NASA Reference Publication 1080

November 1981

NASA-RP-1080-VOL-5
19820008278

LANGLEY RESEARCH CENTER
LIBRARY, NASA
HAMPTON, VIRGINIA

ATS-6 Final Engineering Performance Report

Volume V - Propagation Experiments

NASA

NASA Reference Publication 1080

1981

ATS-6 Final Engineering Performance Report

Volume V - Propagation Experiments

Robert O. Wales, *Editor*
Goddard Space Flight Center
Greenbelt, Maryland

National Aeronautics and Space Administration

Scientific and Technical Information Branch

An Engineering Evaluation

in

Six Volumes

This document makes use of international metric units according to the Système International d'Unités (SI). In certain cases, utility requires the retention of other systems of units in addition to the SI units. The conventional units stated in parentheses following the computed SI equivalents are the basis of the measurements and calculations reported.

For sale by the National Technical Information Service
Springfield, Virginia 22161
Price

VOLUME V
CONTENTS

VOLUME V
CONTENTS (continued)

VOLUME V
CONTENTS (continued)

VOLUME V
CONTENTS (continued)

VOLUME V
CONTENTS (continued)

VOLUME V
CONTENTS (continued)

PART C
EXPERIMENTS ABOVE 10 GHz

VOLUME V
CONTENTS (continued)

VOLUME V
CONTENTS (continued)

VOLUME V
CONTENTS (continued)

LIST OF ILLUSTRATIONS

VOLUME V
LIST OF ILLUSTRATIONS (continued)

VOLUME V
LIST OF ILLUSTRATIONS (continued)

VOLUME V
LIST OF ILLUSTRATIONS (continued)

VOLUME V
LIST OF ILLUSTRATIONS (continued)

VOLUME V
LIST OF ILLUSTRATIONS (continued)

VOLUME V
LIST OF ILLUSTRATIONS (continued)

VOLUME V
LIST OF ILLUSTRATIONS (continued)

LIST OF TABLES

VOLUME V
LIST OF TABLES (continued)

VOLUME V
LIST OF TABLES (continued)

FOREWORD

ATS-6 has been referred to as Arthur C. Clarke's "Star," because Mr. Clarke originated the idea for synchronous communications satellites in an article that he wrote in 1945. In 1975, Mr. Clarke was actively engaged in monitoring the Indian Satellite Instructional Television Experiment on ATS-6 and giving feedback to the Indian Space Research Organization. We, therefore, felt that it would be appropriate for him to contribute the foreword for this report.

An excerpt from his response to our request and selected paragraphs from his contribution, "Schoolmaster Satellite," follow.

ශ්‍රී ලංකා මොරටුව විශ්වවිද්‍යාලයේ
කුලපති කාර්යාලයෙනි

FROM THE DESK OF THE CHANCELLOR
UNIVERSITY OF MORATUWA, SRI LANKA

ආතර් සී. ක්ලාර්ක්
බී.ඇස්.සී., ඇෆ්.ආර්.ඒ.ඇස්., ඇෆ්.බී.අයි.ඇස්.
ලන්ඩනයේ කිංග්ස් විද්‍යාලයේ අයි සාමාජික
Arthur C. Clarke
B.Sc., F.R.A.S., F.B.I.S.
Fellow of King's College, London.

වැලිසර: 94255
කේබල්: අන්ඩර්සී
කොළඹ
Tel: 94255
Cable: Undersea
Colombo

"ලෙස්ලිගෙ නිවස"
25, බාන්ස් පෙදෙස,
කොළඹ 7.
"Leslie's House"
25, Barnes Place,
Colombo 7.

24th September 1980

The extracts that follow are from an essay that was written in 1971, almost five years before the SITE program became fully operational, and originally appeared in the *Daily Telegraph Colour Magazine* for 17 December 1971. It was later read into the *Congressional Record* (27 January 1972) by Representative William Anderson, first commander of the nuclear submarine *Nautilus*, and now forms Chapter 12 of *The View From Serendip* (Random House, 1977; Ballantine, 1978).

To me, it brings back vivid recollections of my meetings with Dr. Sarabhai, the chief instigator of the program. I would like to dedicate it to his memory – and to that of another good friend, also closely associated with the project – Dr. Wernher von Braun.

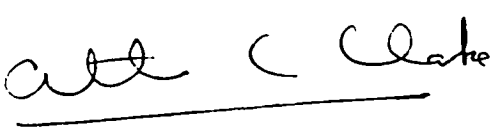

Arthur C. Clarke
Chancellor
University of Moratuwa
Sri Lanka

Vikram Sarabhai Professor, Physical Research
Laboratory, Ahmedabad
India

SCHOOLMASTER SATELLITE

"For thousands of years, men have sought their future in the starry sky. Now this old superstition has at last come true, for our destinies do indeed depend upon celestial bodies—those that we have created ourselves . . .

"In 1974 there will be a new Star of India; though it will not be visible to the naked eye, its influence will be greater than that of any zodiacal signs. It will be the satellite ATS-F (Applications Technology Satellite F), the latest in a very successful series launched by America's National Aeronautics and Space Administration. For one year, under an agreement signed on September 18, 1969, ATS-F will be loaned to the Indian Government by the United States, and will be "parked" 22,000 miles above the Equator, immediately to the south of the sub-continent. At this altitude it will complete one orbit every 24 hours and will therefore remain poised over the same spot on the turning Earth; in effect, therefore, India will have a TV tower 22,000 miles high, from which programmes can be received with almost equal strength over the entire country . . .

"ATS-F, now being built by the Fairchild-Hiller Corporation, represents the next step in the evolution of communications satellites. Its signals will be powerful enough to be picked up, not merely by multi-million dollar Earth stations, but by simple receivers, costing two or three hundred dollars, which all but the poorest communities can afford. This level of cost would open up the entire developing world to every type of electronic communication—not only TV; the emerging societies of Africa, Asia and South America could thus by-pass much of today's ground-based technology, and leap straight in to the space age. Many of them have already done something similar in the field of transportation, going from ox-cart to aeroplane with only a passing nod to roads and railways.

"It can be difficult for those from nations which have taken a century and a half to slog from semaphore to satellite to appreciate that a few hundred pounds in orbit can now replace the continent-wide networks of microwave towers, coaxial cables and ground transmitters that have been constructed during the last generation. And it is perhaps even more difficult, to those who think of television exclusively in terms of old Hollywood movies, giveaway contests and soap commercials to see any sense in spreading these boons to places which do not yet enjoy them. Almost any other use of the money, it might be argued, would be more beneficial . . .

"Those who actually live in the East, and know its problems, are in the best position to appreciate what cheap and high-quality communications could do to improve standards of living and reduce social inequalities. Illiteracy, ignorance and superstitution are not merely the results of poverty—they are part of its cause, forming a self-perpetuating system which has lasted for centuries, and which cannot be changed without fundamental advances in education. India is now beginning a Satellite Instructional Television Experiment (SITE) as a bold attempt to harness the technology of space for this task; if it succeeds, the implications for all developing nations will be enormous.

"Near Ahmedabad is the big 50-foot diameter parabolic dish of the Experimental Satellite Communication Ground Station through which the programmes will be beamed up to the hovering satellite. Also in this area is AMUL, the largest dairy co-operative in the world, to which more than a quarter of a million farmers belong. After we had finished filming at the big dish, our camera team drove out to the AMUL headquarters, and we accompanied the Chief Veterinary Officer on his rounds.

"At our first stop, we ran into a moving little drama that we could never have contrived deliberately, and which summed up half the problems of India in a single episode. A buffalo calf was dying, watched over by a tearful old lady who now saw most of her worldly wealth about to disappear. If she had called the vet a few days before—there was a telephone in the village for this very purpose—he could easily have saved the calf. But she had tried charms and magic first; they are not always ineffective, but antibiotics are rather more reliable . . .

"I will not quickly forget the haggard, tear-streaked face of that old lady in Gujerat; yet her example could be multiplied a million times. The loss of real wealth throughout India because of ignorance or superstition must be staggering. If it saved only a few calves per year, or increased productivity only a few per cent, the TV set in the village square would quickly pay for itself. The very capable men who run AMUL realise this; they are so impressed by the possibilities of TV education that they plan to build their own station to broadcast to their quarter of a million farmers. They have the money, and they cannot wait for the satellite—though it will reach an audience two thousand times larger, for over 500 million people will lie within range of ATS-F . . .

"And those who are unimpressed by mere dollars should also consider the human aspect—as demonstrated by the great East Pakistan cyclone of 1971. That was tracked by the weather satellites—but the warning network that might have saved several hundred thousand lives did not exist. Such tragedies will be impossible in a world of efficient space communications.

"Yet it is the quality, not the quantity, of life that really matters. Men need information, news, mental stimulus, entertainment. For the first time in 5,000 years, a technology now exists which can halt and perhaps even reserve the flow from the country to the city. The social implications of this are profound; already, the Canadian Government has discovered that it has to launch a satellite so that it can develop the Arctic. Men accustomed to the amenities of civilisation simply will not live in places where they cannot phone their families, or watch their favourite TV show. The communications satellite can put an end to cultural deprivation caused by geography. It is strange to think that, in the long run, the cure for Calcutta (not to mention London, New York, Tokyo), may lie 22,000 miles out in space . . .

"The SITE project will run for 1 year, and will broadcast to about 5,000 TV sets in carefully selected areas. This figure may not seem impressive when one considers the size of India, but it requires only one receiver to a village to start a social, economic and educational revolution. If the experiment is as great a success as Dr. Sarabhai and his colleagues hope (and deserves), then the next step would be for India to have a full-time communications satellite of her own. This is, in any case, essential for the country's internal radio, telegraph, telephone and telex services . . .

"Kipling, who wrote a story about "wireless" and a poem to the deep-sea cables, would have been delighted by the electronic dawn that is about to break upon the sub-continent. Gandhi, on the other hand, would probably have been less enthusiastic; for much of the India that he knew will not survive the changes that are now coming.

"One of the most magical moments of Satyajit Ray's exquisite Pather Panchali is when the little boy Apu hears for the first time the Aeolean music of the telegraph wires on the windy plain. Soon those singing wires will have gone forever; but a new generation of Apus will be watching, wide-eyed, when the science of a later age draws down pictures from the sky—and opens up for all the children of India a window on the world."

A. C. Clarke

ACKNOWLEDGMENTS

Many scientists, engineers, and technicians, too numerous to mention by name, have contributed to these volumes. Engineers at Fairchild Space and Electronics Company and Westinghouse Defense and Electronic Systems Center composed the chapters from material supplied by subsystems designers of the various systems and experiments, and have worked closely with the editors to complete this report. They have the editor's gratitude.

In particular, thanks go to Mr. Ralph Hall at Fairchild Space and Electronics Company and Mr. James Meenen of Westinghouse Defense and Electronic Systems Center for their patient cooperation, thorough review, and constructive comments and suggestions.

INTRODUCTION

ATS-6 was the final satellite in a series of six of the Applications Technology Satellite Program of the National Aeronautics and Space Administration. It was designed and built by Fairchild Space and Electronics Company, Germantown, Maryland, under NASA Contract NAS5-21100 from NASA Goddard Space Flight Center.

At the time of its launch, it was the largest and most powerful communications satellite to go into orbit.

The mission of ATS-6 was to demonstrate and evaluate the application of new technologies for future satellite systems. This it accomplished by demonstrating the first direct-broadcast television from geosynchronous orbit; by demonstrating many new communications technologies; by relaying data from, and tracking, low-orbiting satellites; by relaying communications and positions of ships and aircraft; and by supporting a variety of other experiments involving communications, meteorology, particle and radiation measurements, and spacecraft technology.

The purpose of this report is to document the lessons learned from the 5-year ATS-6 mission that might be applicable to spacecraft programs of the future. To satisfy this purpose, the six volumes of this report provide an engineering evaluation of the design, operation, and performance of the system and subsystems of ATS-6 and the effect of their design parameters on the various scientific and technological experiments conducted.

The overall evaluation covers the following:

- A summary of the ATS-6 mission objectives, operations, and results
- A summary description of the spacecraft system and subsystem requirements, the designs evolved to meet these requirements, and special analyses and ground testing performed to validate these designs and to confirm the flight integrity of the spacecraft
- A comparative evaluation of the 5-year performance and operations in orbit relative to those specified and demonstrated during ground tests prior to launch
- A summary of anomalies that occurred in the hardware, probable causes, and recommendations for future spacecraft systems
- A summary evaluation of the various technological and scientific experiments conducted
- A summary of conclusions and recommendations at the spacecraft system and subsystems levels that address considerations that might be relevant to future spacecraft programs or similar experiments.

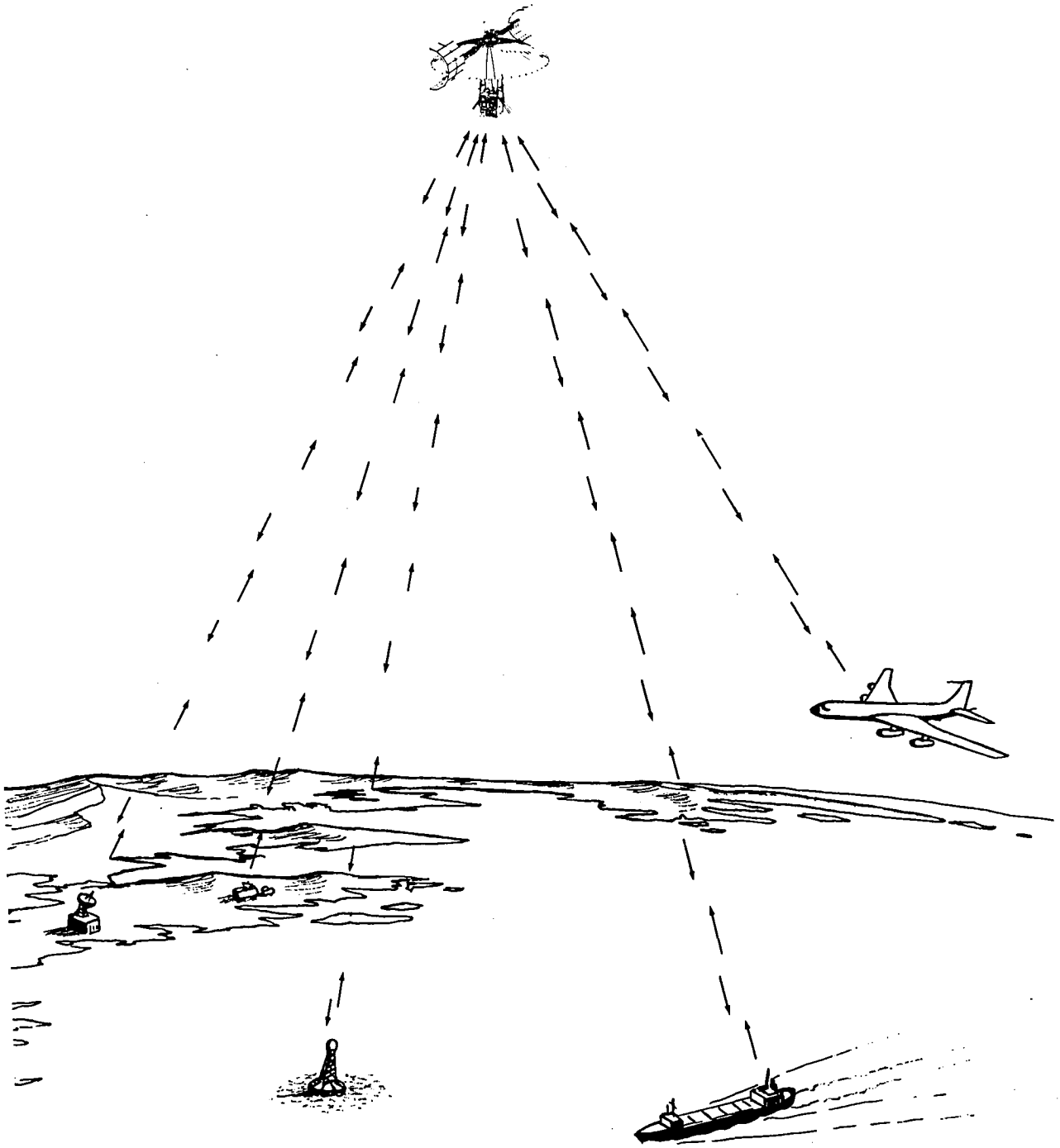

Communication and Propagation Experiments

Part A
Experiments at 1550 MHz to 1650 MHz

CHAPTER 1

"INTEGRATED L-BAND EXPERIMENTS" SYSTEM

PURPOSE AND SYSTEM PARAMETERS

Objective of Experiments

ATS-6 contained L-band capability that was specifically intended for use in the aircraft and maritime bands. The intended tests were to investigate various methods of communications, data transmission, and position determination of aircraft and ships in conjunction with a ground station. During the early planning stages of the experiment, it became apparent that many organizations in the maritime and aeronautical communities wished to participate in the L-band tests. Interested parties were invited by NASA/GSFC to submit experiment proposals that were evaluated by GSFC and eventually used as inputs to formulate an overall experiment that maximized the use of the NASA resources and still accommodated each experiment. The resulting experiment plan provided the basis for the integrated L-band experiments.

The L-band communication system provided by ATS-6 allowed the performance of integrated L-band experiments of international scope consisting of aeronautical and maritime communications that included air traffic control (ATC) and air-sea navigation. The purpose of these experiments was to demonstrate and evaluate the basic capabilities and conceptual methods of operations pertaining to the use of geostationary satellites, one of which was the Position Location and Communication Experiment (PLACE).

PLACE was originally conceived by NASA in 1967, and was later supported in a joint effort by other participants in the United States, Canada, and Europe. Aircraft flying near the coast make use of line-of-sight vhf communications that are limited to less than 400 miles. Flights in most oceanic areas rely on hf frequencies, which is not a reliable communications system. The present oceanic air traffic control system uses widely spaced planned tracks across the ocean and periodic reports by the onboard crew, as they pass certain check points along the track. Navigation and periodic reporting of position to the ATC centers depends strictly on the performance of the crew and equipment. As air traffic increases, it will be necessary to provide additional ATC system capacity by a reduction of aircraft separation standards.

A solution to the inadequacies of the present oceanic ATC service is a satellite relay system that provides continuous surveillance and communication coverage over the oceanic areas. The existence of such a satellite relay system would provide the basis for establishing positive control of an oceanic ATC system.

To conduct the integrated L-band experiments required the use of geostationary satellites (ATS-6 and ATS-5), aircraft, ships, and ground station facilities. The United States Department of Transportation and the Federal Aviation Administration (FAA) conducted a series of experiments with ATS-6 during 1974 to 1975, as participants in the integrated L-band experiments. The general objectives for the development of ATC systems using satellite communications and surveillance techniques fall into two major categories:

- System technology and equipment development
- System demonstration of operational concepts

The FAA was joined by the European Space Agency (ESA) and the Canadian Ministry of Transport for the civil aviation experiments. In the maritime activity, the United States Coast Guard, the FAA, and the ESA conducted search and rescue (SAR) demonstrations and voice and data L-band satellite communications experiments.

During the past decade, the FAA has conducted various satellite communications studies and experiments in support of Oceanic and Continental (CONUS) ATC systems. The FAA, the ESA and Canada have performed L-band experiments for the aeronautical satellite (Aerosat) program. This program was designed to test alternative ATC techniques and operational procedures for a future satellite-based oceanic communications system.

Participants

The participants in the ATS-6 integrated L-band experiments were as follows:

Goddard Space Flight Center (GSFC)
Department of Transportation (DOT)
Federal Aviation Administration (FAA)
Maritime Administration (MarAd)
European Space Agency (ESA)
Canadian Ministry of Transport (Canada)
U.S. Coast Guard (USCG)

INTEGRATED L-BAND SYSTEM

The major facilities or terminals of the operational network for the integrated L-band experiments consisted of the following:

1. Three NASA Satellite Tracking and Data Network (STDN) stations (Rosman, Mojave, Santiago)

2. Kings Point Earth Station (Kings Point, N.Y.)

3. National Aviation Facilities Experiment Center (NAFEC)
4. Mobile terminals (aircraft, ships)
5. U.S. Coast Guard Radio Station (Radsta)
6. ATS Operations Control Center (ATSOCC)
7. Canadian Ground Station (Ottawa, Canada)
8. NASA Communication Division (NASCOM)
9. Information Processing Division (IPD)

The three NASA ground stations consisted of the Rosman Ground Station (North Carolina) as the primary station and the remote stations located in Santiago, Chile and the Mojave Ground Station, near Barstow, California. The Rosman station had C-band transmit and receive capabilities with an 25.9-meter antenna, transmit only at C-band on a 4.6-meter antenna, and transmit and receive at L-band on another 4.6-meter antenna. The Mojave station had C-band transmit and receive capabilities with a 12.2-meter antenna and a 4.6-meter antenna for L-band. Santiago had transmit and receive capabilities for L-band only (using a 4.6-meter antenna).

The Kings Point Earth Station was housed at the National Maritime Research Center (NMRC) in Kings Point, New York, and served as the control center for the Maritime Administration tests. The Kings Point Earth Station was capable of transmitting and receiving at C-band frequencies of 6359 and 3959 MHz on a 10-meter antenna system. It also had two L-band receive-only capabilities with 1.2-meter antennas. MarAd's Kings Point ground station communicated with ATS-6 as scheduled by ATSOCC. Rosman monitored the L-band forward signal level to determine the C-band carrier level received by the spacecraft from the Kings Point transmitter, which was adjusted to the agreed upon level.

The National Aviation Facilities Experiment Center was the control center for the FAA tests and was shared by ESA during the fall of 1974. The NAFEC center had no satellite communication facilities and, therefore, performed all of their tests with their equipment located at the Rosman Ground Station. NAFEC was connected to their equipment by three dedicated telephone lines between NAFEC and Rosman. This center also had a dedicated telephone line to NASCOM at GSFC.

There were a number of mobile terminals communicating with ATS-6 during the L-band experiments. The mobile terminals of the participating agencies are listed below:

Agency	Mobile Description
FAA	1 – KC-135 airplane
ESA (aircraft)	1 – Comet airplane
Canada	1 – Lockheed Jetstar airplane

Agency (cont)	Mobile Description (cont)
MarAd	2 – Cargo ships American Ace and Lash Atlantico
U.S. Coast Guard	2 – Cutters "Gallatin" and "Sherman"
ESA (maritime)	The German ship, "Otto Hahn" The Norwegian ship, "Skiensfjord" Bouy-emergency position indicating radio beacon (EPIRB) Indicating radio beacon (EPIRB)

The U.S. Coast Guard Radio Station, located near Washington, D.C., was used by participants to communicate with their mobile stations. The Radsta had no spacecraft communication capabilities, but was equipped with a 10-kW hf/mF transmitter capable of services to the Atlantic Ocean region. The radio station was connected to NASCOM by a dedicated telephone line.

The Canadian ground station was located in Ottawa, Canada, and was housed at the Communications Research Center of the Department of Communications. The station had transmit and receive capabilities in the L-band frequency range and used a 50-watt transmitter and a 4.2-dB noise figure receiver that were connected to a 8.5-meter antenna. Basically, the station was used to receive signals transmitted from its equipment located at Rosman and translated through ATS-6. When time permitted, some of the L-to-L frequency translation tests were performed between Ottawa, ATS-6, and their aircraft. Communications between Ottawa and ATSOCC was by a telephone line between NASCOM at GSFC and the Canadian embassy in Washington, D.C.

The General Electric Radio Optical Observatory near Schenectady, New York, performed ranging tests through ATS-5 to transponding stations located in Hawaii and Buenos Aires. The position of ATS-5 was determined and predicted for 90-minute increments. Once an hour, ATS-5 predictions were teletyped to Rosman and Kings Point as part of the two satellite-position-determination experiments. The predictions covered 90-minute periods. General Electric's Observatory trilateration experiment used the L-to-L translation mode of ATS-5.

ATS-6 System

General

Refer to Volume I of this report for a description of the spacecraft, a spacecraft systems summary, an operations summary, and a mechanical subsystem summary; to Volume II, "Orbit and Attitude Control" for attitude control and propulsion information; and to Volume III "Telecommunications and Power" for data on communications, telemetry, command, tracking, and relay of data.

Ground Terminals

Rosman Ground Station

The Rosman Ground Station, near Brevard, North Carolina, was NASA's primary spacecraft control and communication interface, and data acquisition facility for the operation with ATS-6 and ATS-5. The function of this ground terminal for the ATC demonstration system was fourfold:

1. It provided the interface to ATS-6 through the ground and aircraft equipment of the NASA PLACE subsystems and furnished all of the signal processing.

2. It housed the FAA simulated aircraft terminal.

3. It monitored the status of satellite communication channels and the quality of performance, and recorded the voice and data communications for postanalysis.

4. It furnished, through its resources, the collection and computation of aircraft independent surveillance data.

Voice and data communications were transmitted to and from ATS-6 through a 25.9-meter diameter C-band parabolic reflector antenna. A 4.6-meter diameter antenna provided the backup for the primary C-band transmissions to ATS-5 in support of the two-satellite-position-determination experiment and also for communications to airborne terminals by ATS-6.

The primary interface with the station equipment was by the L-band experimenter ground equipment that provided up to three data channels, one surveillance and one ranging channel, which permitted the use of seven separate communication channels. Two computers at the station had two digital recorders each for use of the experimenters. In addition, various types of hard-copy recorders were available, such as 8-channel strip-chart recorders and X-Y plotters.

Ground communications were available to and from the ground station by the switching, conferencing, and monitoring arrangement (SCAMA) network, voice, voice or data telephone lines, full-duplex teletype, and commercial telephone lines. The SCAMA voice lines provided communications between the ground station and the control center. Commercially leased telephone lines were available and had the capability of duplex voice or data communications. The ground station had the teletype capability for both receive and transmit, and carried operational traffic to and from the network stations, ATSOCC, and the experimenters. Some of the principal characteristics of the Rosman station are presented in Table 1-1.

Mojave Station

The Mojave Ground Station, located near Barstow, California, had the capability of transmitting and receiving in L-band to ATS-6 with a 4.6-meter antenna. A maximum L-band transmitter power of 1 kW was available for the experiments. A backup PLACE modem was available when required.

Table 1-1
Rosman Ground Station Capabilities

Location			
Latitude	35° 11′ 55″ North		
Longitude	82° 52′ 22″ West		
Elevation	888 meters		
Antennas			
C-Band			
Diameter	4.6 meters (ATS-5)	25.9 meters (ATS-6)	
Type	Parabolic reflector with Cassegrain C-band feed		
Polarization	Linear	Linear	
Mount	AZ-EL	X-Y	
Receive frequency	860 MHz	3.7 to 4.2 GHz	
Transmit frequency	5.9 to 6.4 MHz	5.9 to 6.4 GHz	
Net receive gain (peak)	28.3 dB	57.5 dB/3750 MHz	±0.5 dB
		58.3 dB/3950 MHz	
		58.2 dB/4150 MHz	
Net transmit gain (peak)	43.1 dB	58.1 dB/4178 MHz	
		59.1 dB/5950 MHz	+1.0 dB
		59.7 dB/6150 MHz	-0.0 dB
		59.9 dB/6350 MHz	
System noise temperature	600 K	100 K	
System G/T	0.5 dB/K	38.3 dB/K/3950 MHz	
L-Band			
Diameter		4.6 meters (ATS-6)	
Type	Parabolic reflector with prime-focus feed		
Polarization		Circular	
Mount		AZ-EL	
Receive frequency		1.5 to 1.58 GHz	
Transmit frequency		1.62 to 1.7 GHz	
Net receive gain (peak)		34.2 dB, ±1.5/1.55 GHz	
Net transmit gain (peak)		33.4 dB, ±1.5/1.65 GHz	
System noise temperature		22.7 dB/K (188 K)	
G/T		11.5 dB/K, ±1.5	

Table 1-1
Rosman Ground Station Capabilities (continued)

Receivers	
C-Band	
Noise temperature	20 K
Rf bandwidth	500 MHz
I.f. bandwidth	70 MHz
L-Band	
Noise temperature	99 K
Rf bandwidth	80 MHz
I.f. bandwidth	70 MHz, ±15 MHz
Transmitters	
C-Band	
Maximum power output	2 KW at 4.6-meter antenna 8 KW at 25.9-meter antenna
Instantaneous rf bandwidth	50 MHz
L-Band	
Maximum power output	1 KW at 4.6-meter antenna
Rf bandwidth	10 MHz

Santiago, Chile Station

The Santiago Ground Station was provided with an L-band receive and transmit capability and used a 4.6-meter antenna. A PLACE modem was also included in this station.

FAA (NAFEC) Ground Terminal

The National Aviation Facilities Experiment Center ground terminal consisted of two minicomputers, each with associated teletypewriter input/output (I/O) devices, and a seven-channel magnetic tape recorder for recording voice communication transactions. One computer controlled the information displays, and the second computer processed the incoming and outgoing digital data communications. One of the information displays was used as the primary controller's I/O position.

Data messages, sent from the airborne terminals, were processed first in the processing computer and then applied to the second computer for display on the I/O machine information displays.

The telephone circuits that interconnected the NAFEC ground terminal and the NASA Rosman facility consisted of three dedicated, alternate voice or data, full-duplex channels with customer switching provisions for configuration of each channel to either voice or data transmissions. The data circuits were interfaced to the Bell Telephone System. The data rate was selectable at 600, 1200, or 2400 bits per second. Provisions for two other voice circuits were also made at the NAFEC ground terminal. These were full-duplex voice channels between NAFEC and the NASA GSFC communications center. The formerly described voice circuit was used for alternate access to the Rosman Ground Station through the NASA SCAMA network.

Canada Terminal

The Ottawa, Canada ground station configuration for the ATC demonstration system consisted of a transmitter, receiver, and a 5.8-meter diameter L-band parabolic reflector antenna. This equipment configuration, which provided the capability for voice communication only, was used by the Canadian Ministry of Transport. The Ottawa terminal functioned as a simulated aircraft terminal participating in voice communication exchanges with the NAFEC ground terminal through the Rosman Ground Station PLACE C-band channels and the dedicated telephone lines between Rosman and NAFEC. Prepared scenarios of simulated aircraft operations were used by the Canadian communicators to provide additional voice-only aircraft traffic loadings for the ATC demonstrations.

ATSOCC Terminal

All operations with ATS were controlled by ATSOCC. ATSOCC coordinated all experimenter requirements and scheduled the spacecraft operations and the activities of the Rosman Ground Station. This control center maintained real-time voice contact with the Rosman Ground Station and monitored the status of the spacecraft through the use of telemetry data from Rosman.

ATSOCC also coordinated all the activities between the various channels of GSFC, such as data processing and orbit determinations and provided daily, weekly, and monthly summary reports of all operational activities. Logs, data sheets, and plots were kept of the selected parameters and activities. The control center also kept an account of all the data to and from the ground stations.

Airborne Terminals

FAA KC-135 Aircraft Terminal

FAA KC-135 aircraft provided the test-bed terminal for both the United States dedicated ATC demonstrations and the joint United States, ESA, and Canadian demonstrations. The KC-135 aircraft terminal consisted of the data link subsystem, PLACE transponder, an inertial navigation system, L-band antennas, selective calling digital message processor, and the required interfaces that provided aircraft altitude, heading, position in latitude, and longitude. The PLACE transponder contained a data modem and an L-band transmitter and receiver.

In the operation of the ATC demonstration system, the data link subsystem accepted digital signals from the PLACE data channel, decoded the message according to a fixed format, and displayed the information on the particular output device designated by the incoming message. The data link subsystem also accepted digital signals from the various input devices of the ATC demonstration system on the aircraft, arranged the information in the proper format, and presented it to the PLACE transponder for transmission to the ground terminal. To increase the data link aircraft traffic loading, software programs were used in the data link subsystem computer to generate simulated position reports and flight progress messages for up to 6 simulated aircraft and 14 prestored routes. The INS data input to the data link subsystem were the following: Present position, groundspeed, track angle, true heading, windspeed, and wind angle. Present position was also available for display on a slave indicator unit for use in the two-satellite-position-determination experiment. All messages in and out of the airborne data link terminal were logged by a paper tape punch and hard-copy printer.

The aircraft L-band antenna system used for the ATC demonstrations consisted of three flush-mounted slot dipole antennas as shown in Figure 1-1. These two antennas provided ±4 dB gain (with respect to a right-hand circular isotrope) side coverage from approximately 10 degrees to 165 degrees in the azimuth plane (point of reference being the nose of the aircraft) and from 10 degrees to 75 degrees above the horizon in the vertical plane. The third antenna provided +4 dB gain (with respect to a right-hand circult isotrope) overhead and the fore and aft coverage from 10 degrees above the horizon to the zenith. Since the flight paths were all made at aircraft-to-satellite elevation angles between 40 degrees and 10 degrees, the right and left wing root slot dipole antennas were used during the major portion of each demonstration period.

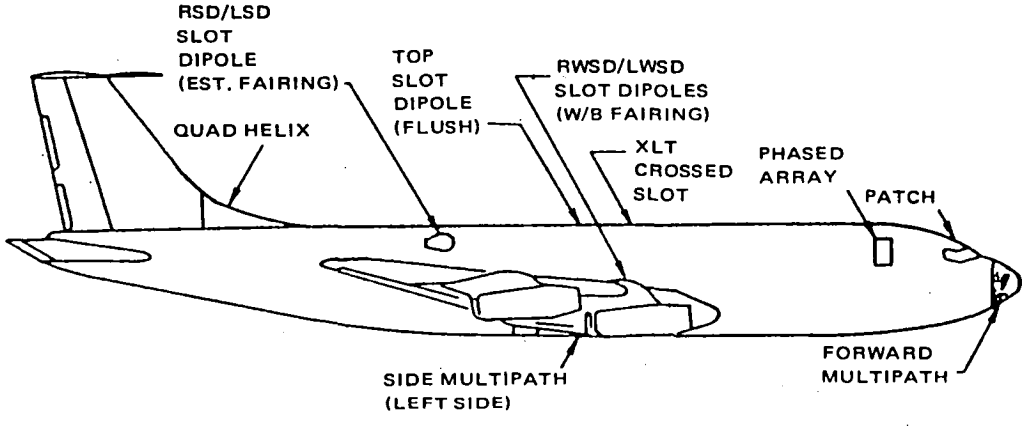

NOTE:
RWSD RIGHT WING SLOT DIPOLE
LWSD LEFT WING SLOT DIPOLE

Figure 1-1. KC-135 Antenna Locations

ESA Comet IV Terminal

The Comet IV aircraft was used by the ESA in support of the joint ATC demonstrations. The data link subsystem and audio communications patching and switching unit furnished by the FAA were similar to that installed in the FAA KC-135 aircraft. The data link subsystem was interfaced to the ESA L-band avionics equipment (receiver, transmitter, and modem) that provided similar performance and had compatible functions with that of the PLACE equipment used in the FAA aircraft. Other equipment provided by ESA were L-band antennas and an omega navigation system that was used as the data source for the automatic-positioning reporting function.

Canada Jetstar Aircraft Terminal

The Jetstar aircraft was used by Canada in their aeronautical experiments primarily to evaluate simultaneously four voice modulation techniques and the performance of an antenna system in conjunction with the onboard equipment in a ground-to-satellite-to-aircraft environment. The communications experiments were conducted between the Ottawa, Canada ground station and the aircraft by ATS-6. Equipment in the aircraft consisted of two vhf-amplitude modulated modems, one i.f.-single sideband modem, a receiver in the medium frequency band and a phased-array antenna.

Maritime Terminals

The integrated L-band experiments on communications and oceanic surveillance/navigation tests were performed by the following maritime participants and their corresponding ships:

Dept. of Commerce/Maritime Administration	Cargo ships *American Ace* and *Lash Atlantico*
Dept. of Transportation/U.S. Coast Guard	Cutters *Gallatin* and *Sherman*
European Space Agency	German ship *Otto Hahn* EPIRB (buoy-emergency position indicating Radio Beacon)

The maritime equipment used on board the Maritime Administration (MarAd) ships, *American Ace* and *Lash Atlantico*, consisted of a parabolic antenna inside a radome, three types of voice modems, and three types of digital data modems having the capability of the following types of modulation:

Voice	Data
Narrowband frequency modulation	Phase shift keying–pseudonoise (PSK-PN)
Frequency modulation (companded)	Phase shift keying (PSK)
Pulse duration modulation	Frequency-shift keying (FSK)

Voice and data communication experiments in L-band were performed between the two maritime ships and the ground facilities at the National Maritime Research Center at Kings Point, N.Y., by ATS-6. A navigation L-band experiment was also conducted with the above two ships, ATS-6, and the ground facilities at Kings Point, N.Y. Position of the ships was determined by performing four different ranging measurements with the use of the ATS-6 and ATS-5 and using the pseudorandom code (PN) method. The 10-meter antenna at the Kings Point facility was used for the ranging measurements. A 1.22-meter stabilized antenna on board both ships was engaged in performing the L-band experiments.

The U.S. Coast Guard participated in the L-band experiments by providing two of their cutters, the *Sherman* and the *Gallatin*. The same type of experiments was performed with the Coast Guard ships as that with MarAd, with the addition of a multipath test and the Search and Rescue (SAR) demonstration that involved the use of the European Space Agency (ESA) EPIRB buoy. The L-band communications link was composed of the U.S. Coast Guard ship to the ATS-6 satellite to the NASA Rosman Ground Station. Communications from ship to the Coast Guard Radio Station shore facilities was also provided for the purpose of conveying operational administrative information. This facility had the capability of operating in full-duplex voice, carrier wave, teletype or facsimile modes.

ESA participated in the European maritime communications L-band experiments by using the Norwegian ship *M. V. Skiensfjord*, the German ships *M. S. Otto Hahn*, *M. S. Lukastrum*, and *M. S. Tabasis*, and the German ocean buoy emergency position indicating radio beacon (EPIRB).

The Norwegian ship *M. V. Skiensfjord* had an L-band communications capability for receive only and used a phased array antenna that provided a hemispherical coverage with the combined electronics scanning and mechanical movement. Automatic tracking of ATS-6 was also available with this antenna and used the monopulse technique. The mount for the antenna provided one axis of rotation. L-band experiments were performed in a communications link between the ship and the Rosman Ground Station by ATS-6. Equipment for these experiments was provided to determine the performance in the reception of PN coded data using PSK modulation and a narrowband frequency modulated voice signal.

The L-band communications link for the German ship *Otto Hahn* was between the ship and the Rosman Ground Station by ATS-6. Primary maritime experiments that were performed with this ship consisted of the following:

- Multipath measurements
- Bit error rate measurement for data reception
- Voice reception quality for modulation types of companded narrowband frequency (NBFM) and delta modulation for three sampling rates
- Ship's position location by range measurements.

The ship-terminal equipment had the capability of transmitting and receiving signals by an L-band transponder that used the time-division-multiplex carrier system. Two antennas were employed on the *Otto Hahn* ship, both mounted on individual stabilized platforms. One antenna was a quad-helix type, while the other antenna had a quadrafiliarshort backfire configuration. A 10-watt solid state transmitter was located on the back of each antenna to minimize transmission losses.

Two additional German ships, the *M. S. Lukastrum* and the *M. S. Tabasis*, took part in the ESA maritime L-band experiments. The *M. S. Lukastrum* performed tests in November and December 1974, while the *M. S. Tabasis* participated in March and April 1976. Both ships had similar equipment, although the *M. S. Tabasis* had additional equipment that provided greater communications capability.

A stabilized antenna pedestal on each ship contained two antennas, one a 3-meter parabolic dish and the other an array of helixes that provided a monopulse tracking capability. Three channels were available in the array antenna: two that were the difference channels for monopulse tracking, and the third that was the sum channel that was allocated for transmitting and receiving communications signals. Transmission of signals in the L-band was supplied by a 50-watt transmitter through a diplexer.

The distress buoy experiment, whose function was to provide a distress radio call from a sinking ship, was also conducted by ESA and the German ship *Otto Hahn*. The objective of this experiment was to demonstrate operational feasibility of using a maritime distress buoy with ATS-6 to improve the search and rescue (SAR) operation. A distress buoy would normally be placed on the top deck of a ship and allowed to float in the ocean if the ship began to sink. In this experiment, the distress buoy was dropped into the ocean from the nuclear ship *Otto Hahn*. The buoy was automatically energized as soon as it was immersed in the ocean water, and then it transmitted the ship's call signal to ATS-6, which relayed the information by C-band to the Rosman Ground Station, where the signal was processed and the ship identification determined. Rosman relayed the information by land lines to the U.S. Coast Guard, which controlled the rescue effort. A homing beacon operating on the international distress frequency of 2182 kHz was also employed in the buoy to guide the ships of the SAR system in the vicinity and to allow the determination of the bearing of the ship in distress.

An L-band right-hand circular polarization conical spiral antenna having an omnidirectional pattern was used on the buoy for continuous transmission of the distress signal. The buoy contained an L-band FM transmitter that provided the coded identification signal.

CHAPTER 2

"INTEGRATED L-BAND EXPERIMENTS" TEST RESULTS

PLACE AERONAUTICAL EXPERIMENTS

The Position Location and Communications Experiment (PLACE) consisted of determining the location of an aircraft in flight over the Atlantic Ocean by using a sidetone ranging technique and evaluating the performance of two-way voice and digital data communications between the aircraft and the selected ground facilities. The facilities used for this test were two satellites, ATS-6 and the ATS-5, FAA KC-135 jet aircraft, and Rosman Ground Station, the primary facility, as shown in Figure 2-1.

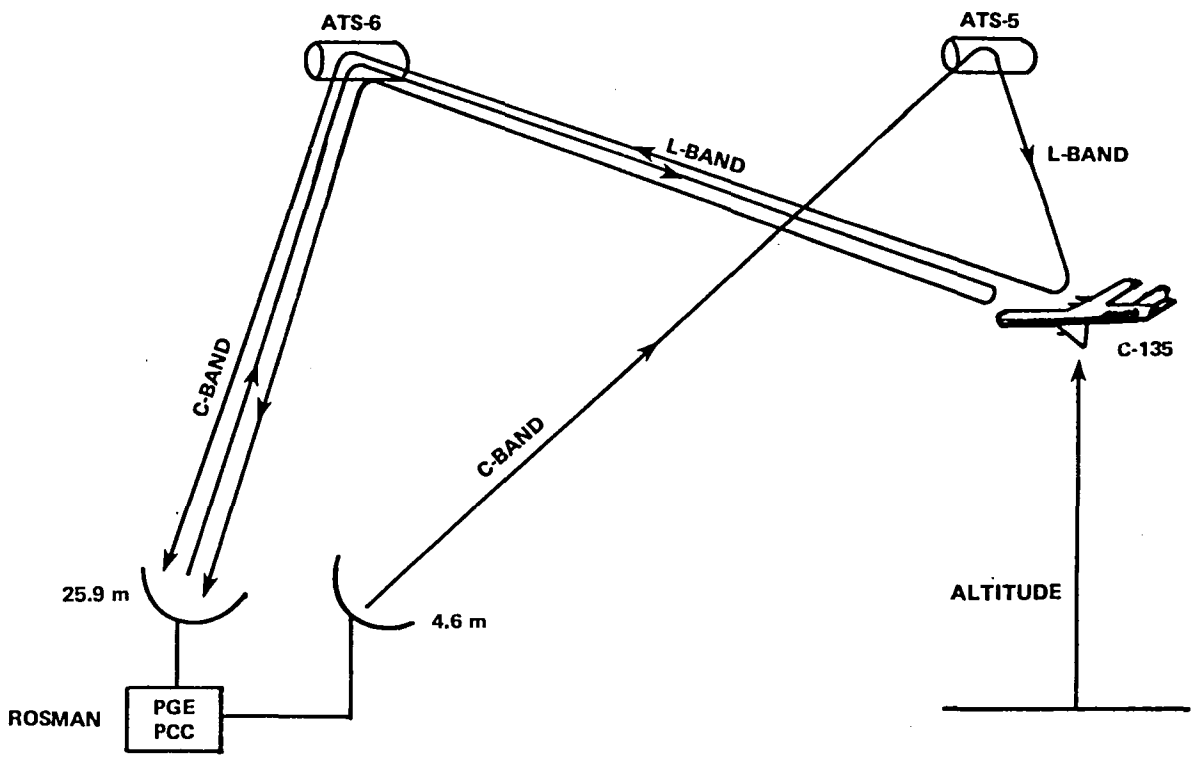

Figure 2-1. Dual Satellite PLACE Ranging Configuration

In the NASA ranging test for locating the position of the aircraft, Rosman transmitted the surveillance and ranging (S&R) signal containing four ranging tones that were Double sideband/amplitude modulation modulated on a carrier of 6350 MHz to the satellite. Supervisory data at a 600 bits per second (bps) rate were phase shift keying (PSK) modulated in phase quadrature on the S&R carrier. The C-band carrier was translated to an L-band frequency of 1550 MHz in the satellite and relayed to the KC-135 aircraft. The aircraft converted this received frequency to 1650 MHz that was relayed back to ATS-6 where it was converted to a C-band frequency of 4150 MHz, and then transmitted back to Rosman. Similarly, the ranging tones were transmitted to ATS-5 at C-band, translated to L-band, relayed to the aircraft where it was retransmitted on L-band to ATS-6, converted to C-band, and relayed back to Rosman. Simultaneously, the aircraft sent its altitude data to Rosman through ATS-6. The PLACE ground equipment at Rosman processed the received range tones where data, in conjunction with ATS-6 and ATS-5 ephemeris data, were used to compute the position of the KC-135 aircraft. Each tone phase was computed by baseband correlation with reference tones. A digital computer resolved phase ambiguities and computed the round-trip range.

Voice and digital data communications were conducted individually and combined with their respective modems between the KC-135 aircraft and the Rosman PLACE Ground Equipment by ATS-6. Voice signals (300 to 3500 Hz) were adaptive narrowband frequency modulated, whereas the digital data at 1200 bps were differentially encoded coherent phase shift keying (DECPSK) modulated.

Experiment Results

Results of the tests performed on the ranging experiment are presented in Table 2-1. The parameters shown in the table are the total number of points, the accepted number of points, the standard deviation of error, the chi-squared fit result and the measured link carrier-to-noise power density ratio (C/N_o).

The PLACE voice tests were performed with the NASA voice modem, Hybrid No. 1, which used the adaptive narrowband frequency modulation (ANBFM). Measurements were performed in a one-way forward-link configuration. Voice transmission quality was measured by determining the percent of word intelligibility from a phonetically balanced (PB) word list for various values of the received C/N_o. The results are presented in Figure 2-2.

The PLACE data tests were performed with a modem having a data rate capability of 1200 bps and a differentially encoded coherent phase shift keying modulation. The bit-error rate (BER) performance was measured with a computer for a range of C/N_o values, the results of which are presented in Figure 2-3. Simultaneous transmission of voice, with DSB/AM modulation, and data, with phase shift keying (PSK) quadrature phase modulation, were performed with the results being shown in Figure 2-4. The modem tests were performed in two configurations, Type I and Type II as follows:

Type I tests used the aircraft slotted dipole antenna that discriminated against multipath effects.

Type II tests used the quad-helix antenna that was used so as to enhance the multipath effects observed over the ocean.

Table 2-1
PLACE Ranging Summary

Date Mo/Day/Yr	Test Type	Start Time	Stop Time	Total Points	Points Accep	σR Meter	P (x^2 >t)	C/N_o dB-Hz
11-13-74	II	0941	0946	42	32	298	0.70	42.0
11-13-74	I	0958	1007	79	69	248	0.27	–
11-13-74	II	1011	1016	32	23	332	0.62	44.5
11-19-74	II	1203	1208	43	23	225	0.79	–
1-29-75	I	1020	1028	76	76	56	0.35	60
1-29-75	I	1030	1038	67	67	125	0.92	46
3-27-75	II	1220	1233	127	120	334	0.03	44.6
3-28-75	I	1353	1359	48	45	236	0.75	42.7
3-31-75	II	1217	1221	33	27	263	0.27	42.0

DOT/TSC AERONAUTICAL EXPERIMENTS

The Department of Transportation/Transportation Systems Center (DOT/TSC) conducted L-band experiments consisting of the following three major categories:

1. Modem Evaluation
2. Multipath Characteristics
3. Antenna Evaluation

The tests were performed by using the FAA KC-135 aircraft, ATS-6, and the NASA Rosman Ground Station as shown in Figure 2-5. All of the modem evaluation tests were performed in a one-way forward link system where test signals were transmitted from the Rosman Ground Station to ATS-6 and then relayed to the KC-135 aircraft. The principal antennas installed on the aircraft consisted of the three-element slot-dipole used for the Type I tests and the quad-helix used for the Type II tests shown in Figure 2-1.

Modem Evaluation

The modem used for the TSC ranging used a binary ranging code that had 9 or 12 binary sub-multiples that provided a rapid acquisition of the code. A narrowband and a wideband mode of operation were used in the ranging tests.

The range error in meters was measured over a wide range of C/N_o for both the narrowband and wideband modes, and the results are presented in Figure 2-6. Best fit curves to laboratory measured

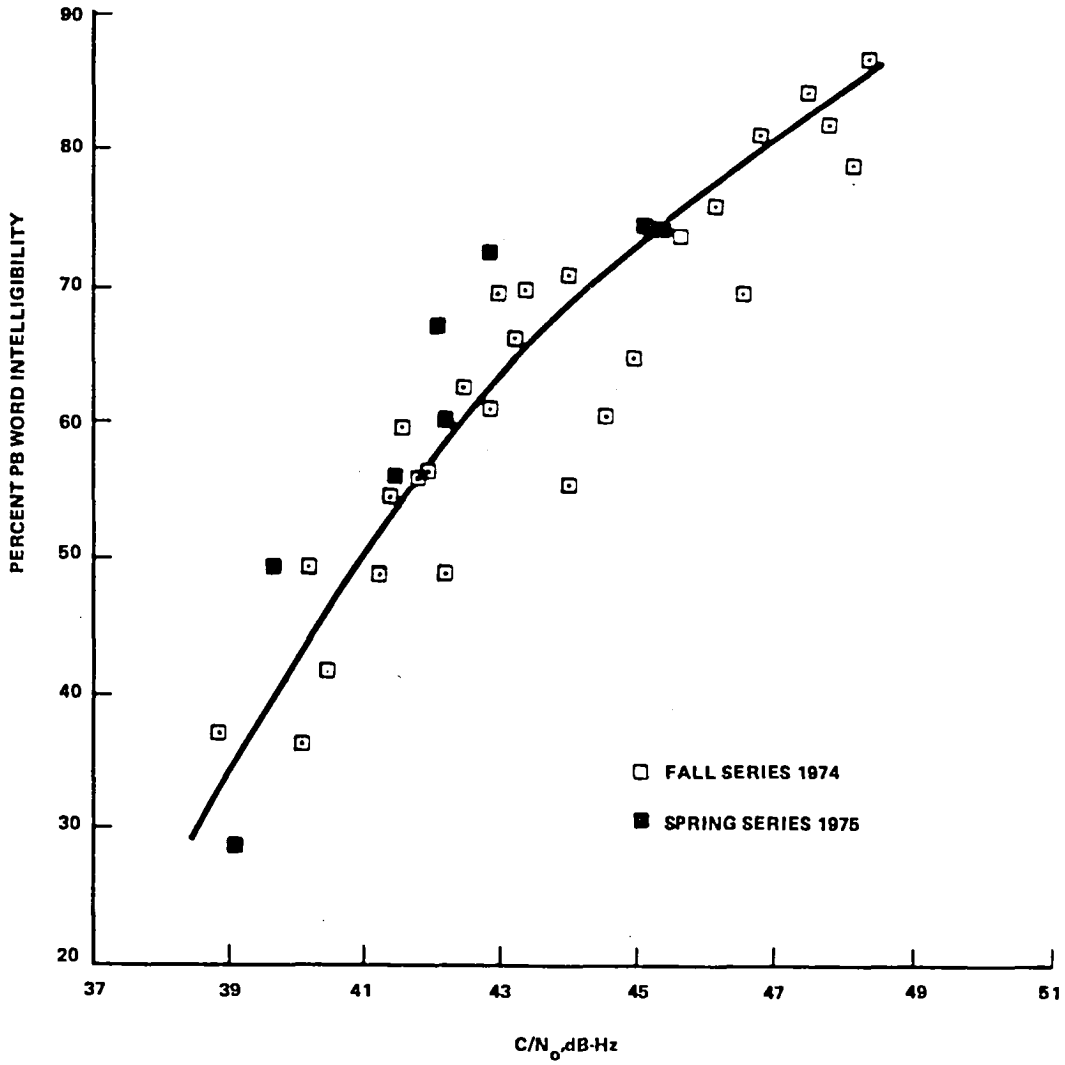

Figure 2-2. Adaptive Narrowband Frequency Modulation Voice Modem, Type I Results

data are superimposed on the data for comparison. The measured range errors can be compared to the theoretical results shown in Figure 2-7.

Three distinct voice modulation techniques were tested by TSC consisting of quadrature phase modulation/PSK (Q-M/PSK) Hybrid No. 1 modem, pulse duration modulation/PSK (PDM/PSK) Hybrid No. 2 modem, and adaptive delta voice modulation (ADVM). The results of the tests for the above three types of modulation are presented in Figure 2-8 as percent of phonetically balanced (PB) word intelligibility for a wide range of C/N_o. Best fit curves of the data obtained are exhibited in this figure.

Digital data tests that were performed with the TSC modems consisted of Hybrid No. 1 and Hybrid No. 2, both of which have DECPSK modulation. The results of the digital data tests at a 1200 bps

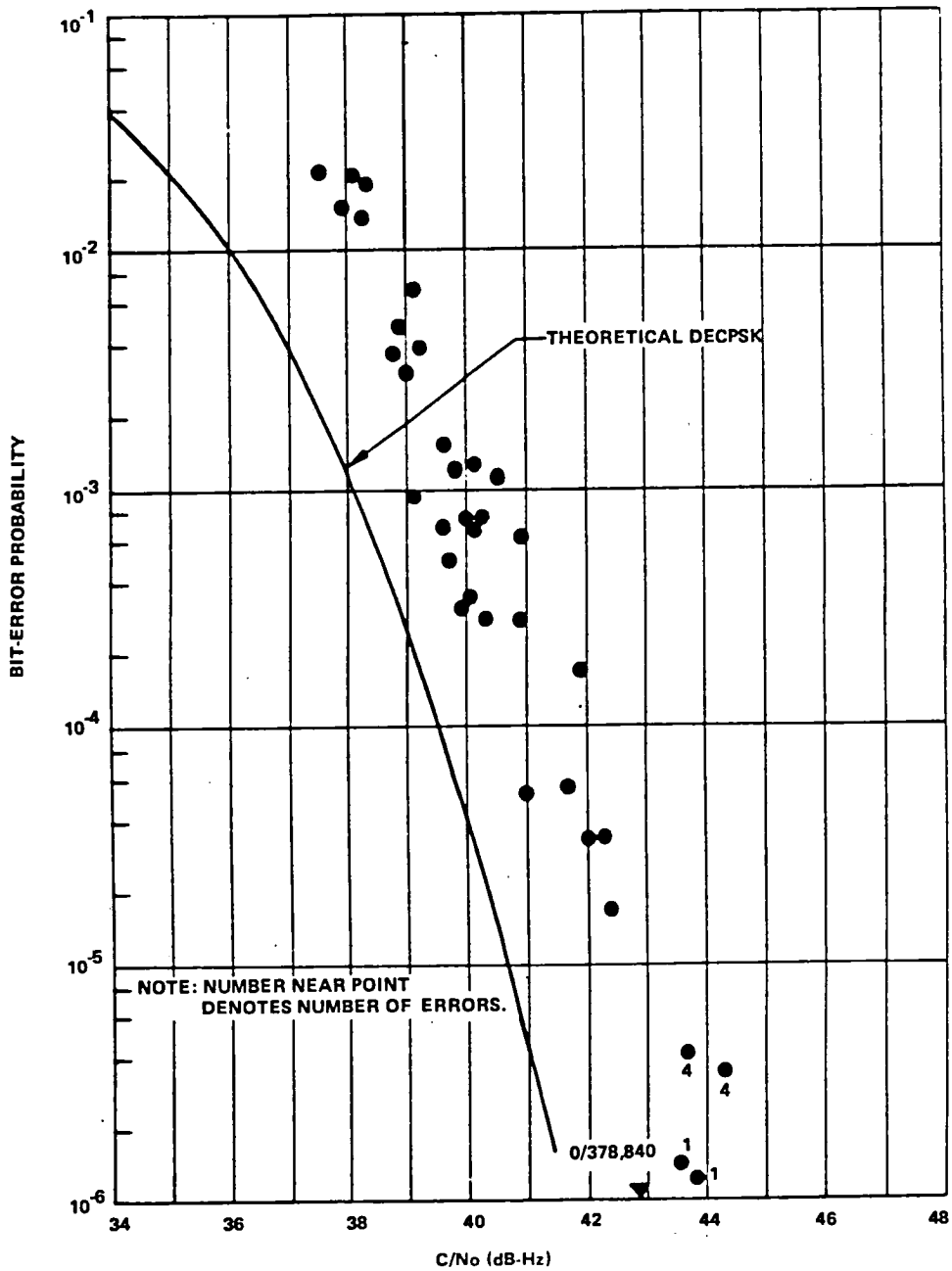

Figure 2-3. Bit-Error-Rate Performance of NASA DECPSK Demodulators, 1200 bps, Type I Tests

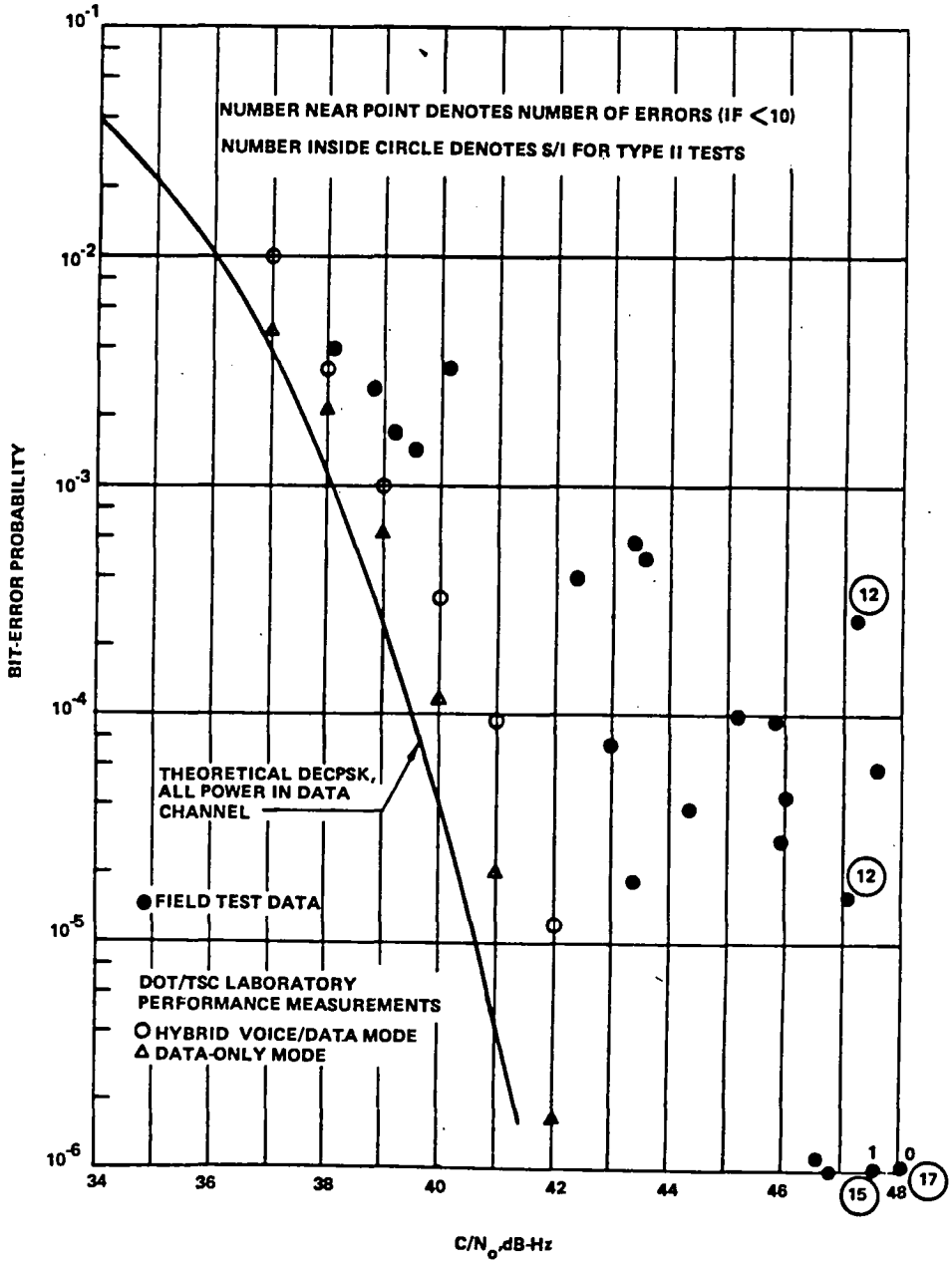

Figure 2-4. Bit-Error-Rate Performance, Hybrid No. 1 Modem, Hybrid Voice and Data Mode, 1200 bps

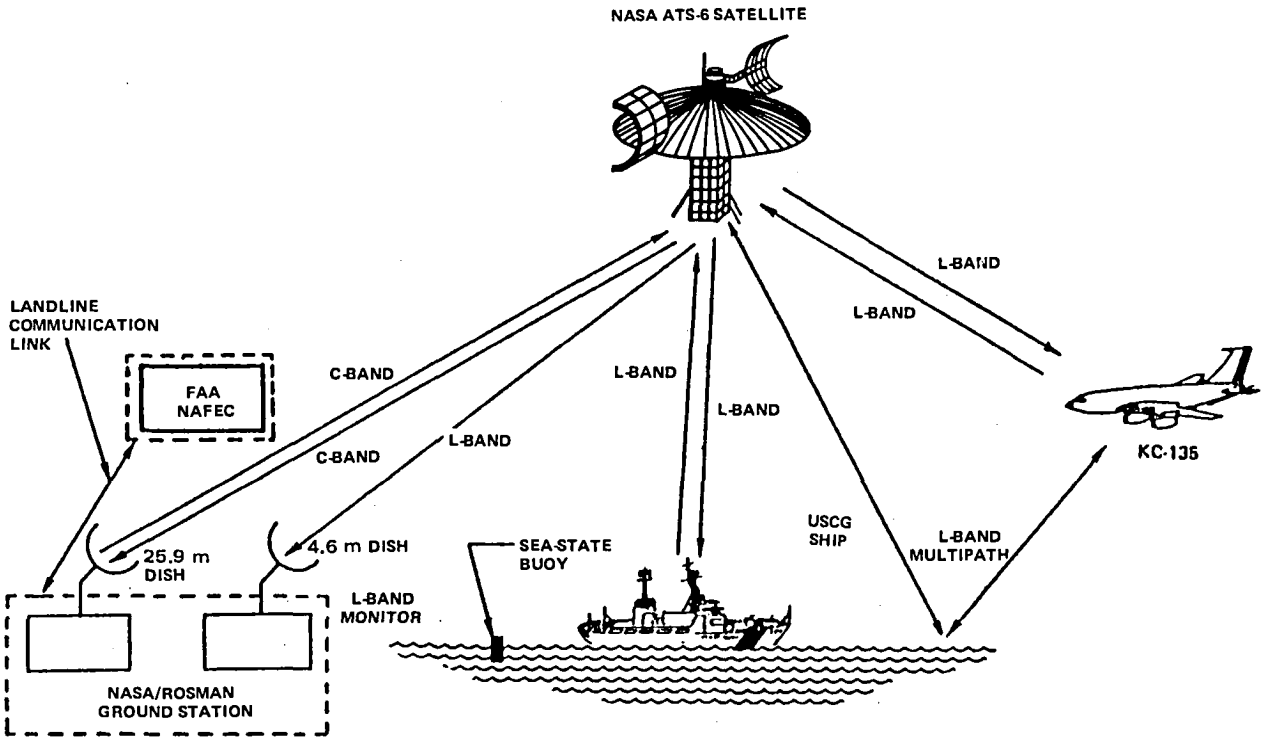

Figure 2-5. Link Configuration for DOT ATS-6 L-Band ATC Experiment and Evaluation Tests

rate obtained with Modem No. 1 are presented in Figure 2-9 as bit-error rate for values of C/N_o. Theoretical curves are exhibited in the above figure to allow a comparison with the data obtained.

Simultaneous transmission of voice and data was performed with the Hybrid No. 1 modem with the results presented in Figure 2-10. The graph exhibits the effect of the data bit-error rate for values of C/N_o when the modem was operated in a hybrid mode. A theoretical performance curve is shown on the graph for a DECPSK modulation to allow a comparison with the measured data.

Multipath Characteristics

Multipath tests were performed in a forward link from the KC-135 aircraft to ATS-6 and then relayed to the Rosman Ground Station. Three pseudo-noise (PN) codes on different L-band frequencies were transmitted from the aircraft over two types of surfaces, the U.S. land (ConUS) and the Atlantic Ocean. The primary parameters that were measured for oceanic multipath tests are presented in Table 2-2 and for that over the land (United States) are listed in Table 2-3.

Aircraft Antenna Evaluation

This experiment provided performance characteristics of three types of antennas mounted on the KC-135 aircraft in an L-band communications link from the aircraft to ATS-6 and to the Rosman

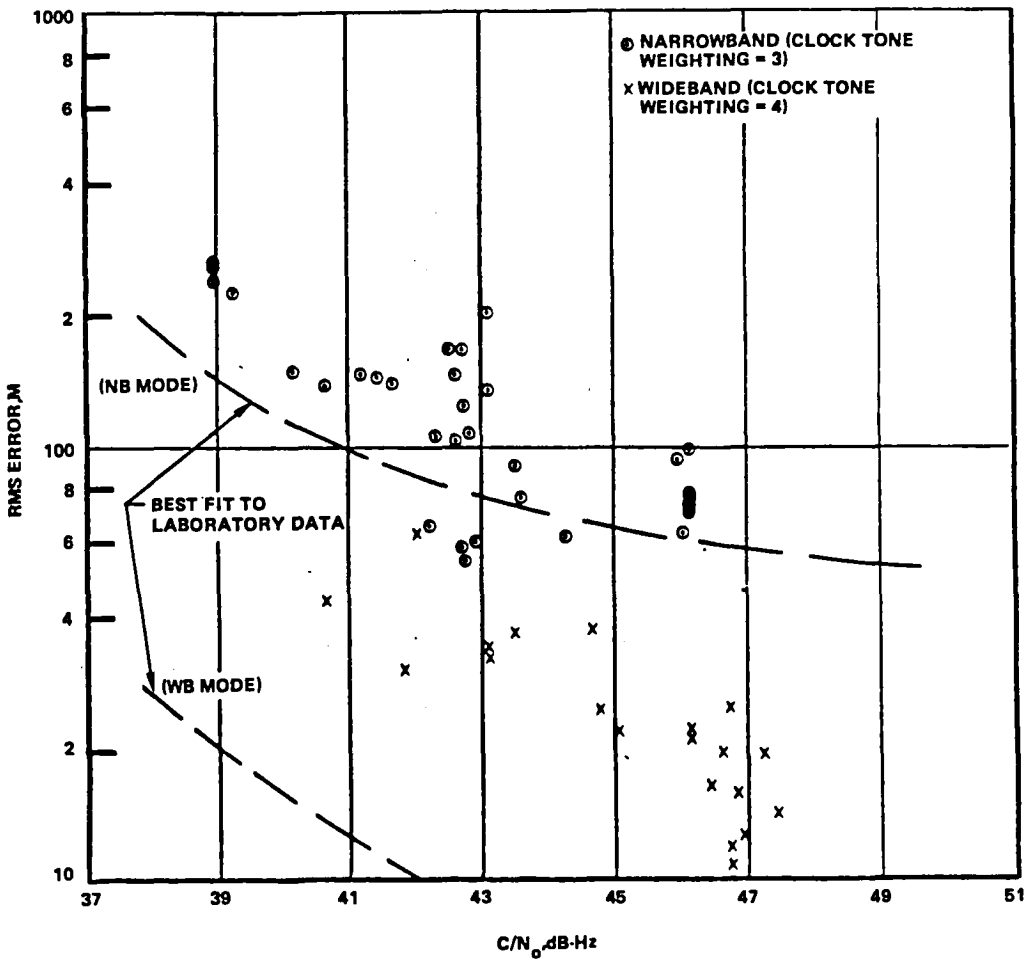

Figure 2-6. RMS Error Performance, TSC Ranging Modem, Type I Tests

Ground Station. The antennas used in this test consisted of a three-element slot-dipole, a phased array, and a patch antenna. The primary parameters that were measured that determine the performance of the antenna are the gain and the multipath interference ratio signal interference (S/I). For the three antennas, the measured parameters are as follows:

1. Slot-Dipole Antenna

   Gain = >4 dB
   S/I = >20 dB

2. Phased Array Antenna

   Gain = 11 to 12 dB peak
   S/I = >20 dB

3. Patch Antenna

   Gain = 3.7 dB
   S/I = 13 dB

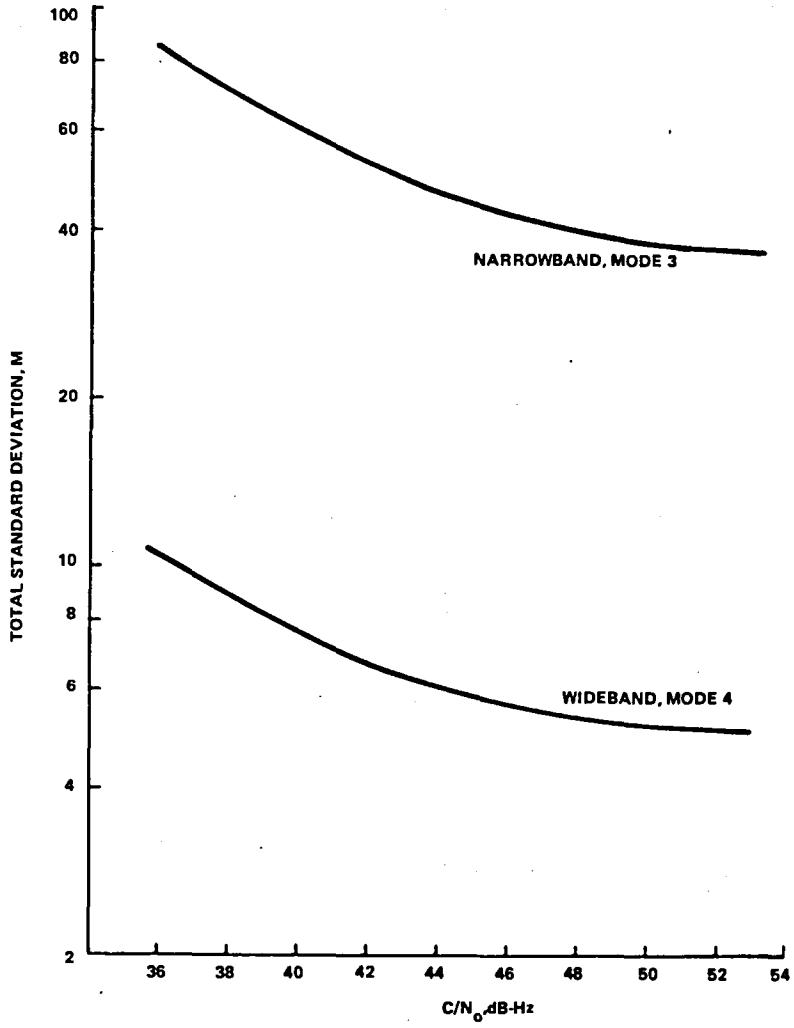

Figure 2-7. Theoretical RMS Range Error, TSC Ranging Modem, Additive Gaussian Noise Channel

DEPARTMENT OF TRANSPORTATION/FEDERAL AVIATION ADMINISTRATION ATC TESTS

The Department of Transportation/Federal Aviation Administration (DOT/FAA) conducted air traffic control (ATC) L-band experiments with aircraft over the Atlantic Ocean. Air traffic control tests consisted of voice, real-time data, and ranging. The transmission link consisted of the FAA KC-135 aircraft, ATS-6, and the FAA National Aviation Facilities Experiment Center ground station as shown in Figure 2-5.

The method used for determining the position of the KC-135 aircraft was the PLACE ranging technique, the results of which were presented previously.

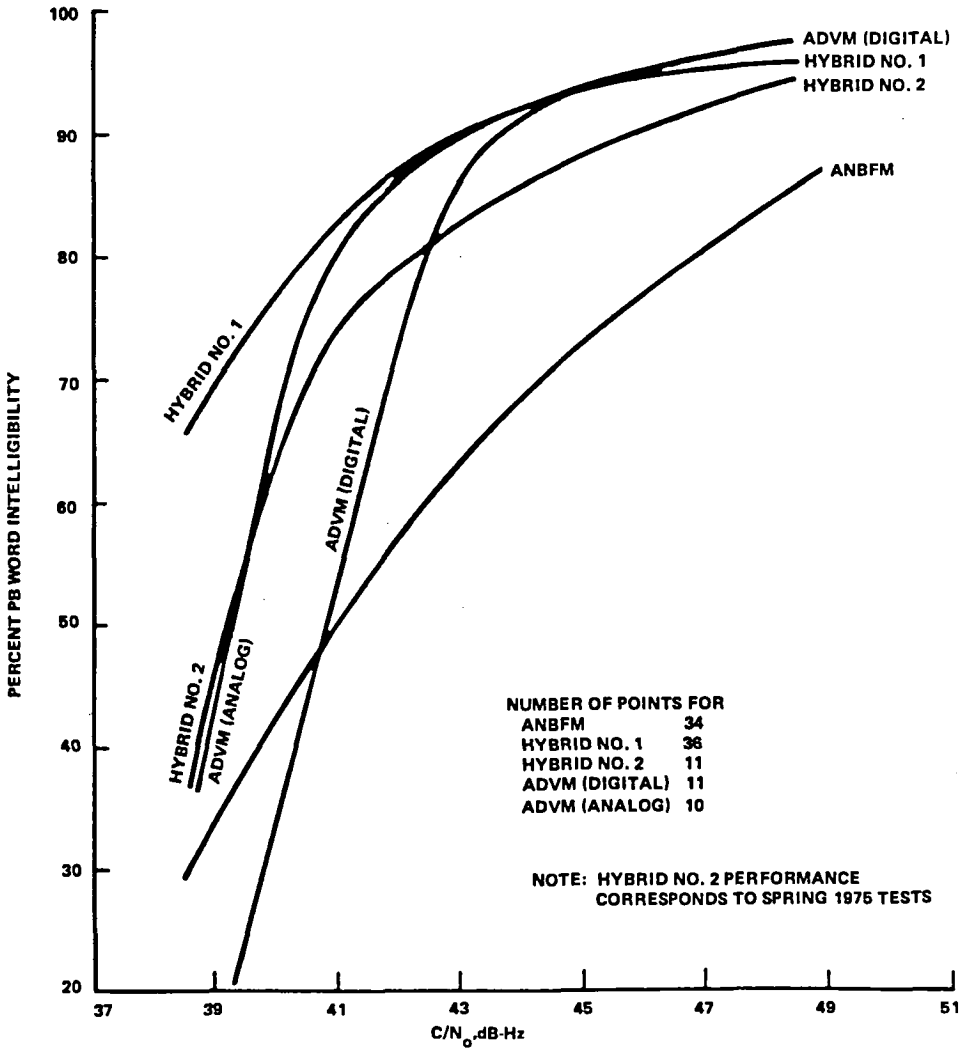

Figure 2-8. Summary Comparison of Voice Modem Performance, Type I Tests

Two-way voice only communications tests were conducted resulting in good quality operational performance. Variations in performance occurred only during aircraft maneuvers that were caused by the aircraft and ATS-6 antenna pattern effects. The results measured during this demonstration showed an average C/N_0 value of 43 dB-Hz.

Digital data only communications was demonstration at the 1200 bps rate. For a number of messages transmitted over a period of time, 88 percent of them were successfully received. Results of the data communications was considered of good quality and reliability.

CANADIAN AERONAUTICAL TESTS

The Canadian Government conducted L-band aeronautical tests by using their Jetstar aircraft, ATS-6, and their ground station located in Ottawa, Canada. The tests performed consisted basically

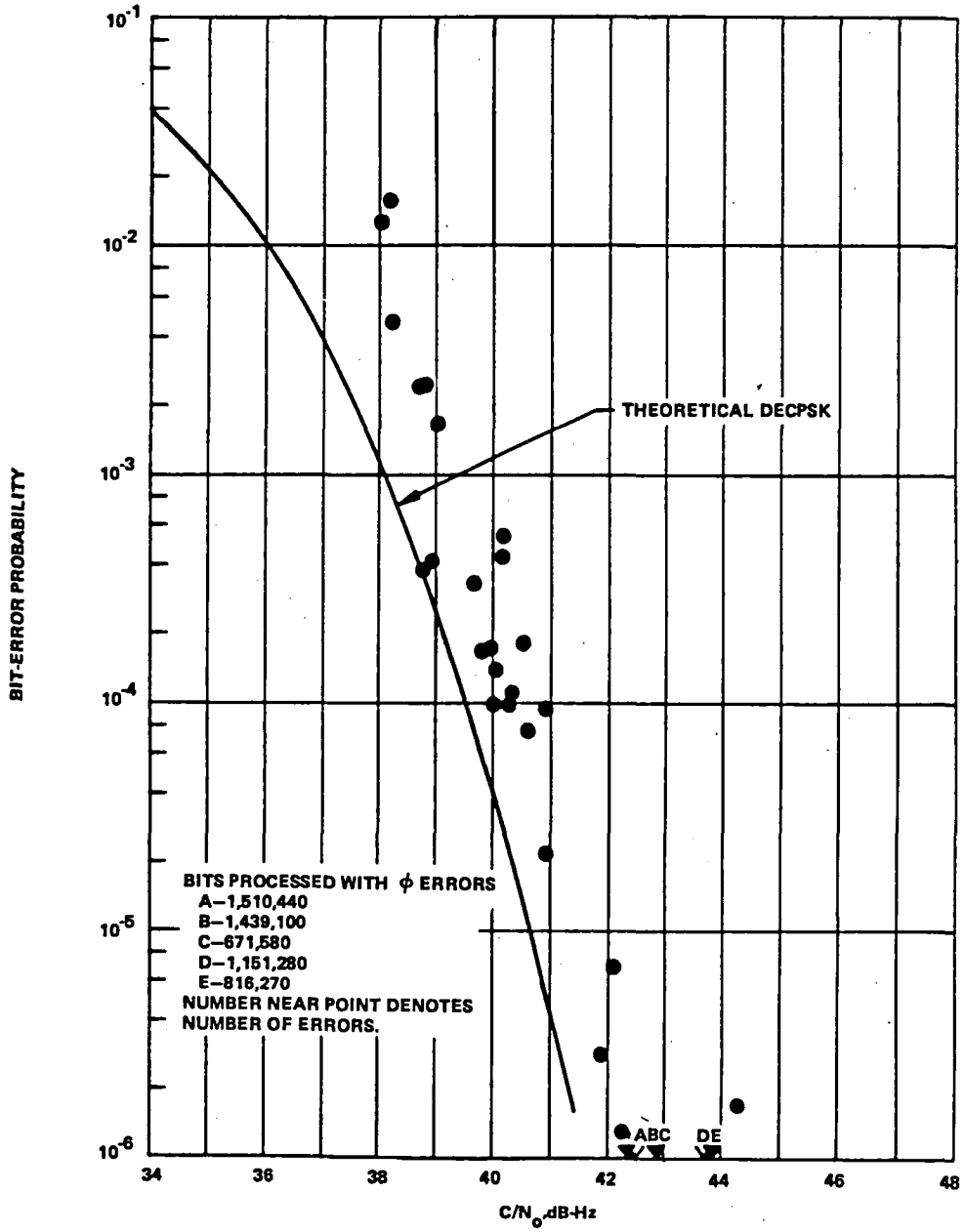

Figure 2-9. Bit-Error-Rate Performance at Hybrid No. 1 DECPSK Demodulator, 1200 bps, Type I Tests

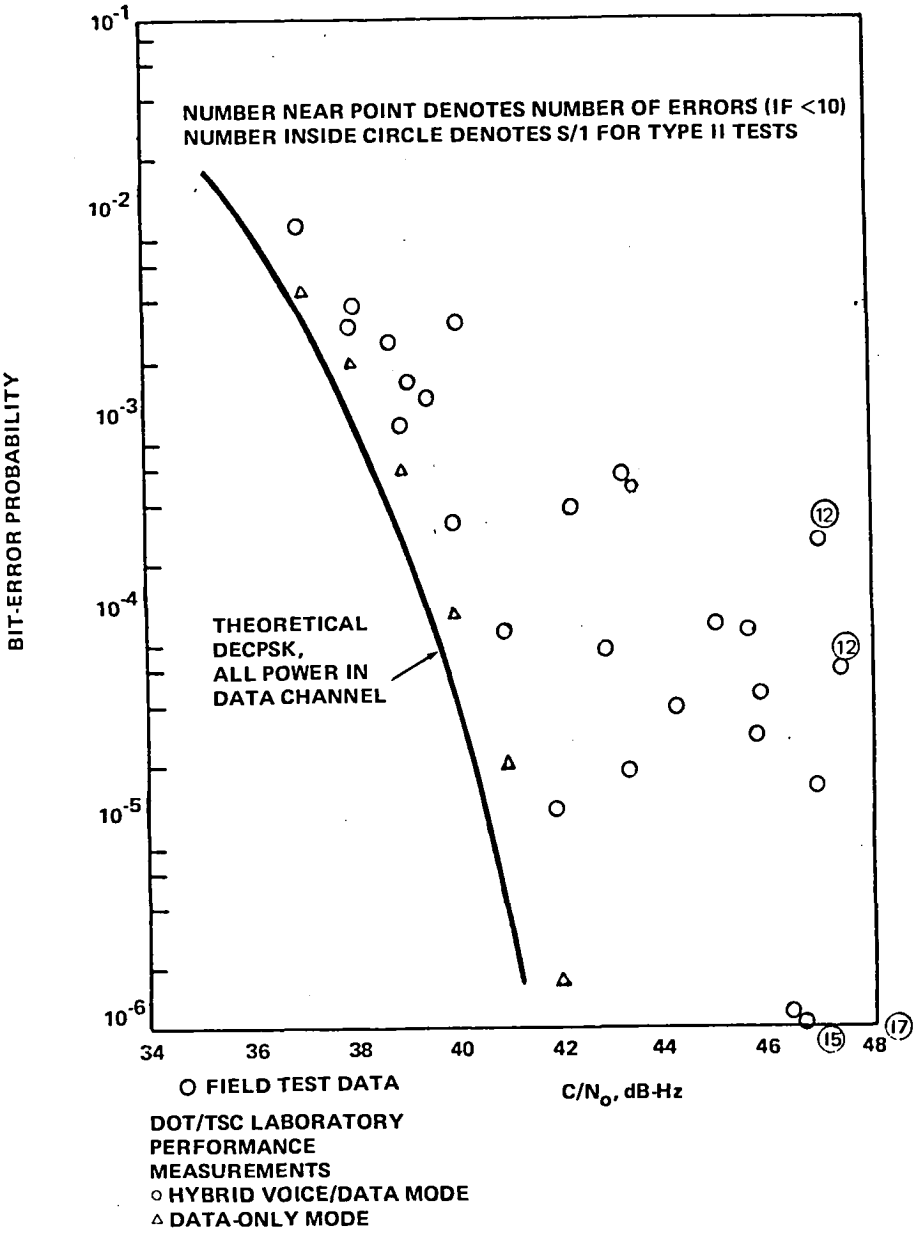

Figure 2-10. Bit-Error-Rate Performance, Hybrid No. 1 Modem, Hybrid Voice and Data Mode, 1200 bps

Table 2-2
Summary of Selected Oceanic Multipath Parameter Measured Values

Parameter	Notes	Measured Range	Typical Value at Grazing Angle Specified		
			8°	15°	30°
RMS scatter coefficient (horizontal polarization)	b	-5.5 to -0.5 dB	-2.5 dB	-1.0 dB	-1.0 dB
RMS scatter coefficient (vertical polarization)	a	-15.0 to -2.5 dB	-14.0 dB	-9.0 dB	-3.5 dB
Delay spread	b				
3-dB value		0.25 to 1.8 μsec	0.6 μsec	0.8 μsec	0.8 μsec
10-dB value		2.2 to 5.6 μsec	2.8 μsec	3.2 μsec	3.2 μsec
Coherence bandwidth (3-dB value)	b	70 to 380 kHz	160 kHz	200 kHz	200 kHz
Doppler spread (in-plane geometry)	c				
3-dB value		4 to 190 Hz	5 Hz	70 Hz	140 Hz
10-dB value		13 to 350 Hz	44 Hz	180 Hz	350 Hz
Doppler spread (cross-plane geometry)	c				
3-dB value		79 to 240 Hz	79 Hz	110 Hz	190 Hz
10-dB value		180 to 560 Hz	180 Hz	280 Hz	470 Hz
Decorrelation time (3-dB value)	d	1.3 to 10 msec	7.5 msec	3.2 msec	2.2 msec

[a]Strong dependence on grazing angle, especially near Brewster angle
[b]No strong grazing-angle dependence
[c]Strong grazing-angle dependence
[d]Strong inverse dependence on grazing angle
[e]At 10° grazing angle.

Table 2-3
Summary of Measured ConUS Multipath Parameters

Parameter	Measured Range	Typical[a] Value
RMS scatter coefficient (horizontal polarization)	-18 to +2 dB	-9 dB
RMS scatter coefficient (vertical polarization)	-21 to -3 dB	-13 dB
Delay spread (3-dB)	0.1 to 1.2 μsec	0.3 μsec
Delay spread (10-dB)	0.2 to 3.0 μsec	1.2 μsec
Coherence bandwidth (3-dB)	150 kHz to 3.0 MHz	600 kHz
Doppler spread (3-dB)	20 to 140 Hz	60 Hz
Doppler spread (10-dB)	40 to 500 Hz	200 Hz
Decorrelation time (3-dB)	1 to 10 msec	4 msec

[a]Grazing angle dependencies (if any) masked by nonstationary properties.

of two types: the voice only modem test for three modulation modes, and the aircraft antenna performance test.

Modulation modes used for the voice tests were provided by the adaptive narrowband frequency modulation (ANBFM) modem, the pulse duration modulation (PDM) modem, and the pulse zero crossing (PZC) modem. All three modems gave good voice operational performance and the results are presented in Table 2-4. A relatively high percentage of word intelligibility is indicated for the measured C/N_o in the table.

The aircraft phased array antenna patterns were measured by flying the aircraft through fixed bank circles at different satellite elevation angles. From the measured data, an antenna gain of greater than 7 dB was established, which is well within the design specifications. This antenna gain varied with elevation angle of the aircraft to the satellite. A 6-dB change in gain was measured for an elevation angle change from 9 degrees to 20 degrees.

EUROPEAN SPACE AGENCY AERONAUTICAL TESTS

The European Space Agency (ESA) participated in the integrated L-band experiments by using a communications link consisting primarily of their aircraft Comet IV, ATS-6, and the FAA NAFEC ground station in Atlantic City, New Jersey. One other facility, the NASA Rosman Ground Station, was also involved during the ESA aeronautical tests. A configuration for this system is presented in Figure 2-11.

The PLACE ranging technique, using tone frequencies, was used in determining the position location of the ESA aircraft Comet IV. Ranging tones using DSB/AM modulation and 600 bps digital data phase shift keying (PSK) modulated in phase quadrature were transmitted on a single carrier. The results of a number of ranging tests are presented in Table 2-5 where the standard deviation in meters is given for its corresponding C/N_o.

Table 2-4
Voice Intelligibility Results MART Test–(Canadian)

Modem	Modem Location	Preemphasis	C/N_o (dB-Hz)	Percent Intelligibility	Test Time (hr)
ANBFM	Aircraft	Standard	45	80	4.9
ANBFM	Ottawa	Standard	45	80.4	5.2
PDM	Aircraft	Standard	45	81.5	4.2
PZC	Aircraft		45	75.2	6.7
PZC	Ottawa		45	81.6	4.86
ANBFM	Aircraft		42	76.7	3.7
ANBFM	Ottawa		42	74.3	3.86

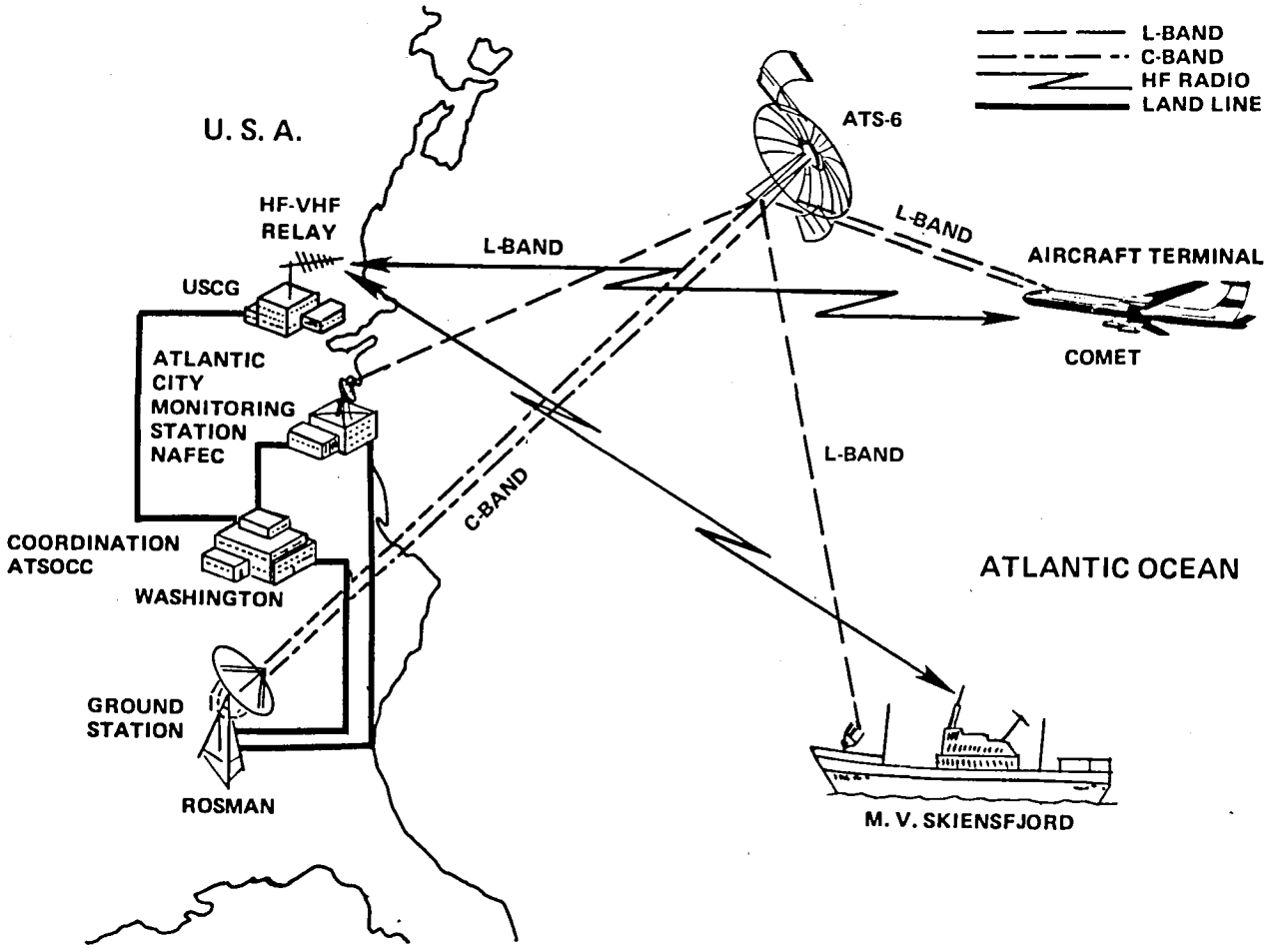

Figure 2-11. ESA Experimental Configuration (*M. V. Skiensfjord*)

Voice transmission tests were performed using narrowband frequency modulation (NBFM) and digital companded delta/PSK modulation at a 19.2-kbps rate. Results of the above two voice modulation techniques are shown in Figures 2-12 and 2-13. The data are presented as a percent of the phonetically balanced intelligibility of words against the C/N_o values. For an articulation index of 0.6, which is an Aerostat system requirement, an intelligibility of 95 percent is obtained for NBFM at a C/N_o of 47 dB-Hz, and for delta modulation, a C/N_o of 44 dB-Hz.

Digital data transmission tests were performed consisting of pseudorandom coded data at a 1200 bps rate and DECPSK modulated on the carrier. The results of this test are presented in Figure 2-14 as bit-error rates (BER) for a range of C/N_o values and for elevation angles from 10 to 15 degrees. Both the Rayleigh and the Gaussian BER are shown in the graph for reference purposes. The test results show that the deviation of the measured data from the laboratory measurement increases with a decrease in the signal-to-multipath interference ratio, S/I.

Table 2-5
Aircraft Ranging Results–PLACE Tones

Day	Elevation Angle	Data Points Analyzed	Correlation Coefficient	Measured C/N_o (dB-Hz)	Range Standard Deviation (meters)
81	11.2°	32	-0.999	45	467
	9.4°	31	-0.998	44	590
	11.6°	32	-0.999	44	545
	12.6°	29	-0.999	44	344
67	7.0°	23	-0.997	47	609
	7.5°	20	-0.998	47	418
	8.0°	11	-0.992	47	654
	9.1°	19	-0.998	47	419
	9.6°	25	-0.997	47	664
	9.6°	28	-0.998	48	705
	8.5°	39	-0.999	48	850

DOC/MARAD MARITIME TESTS

The Department of Commerce/Maritime Administration (DOC/MarAd) conducted maritime tests over a link consisting of the ships *American Ace* and the *Lash Atlantico*, ATS-6, and the National Maritime Research Center (NMRC) ground station located at Kings Point, New York. In voice communications, three types of modulation were used consisting of narrowband frequency modulation (NBFM), companded frequency modulation and pulse duration modulation (PDM). With both ships using NBFM, the mean phonetically balanced (PB) word intelligibility of 85 percent was obtained for a C/N_o range of 46 to 53 dB-Hz. When the ship *American Ace* used companded frequency modulation, good quality voice was achieved for C/N_o values from 50 to 68 dB-Hz. With the AII Systems voice modems employed in both ships, the results of the word intelligibility obtained is presented in Table 2-6. All of the scheduled pulse duration modulation (PDM) voice modem tests were not complete, because of rfi problems caused by high power hf transmitters in the vicinity.

The ship *American Ace* performed digital data tests using modems having frequency shift keying (FSK) and phase shift keying (PSK) modulation at 1200 and 4800 bps rates. Test results showed that a 3 dB higher C/N_o was required than expected to achieve the desired bit-error rates. Digital data tests were also performed by the ship *Lash Atlantico* using the modem having differentially encoded PSK (DECPSK) modulation at 1200 to 9600 bps rates. Results of these tests were in poor agreement with the theoretical performance. With the AII Systems digital data modem used in both ships, the transmission performance is presented in Figure 2-15 as bit-error rate against values of

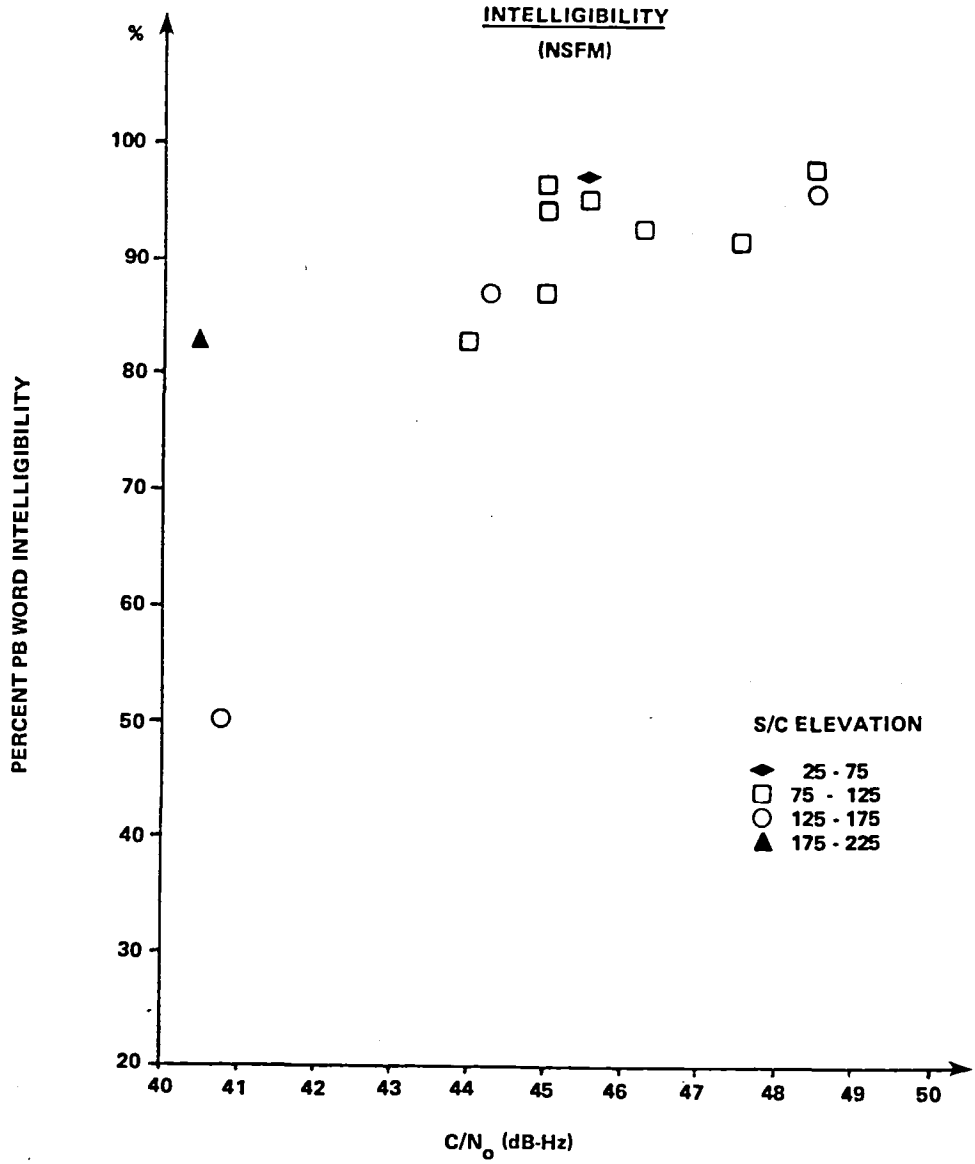

Figure 2-12. Voice Performance Using NBFM

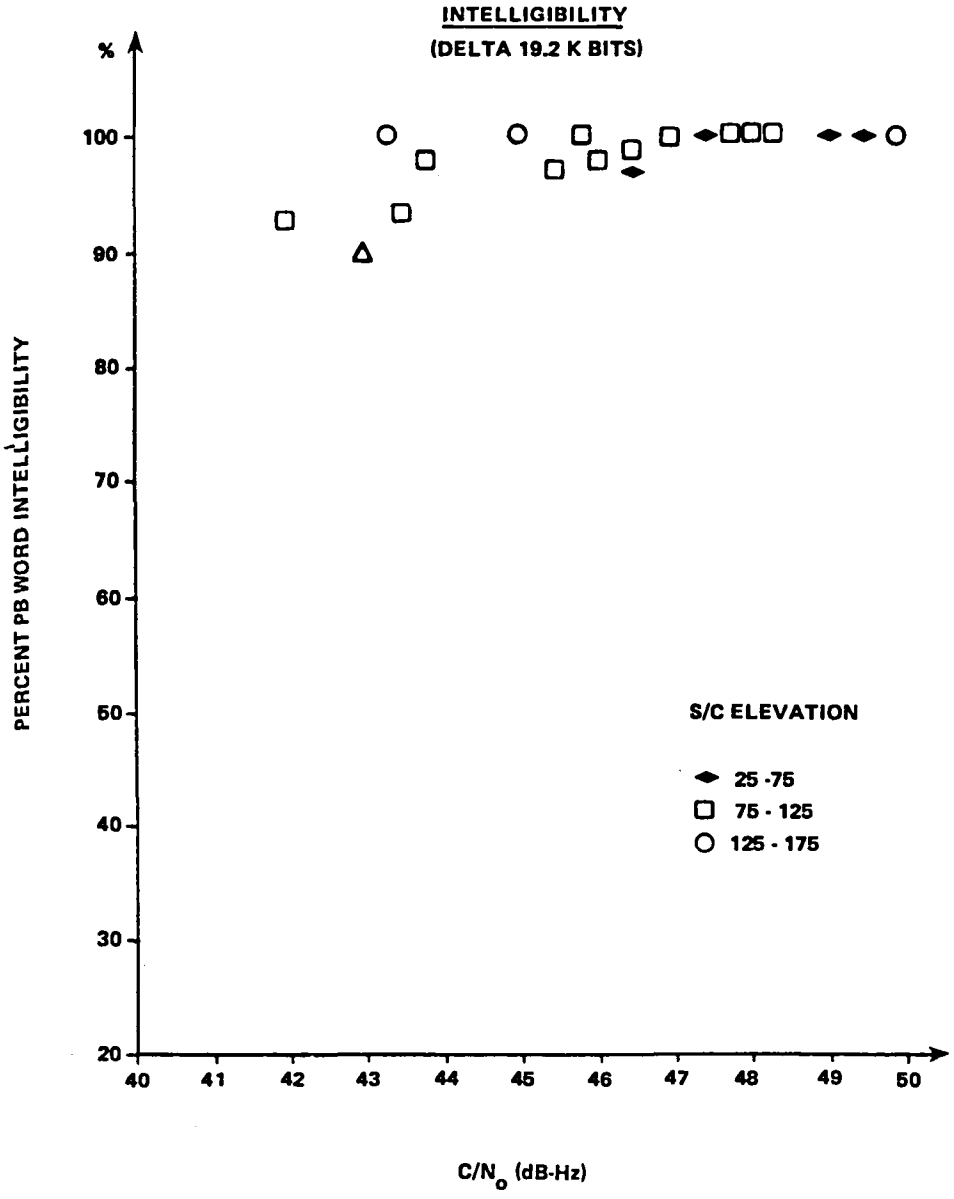

Figure 2-13. Voice Performance Using Companded Delta/PSK Modulation

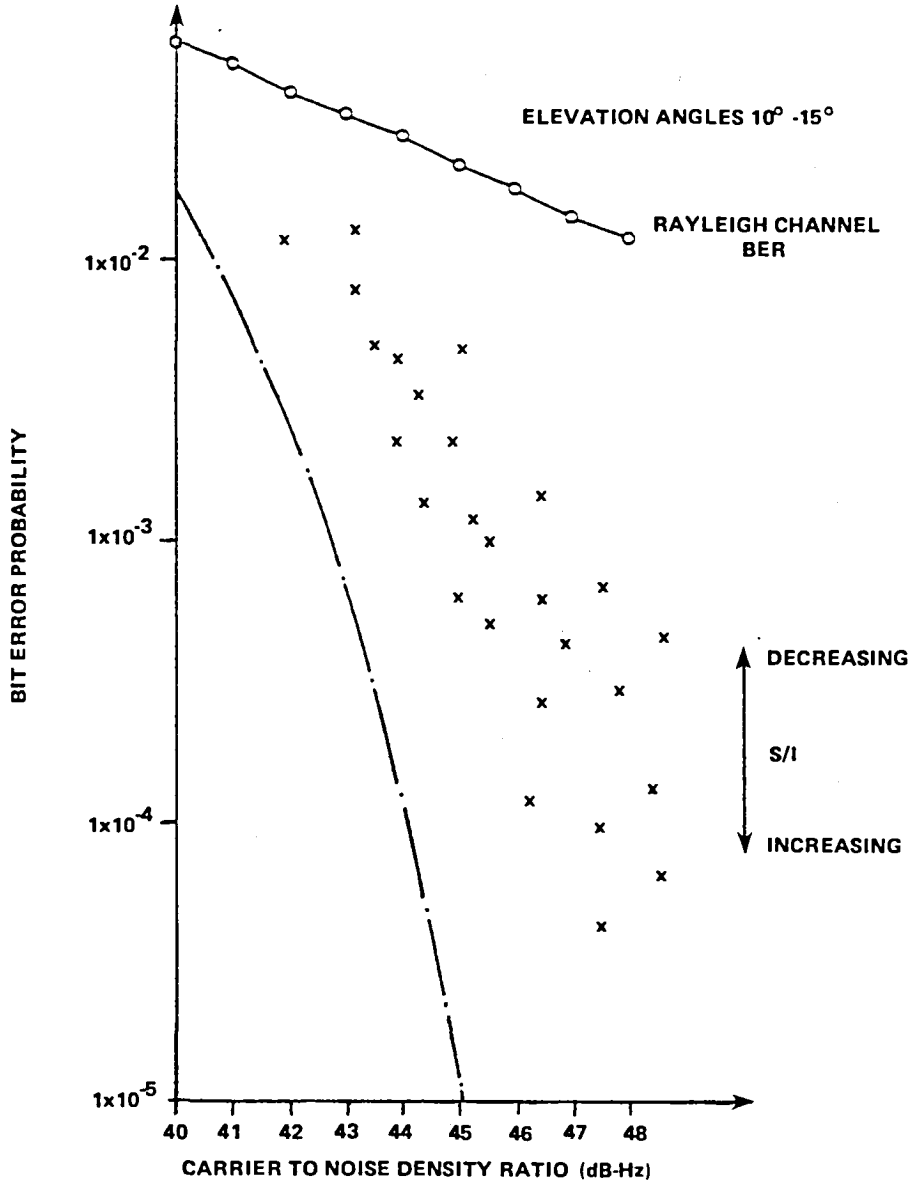

Figure 2-14. Digital PN Coded Data Performance at 1200 bps Using DECPSK Modulation

Table 2-6
Results of PB Word Intelligibility Tests on AII Systems Voice Modem for Calm Sea State

Test No.	Voice Transfer Route	Ship	Mean PB Word Score						C/N_o (dB-Hz)	El ( )°	Az ( )°	Hd ( )°	Date
			Composite		Male		Female						
			Score	σ	Score	σ	Score	σ					
13	MCC to Ship	Lash	93.5	2.1	94.4	1.0	92.6	2.7	53	49	207	67	10/29/74
14	MCC to Ship	Lash	96.7	1.9	98.3	0.7	96.1	1.2	50	44	211	34	10/31/74
15	MCC to Ship	Lash	91.6	4.6	95.6	2.0	87.7	1.9	46	49	207	67	10/29/74
19	MCC to Ship	Ace	93.3	4.4	97.2	2.0	89.4	0.9	50	13	246	72	9/20/74
21	Ship to MCC	Lash	84.7	7.3	91.3	1.9	78.2	2.6	53	44	211	34	10/31/74
22	Ship to MCC	Lash	84.8	8.3	92.2	2.4	77.4	2.8	50	44	211	34	10/31/74
27	Ship to MCC	Ace	90.9	4.4	93.2	3.3	86.9	3.0	50	13	246	72	9/20/74
27A	Ship to MCC	Ace	89.7	5.0	91.4	4.6	88.0	5.4	50	6	250	264	10/31/74

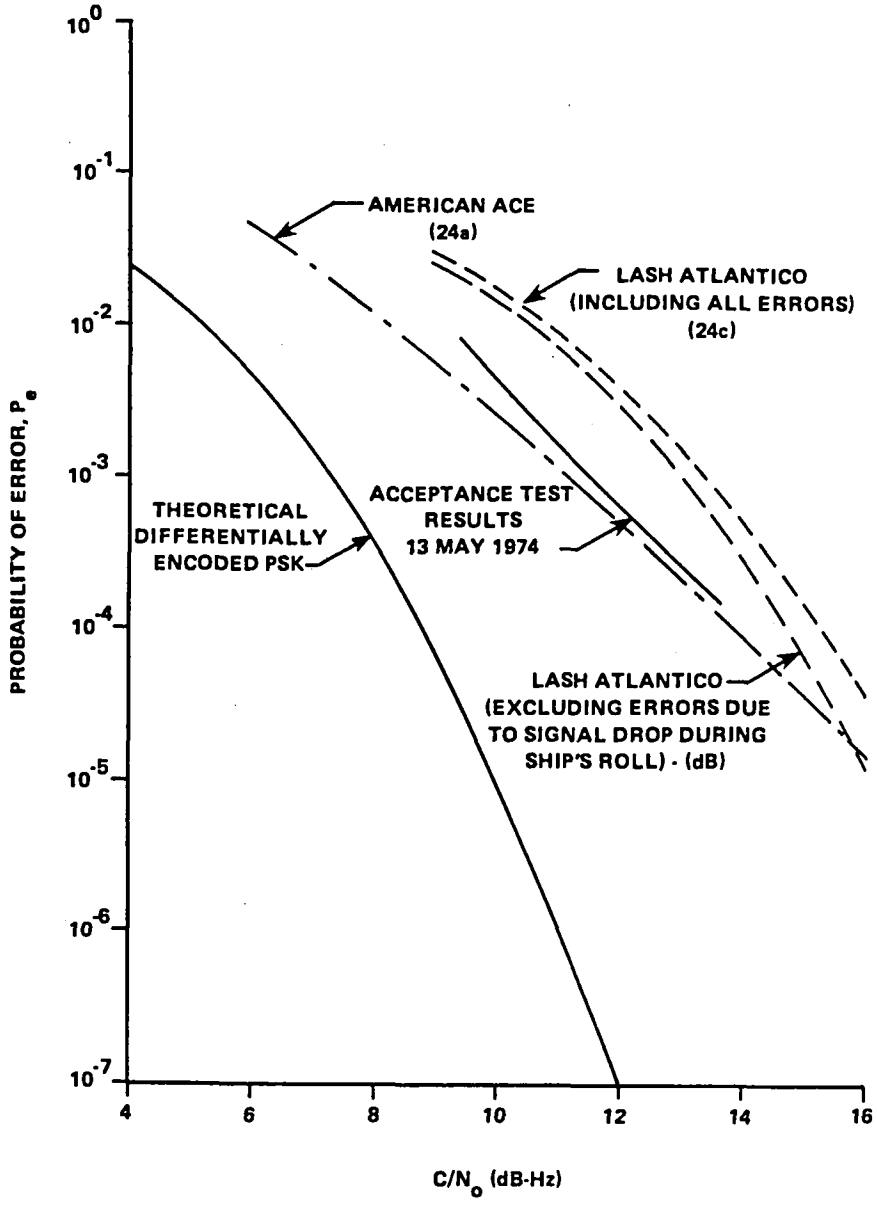

Figure 2-15. MCC to ATS-6 to Ship Performance of All Systems Data Modem (1099 bps)

C/N_o for a bit rate of 1099 bps. A theoretical curve is plotted on the graph for a comparison with the measured data.

The position location test with the ship *American Ace* was performed with only partially successful results. Mean deviations between MarAd and onboard ship computations of the ship's position were roughly from 13 to 39 nautical miles (nmi) in latitude and 17 to 27 nmi in longitude. Also the standard deviation of latitude varied from 0.3 to 5.1 nmi and in longitude varied from 0.7 to 5.2 nmi.

DEPARTMENT OF TRANSPORTATION/UNITED STATES COAST GUARD MARITIME TESTS

In the maritime tests, the Department of Transportation/United States Coast Guard (DOT/USCG) participated in the integrated L-band experiments using a communications link composed of the U.S. Coast Guard cutters *Sherman* and *Gallatin*, ATS-6, and the Rosman Ground Station. The tests that were performed were similar to that of the MarAd experiments and consisted essentially of ranging for position location of ships, voice transmission, digital data transmission at a 1200 bps rate, combined voice and data transmission, and multipath effects. The test data from the ship *Sherman* are addressed in the discussion of the test results that follows.

Voice and digital data communication tests were conducted with three types of modem, two of which were hybrids and were capable of operating in modes of voice only, data only, and combined voice and data. Each hybrid modem employed differentially encoded coherent PSK modulation for data transmission. For voice transmission, one hybrid used narrowband frequency modulation (NBFM) while the other used pulse duration modulation (PDM/PSK). Both hybrid modems employed quadrature phase modulation (Q-M/PSK) when the operating mode was simultaneous voice and data transmission. The third modem provided voice only or data only modes of operation. In the voice mode, NBFM was employed and DECPSK modulation was used for the data mode.

Results in the transmission of digital data at 1200 bps rate for hybrid modem I are presented in Figure 2-16 where the bit-error rate is indicated against the carrier-to-noise power density (C/N_o) ratio. In addition to the measured data on the graph, the theoretical performance curve is plotted and three laboratory derived performance curves are shown for the conditions of different multipath effects that are indicated as carrier-to-multipath (C/M) power ratios.

Figure 2-16 shows that most of the measured data falls between the theoretical performance curve and the curve with the lowest multipath effect having a C/M ratio of 11 dB. The results shown in the figure indicate that the data transmission link was operating near optimum performance with an apparent C/M ratio in excess of 11 dB. A C/N_o of approximately 44 dB-Hz was established from the measured data for a bit-error rate of 10^{-5} bps.

Voice transmission performance was determined by conducting a phonetically balanced (PB) word test. Complete processed data from the measured voice data were not obtained: a sample of the results obtained consisted of the following:

Mean (PB) word score = 78.8 percent
Standard deviation = 7.85

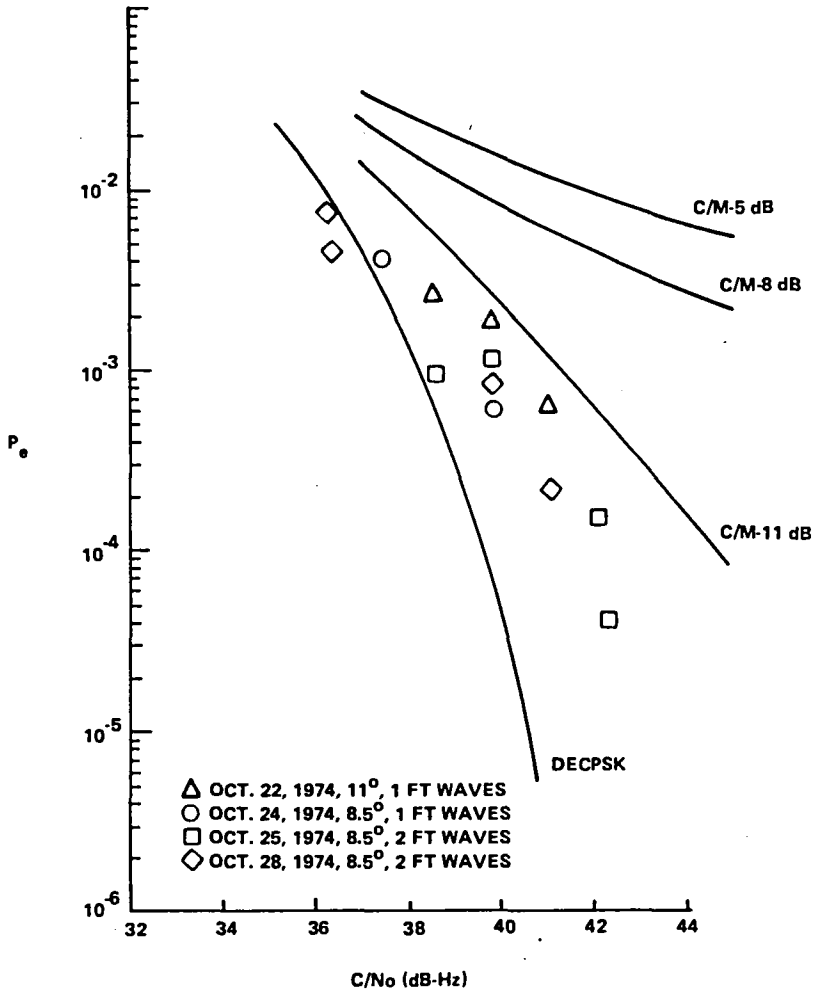

Figure 2-16. Error Performance of Hybrid I Modem at 8.5 and 11 Degrees Elevation Angle, 1200 bps Data Only

A more meaningful evaluation of the voice performance could be established if the C/N_o values were available for the corresponding percent PB word intelligibility that was measured.

Ranging tests for determining the position location of the ship *Sherman* were performed. However, the equipment needed for processing the data at that time was not completed, so that no data were obtained. Some of the variable factors affecting the ranging accuracy that were considered during the tests consisted of the inherent jitter, the multipath effects, and the motion of the ship. The parameters that were computed from the measured data of the ranging tests were as follows: The number of points accepted, the mean error in meters, the rms error in meters, and the chi-square variance.

Final results for the U.S. Coast Guard cutter *Gallatin* have not been provided; However, preliminary results indicated that the quality of the data was satisfactory.

EUROPEAN SPACE AGENCY MARITIME TESTS

The European Space Agency (ESA) conducted maritime L-band experiments by using a communications link consisting of two ships, ATS-6, and the Rosman Ground Station. The two ships involved in the ESA tests were the German ship *Otto Hahn* and the Norwegian ship *Skiensfjord* in a system configuration as shown in Figures 2-11 and 2-17.

The primary L-band tests that were performed by the ship *Otto Hahn* were composed of the tone ranging for position location, voice and digital data transmission, and multipath effects.

In the ranging measurement, the PLACE technique was used where four tone frequencies were DSB/AM and PSK modulated in quadrature phase on a single carrier. The results of this test are presented in Figure 2-18 as standard deviation range in meters against a range of C/N_o values. Data in the figure indicate an increase of standard deviation for a decrease in the elevation angle. A doubling of the standard deviation for a 6-dB decrease in the signal-to-noise (S/N) ratio was established from the data.

Two techniques of voice transmission were performed. One was the narrowband frequency modulation (NBFM) and used preemphasis/deemphasis of 6 dB per octave. The second voice system was digital companded delta modulation at a 19.2 kbps rate and PSK modulated onto the carrier. Results of the two voice modulation techniques are presented in Figures 2-19 and 2-20 respectively as the percent of word intelligibility against a range of C/N_o values. From the data, it was established that for an articulation index of 0.6, the word intelligibility of both systems was 95 percent for NBFM at a C/N_o of 48 dB-Hz and a C/N_o of 45 dB-Hz for delta modulation.

Digital data transmission tests were performed using pseudonoise (PN) random coded data at a 1200 bps rate and PSK modulated on the carrier. Results of this test are shown in Figure 2-21 with bit-error-rate probability plotted against C/N_o values, including a laboratory measured curve for performance comparison.

The L-band tests performed by the Norwegian ship *Skiensfjord* consisted essentially of voice and digital transmission similar to that performed by the ship *Otto Hahn*. Voice transmission was performed by narrowband frequency modulation.

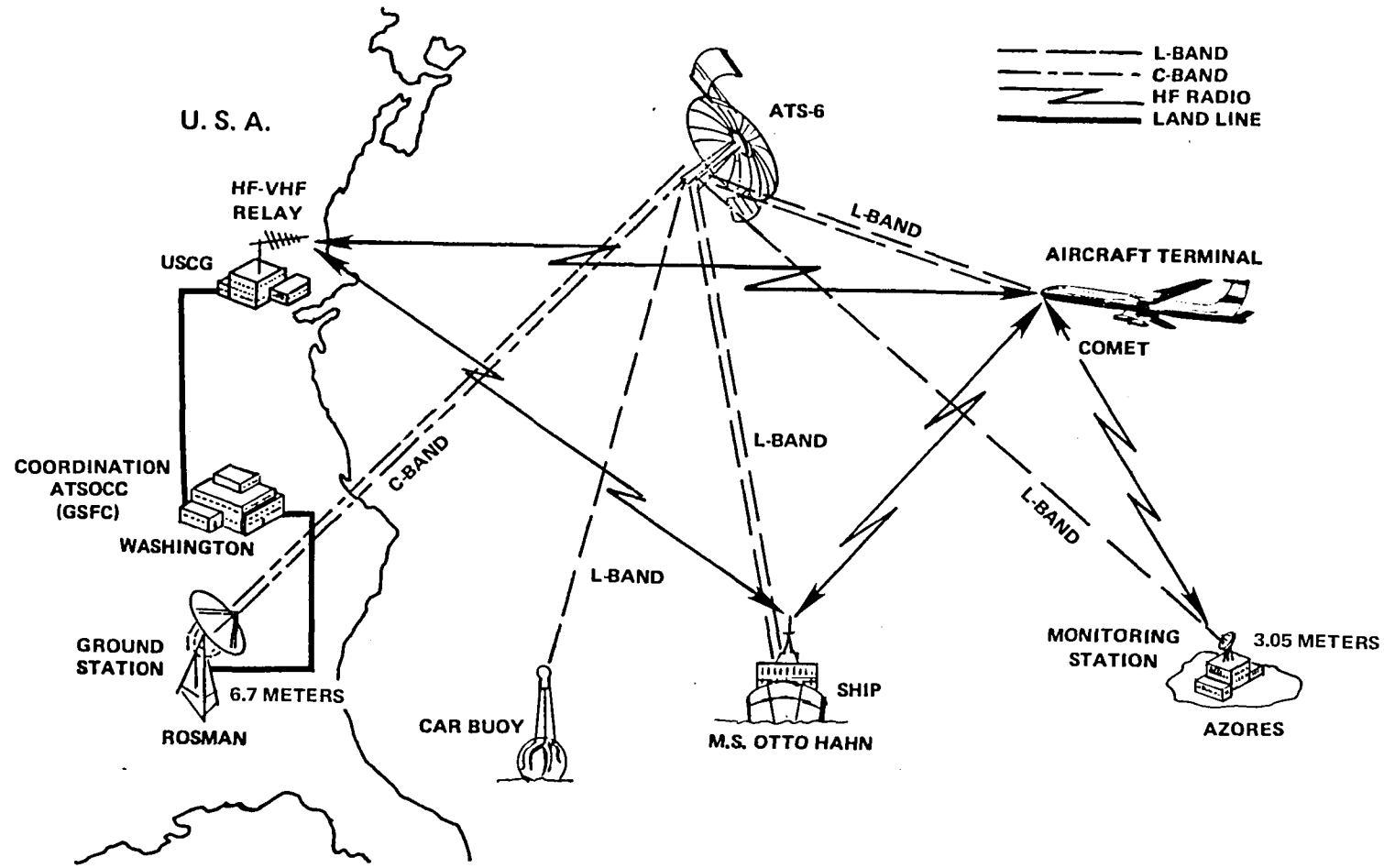

Figure 2-17. ESA Experimental Configuration (*M. S. Otto Hahn*)

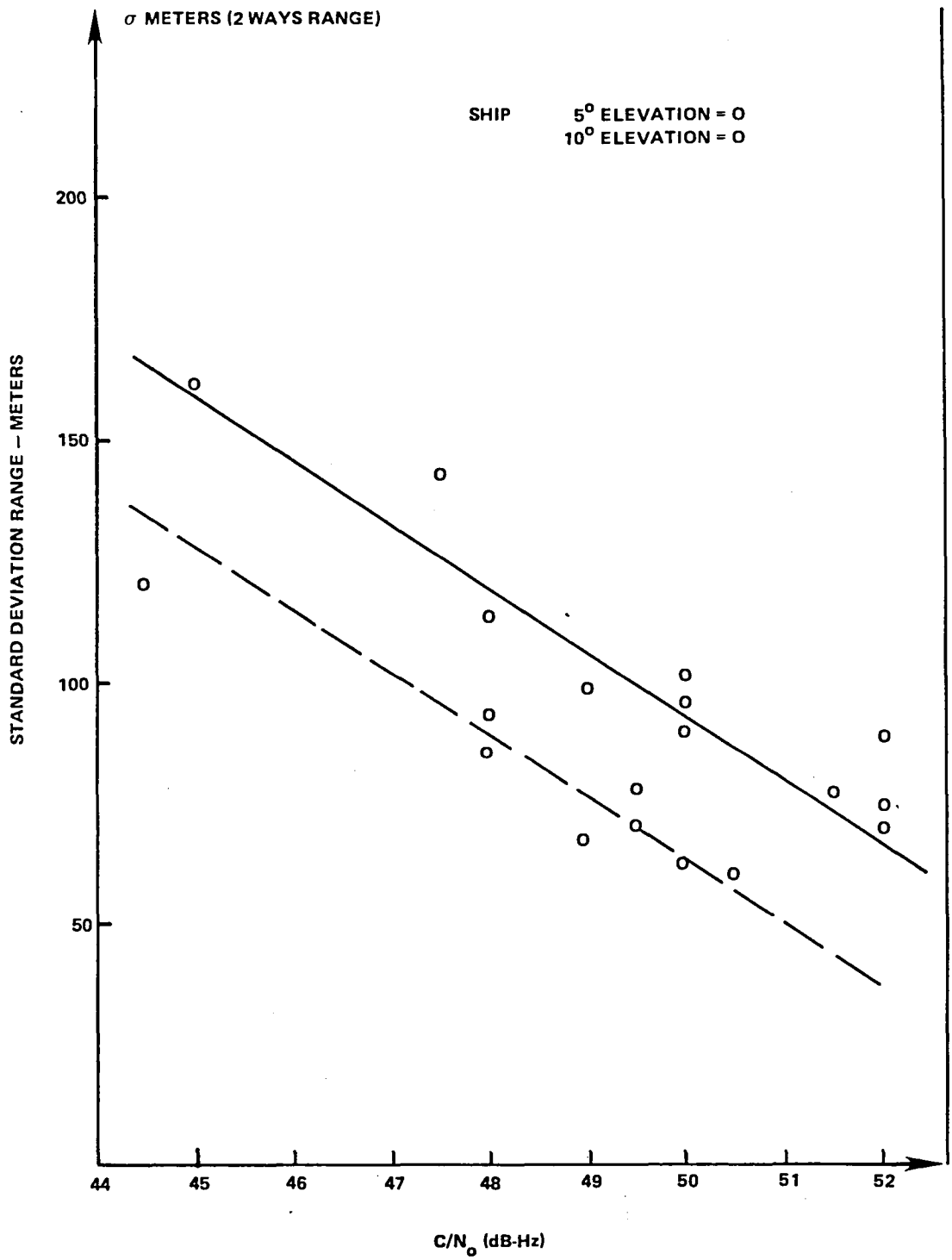

Figure 2-18. Ranging Results

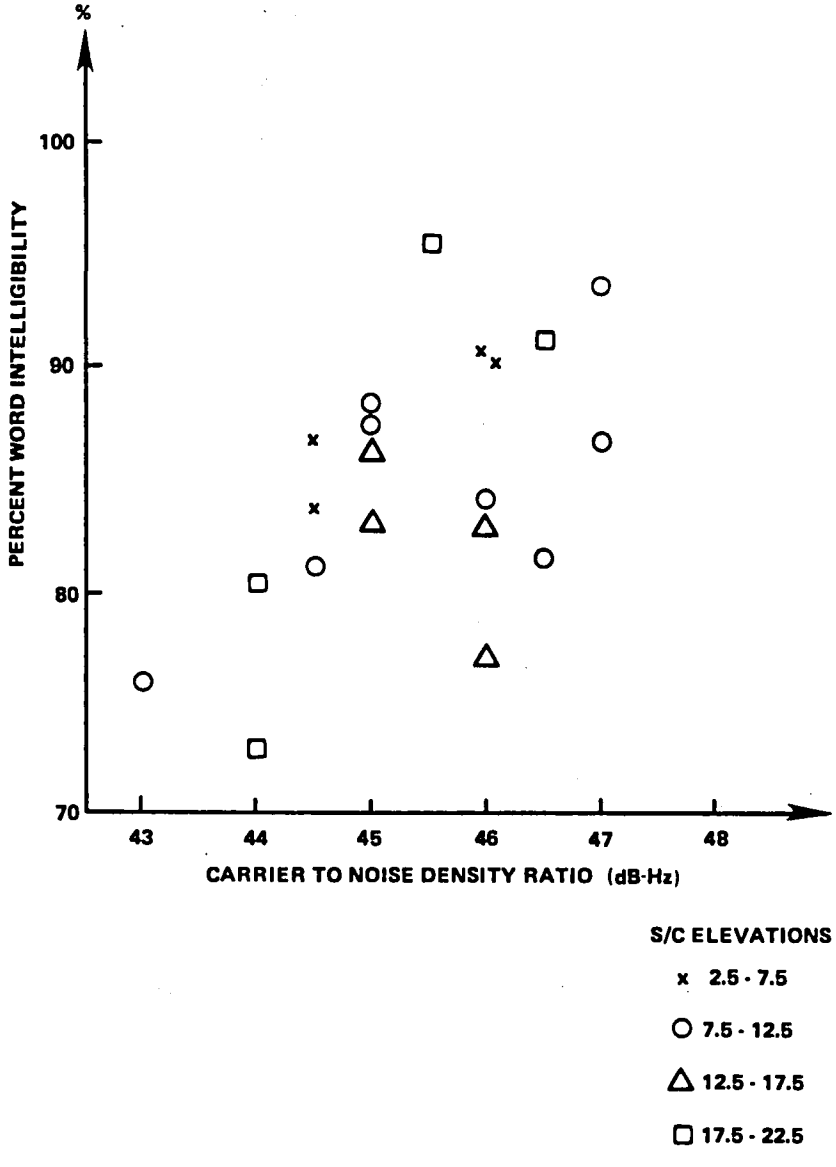

Figure 2-19. PB Words (NBFM)

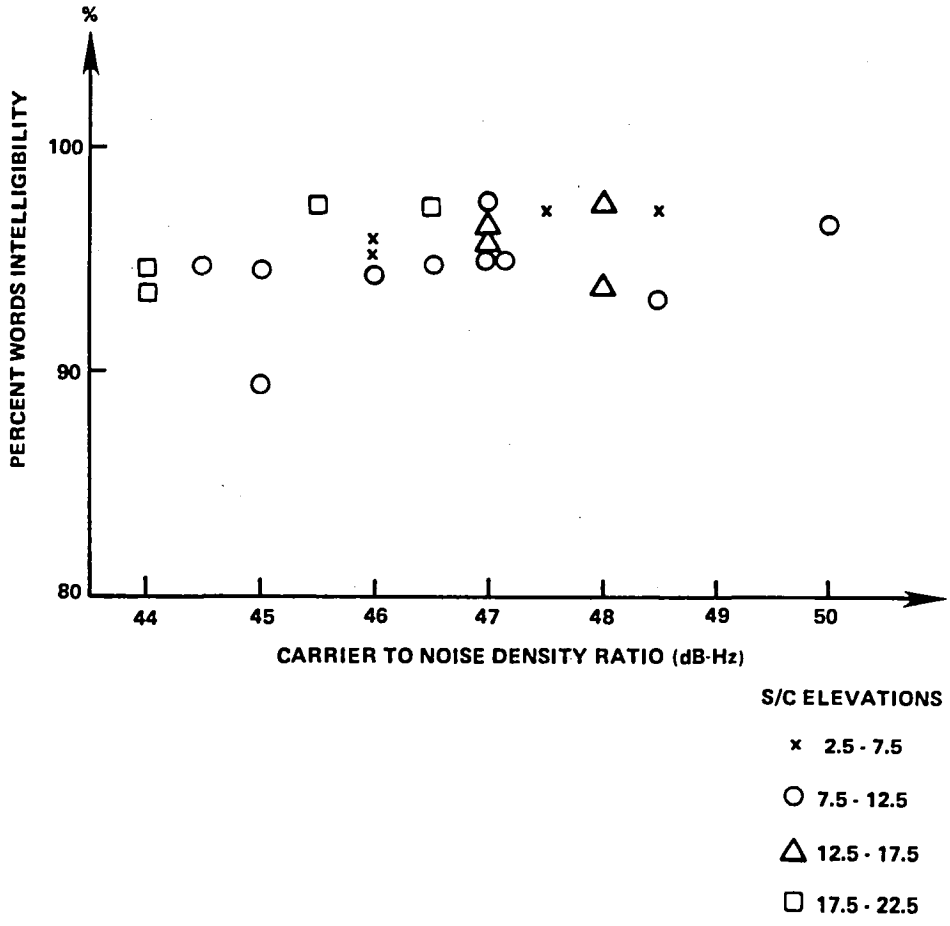

Figure 2-20. PB Words (Delta)

Digital data was transmitted by using pseudonoise (PN) random coded data at a rate of 1200 bps and PSK modulated on the carrier.

No received data on the voice reception performance was obtained.

Results for the digital data transmission are presented in Figure 2-22 as percent probability against the received carrier input level for an elevation angle of 16 degrees. From the data a mean signal level of -127.5 dBm, a standard deviation of 0.7 dB, and bit-error rate of 1.7×10^{-4} was established.

EUROPEAN SPACE AGENCY DISTRESS BUOY SYSTEM TESTS

The European Space Agency conducted L-band communications experiments with a distress ocean buoy that was supported by the ship *Otto Hahn*, ATS-6, and the Rosman Ground Station. The data

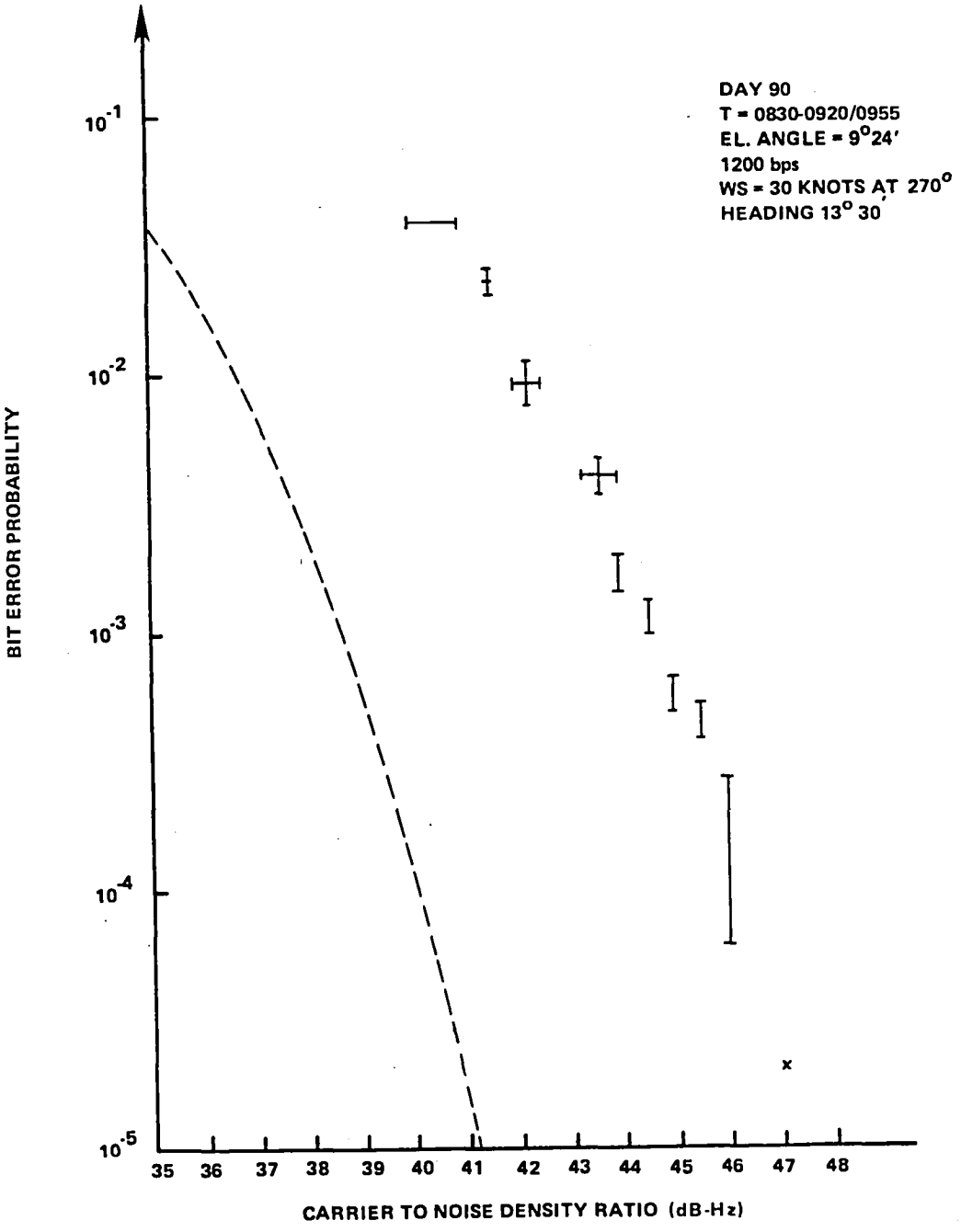

Figure 2-21. Digital PN Coded Data Performance at 1200 bps

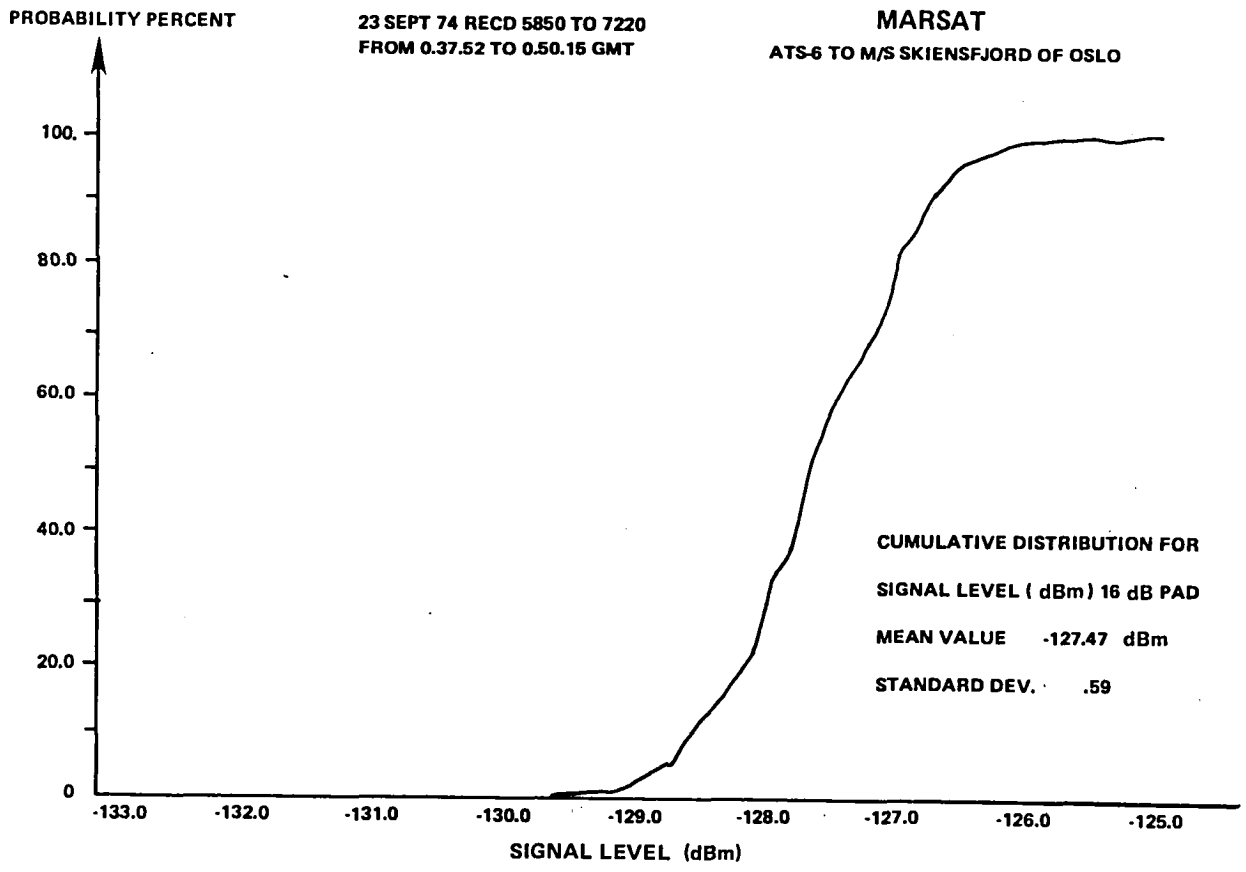

Figure 2-22. Digital Data Performance at an Elevation Angle of 16 Degrees

from a number of tests are presented in Table 2-7. The test results obtained verified that a distress buoy with a 3-watt transmitter and an omnidirectional antenna is capable of sending a coded identification signal to a ground station by ATS-6 at elevation angles down to 0.5 degree with sufficient reliability.

CONCLUSIONS

PLACE Aeronautical Experiments

Calculated ranging parameters are in reasonable agreement with those presented in Table 2-1. For a total of C/N_o = 42 dB-Hz, the theoretical rms range error is 285 meters (m). In a forward link having a C/N_o = 42 to 44 dB-Hz, the typical observed standard deviation is 276 m. The PLACE modem exhibited one undesirable ranging result, i.e., a high frequency of errors occurred, probably due to incorrect ambiguity resolution.

Results of the voice modem presented in Figure 2-2 shows that for a C/N_o of 43 dB-Hz, the PB word intelligibility is below 70 percent, a value which is exceeded by other modems tested. No apparent degradation in word intelligibility was observed for a high multipath signal interference (S/I) of 3 dB.

Table 2-7
Details of the Communication Link and Results

DFVLR* No.	Transmitter Power (watt)	Attenuators	Rec'd Level (dBW) (min)	Signal (dBW)** (max)	Fading** Period (sec)	Percentage of Error Free Messages at Number Superpositions							Other Users on Return Link	Remarks
						1	2	4	8	16	32	64		
1	10	9	-171	-163	3, 5	–	45	100	100	100	100	100	No	
2	10	12	–	–	–	–	10	85	100	100	100	100	No	Interference by spurious signal at Rosman
3	10	12	-178	-171	3, 5	–	–	–	–	–	40	90	No	Signal degradation by defect. antenna cable
4a	10	9	–	–	–	75	95	100	100	100	100	100	MarAd	New antenna cable
4b	10	15	–	–	–	–	35	70	100	100	100	100	MarAd	6 dB more att.
5	10	15			3, 3	–	30	65	90	100	100	100	MarAd from 13.00	Finite configuration
SAR DEMO	10	15	–	–	–	–	–	80	–	–	–	–	MarAd	Buoy operates from deck of *Otto Hahn*
6	10	15	-178	-171	3, 0	–	–	20	80	95	100	100	MarAd	
7	10	15	-175	-165	3, 0 12, 2	–	–	60	85	100	100	100	VOICE	SAR demonstration
8	10	15	-171	-166	3, 7 10, 5	–	45	65	100	100	100	100	VOICE	
9	10	15	-179	-170	2, 9 7, 5	–	–	–	–	40	90	100	DOT	Linear antenna horiz. and vert. pol.
10	10	15	-176	-166	3, 3 8, 3	–	35	95	100	100	100	100	FAA/ DOT	
11	10	15	-179	-165	4, 8	–	–	25	80	100	100	100	No	
12	10	15	– -179	-172 -163	5, 1 6, 3	– –	– –	– –	– –	– –	50 –	65 100	No	Normal level Peculiarity for 2 min.

*Deutsche Forschungs-und Versuchsanstalt für Luft-und Raumfahrt
**The levels are evaluated only if a record of 1-sec integration time is available.

For simultaneous transmission of voice and data, Figure 2-4 shows a large deviation of performance from the theoretical data at the low bit-error rates.

Department of Transportation/Transportation Systems Center Aeronautical Experiments

Results in the Transportation Systems Center ranging test showed that a typical rms range error of 100 m at a C/N_o of 43 dB-Hz was obtained for the narrowband mode and for the wideband mode, and an approximate error of 30 m was determined. These results are generally larger than the corresponding laboratory measurements, particularly for the wideband mode. The multipath interference caused the test range error to be higher than the laboratory measurements.

The TSC voice-only test presented in Figure 2-7 indicated Hybrid No. 1 modem had the best performance. All three TSC modems, Hybrid No. 1 (Q-M/PSK), Hybrid No. 2 (PDM/PSK) and adaptive delta voice modulation (ADVM), exceeded the 70 percent PB word intelligibility for a C/N_o of 43 dB-Hz. No apparent degradation in word intelligibility was observed for a relatively high multipath S/I of 3 dB.

The results of the digital data tests shown in Figure 2-9 indicated a bit-error rate of less than 1×10^{-5} for a C/N_o = 43 dB-Hz. This value corresponds to the AeroSat system specification. When the multipath interference ratio was S/I* = 10 dB or less, the bit error rate increased for the same C/N_o and for a DECPSK type modulation.

The results for Hybrid No. 1 modem shown in Figure 2-10 indicated a large divergence of the data from the theoretical curve at the low bit-error rates.

The analyzed results from the L-band multipath tests over land and ocean provided essential data required for appropriate communications signals structure design and the definition of an aircraft antenna for optimum multipath rejection characteristics. The mathematical model characteristics agreed closely with that of the measured multipath results.

The results obtained from the three aircraft antennas showed that the measured gain is in close agreement with the predicted values. All three antennas indicated a relatively high multipath interference rejection characteristic.

DOT/FAA Aeronautical (ATC) Tests

Since the ranging technique used by the Federal Aviation Administration (FAA) in their air traffic control (ATC) experiments was the same as that of the PLACE system, the results are referred to previously. Many difficulties that were caused by hardware and software problems were encountered during the ATC aircraft position demonstration.

The voice-only test results indicated that continuous voice communications were provided and momentary variations occurred only when the aircraft performed turn maneuvers.

*S/I is defined as the signal to interference ratio.

The objective of the FAA ATC experiment was not to evaluate the system's equipment and techniques but to provide a qualitative demonstration on the performance of the system. For this reason, very little data on the tests were obtained. Essential objectives of the ATC demonstration were accomplished and the program was considered a success.

Canadian Aeronautical Tests

From the results shown in Table 2-4, it can be concluded that good voice operational performance can be expected from each modem when they are properly calibrated.

The aircraft phased array antenna test showed that the measured gain was in agreement with the design specification for the region required to cover. A significant antenna parameter that was not measured, because of a lack of time, was the multipath rejection characteristic.

European Space Agency Aeronautical Tests

The ranging results shown in Table 2-5 indicate the standard deviation varied in range from 500 to 600 meters for the short integration time of 120 msec. This standard deviation was relatively large when compared with that of 100 meters obtained when a pseudorandom code data system is used.

In the transmission of voice, the word intelligibility data obtained were reasonably flat above the threshold region for both modulation techniques, indicating that the system background noise did not greatly affect the intelligibility. A 3-dB improvement of delta modulation was shown over that of the narrowband frequency modulation (NBFM). These tests have shown that digitally commanded delta modulated data that is phase shift keying (PSK) modulated onto an rf carrier is more effective in speech transmission than that of NBFM, particularly under the conditions of multipath interference.

The digital data transmission tests showed that data encoding is required, since the Comet aircraft antenna did not have sufficient multipath interference rejection to permit satisfactory reception of coherent data on a PSK signal at a 1200-bps rate and elevation angles down to 10 degrees.

Department of Commerce/Maritime Administration Maritime Tests

Results from the voice modems that were tested showed good quality performance for a reasonably wide range of C/N_o values.

Unsatisfactory performance resulted from the two digital data modem tests. To improve the performance, modifications to the modems were required.

A wider deviation of the location of the ship's position resulted between the MarAd and the onboard ship computations than was expected.

Department of Transportation/U.S. Coast Guard Maritime Tests

A comparison of the measured and theoretical digital data obtained with the ship *Sherman* showed that to have a minimum multipath interference, the carrier-to-multipath (C/M) ratio must be greater than 11 dB.

The sample of voice data that was obtained was minimal and an evaluation of the phonetically balanced word intelligibility versus the C/N_o ratio could not be performed.

No conclusion can be made on the ranging test results because reduced data were not obtained, since the construction of the data processing equipment was not completed.

Test results from the U.S. Coast Guard cutter *Gallatin* were not provided; therefore, a conclusion could not be formulated.

European Space Agency Maritime Tests

Satisfactory results were provided by the side-tone ranging tests with the ship *Otto Hahn* as the mobile terminal. A standard deviation of 60 to 70 meters was achieved at a C/N_o of 52 dB-Hz and an elevation angle of 5 degrees.

Performance of the two-voice modulation techniques shown in Figures 2-20 and 2-21 indicated that a greater spread of data occurred from the narrowband frequency modulation. This result shows that multipath interference has a greater effect on narrowband frequency modulation than that on delta modulation.

From the digital data test results, it was established that the difference multipath interference has considerable effect on the bit-error rate for PSK modulation particularly at low elevation angles. This multipath effect can be reduced by narrowing the antenna beamwidth and encoding the data.

With the Norwegian ship *Skiensfjord* as the mobile terminal, the results of the digital data transmitted indicated that there is little effect from multipath interference for elevation angles above 5 degrees and for received carrier levels above -129 dBm or for a C/N_o of 42 dB-Hz.

European Space Agency Distress Buoy System Tests

All of the tests performed with the distress buoy for elevation angles from 0.5 degree to 20 degrees were successful. The search and rescue demonstration was conducted in conjunction with the distress buoy and the results were very successful.

CHAPTER 3

"MOBILE L-BAND TERMINALS FOR SATELLITE COMMUNICATION" SYSTEM

INTRODUCTION

Objectives of Experiments

Mobile L-band terminals were used with ATS-6 to perform experiments involving voice communications and to characterize propagation effects due to the local environment.

Two different designs of mobile L-band transceivers were used to perform the voice communication experiments. One of the transceiver configurations was a NASA/GSFC design, built by Westinghouse Electric Corp., that had all of the components except the antenna mounted inside a briefcase. The second type of transceiver was a General Electric (G.E.) design that was packaged in a configuration suitable for use in mobile vehicles, such as jeeps and trucks, and was also adaptable for fixed base stations. Both types of transceivers could easily be hand-carried to remote areas or over rough terrain.

The L-band propagation experiments were performed by Motorola Communications and Electronics, Inc., and used the ATS-6 L-band downlink (1550 MHz) to characterize the local environment effects expected to be encountered during mobile operations. Data were also taken at uhf (860 MHz) to determine frequency dependence. Both downlinks were provided by ATS-6.

Communications Experiments

The National Association for Search and Rescue (NASAR), a member of the Emergency Response Communications Program (ERCP), and NASA/GSFC recognized the need for emergency voice communications in remote areas and over rough terrain, to prevent critical delays in response to disasters. A study of this problem revealed that a small, low cost L-band mobile ground terminal, used in conjunction with ATS-6 and a ground station, could provide the required communications. In a joint effort between NASAR and NASA/GSFC, a number of communications experiments were conducted to demonstrate voice communications between mobile units and a base station via ATS-6. Demonstrations of the "briefcase" unit were also given to many other interested agencies.

Propagation Experiments

Practical design of two-way mobile communications via satellite requires accurate knowledge of the additional path loss over free space (line-of-sight). The additional or excess path loss arises from local environment shadowing and multipath cancellation at the mobile Earth terminals. In an effort to

quantify these losses, the ATS-6 L-band and uhf downlink signals were used to determine the additional path loss as a function of the following:

- Local environment
- Vehicle heading
- Link frequency
- Satellite elevation angle
- Street side (city block orientation relative to line-of-sight to the spacecraft).

SYSTEM DESCRIPTION

General

Two system configurations were used in performing the experiments as shown in Figures 3-1 and 3-2. Both system configurations involved ATS-6, at least two mobile ground terminals, and a "turnaround" ground station to support voice communications. A turnaround ground station (NASA Rosman Ground Station or a General Electric Base Station) was required so that an adequate downlink carrier-to-noise (C/N) ratio could be provided to the mobile ground terminal. The system constraints on the forward uplink from a mobile ground terminal produced a negative C/N value in the satellite; the resultant downlink signal to the mobile ground terminal was not sufficient to provide satisfactory voice communications. The problem was resolved by processing the downlink signal received from the satellite by a turnaround ground station and transmitting the processed signal back to the satellite. The signal received by the satellite was then transmitted to the ground mobile unit with an adequate signal level to support satisfactory voice communications.

Figure 3-1 shows the L-band to L-band (L X L) configuration used in ATS-6, where the mobile ground terminal transmitted an uplink L-band frequency of 1655.05 MHz and received a frequency of 1552.00 MHz from the satellite. The turnaround ground station received an L-band frequency of 1555.05 MHz and transmitted at a frequency of 1652.00 MHz. A mobile van with a 1.2-meter diameter antenna was also used as a mobile ground terminal on some of the demonstrations.

The second system configuration (Figure 3-2) used two of the spacecraft i.f. amplifiers configured to provide frequency conversion of L-band to C-band (L X C) in the forward link; and C-band to L-band (C X L) in the return link. An uplink frequency of 1655.05 MHz was received by the satellite from the mobile ground terminal and retransmitted to the turnaround ground station after a conversion to the C-band frequency of 3955.05 MHz. The turnaround station then processed and transmitted the uplink signal to the satellite at a C-band frequency of 6152.00 MHz. In the satellite, the signal was then converted to the L-band frequency of 1552.00 MHz and transmitted downlink to the mobile ground terminal. Most of the experiments that were performed used the Rosman Ground Station, North Carolina for the turnaround station (either L X L or L X C:C X L). When the Rosman Ground Station was not available, the General Electric Base Station in Schenectady, New York, was used (L X L only).

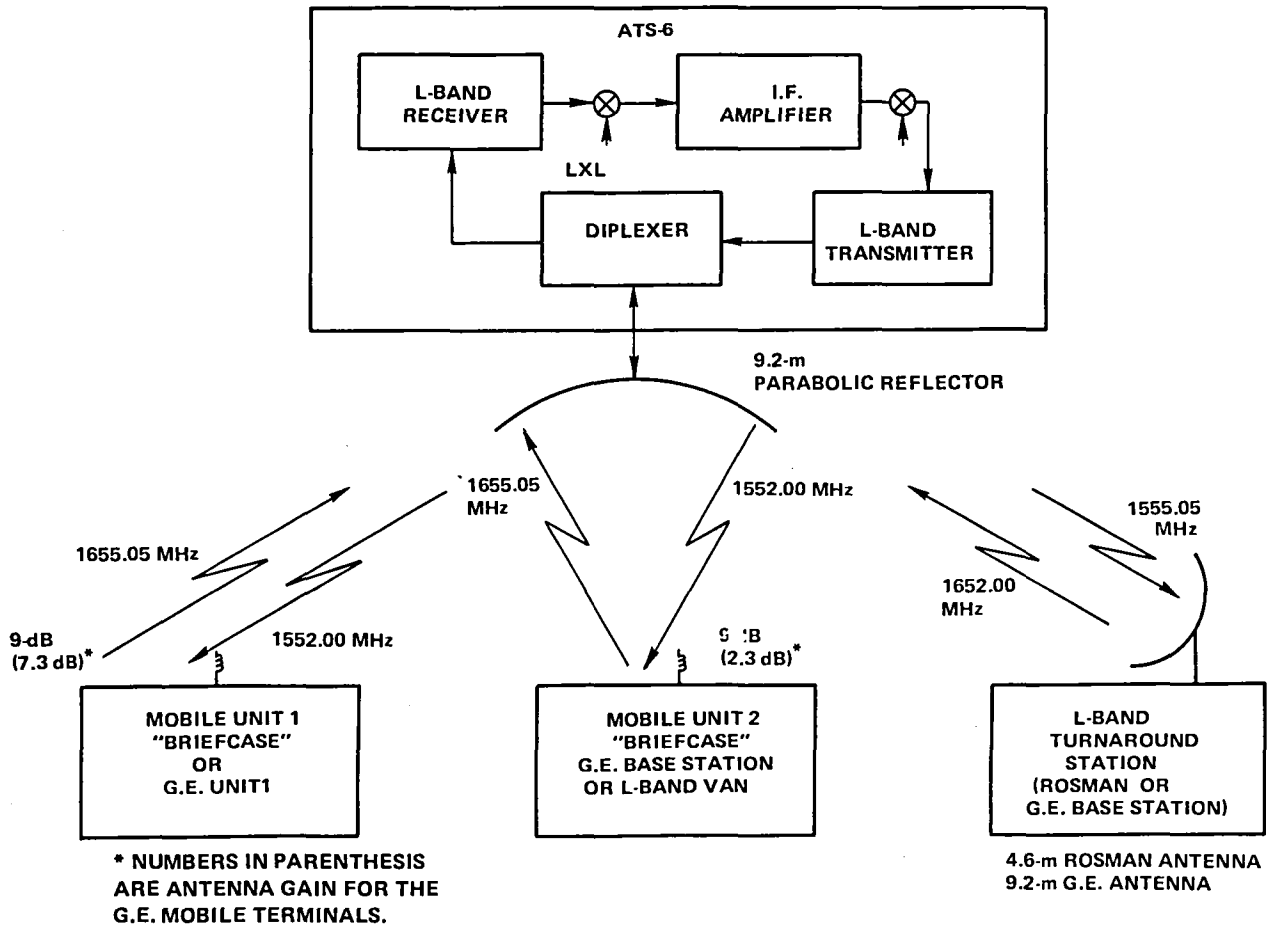

Figure 3-1. Mobile Terminal Communications System (L X L)

NASA "Briefcase" Terminal

The function of the "briefcase" L-band transceiver was to provide half-duplex (push to talk) voice communications to another terminal via ATS-6, primarily to demonstrate the feasibility of providing voice communications with a small portable Earth terminal under typical environmental conditions. The portable transceiver was built by Westinghouse Electric Corp. for Goddard Space Flight Center (GSFC) and essentially consisted of a commercial uhf/FM transceiver, an upconverter, a 20-watt power amplifier, a preamplifier, a downconverter, a power supply, and helical antenna. Three units were built, two of which were mounted inside a standard briefcase. The third unit was mounted in an aluminum camera case that measured 45.7 cm X 33 cm X 11.4 cm. The antenna was mounted either on the case, as illustrated in Figure 3-3, or on an adjustable tripod. Primary power for the transceiver was provided by either two internal 12-volt batteries, an external 12 Vdc source or an internal power supply requiring a 120-volt, 60-Hz source.

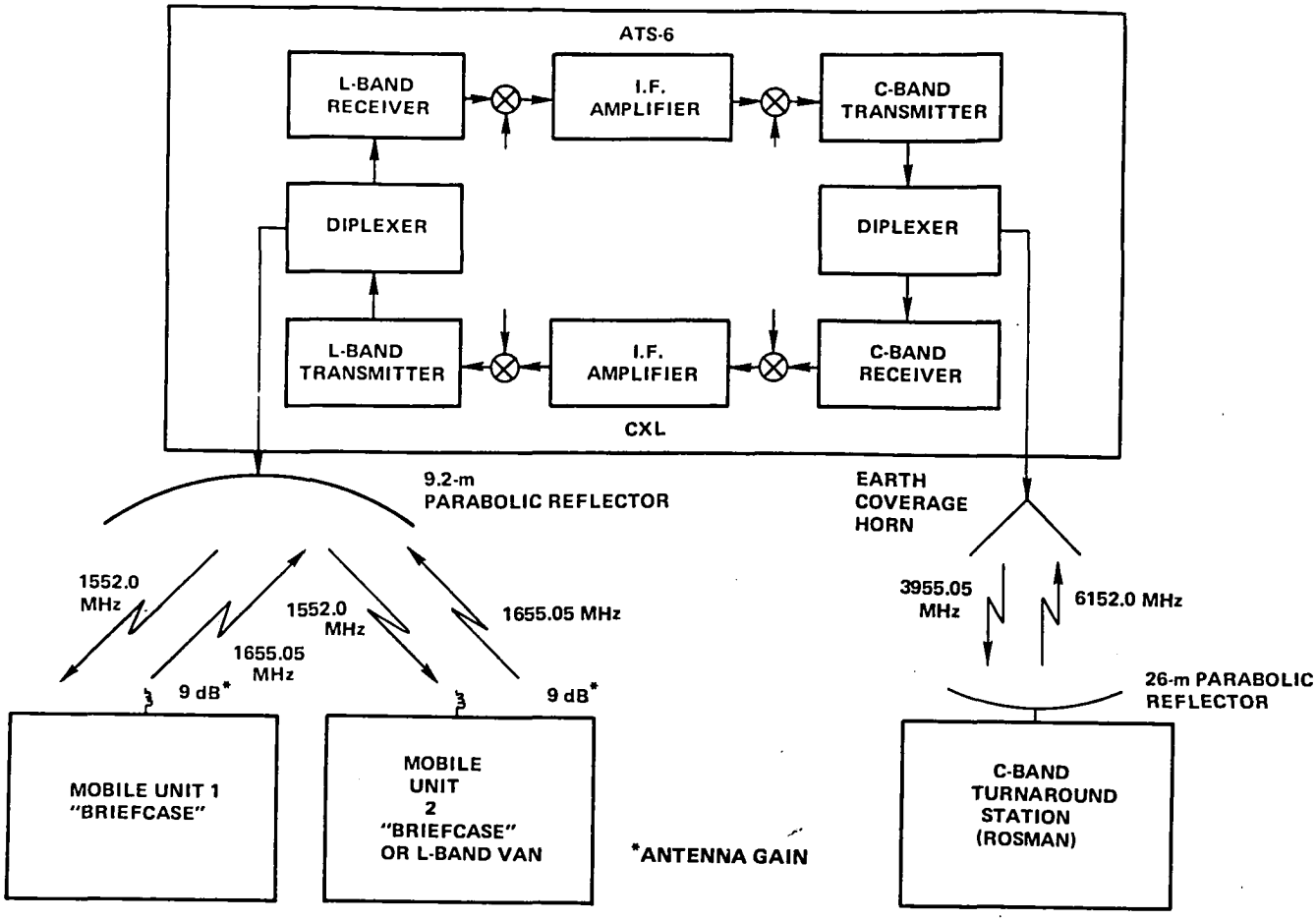

Figure 3-2. Mobile Terminal Communications System (L X C; C X L)

Voice transmission was provided by a narrowband frequency modulated carrier from a commercial uhf/FM voice transceiver having an output of +30 dBm at a frequency of 444.05 MHz and contained a push-to-talk microphone that was detachable. A block diagram of the "briefcase" transceiver is shown in Figure 3-4. The uhf output frequency of 444.05 MHz was upconverted to the transmitting L-band frequency of 1655.05 MHz and amplified to an output power of 20 watts (43 dBm). When a helical antenna with a gain of 9 dB was used, an e.i.r.p. of 52 dBm was obtained (right-hand circular polarization).

The 1 watt output (+30 dBm) from the uhf transceiver was attenuated to +20 dBm to provide the proper input level to a high level double balanced mixer. A local oscillator frequency of 1211 MHz at +7 dBm was used to upconvert from uhf to the L-band frequency. A four-pole bandpass filter with a 30-MHz (-3 dB) bandwidth was provided at the input to the power amplifier to reject the transmission of unwanted frequencies from the mixer. The solid-state amplifier was operated Class C to produce an output power of 20 watts for an input of approximately +12 dB. An isolator at the output of the power amplifier provided protection for the amplifier from the occurrence of a high voltage standing wave ratio at the antenna port.

Figure 3-3. GSFC "Briefcase" Mobile Transceiver

The antenna most often used with the transceiver was a simple right-hand circular polarized helix with a gain of 9 dB and a 3-dB beamwidth of 40 degrees. To allow pointing of the antenna to ATS-6, the antenna was mounted on an adjustable tripod. Occasionally, a crossed dipole antenna with a gain of 6 dB was used.

Voice signals received at the L-band carrier frequency of 1552.00 MHz by the 9-dB gain helical antenna were applied to the receiver input through a circulator. A four-pole bandpass filter having a -3 dB bandwidth of 30 MHz was provided at the preamplifier input, primarily to reject the transmitter signal received from the isolator with an attenuation of approximately 60 dB. The receiver contained a low noise preamplifier with a noise figure of 3.5 dB and a gain of 25 dB. A similar type of bandpass filter was also provided at the output of the preamplifier to reject the image frequency originating at the double balanced mixer that was used as a downconverter.

The received L-band signal was downconverted to the uhf frequency of 449.0 MHz and applied to channel 1 of the uhf transceiver. Demodulation of the carrier was performed in this unit and the resulting voice signal was applied to an audio speaker. A local oscillator, at a frequency of 1103 MHz

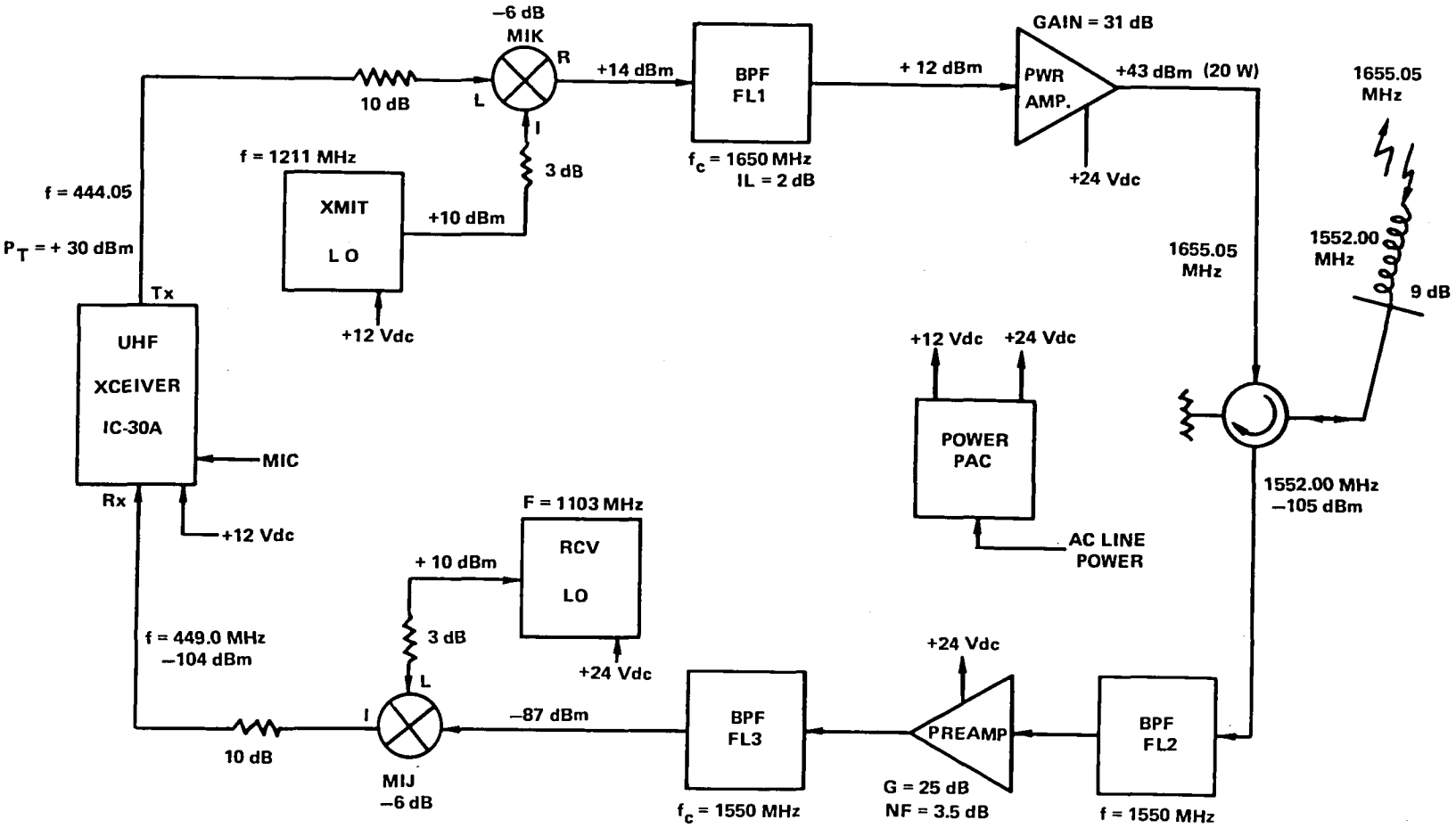

Figure 3-4. "Briefcase" Transceiver Block Diagram

and an output of +10 dBm, was used by the double balanced mixer in the downconverter. The overall characteristics for the uhf/FM transceiver were as follows:

GENERAL:

Parts	Quantity
Transistors	40
Field effect transistors	24
Diodes	3
Integrated circuits	3

Frequency range	440 to 450 MHz;
Frequency stability	1 X 10E–5 (0.001 percent)
Impedance	50 ohms
Voltage	13.8 V, ±15 percent
Polarity	Negative ground
Current	Receiver squelched . . . . . 250 mA Receiving signal. . . . . 550 mA Transmitter (10 W) . . . . . 2.8 A Transmitter (1 W) . . . . . 1.3 A
Size	58 X 156 X 244 mm
Weight	2.4 kg
Modulation type	F3
Antenna input	50 ohms

TRANSMITTER:

Frequency range	444.00 to 449.99 MHz, 22 channels
RF power output	HI . . . . . .10 W (10-watt output disabled) LOW . . . . 1 W
Maximum frequency deviation	Adjustable between 3 to 16 kHz
Audio input	500 ohms
Modulation system	Variable reactance phase modulation
Microphone	500 ohms–dynamic microphone with push-button switch
Crystal multiplier factor	24
Crystal range	18 MHz
Spurious response	-60 dB or less

RECEIVER:

Frequency range	444.00 to 449.99 MHz, 22 channels
I.f. frequencies	First–10.69 MHz Second–455 kHz
20 dB quieting sensitivity	-4 dB or less (0 dB = 1 microvolt)
Bandwidth	±15 kHz at the -6 dB point
Selectivity	±25 kHz (-50 dB) point
Squelch sensitivity	-80 dB or less (0 dB = 1 microvolt)
Spurious rejection	60 dB or more
Audio power output	1.2 W

Primary characteristics for the L-band "briefcase" transceiver were as follows:

Transmit	
Power out	20 watts (+43 dBm)
Frequency range	1655.000 to 1656.000 MHz
Frequency stability	1 part in 10^6
Modulation	Narrowband FM
Audio bandwidth	300 to 3000 Hz
Peak deviation	5 kHz
Preemphasis	0.2 millisecond
Receive	
Noise figure	3.5 dB
Frequency range	1552.000 to 1553.000 MHz
Frequency stability	1 part in 10^6
Audio bandwidth	300 to 3000 Hz
Deemphasis	0.2 millisecond
I.f. bandwidth	15 kHz
Power	+11 to +15 volts dc
Temperature	0°C to 50°C

A measured FM quieting of 35 dB was obtained for this transceiver.

Land Mobile Vehicle Terminal (General Electric Corp.)

One major objective of this experiment was to demonstrate that a practical satellite-aided land mobile radio set could be manufactured using current mass production technology. To meet this goal, the experimental equipment was designed as similar as possible to current land mobile equipment. Standard mobile radio equipment was modified to implement the design, but several parts of the experimental radio set were specifically designed.

The radio set was packaged like a standard mobile radio set, so that it would be familiar to the users. The packaging assured mechanical integrity in rough field tests encountered in long haul tractor trailer trucks. As is typical in mobile radio installations, the controls of the radio set were mounted separately from the main chassis of the radio to conserve space near the dashboard of the truck. A multiconductor cable connected the control head with the main chassis of the radio set.

The General Electric mobile radio transceiver set was designed to meet the specifications that follow:

Transmitter:	
Frequency	1655.050 MHz
Power output	16 watts nominal 12 watts minimum

Transmitter (cont):	
Frequency stability	±0.0002 percent (-30° to +60°C)
Modulation	Adjustable from 0 to ±5 kHz swing FM with instantaneous modulation limiting
Audio frequency response	Within +1 dB and -3 dB of a 6 dB/octave preemphasis from 300 to 3000 Hz per EIA standards
Duty cycle	EIA 20 percent intermittent
Maximum frequency spread	±6 MHz with center tuning
Rf output impedance	50 ohms
Receiver:	
Frequency	1552.000 MHz
Frequency stability	±0.0002 percent (-30° to +60°C)
Noise figure	2.6 dB referenced to transceiver antenna jack
Equivalent receiver noise temperature	238 K
Selectivity	-75 dB by EIA two-signal method
Audio output	5 watts at less than 5 percent distortion
Frequency response	Within +1 and -8 dB of a standard 6 dB per octave deemphasis curve from 300 to 3000 Hz
Modulation acceptance	±7 kHz
Rf input impedance	50 ohms
Antenna System:	
Antenna type	"Wheeler" transposed coaxial segment array
Polarization	Linear (vertical)
Gain	7.3 dBi (peak)
Vertical pattern (all angles with reference to the horizon = 0)	At 1550 MHz—receive Beam peak—+11° -3 dB points—+4° and +19° At 1650 MHz—transmit Beam peak—+18° -3 dB points—+11° and +28°
Horizontal pattern	Omnidirectional (< ±1 dB)
Feed line loss	1.8 dB (4.57 m of RG-214)
Receive system noise figure referenced to antenna terminals	4.4 dB, including feedline loss (509 K equivalent temperature)

Antenna System (cont):	
Estimated antenna background temperature	290 K
Total receive system equivalent noise temperature	799 K

These specifications represented only a moderate extension of the present state-of-the-art in mobile radio transceivers. The transmitted power specification was limited to that of a varactor doubler connected to the output of a medium power 800-MHz mobile radio transmitter. Approximately the same amount of power could be generated in a single transistor package without the aid of splitters and combiners. The noise figure specified was somewhat lower than that obtained with inexpensive plastic case transistors, but only by approximately 1 dB. A $15.00-device was used as the first rf amplifier in the experimental satellite transceiver, but devices having the specified noise figure are available for less. Construction methods used in the mobile transceivers can be readily adapted to mass production.

The base station equipment deployed at the trucking company central dispatch facility had essentially the same specifications as the mobile radio equipment described previously. A larger antenna was chosen for the base station, so that it could receive any truck signal and retain control of the communications network.

Although several alternate antenna designs were considered for the mobile radio transceiver, the primary antenna requirement was that it be relatively small with convenient installation. The antenna required an omnidirectional azimuth pattern, so that the truck could travel in any direction without requiring the driver to point the antenna. A transposed coaxial antenna, with a net peak gain of 7.3 dB, met these requirements and was chosen for the truck. A 1.3-meter parabolic reflector was available and was used at the central dispatching facility for the base station. This provided more than adequate gain.

The equipment at the General Electric Earth Station Laboratory could have been configured in a variety of ways to complete the experimental communications system. A fixed 2-meter parabolic reflector and a fully steerable 10-meter parabolic reflector were available; the L-band power amplifiers could generate as much as 300 watts. Assorted low noise amplifiers, duplexers, downconverters, local oscillators, tape recorders, transmitting exciters, and a PDP-11 computer were also available. Various equipment was selected from inventory to meet the system requirements.

General Electric equipped five vehicles and a base station with the mobile transceiver. The mobile radio transceiver block diagram is shown in Figure 3-5. Much of the basic circuitry and the case is from production models of their 800-MHz radio set and 238-MHz receiver. Modifications required for the transceiver follow:

- Preselector Filter

  The preselector filter used to protect the rf amplifier of the satellite receiver did not represent any new technology beyond the techniques currently applied to land mobile receivers.

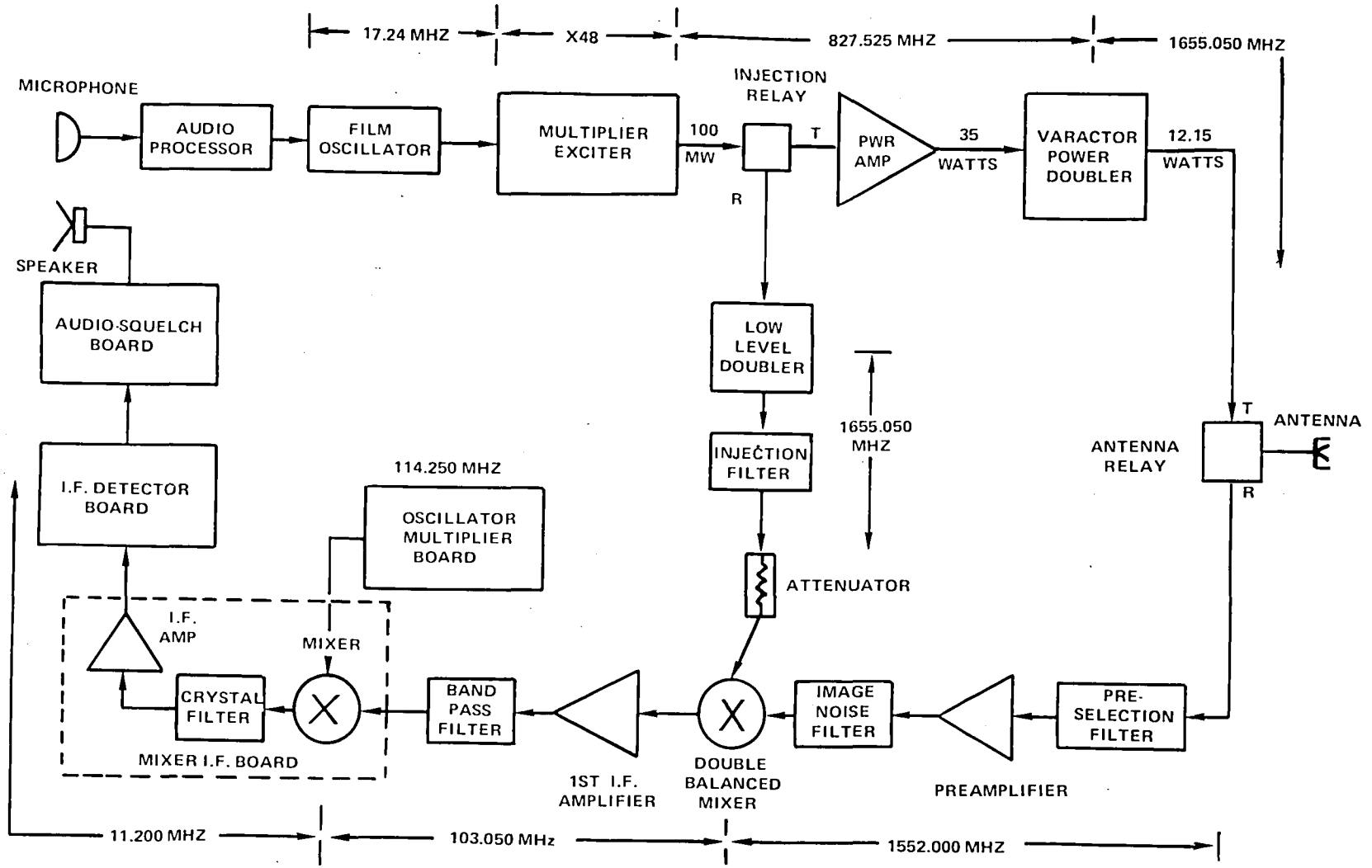

Figure 3-5. General Electric Mobile Radio Transceiver

- Preamplifier

During the construction phase of this experiment, a substantial effort was devoted toward constructing a very low noise preamplifier using inexpensive mass production techniques. The two-stage preamplifier designed for these receivers provided approximately 24 dB of gain over a broad frequency band that was limited by the bandpass characteristic of the preselector filter.

In the first stage, a low noise, high gain bipolar transistor provided an optimum noise figure of 1.4 dB with an associated gain of 13 dB.

The second stage of the preamplifier provided at least an additional 10 dB of gain, with a device that cost less than two dollars. The 3-dB typical noise figure of the second stage degraded the overall performance only slightly.

The preamplifier design included only one adjustable piston trimmer capacitor in the output circuit of the second stage. No other adjustment or microstrip trimming was required to optimize various units of the final design.

- RF Filter, First Mixer, and First I.F. Board

All the components associated with the first frequency downconverter of the 1550-MHz receiver were assembled on a common circuit board mounted in a free space within the modified 138-MHz receiver casting. Ordinary "G-10" glass epoxy circuit board exhibited sufficiently low loss to provide a good performance in this design at 1550 MHz.

The image noise rf bandpass filter was the most critical circuit etched on this circuit board. This filter, centered at 1550 MHz, prevented broadband noise generated within the preamplifier from reaching the first mixer at the first mixer image frequency. If noise at the 1750 MHz first mixer image frequency was not filtered, the receiver sensitivity could suffer by as much as 3 dB. The image noise filter provided at least 20-dB rejection. The three-pole bandpass filter, etched on this circuit board, used a coupled microstrip technique to provide an image rejection of more than 35 dB with an insertion loss of 1.25 dB in the pass band at 1550 MHz. The output of the filter fed the rf port of the first mixer.

The first mixer was double-balanced and housed in a hermetically sealed PC mounted module. The manufacturer specified a 6-dB conversion loss and 40 dB of isolation between ports. The mixer required the standard level of +7 dBm of local oscillator injection at 1655 MHz. The output of the mixer was fed into the input of the first i.f. amplifier.

The first i.f. amplifier used a single bipolar transistor that provided 18 dB of gain with a noise figure under 2 dB. The low noise i.f. preamplifier made up for losses in the 103-MHz bandpass filter that followed it to assure good overall receiver sensitivity. The circuit incorporated a second transistor in an active bias network to stabilize the dc operating point of the low noise transistor.

Finally, the circuit board included an attenuator for the local oscillator signal provided from the low level doubler. Three 1/8-watt metal film resistors arranged in a π configuration provided approximately 10 dB of attenuation to reduce the +17 dBm doubler output to +7 dBm required by the first mixer.

- Low Level Doubler and Injection Filter

In the receive mode, the low level doubler multiplied the frequency of the signal from multiplier exciter to the final 1655.050 MHz transmit frequency but at a much lower power level than the varactor power doubler used in the transmit mode. The multiplier exciter provided as much as 100 mW of drive to the low level doubler at approximately 827 MHz. Two bipolar transistors configured in a push-push circuit delivered more than 40 mW of output at 1655 MHz from 60 mW or more drive power at 825 MHz. Like the preamplifier and the first mixer board, the low level doubler was constructed on G-10 glass epoxy circuit board and was successfully duplicated in small quantities. The 1655-MHz output from the low level doubler circuit board was fed directly to the injection filter to strip unwanted harmonics from the signal applied to the first mixer.

After the injection signal passed through this filter, all unwanted spectrum lines were at least 60 dB below the desired injection signal.

- First I.F. Band Pass Filter

Three helical resonator cavities of the 138-MHz receiver casting continued to serve as a preselector filter for the following mixer.

- Oscillator-Multiplier Board

The oscillator-multiplier board of the 138-MHz receiver required minor modification to make the entire 138-MHz receiver operate at 103.050 MHz. Two small additional capacitors were required to tune the circuit board output down to 114.250 MHz as required for the L-band receiver.

All remaining portions of the 138-MHz receiver required no modification.

- Transmitter

The standard General Electric Master Executive II 800-MHz transmitter exciter served as the first part of the satellite radio transmitter, providing a deviation of the exciter of ±2.5 kHz and a center frequency of 825 kHz. The output of the exciter was then doubled to the 1650-MHz satellite uplink frequency, resulting in a transmitted signal having ±5 kHz deviation.

Land Mobile Path Loss Measurements

Signal power from ATS-6 was recorded as a function of five main variables: (1) local environment, (2) vehicle heading, (3) link frequency, (4) satellite elevation angle, and (5) street side.

Local environment was divided into four broad categories: urban, semiurban, suburban, and rural. Carrier frequencies of 860 MHz and 1500 MHz originating at the satellite were used. The satellite elevation angle varied from 19° in Chicago to 43° in San Francisco. The importance of street heading became clear during the data collection phase, so this parameter was quantized into 45° steps. For example, in cities like Denver and San Francisco with streets running northeast and southwest, little signal shadowing was apparent, despite the presence of large buildings on both sides of the streets. This is because the satellite itself was located to the southwest, and so a line-of-sight signal component could readily be maintained. Conversely, when traveling at right angles (northwest and southeast), building shadowing was particularly severe. The fifth and final parameter, street side, was added to avoid misleading conclusions about the effect of satellite elevation angle. In a given city, it was observed that the signal generally improved when one was on the street side opposite from the satellite. This is because a line-of-sight signal component could then more readily reach the receiving antenna.

Figure 3-6 presents a block diagram of the receiving and data recording equipment. The blocks drawn above and to the right of the dashed line were located in the mobile test van. ATS-6, operating in the PLACE mode, transmitted right-hand circularly polarized downlink carriers at 860 or 1550 MHz. These carriers were received by conventional quarter wave whips located on the van roof. A seven-pole combine bandpass filter was used, as necessary, to prevent strong local signals such as television channels from overloading the wideband low-noise preamplifier. The preamplifier was included to establish a low overall system noise figure, and thus maximize the depth of signal fade that could be tracked. A spectrum analyzer operating in the fixed tune mode served as a selectable bandwidth receiver.

An onboard analog-to-digital converter and microprocessor allowed simple real-time histogram analysis of received signal strength. The resulting real-time histograms were storable on cassette tape for more detailed analysis later on a Sigma 9 time-sharing system. The satellite signal, along with odometer information and voice commentary was also tape recorded, for detailed analysis later, on a dedicated PDP 11 computer.

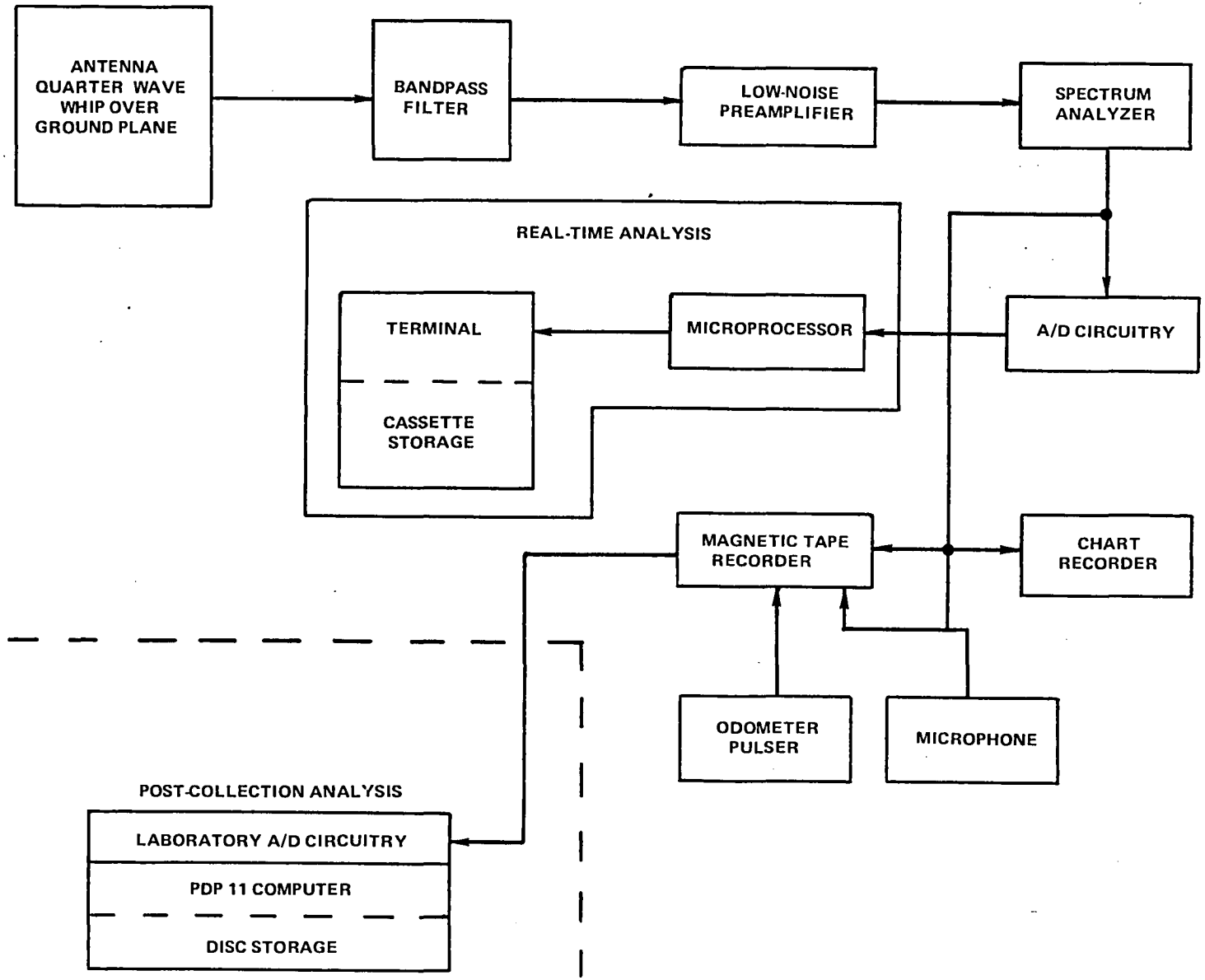

Figure 3-6. Block Diagram of Receiving and Data Recording Equipment

CHAPTER 4

"MOBILE L-BAND TERMINALS FOR SATELLITE COMMUNICATION" TEST RESULTS

TEST DESCRIPTION

Briefcase Terminal

The voice communications tests that were performed with the "briefcase" transceiver used either of the two operational configurations shown in Figures 3-1 and 3-2 in Chapter 3, "Mobile L-Band Ground Terminals for Satellite Communication System." The satellite configuration for the system shown in Figure 3-1, Chapter 3, was L-band to L-band frequency translation (L X L). Most of the tests performed used the Rosman Ground Station as the "turnaround" ground station for this configuration. During some of the demonstrations, the General Electric Company's base station participated as the turnaround station when Rosman was not available. The L-band van was used on some of the demonstrations as a second mobile ground terminal.

The second satellite configuration, shown in Figure 3-2, operated in the L-band to C-band frequency translation: C-band to L-band frequency translation (L X C:C X L) mode and used Rosman as the turnaround station. For this configuration, the L-band van was also used as the second mobile terminal.

The link calculations for the forward and return links were performed for both system configurations shown in Figures 3-1 and 3-2 and are presented in Table 4-1. These calculations indicate that a C/N_o of greater than 50 dB-Hz was obtained with the use of the briefcase terminal. Good quality voice communications were achieved when a C/N_o of 50 dB-Hz or greater was obtained.

Many demonstrations of voice communications were performed using both system configurations shown in Figures 3-1 and 3-2. Qualitative results of typical demonstrations using the briefcase terminal are presented in Table 4-2.

Land Mobile Terminal (General Electric)

Voice communication experiments using the General Electric (G.E.) transceiver were performed with two types of mobile terminals and a base station via ATS-6. One of the experiments, conducted at the Yosemite National Park, California, used two jeeps as the mobile terminals: the Air Force Coordination Center, Scott Air Force Base, Illinois, as the base station; and ATS-6. On occasions, the Goddard briefcase portable terminal was also used. Both jeeps traveled over most of the park area through heavy forest and mountainous terrain and successfully performed voice communications via ATS-6, with each other, with the base station, and with the briefcase unit. This

Table 4-1
Link Calculation Using GSFC Briefcase Terminals

Link	C-Band Turnaround Forward L X C	C-Band Turnaround Return C X L	L-Band Turnaround Forward L X L	L-Band Turnaround Return L X L
Transmitter				
Power (dBm)[1]	43 (20 W)	60 (1 kw)	43	30.0
Net antenna gain (dB)	6	58.8	6	32.6
E.i.r.p. (dBm)	49	118.8	49	76.6
E.i.r.p. per channel (dBm)	49	118.8	49	62.6
Free space loss (dB)	188.8	200.2	188.8	188.8
Transmitter antenna pointing loss (dB)	1.0	1.0	1.0	1.0
Spacecraft antenna pointing loss (dB)	4.0	1.0	4.0	4.0
Spacecraft				
P_{rsi} per carrier (dBm)[6]	-144.8	-83.4	-144.8	-131.2
Receive antenna peak gain (dB)	28.0	15.7	28.0	28.0
Receive AGC (dBm)[2]	-116.8	-67.7	-103.0	-103.0
Gain/temperature peak (dB)	-0.6	-18.4	-0.6	-0.6
Uplink C/N_o (dB-Hz^{-1}) due to reradiated noise[3]	53.2	96.8 (53.1)	53.2	66.8 (53.2)
Spacecraft i.f. bandwidth (dB-Hz)	70.8	70.8	66.8	70.8
Uplink C/N (dB)[4]	-17.6	26.0	-4.0	-4.0
Spacecraft transmitter e.i.r.p. (dBm)	54.1	74.2	74.2	74.2
Carrier power sharing (dB)[5]			-13.6	
Spacecraft noise power sharing (dB)	-18.6	-0.1	-4.6	-4.6
Free space loss (dB)	196.8	188.3	188.3	188.3
Spacecraft antenna pointing loss (dB)	1.0	4.0	4.0	4.0
Ground antenna pointing loss (dB)	1.0	1.0	1.0	1.0
Ground P_{rgi} per carrier (dBm)[6]	-162.4	-119.2	-137.3	-123.7
Ground gain/temperature (dB)	36.1	-22.2	11.5	-22.2
Downlink C/N_o per carrier (dB-Hz^{-1})	-71.4	57.2	72.8	52.7
Overall C/N_o (dB-Hz^{-1})	53.1	51.7	53.2	50.0

[1]The ground station L-band transmitter is adjusted to provide optimum power sharing in the spacecraft i.f. with the forward uplink signal (based on prior experience the turnaround e.i.r.p. = 62.6 dB).

[2]The spacecraft receive signals are due to all carriers in the spacecraft i.f.

[3]The return uplink consists of noise retransmitted from the forward link. The C/N_o in parenthesis is the combination of the overall forward link and the return uplink.

[4]Uplink C/N is a function of all signal power in the spacecraft i.f. and is used to determine noise power sharing of the spacecraft transmitter output. It is computed from the C/N_o of each carrier plus (in dB) the number of carriers present minus (in dB) the noise power bandwidth of the spacecraft i.f.

[5]The carrier power sharing in the L X L forward downlink is due primarily to the return downlink signal.

[6]P_{rsi}—Power received at the spacecraft into an isotropic antenna; P_{rgi}—Power received at the ground into an isotropic antenna.

Table 4-2
Qualitative Results of Briefcase Terminal Voice Communication Tests

Date	Terminal Location: Briefcase 1	Terminal Location: Briefcase 2	L-Band Van	ATS-6 Config.*	Turn-around Station	Voice Quality: Briefcase 1	Voice Quality: Briefcase 2	Voice Quality: L-Band Van	Remarks
8/23/77	Enroute to Kingspoint Long Is., NY	–	GSFC	L X L	G.E. Base Station	Very Good	–	Very Good	C/N_o = 60 dB/Hz
8/24/77	Park Police HQ (Brooklyn, NY)	–	GSFC	L X L	G.E. Base Station	Very Good	–	Very Good	One terminal in moving vehicle, both cases
8/7,8/77	NWS HQ Silver Spring, MD	–	Dulles Airport	L X C: C X L	Rosman	Good	–	Degraded	LO drift in L-band van
9/12/77	Gatlinburg, TN	GSFC	Scott AFB St. Louis, MO	L X C: C X L	Rosman	Good	Good	Good	High and low gain antennas used
9/13/77	GSM Park HQ, TN	Rayburn Bldg., Washington, D.C.	Scott AFB	L X C: C X L	Rosman	Unsatis-factory	Good	Good	Mountains blocked LOS to ATS-6
9/14/77	Clingmans Dome (GSM Park)	Rayburn Bldg., Washington, D.C.	Scott AFB	L X C: C X L	Rosman	Good	Good	Good	
9/15/77	GSM Park Valley View	Nashville, TN	Scott AFB	L X L	G.E. Base Station	Good	Good	Good	
9/23/77 9/24/77	CAP Aircraft Frederick, MD	CAP HQ Frederick, MD	GSFC	L X C: C X L	Rosman	Fair	Fair	Fair	High aircraft eng. audio noise
9/29/77	Agency Off., Washington, D.C.	–	–	L X C: C X L	Rosman	Good	–	–	
9/29/77	Agency Off., Washington, D.C.	–	–	L X L	G.E. Base Station	Good	–	–	

Table 4-2
Qualitative Results of Briefcase Terminal Voice Communication Tests (continued)

Date	Terminal Location		L-Band Van	ATS-6 Config.*	Turn-around Station	Voice Quality			Remarks
	Briefcase 1	Briefcase 2				Briefcase 1	Briefcase 2	L-Band Van	
10/3/77	Agency Off., Washington, D.C.	Princeton Battle Grnd.	GSFC	L X L	G.E. Base Station	Good	Good	Good	Quality good at all stations
10/11/77	NFC/NEC	–	GSFC	L X L	G.E. Base Station	Good	–	Good	Rosman not available
10/25/77	Pentagon, Washington, D.C.	Thomasville, GA	GSFC	L X L	Rosman	Good	Good	Good	Demonstration for DCPA
10/28/77	NASA HQ	–	GSFC	L X L	Rosman	Good	–	Good	Solar cells and gell cell batteries used for power
11/18/77	Santo Domingo (Dom. Repub.)	Santiago (Dom. Repub.)	GSFC	L X C: C X L	Rosman	Very Good C/N_o = 67 dB-Hz	Very Good C/N_o = 64 dB-Hz	Very Good C/N_o = 62 dB-Hz	Satellite pencil beam used
11/21/77	HEW, Prince Georges Plaza, MD	University Hosp., Baltimore, MD	GSFC	L X C: C X L	Rosman	Very Good C/N_o = 62 dB-Hz	Very Good C/N_o = 56 dB-Hz	Very Good C/N_o = 81 dB-Hz	Heavy rain had no effect on quality
11/29/77	Ft. Eustis, VA, Bldg. 1728	Ft. Eustis, VA, Bldg. 1726	GSFC	L X L	Rosman	Good	Good	Good	G.E. base station participated
12/8/77	FBI HQ, Washington, D.C.	G.E. Field Office, Baltimore, MD	GSFC	L X C: C X L	Rosman	Very Good	Very Good	Very Good	FBI was very impressed
12/13/77	Boulder, Colorado	Private home, Washington, D.C.	GSFC	L X C: C X L	Rosman	Fair C/N_o = 54 dB-Hz	Fair C/N_o = 54 dB-Hz	Fair	G.E. base station provided support, good quality

Table 4-2
Qualitative Results of Briefcase Terminal Voice Communication Tests (continued)

Date	Terminal Location			ATS-6 Config.*	Turn-around Station	Voice Quality			Remarks
	Briefcase 1	Briefcase 2	L-Band Van			Briefcase 1	Briefcase 2	L-Band Van	
1/17/78	GSFC, Bldg. 3	State Dept., Springfield, VA	GSFC	L X C: C X L	Rosman	Good	Good	Good	G.E. and Magnavox participated
2/24/78	IEEE, San Francisco, CA	IEEE, Los Angeles, CA	–	L X C: C X L	Rosman	Good	Good	–	
7/12/78	CRC, Ottawa, Canada	GSFC	GSFC	L X L	G.E. Base Station	Good	Good	Good	Briefcase 3 at Ottawa, Canada Good quality
7/19/78	CRC, Ottawa, Canada	GSFC	GSFC	L X L	G.E. Base Station	Good		Good	Briefcase 3 at Ottawa, Canada Deviation low

*L X L = L-band to L-band frequency translation.
L X C = L-band to C-band frequency translation.
C X L = C-band to L-band frequency translation.

experiment consisted of 4 days of tests with each day of tests performed under different conditions and locations in the National Park.

On the first day of the tests, the jeeps traveled through clearings and heavy forest and conducted successful voice communications with each other and the briefcase terminal via ATS-6. The quality and reliability of the test conducted the first day were considered excellent.

The second day, the tests were also conducted in the National Park with the mobile terminals located in four different areas. One of the jeeps was positioned at the highest elevation, approximately 3,000 feet above the valley floor. A second jeep was placed on the valley floor of the park while the briefcase transceiver was mounted in a helicopter. Very good voice communication were obtained between the three transceivers and the base station (Scott Air Force Base) via ATS-6. In addition to the above tests, voice communications were conducted with the helicopter at different altitudes above the valley floor. The performance of all of these tests resulted in very good quality voice communication.

The third day of the tests performed at the park consisted of voice communication between one of the jeeps, the Air Force Coordination Center, Scott Air Force Base, and the State of California Emergency Operations Center, Park Headquarters, via ATS-6. Very good quality voice communication was also obtained with these tests.

On the fourth and last day of the tests performed at the park, the participants involved were one jeep, the Goddard briefcase transceiver, and the California mobile unit. These transceivers were located in five different areas in the National Park that were known for difficult communication. Voice communication between the vehicles via ATS-6 was of very good quality. The Goddard briefcase unit was also tested when flown in a Navy helicopter and provided excellent results both on the ground and under flight conditions.

Another experiment involved equipping several commercial trucks with the G.E. mobile terminals. Smith's Transfer Corporation of Staunton, Virginia, participated in the experiment by allowing its drivers to use the G.E. radio equipped trucks to pass routine traffic to the central dispatch office. The trucks operated primarily over Eastern U.S. routes between cities listed in Table 4-3. Figure 4-1 shows the location of the cities within the L-band spot beam footprint.

During the early part of the experiment, G.E. requested NASA to point the ATS-6 L-band pencil beam at 40°N latitude and 85°W longitude. The dashed curve of Figure 4-1 represents the -3 dB contour of the ATS-6 pencil beam at this pointing. Signals received from the vicinity of Atlanta, Georgia, were at least 6 dB weaker than signals received from trucks in areas near the center of the satellite beam. Signals from trucks near Atlanta were much weaker because of the off-beam loss of the satellite antenna. The southern edge of the ATS-6 beam was located too far north for this experiment. On December 29, 1978, G.E. requested NASA to point the ATS-6 L-band pencil beam further south to 38.5°N latitude and 85°W longitude. That pointing, illustrated by the solid curve in Figure 4-1, was used for the experiment during the months of January and February 1979.

Table 4-3
Elevation Angle of ATS-6 at 140° West Longitude from Various U.S. Cities

City and State	City Latitude (°N)	City Longitude (°W)	ATS-6 Elevation (degrees)
New York, New York	40	74	9
Washington, D.C.	39	77	13
Cleveland, Ohio	42	82	15
Cincinnati, Ohio	39	85	18
Chicago, Illinois	42	88	19
Des Moines, Iowa	42	94	23
St. Louis, Missouri	39	90	22
Memphis, Tennessee	35	90	24
Atlanta, Georgia	34	84	19
Charlotte, North Carolina	35	81	17
Staunton, Virginia	38	79	14
Schenectady, New York	43	74	9

The "double hop" system configuration illustrated in Figure 3-1, Chapter 3, was chosen to overcome noise power sharing and the spacecraft transmitter noise desensitization effect. In this configuration, the Earth Station Laboratory (ESL) continuously transmitted a carrier through ATS-6 to prevent transmitter noise desensitization of the spacecraft receiver. When no truck or base station was using the system, the ESL transmitted an "idle carrier" through ATS-6 on a frequency that could not be heard by the trucks or the base station. The carrier quieted the spacecraft transmitter noise when the system was not in use. When a truck or base station made a transmission, the spacecraft retransmitted the signal. Very little satellite transmitter power was devoted to retransmitting the truck or base station signal, because it was much weaker than the ESL carrier, but the ESL received the weak truck or base station signal clearly with its large receiving antenna.

Upon receiving a truck or base station signal, the ESL transmitter immediately and automatically changed its frequency to the one the trucks and base station could hear, so any message transmitted by the truck or base station was relayed to all other stations in the network. Only one station in the network could transmit at any given time. A message originated by one station passed through the spacecraft and was detected and repeated by the ESL and then retransmitted through the spacecraft a second time, explaining the designation: "Double-hop configuration."

The transmit power of the ESL was adjusted to nearly saturate the spacecraft transponder, capturing most of its transmitter power. The trucks could then receive satellite signals with small antennas. If the ESL transmitted more than just enough power to saturate the spacecraft transponder, less power would have remained for the weaker truck transmissions, making them more

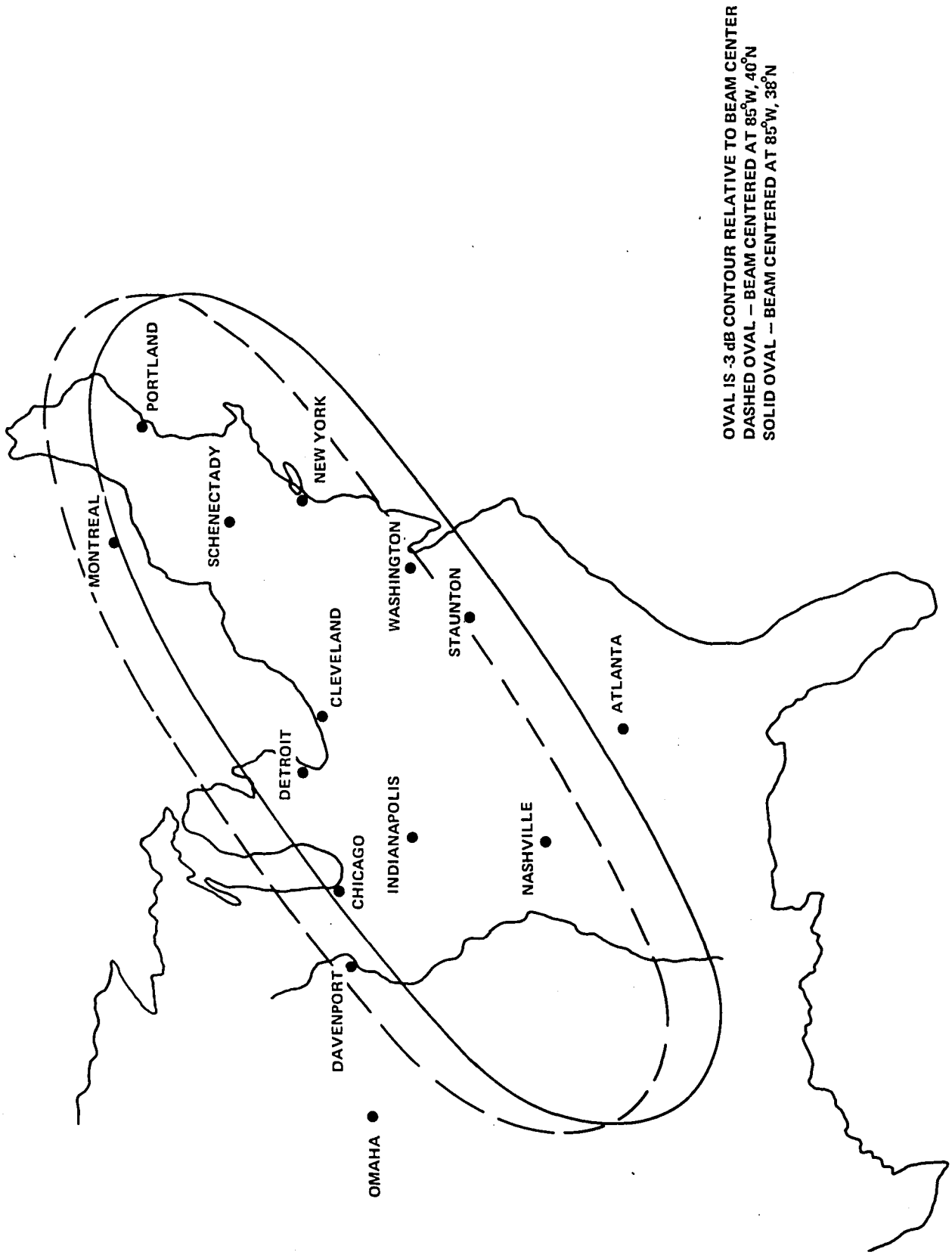

Figure 4-1. ATS-6 Pencil Beam Footprint

difficult to receive at the ESL. It should also be noted that the ESL equipment functioned in the full duplex mode. The filter duplexer mounted at the Earth Station Laboratory antenna permitted the simultaneous transmission and reception of ATS-6 signals.

Two types of selective tone signalling were employed in the experimental system. The base station transmitted a low frequency continuous tone-coded squelch systems (CTCSS) tone to distinguish its transmissions from those made by the trucks. If the Earth Station Laboratory receiver detected the CTCSS tone, the low frequency tone encoder in the laboratory transmitter was automatically enabled. It was necessary to decode and regenerate the CTCSS tone, because the voice audio circuits in the Earth Station Laboratory receiver and transmitter would not pass the low frequency tones. All base station messages repeated by the Earth Station Laboratory contained the CTCSS tone. Each of the trucks contained a CTCSS tone decoder to receive messages from the base station.

Although the satellite transceivers installed in the trucks could receive only CTCSS tone coded signals, they did not transmit a subaudible tone. The Earth Station Laboratory repeated truck signals that did not contain a subaudible tone as it received them—without a tone. Trucks could normally hear only those messages transmitted from the base station that contained tones but could not hear radio transmissions made from any other truck. The base station could hear all transmissions repeated by the Earth Station Laboratory, because it contained an ordinary carrier squelch receiver.

Although the trucks were normally prevented from communicating with each other as described previously, the tone was sometimes transmitted continuously from the Earth Station Laboratory to accumulate propagation data as the truck drivers spoke to each other.

The experimental system also included a dual-tone multiple frequency (DTMF) selective signalling system that permitted automatic vehicle identification, and individual and group selective calling. Encoding and decoding equipments manufactured by Speedcall Corporation were added to the radio equipment at the base station and in the trucks. An individually addressable DTMF decoder was added to the satellite transceiver in each truck. The decoder contained both visual and audible alarms that actuated when the satellite transceiver received the individual address code. The decoder was placed in series with the radio transceiver speaker, enabling the speaker only on receipt of the correct address code. The radio set therefore remained silent, except when it was addressed. To call a specific truck, the dispatch operator at the base station entered the address code of the desired truck through the keyboard on the DTMF encoder. The dispatcher then depressed a key, sending the address code to the truck via the voice communications link. The decoder alarm in the truck sounded to alert the driver. When the driver finished the conversation, he pressed the reset button, silencing his radio until the next call.

Each truck also included a DTMF encoder that automatically transmitted a short sequence of touch-tone digits at the beginning of each radio transmission. The number sequence automatically identified each truck transmission on a decoder and display at the base station. The identification sequence did not interrupt conversation, because it lasted only a fraction of a second.

All voice conversations and selective signalling tones were recorded at the Earth Station Laboratory for later analysis. The ESL also contained DTMF encoders and decoders equivalent to those at the base station for system test and control.

The power budgets in Tables 4-4 and 4-5 summarize the performance of the experimental satellite land mobile communications system. The tables detail the link calculation in the forward direction from the ESL through ATS-6 to the trucks and transmissions from the trucks through ATS-6 to the ESL (the return link). The links were calculated simultaneously, because the ESL continuously retransmitted everything it received to all other stations in the network.

Even in worst case conditions, the ESL forward link carrier was 7.5 dB stronger than the total noise power in the spacecraft 12-MHz i.f. Thus, the saturating forward link carrier captured almost all of the satellite transmitter power as it retransmitted to the trucks. The saturating forward link carrier also depressed the broadband noise transmitted by the satellite by at least 7.5 dB, an amount found sufficient to prevent desensitization of the spacecraft receiver.

Downlink calculations showed that the forward link signals had a signal-to-noise ratio of approximately 22 dB in the mobile transceiver even under worst case conditions. The signal received in the truck was degraded only by thermal noise inherent to the mobile receiver itself. The high power ESL-to-ATS-6 uplink made no substantial thermal noise contribution to the forward link.

In the case of the relatively weak return link transmissions from the trucks, both the uplink and downlink added noise to the signal received at the ESL. In all cases, the uplink portion of the return link contributed more noise to the truck signal than the downlink between ATS-6 and the ESL. In fact, measurements at the ESL showed that the spacecraft receiver noise power retransmitted by ATS-6 on the truck frequency exceeded the inherent ESL receiver noise by at least 6 dB.

The performance of the experimental system was also checked using the 10-meter dish for receive at the ESL rather than duplexing through the 2-meter antenna. Although all the signals received from ATS-6 were much stronger with the 10-meter antenna, no change could be measured in the signal-to-noise ratio of even weak signals from the trucks. These two tests confirmed that the links from ATS-6 to the trucks limited the performance of the experimental system. The 10-meter dish was not used for much of the experiment, because an operator had to repoint its narrow beam at the satellite at least twice a day to ensure adequate systems performance.

Land Mobile Vehicle Path Loss Measurements

The tape recorded data were analyzed with a PDP-11 computer. The 8609-MHz carrier data were sampled at a rate of 100 per second and the 1550-MHz carrier was sampled at 200 per second. A FORTRAN analysis program provided statistical information about individual files and file groups where each file contained the probability density functions (PDF) and cumulative distribution functions (CDF). Signal levels occurring at 10, 50, 70, 90 and 95 percent of the time were measured for each file. By selecting the level above which the signal appears for a specified percentage of samples in a single file, temporal coverage values were obtained. When such temporal coverage values for many files were determined having the same attributes, such as the same link frequency, the same local environment, etc., the cumulative distribution function was formed. This resulted in large scale spatial coverage information at the specified small scale temporal coverage value.

Table 4-4
Best Peak Beam Case ATS-6 "Double-Hop" Power Budget

	Uplink Carriers at 1650 MHz	
	Forward Link ESL, ATS-6	Return Link Truck, ATS-6
Ground Station		
Transmitter power (dBW)	11.0	12.0
Antenna gain (dBi)	27.5	7.3
Pointing loss (dB)	0	0
Polarization loss (dB)	-3.0	-3.0
Feedline loss (dB)	-1.7	-1.8
Effective isotropic radiated power (dBW)	33.8	14.5
Space loss at 1650 MHz (dB)	-188.4	-188.4
Spacecraft G/T at beam peak (dB/K)*	8.1	8.1
Spacecraft received signal (dBW/K)	-146.5	-165.8
Boltzmann's constant (dBW K/Hz)	-228.6	-228.6
Received signal-to-noise power density (dB-Hz)	82.1	62.8
Satellite noise bandwidth, 12 MHz* (dB) (relative to 1 Hz)	70.8	70.8
C/N in spacecraft i.f. (dB)	11.3	-8.0
C/N in 15 kHz communication bandwidth (dB)	40.3	21.0
Limiter degradation factor (dB)	0	-6.0
Power sharing factor (dB)	-0.4	-25.6
	Downlink Carriers at 1550 MHz	
	Forward Link ATS-6, Truck	Return Link ATS-6, ESL
Spacecraft Transmitter*		
Transmitter power (dBW)	15.3	15.3
Antenna gain, peak (dBi)	37.7	37.7
Antenna pointing loss (dB)	0	0
Power sharing factor (dB)	-0.4	-25.6
Spacecraft e.i.r.p. (dBW)	52.6	27.4
Ground antenna gain (dBi)	7.3	26.9
Pointing loss (dB)	0	0
Circuit losses (dB)	Included in system temperature	
Polarization loss (dB)	-3.0	-3.0
Space loss at 1550 MHz (dB)	-187.8	-187.8
Power at ground receiver (dBW)	-130.9	-136.5
Total receive system noise temperature (K)	799	600
Boltzmann's constant (dBW/Hz/K)	-228.6	-228.6
Receiver noise power density (dBW/Hz)	-199.6	-200.8
15-kHz communication bandwidth, referenced to 1 Hz (dB)	41.8	41.8
Downlink C/N in communication bandwidth (dB)	26.9	22.5
Uplink C/N in communication bandwidth (dB)	40.3	21.0
System C/N in communication bandwidth (dB)	26.7	18.6

*Spacecraft configured in the L-band narrowband frequency translation mode using the pencil beam.

Table 4-5
Worst Case ATS-6 "Double Hop" Power Budget

	Uplink Carriers at 1650 MHz	
	Forward Link ESL, ATS-6	Return Link Truck, ATS-6
Ground Station		
Transmitter power (dBW)	11.0	10.8
Antenna gain (dBi)	27.5	7.0
Pointing loss (dB)	-2.0	-1.0
Polarization loss (dB)	-3.0	-3.0
Circuit loss (dB)	-1.7	-1.8
Effective isotropic radiated power (dBW)	31.8	12.0
Space loss at 1650 MHz (dB)	-188.4	-188.4
Spacecraft G/T, over field of view (dB/K)*	4.3	4.3
Spacecraft received signal (dBW/K)	-152.3	-172.1
Boltzmann's constant (dBW/K/Hz)	-228.6	-228.6
Received signal-to-noise power density (dB-Hz)	76.3	56.5
Satellite 12-MHz noise* bandwidth, referenced to 1 Hz (dB)	70.8	70.8
C/N in spacecraft i.f. (dB)	+5.5	-14.3
C/N in a 15-kHz communication bandwidth (dB)	+34.5	+14.7
Limiter degradation factor (dB)	0	6.0
Power sharing factor (dB)	-1.1	-26.9

	Uplink Carriers at 1550 MHz	
	Forward Link Truck, ATS-6	Return Link ATS-6, ESL
Spacecraft Transmitter*		
Transmitter power (dBW)	15.3	15.3
Antenna gain (dBi)	37.7	37.7
Antenna pointing loss (dB)	-3.0	-3.0
Power sharing factor (dB)	-1.1	-26.9
Spacecraft e.i.r.p. (dBW)	48.9	23.1
Ground antenna gain (dBi)	7.0	26.9
Pointing loss (dB)	-1.0	-2.0
Circuit losses (dB)	Included in System Temperatures	
Polarization loss (dB)	-3.0	-3.0
Space loss at 1550 MHz (dB)	-187.8	-187.8
Power at ground receiver (dBW)	-135.9	-142.8
Total receive system noise temperature (K)	799	600
Boltzmann's constant (dBW/K/Hz)	-228.6	-228.6
Receiver noise power density (dBW/Hz)	-199.6	-200.8
15-kHz communication bandwidth, referenced to 1 Hz (dB)	41.8	41.8
Downlink C/N in communication bandwidth (dB)	21.9	16.2
Uplink C/N in communication bandwidth (dB)	+34.5	+14.7
System C/N in communication bandwidth (dB)	21.7	12.4

*Spacecraft configured in the L-band narrowband frequency translation mode using the pencil beam.

The CDF for urban Denver at a frequency of 860 MHz is shown in Figure 4-2 with received power in dBm on the vertical axis and the percent spatial coverage on the horizontal axis. On the vertical axis, the line-of-sight satellite level is indicated and also the noise-floor level of -136 dBm for a 3-kHz spectrum analyzer bandwidth. In the figure, four curves are presented relating to temporal coverages from 95 to 50 percent. The two lines representing temporal/spatial coverages of 90 and 70 percent indicate that a line-of-sight margin of 25 dB and 12 dB respectively are required. Effects of the direction of streets in Denver on the temporal/spatial coverage are shown in Figure 4-3, where a line-of-sight margin of only 6 dB is indicated for a temporal/spatial coverage of 90 percent.

The line-of-sight margins of the 90 percent temporal/spatial coverage of the entire experiment is summarized in Table 4-6. In this table, the line-of-sight margin consists of three forms: the "merged" column values that results from grouping all small scale files into a single master file for the overall 90 percent coverage level; the "AZ equiprob" column that gives the margin assuming each vehicle azimuth is equally likely; and the "individual" column that provides a standard deviation as an indicator of accuracy. The last two columns of parameters were obtained by fitting log-normal curves to the signal strength distribution functions of each observation category that yielded a mean corresponding to the excess path loss. The log-normal fit coefficients in the last two columns can be used to generate a model for prediction of the excess path loss requirements to provide 90 percent temporal or small scale coverage over any specified percentage of the large scale area to be covered. Both the excess path loss and the slope values were independently fitted to polynominals of the five measured parameters as follows:

Margin: EXCESS PATH LOSS + k * SLOPE

Excess Path Loss: $A0 + A1 * ENVIR + A2 * ADJAZ + A3 * FREQ + A4 * SIDE + A5 * ELEV$

Slope: $B0 + B1 * ENVIR + B2 * ADJAZ + B3 * FREQ + B4 * SIDE + B5 * ELEV$

k	Spatial Coverage
0	50%
1.3	90%
1.65	95%
2.33	99%

Variable	Range of Values
ENVIR	UR = 1, SU = 0, SB = -1
ADJAZ (heading)	-COS (2(AZ - ATS-6 AZ))
FREQ	U = 1, L = 1.8
SIDE	+1 away, -1 toward
ELEV	19° to 43°

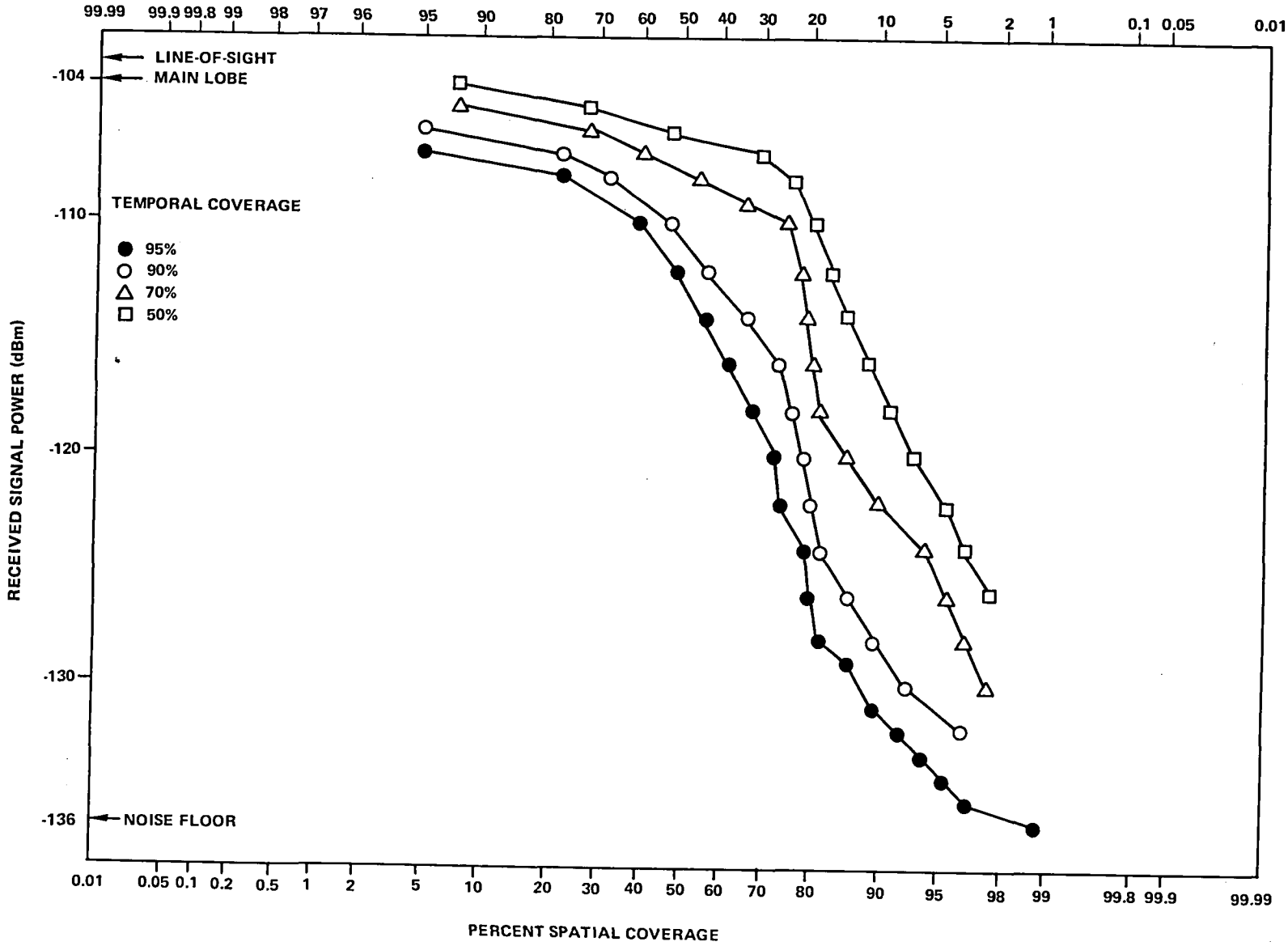

Figure 4-2. CDF: Urban Denver, 860 MHz, All Azimuths

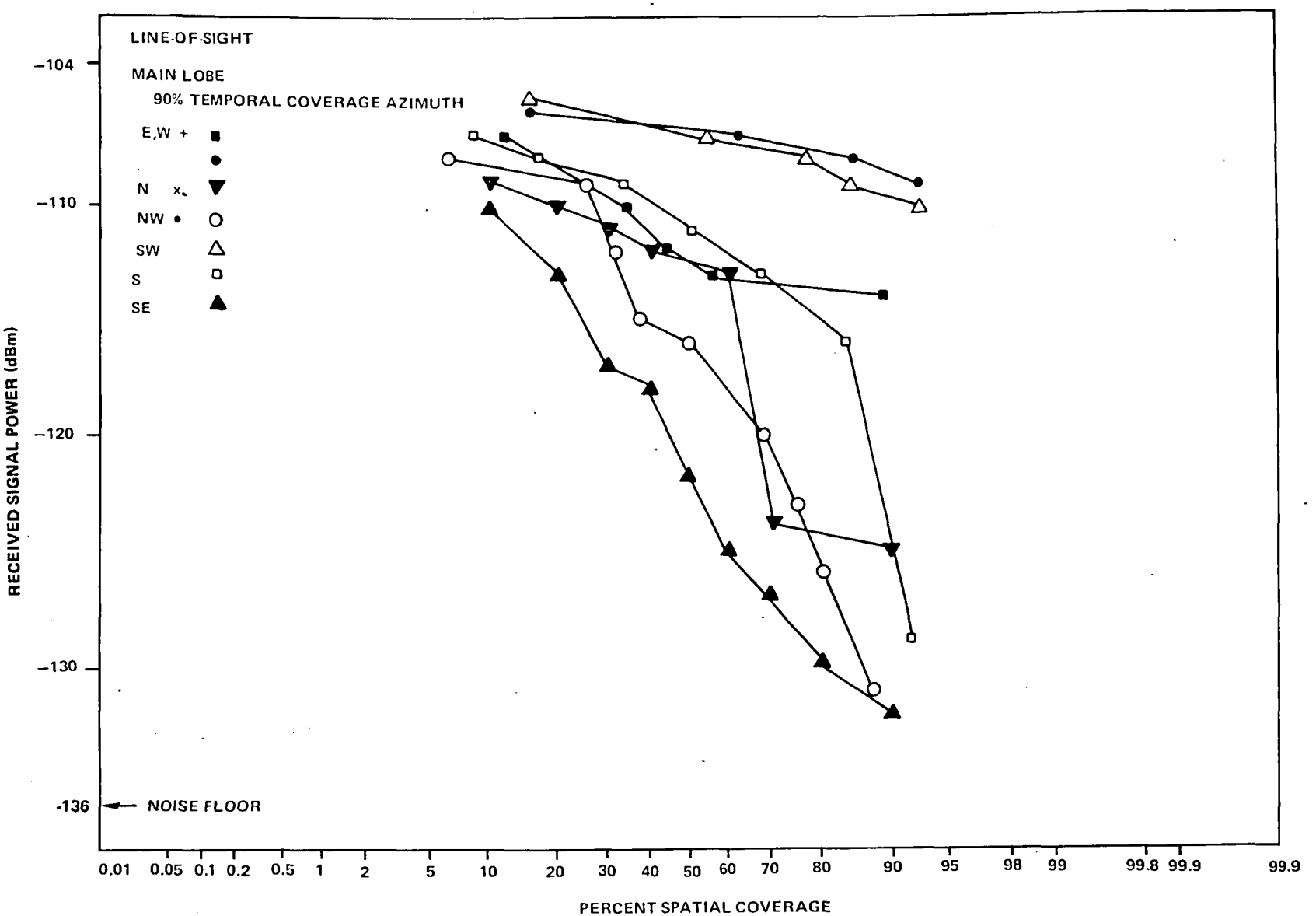

Figure 4-3. CDF: Urban Denver, 860 MHz, Segregated Azimuths

Table 4-6
Satellite Link Excess Path Loss Summary

City	Environment	Band	Azimuth	90% Spatial/Temporal Excess Path Loss Over Line-of-Sight (dB)			Curvefit[4]	
				Merged[1]	Azimuth Equiprob[2]	Individual[3] (Std Dev)	σ (dB)	Mean (dB)[5] Excess Loss
Chicago	Urban	L	All	29	33	36		
			W	26		30 (4)	8.0	20
			N	34		37 (4.2)	8.9	26
			S	29		33 (2.9)	6.8	22
		U	All	25	31	33		
			E/W	24		32 (5.6)	10.0	18
			N/S	26		31 (3.2)	6.1	22
	Semiurban	L	All	13	22	22		
			E	8		18 (3.0)	4.7	10
			W	11		14 (1.1)	1.7	8
			N	14		25 (5.3)	5.3	12
			S	20		32 (3.4)	7.9	19
Chicago	Semiurban	U	All	12	18	22		
			E	9		14 (1.9)	3.1	8
			W	8		11 (0.7)	0.8	8
			N	11		18 (2.9)	5.5	9

Table 4-6
Satellite Link Excess Path Loss Summary (continued)

City	Environment	Band	Azimuth	90% Spatial/Temporal Excess Path Loss Over Line-of-Sight (dB) Merged[1]	Azimuth Equiprob[2]	Individual[3] (Std Dev)	Curvefit[4] σ (dB)	Mean (dB)[5] Excess Loss
San Francisco (Ant -4 dB)	Urban	L	N			31 (3.7)	11.4	19
			NE			30 (3.6)	9.3	17
			E			29 (1.3)	3.0	26
			S			35 (4.3)	10.7	23
			SW			21 (4.4)	8.2	13
			W			32 (3.5)	6.0	26
		U	N			30 (4.7)	8.5	20
			NE			22 (3.3)	6.1	16
			E			32 (2.8)	6.4	25
			S			29 (4.6)	11.1	16
			SW			24 (3.9)	7.3	14
			W			32 (4.6)	8.8	24
	Semiurban	L	N			26 (2.9)	6.9	15
			E/W			26 (2.8)	5.1	18
		U	N			25 (2.9)	7.3	17
			E			26 (3.6)	6.0	22
			W			28 (4.1)	7.1	17
San Francisco (Ant -4 dB)	Urban	L	N			31 (3.7)	11.4	19
			NE			30 (3.6)	9.3	17

Table 4-6
Satellite Link Excess Path Loss Summary (continued)

City	Environment	Band	Azimuth	90% Spatial/Temporal Excess Path Loss Over Line-of-Sight (dB)			Curvefit[4]	
				Merged[1]	Azimuth Equiprob[2]	Individual[3] (Std Dev)	σ (dB)	Mean (dB)[5] Excess Loss
San Francisco (Ant -4 dB) (continued)			E			29 (1.3)	3.0	26
			S			35 (4.3)	10.7	23
			SW			21 (4.4)	8.2	13
			W			32 (3.5)	6.0	26
		U	N			30 (4.7)	8.5	20
			NE			22 (3.3)	6.1	16
			E			32 (2.8)	6.4	25
			S			29 (4.6)	11.1	16
			SW			24 (3.9)	7.3	14
			W			32 (4.6)	8.8	24
	Semiurban	L	N			26 (2.9)	6.9	15
			E/W			26 (2.8)	5.1	18
		U	N			25 (2.9)	7.3	17
			E			26 (3.6)	6.0	22
			W			28 (4.1)	7.1	17
San Francisco (Ant -4 dB)	Suburban	U	N/S			10 (0.6)	1.7	8
			NE			11 (1.7)	3.1	9
			E			13 (1.5)	2.7	9
			SE			12 (1.0)	2.4	9

Table 4-6
Satellite Link Excess Path Loss Summary (continued)

City	Environment	Band	Azimuth	90% Spatial/Temporal Excess Path Loss Over Line-of-Sight (dB) Merged[1]	Azimuth Equiprob[2]	Individual[3] (Std Dev)	Curvefit[4] σ (dB)	Mean (dB)[5] Excess Loss
San Francisco (Ant -4 dB) (continued)			SW			9 (0.8)	1.4	7
			W			10 (0.4)	1.6	8

NOTES:

[1] Computed by grouping all small-scale files and finding 90 percent coverage level.
[2] Assumes each vehicle azimuth is equally likely.
[3] Computed for a specific azimuth reading.
[4] Parameters obtained by fitting log-normal curves to computed distributions. Used lease squares linear curve fit.
[5] For 50 percent of spatial coverage.

Excess Path Loss		Slope	
Coefficient	STD ERR	Coefficient	STD ERR
A0 = 9.55 dB		B0 = 3.75 dB	
A1 = 4.46 dB	0.42 dB	B1 = 2.62 dB	0.29 dB
A2 = 3.41 dB	0.61 dB	B2 = 0.98 dB	0.42 dB
A3 = 1.66 dB	0.91 dB	B3 = 0.046 dB	0.62 dB
A4 = -0.35 dB	0.36 dB	B4 = -0.24 dB	0.25 dB
A5 = -0.052 dB	0.045 dB	B5 = 0.040 dB	0.031 dB
Estimate	3.65 dB	Estimate	2.5 dB

The margin was then obtained by the sum of the predicted excess path loss plus k times the predicted slope, where k is 1.3 corresponded to the 90 percent large scale area coverage. The local environment and vehicle heading were the most important in setting margin levels. The frequency, street side, and satellite elevation coefficients were at best marginally statistically significant.

A useful quantity to characterize the small-scale behavior of a signal is the level crossing rate (LCR). The LCR is the expected rate at which the signal envelope passes through a specified level with a positive slope. A normalized LCR, which is independent of the vehicle speed and link frequency, was obtained by dividing the parameter by the maximum Doppler frequency. A graph of the normalized LCR versus, RHO, the difference between the comparison level and the average signal power, is presented in Figure 4-4. The graph shows that the LCR behavior was not strongly affected by the link frequency and was also generally unaffected by the heading differences of 180 degrees. In the graph, the solid curve with circles indicates the LCR behavior that would be found for Rayleigh fading signals. Characteristics of the normalized fade duration for the same conditions as given in Figure 4-4 are shown in Figure 4-5. Normalization was accomplished by multiplying the average duration of the fades below a specified level by the maximum Doppler frequency.

RESULTS

Briefcase Terminals

The results of all the briefcase terminal demonstrations that were performed, as shown in Table 4-2, indicated that good quality voice communication were achieved in almost all of the tests. For a satisfactory quality of voice communication, a minimum C/N_o of 50 dB-Hz was established. In all of the demonstrations, where the C/N_o was measured, a value greater than 50 dB-Hz was obtained. The quality of voice communication was equally good when either the Rosman Ground Station or the G.E. base station was used as the turnaround ground station. The calculations presented in Table 4-2 indicate a C/N_o of greater than 50 dB-Hz was obtained for both C-band and L-band "turnaround" modes of operation. This predicted data supported the good quality of voice communication results obtained from the demonstrations with the Goddard briefcase terminal.

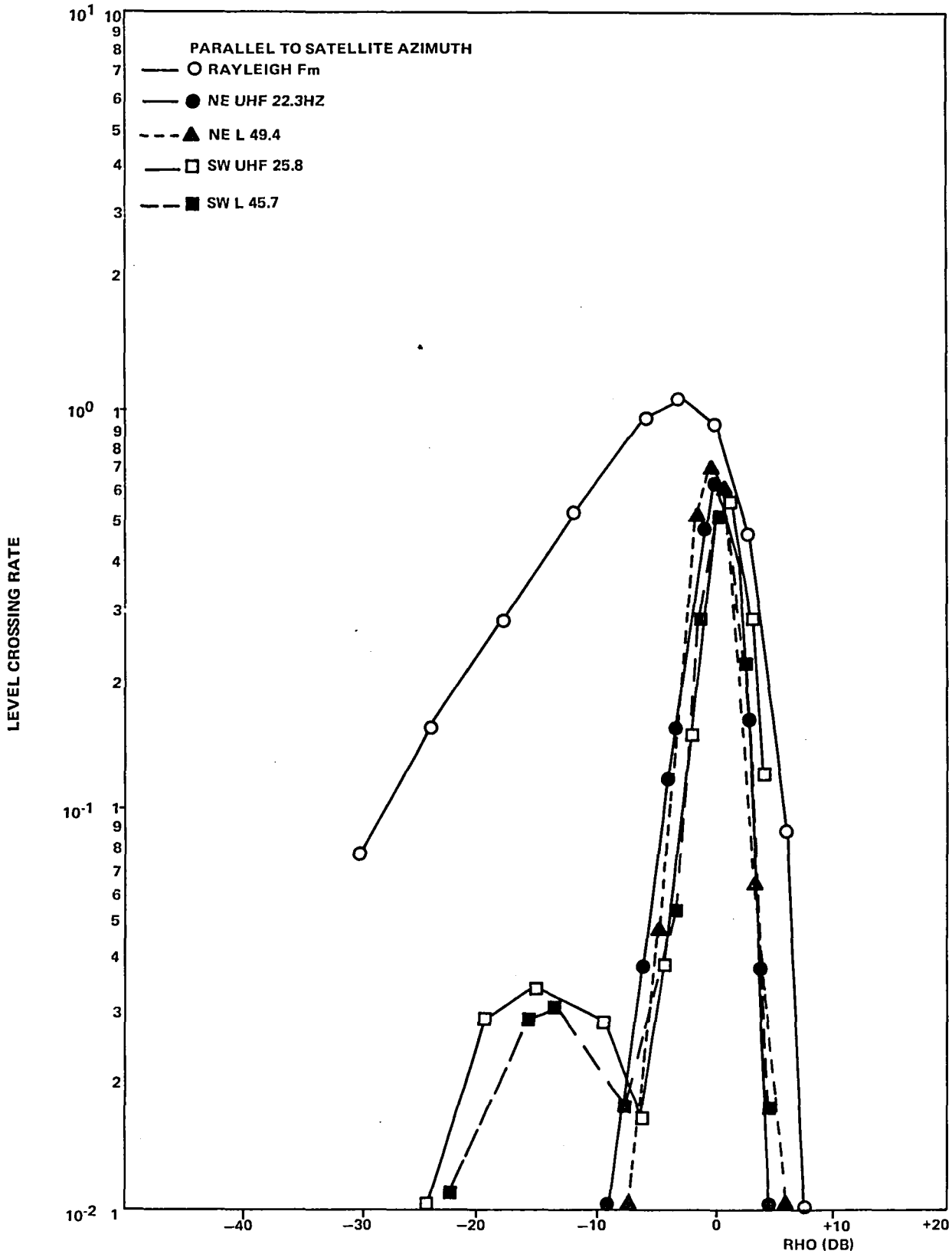

Figure 4-4. Normalized Level Crossing Rate: Urban Denver

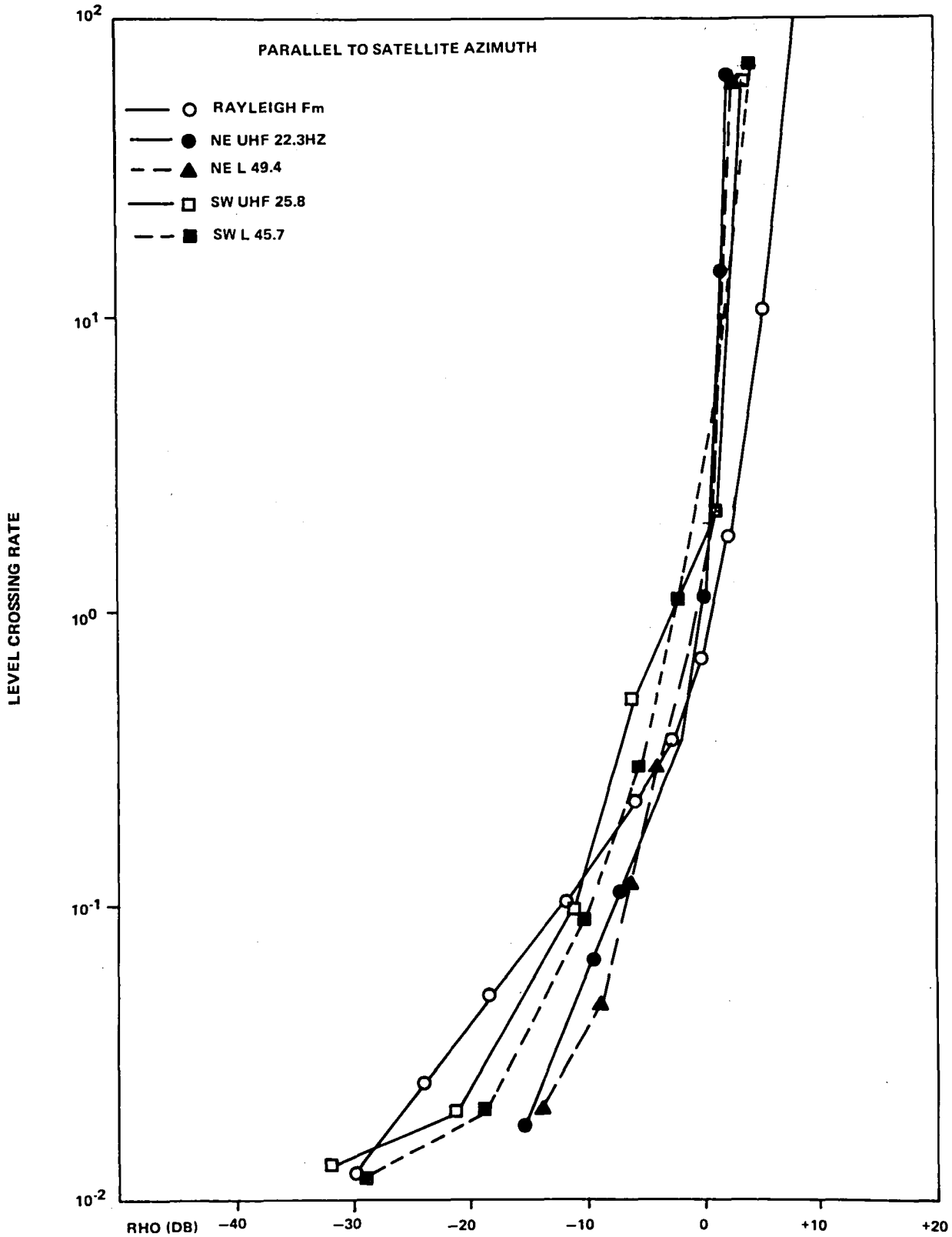

Figure 4-5. Normalized Average Fade Duration: Urban Denver

Land Mobile Terminal (G. E.)

The voice communication tests, which were conducted with the vehicles located in the Yosemite National Park, provided very good voice quality, which was exceptional considering the heavy forest and mountainous terrain encountered in the park area. These tests also demonstrated that successful voice communication could be obtained with a helicopter in flight over mountainous terrain. The trucking experiment yielded preliminary results indicating that practical mobile terminals could be built for operation by unskilled personnel in a commercial environment.

LAND MOBILE PATH LOSS

From the five experimental parameters that were evaluated, the local type of environment and the vehicle heading were the dominant factors in establishing the margins. An increase in excess path loss of only 1.5 dB resulted when the link frequency was increased from 850 to 1550 MHz. The elevation angle of the ground terminal to the satellite also had little effect on the path loss for an angular range from 19 to 43 degrees. The small scale signal behavior of satellite links had been identified as being different from the Rayleigh behavior commonly found in terrestrial links. Measured signal strengths were generally depressed relative to that which Rayleigh fading would give.

Part B

Experiments at 4 GHz to 6 GHz

CHAPTER 5

RADIO FREQUENCY INTERFERENCE MEASUREMENTS SYSTEM

EXPERIMENT OBJECTIVES

The objective of this experiment was to make measurements in geosynchronous orbit of the radio frequency interference (rfi) in the 5925 megahertz (MHz) to 6425 MHz frequency range caused by C-band terrestrial microwave relay systems and by other sources. The purpose of conducting these measurements was to demonstrate the feasibility of making rfi measurements from space and to provide a basis for further evaluation of frequency sharing between satellite telecommunication and terrestrial microwave systems. The specific objectives of this experiment were as follows:

- Determine the total power flux density of the rfi at geosynchronous altitude
- Determine the geographical and frequency distribution of the terrestrial emitters producing the rfi
- Establish maximum satellite gain/temperature (G/T) values that would permit satisfactory satellite system operation in the presence of in-orbit rfi (satellite uplink protection)
- Establish the minimum satellite power required for satisfactory operation of a satellite system in the presence of terrestrial rfi (downlink receiver protection)
- Investigate model utility by comparing the measurement results with a Government-generated mathematical model

BACKGROUND

The phenomenal growth of both space and terrestrial radio communications systems over the past 15 years or so produced a complex sharing problem in portions of the spectrum allocated to both space and terrestrial services. The potential of harmful interference between the two services is especially acute in the 5925-MHz to 6425-MHz common carrier band. In arriving at sharing criteria that would ensure compatibility between space and terrestrial systems, emphasis had been placed on the susceptibility of receiving systems on Earth to interference from transmitters on Earth or in space. The possibility of interference to receivers in satellites from emitters on Earth (which had generally been considered negligible as long as terrestrial antenna beams were not pointed directly at orbital regions) will progressively increase as future satellites incorporate higher gain receiving antennas and higher sensitivity front ends. In addition, the cumulative effect of increasing numbers of terrestrial transmitters will increase the total flux density at orbital altitudes. Because the level of radio frequency interference at orbital altitudes has a significant effect on the technical design and economics of future satellite communication systems, it is essential that basic information about expected interference levels be made available to future satellite communication system designers.

Recommendations of the International Telecommunications Union (ITU) directed toward space frequency allocations and frequency spectrum sharing contained criteria developed for global systems involving a relatively few, widely separated Earth terminals. It became evident that these criteria were insufficient for application to the United States domestic satellite systems being proposed. These proposals that were being submitted to the Federal Communications Commission (FCC) were predicated upon further sharing in the 6-gigahertz (GHz) and 4-GHz frequency bands by satellite and terrestrial microwave systems.

Predictions based upon frequency assignment data bases can provide mathematical models of the rfi environment. Much of the essential information however, such as detailed antenna sidelobe characteristics, modulation signatures, harmonic and spurious radiations of transmitters, and the operational habits and schedules of the potential rfi sources are generally unknown or are very unwieldy in a mathematical model. Hence, any such model must be supplemented by actual in-orbit measurements. With these facts in mind, the National Aeronautics and Space Administration ATS-6 RFI Measurement Experiment (RFIME) was conceived.

EXPERIMENT SUMMARY

At the time the RFIME was conducted, approximately 70,000 terrestrial microwave relay transmitters were operating within the Continental United States (ConUS) in the 5925-MHz to 6425-MHz frequency range (6-GHz band) with the transmissions directed parallel to the Earth's surface. Except for the rare instances in which a terrestrial antenna beam may intersect the geosynchronous orbit, the rfi at any point in the geosynchronous orbit is the result of terrestrial relay antenna sidelobe and Earth-reflected emissions toward that point. Another potential source of rfi at geosynchronous altitude in the 6-GHz band is harmonic radiation from high power radars operating at lower frequencies.

The RFIME used the ATS-6 prime-focus feed (PFF) 9.14-meter antenna using right-hand circular polarization that was directed earthward to receive these terrestrial emissions in the 5925-MHz to 6425-MHz band. Its high gain and its beamwidth of a little over one-third of a degree enabled suitable orientation of the spacecraft for geographical surveys over the ConUS and adjacent areas and of Hawaii and Alaska. The bulk of the measurements were conducted while ATS-6 was located above 94°W longitude during August 1974 and June 1975. A few measurements were made on four major metropolitan areas of the United States as they came into Earth horizon position during the earlier part of the drift phase toward 35°E longitude in mid-1975.

An rfi transponder aboard ATS-6 specifically designed for conducting RFIME was employed. This rfi transponder consisted of a low-noise 6-GHz receiver and a frequency translator that translated the entire 500-MHz wide 5925-MHz to 6425-MHz band received on the PFF antenna to the 3750-MHz to 4200-MHz frequency range. This band was subsequently amplified in the spacecraft C-band power amplifier and transmitted by the Earth-coverage horn to the 25.9-meter ATS-6 Earth terminal at the Rosman Ground Station in North Carolina, for processing by the RFIME Data Acquisition Facility (DAF). The combined rfi translator and C-band power amplifier had a dynamic range of about 40 decibel (dB), and the gain could be reduced by 22 dB in four commandable steps for measuring high rfi levels. The maximum sensitivity was such that terrestrial rfi down to the 10 decibels to 1 watt (dBW) level (-152.5 dBW/square meters (m^2) flux density at the spacecraft) could be processed with a signal-to-noise (S/N) ratio of 10 dB in a 10-kilohertz (kHz) bandwidth.

The DAF at Rosman employed a computer-controlled receiver and analyzer that was capable of several modes of operation. In the principal mode, mode 4 (77 percent of all rfi data collected), the DAF receiver was swept across the entire 500-MHz band in 500 seconds, dwelling on each 10-kHz segment for 10 milliseconds (ms) during which 39 samples of the received power were measured. The parameters digitally-recorded for later processing in this mode were the mean and variance of the signal power for each 10-kHz segment. Scanned in this mode were 168 footprints covering ConUS and adjacent southern Canada and northern Mexico, one footprint each for Hawaii and Alaska, and four horizon scans of the Chicago, Baltimore, Washington, New York, and New Orleans metropolitan areas. In addition, 44 of the major metropolitan areas considered to be the most likely candidates for future satellite Earth terminal locations were surveyed periodically.

Other rfi gathering modes included mode 5/11 (20 percent of the data collected) designed to detect hot spots using a continental antenna scan sampling with 100 kHz vice 10 kHz segments, and mode 8, an rfi source geographic location mode (2 percent of data collected), which was invaluable in performing spacecraft PFF antenna pattern measurements.

Mode 5/11 proved to be infeasible however. It involved analog recording of the data that were played back and digitized for mode 4 processing. Not only did difficulty develop in synchronizing the tape capstan speeds during playback, producing a frequency error of variable offset, but also the subsequent data processing time at Goddard Space Flight Center was very lengthy.

The remaining modes of operation involved calibration and noise measurements of the system. Calibration of the system was undertaken by employing a fixed calibration terminal (FCT) at Rosman. A portable calibration terminal (PCT) was housed in a van and deployed as needed to the particular geographic area being surveyed.

Altogether, the RFIME recorded 452 hours of data and produced 4073 files (all data).

The mode 4 ConUS scan resulted in an overall rfi density plot of 10-kHz segments that correlated basically with microwave link density. Some rfi existed though on some nonassigned frequencies. The maximum detected power level referenced to the ground was 23 dBW effective isotropic radiated power (e.i.r.p.) (-139.5 dBW/m^2 power flux density [PFD] at the spacecraft). Generally, the common carrier channels were near the threshold of detection (about -150 dBW/m^2). The mode 4 major metropolitan area surveys showed similar results with the PFD at the spacecraft reaching as high as -128 dBW/m^2. Unidentified wideband rfi sources were found in four distinct areas and represented potential sources of interference, occupying up to as much as 10 MHz of the spectrum. The detected common carrier frequency usage was generally consistent with that expected and confirmed the original prediction that many transmitters would have to occupy one antenna footprint region to produce a detectable rfi signal at geosynchronous altitude.

Basically, the first two objectives of the experiment were met, i.e., the rfi power flux density at geosynchronous altitude was measured and the geographical and frequency distribution, at least over the ConUS and adjacent regions, was determined. The estimated measurement accuracy of the PFD in terms of total root-mean-square (rms) error was -3.5 dB to +1.0 dB for monopulsed operations and -3.5 dB to +6.1 dB for nonmonopulsed operations. The major sources of error for both of

these operations were due to polarization error (-3.0 dB) and integrated source distribution error (-1.5 dB). For nonmonopulsed operation, boresight error of the spacecraft 9.14-meter antenna produced an estimated rms error of +6.0 dB. Analysis of data involving known PCT locations indicated that the geographic location of an rfi could be determined to an accuracy of 133 to 153 kilometers (km), the principal source of error was the misalignment of the antenna boresight axis with the spacecraft X-axis due to solar thermal deformation of the antenna surface.

Data were supplied to the cognizant agencies considering the third and fourth objectives, that of establishment of maximum satellite G/T ratios and minimum downlink power. No feedback occurred; therefore, the impact of the data in establishing these values was unknown.

The last objective, establishing model utility, was not accomplished because of circumstances beyond the control of NASA. Preliminary results about two of the smaller metropolitan areas indicated that while the measurements showed there was a general agreement based on existing terrestrial microwave link user populations, the modeling fell short because measured rfi occurred on unassigned frequencies and broadband rfi was evident from unknown sources.

The rfi transponder was used in orbit to measure the antenna patterns of a number of Intelsat Earth stations.

The remainder of the report is devoted to the experiment design, its detailed description, the methods of conducting the experiment, and the experimental results.

EXPERIMENT REQUIREMENTS

The following paragraphs summarize the derivation of the specific parameters of the Radio Frequency Interference Measurement Experiment (RFIME) that were required to meet the experiment objectives. See Reference 1 for details of the design.

The first step in the design process was to select one of two candidate general configurations that could be employed—one conducting the measurements using a processor aboard the spacecraft and the other conducting the measurements on the ground. The first of these had the advantage of requiring only a minimum downlink capability, because the measured parameters could be transmitted in a very small information bandwidth. The disadvantages of in-orbit signal processing were the high cost of developing and qualifying special purpose tunable microwave receiving equipment, the added command and telemetry complexity required, and the lack of adaptability to unexpected developments during the course of the experiment. Since a substantial satellite downlink capability had already been planned in connection with the other experiments, there was no advantage in performing in-orbit processing. Hence, the second configuration using a simple onboard frequency translator was selected.

The question then arose as to whether to employ a narrow or a wideband repeater. This question was settled in favor of using a 500-megahertz (MHz) wide repeater, since the 4-gigahertz (GHz) C-band power amplifier proposed for the satellite for other reasons, was capable of handling the greater downlink power required for the wideband approach.

The 9.14-meter (m) spacecraft prime-focus feed (PFF) parabolic antenna was admirably suited for receiving the 6-GHz terrestrial signals because of its high gain and the ability to direct its spot beam to particular geographic areas of interest by suitably orienting the spacecraft by ground commands. A 6-GHz to 4-GHz special purpose translator was used in conjunction with the spacecraft C-band power amplifier to transmit the entire 500-MHz spectrum by the Earth-coverage horn (ECH) back to Earth for reception by the 25.9-m Rosman Applications Technology Satellite (ATS) facility in North Carolina.

After reception by the ground receiver, it was proposed to amplify the received signals to minimize contamination by downlink noise, and to feed these signals to a computer-controlled spectrum analyzer. This analyzer measured the pertinent characteristics of the signals, such as frequency, power level, pulse width, and repetition frequency, and then encoded the measured quantities into a format suitable for recording. It was planned to provide a calibration terminal to relay 6-GHz uplink signals of known frequency and power level through the spacecraft and back to the receiver analyzer. Other data were to be introduced into the recorder, such as time signals for correlating the radio frequency interference (rfi) measurements with telemetry data on satellite orientation, orbit location, and transponder status.

As an adjunct to the receiver-analyzer, particularly during initial experiment debugging and the earlier stages of data collection, a quick-look procedure using a visual display was considered necessary to avoid data recording and processing delays.

The remainder of the design procedure consisted of establishing the spacecraft translator parameters, the up and downlink performance requirements, and the receiver-analyzer regimen. The succeeding subsections are devoted to summarizing the design criteria and establishing the parameter bounds requirements.

Minimum Detectable Effective Isotropic Radiated Power

In establishing the required RFIME sensitivity, a judgment was made as to the type of future communication satellite system that would be interfered with, and the level of interference that could be considered significant.

To arrive at a specific interference level that would be of interest, it seemed appropriate to select, as a typical highly interference-susceptible link, a hypothetical one with 24-voice channels employing frequency diversity modulation-frequency modulated (FDM-FM). There were a number of reasons for this selection, one was that many of the smaller country users would probably employ a low capacity link. The lowest significant level of interference in a baseband channel was chosen somewhat arbitrarily as 100 picowatts (pW). This level of interference would cause a 10 percent increase in the customary assumed 1000-pW uplink noise contribution, and represents 1 percent of the 10,000-pW International Radio Consultative Committee (CCIR) telephone channel noise allowance for a complete satellite link. It was further assumed that the uplink interference could be considered to be carrier wave (CW) because the common carrier microwave relay stations employ very low modulation index signals.

In an FDM-FM system, the level of interference in a baseband channel for a given level of radio frequency interference is a function of modulation index. The International Radio Consultative Committee multichannel loading formula was considered to be of doubtful validity for such a low capacity link. Consequently, the mathematical expressions were derived for uplink performance expected in the presence of an interfering CW signal plus thermal noise.

Current practice was (and still is) to define the link performance in terms of baseband noise level in the uppermost (worst) voice channel. Hence, it was convenient in formulating the performance dependence on modulation index to determine the level of radio frequency interference, I, required to produce a given level of interference-to-noise power ratio in the uppermost baseband channel using root-mean-square (rms) modulation index, m, as the independent variable. Parameters relating to the function of m are shown in Equation 5-1. The ratio minimizes at 1.38 near m = 1 and thus

$$\frac{I}{kT} = 1.38\left(\frac{I_{ch}}{N_{ch}}\right) f_m \tag{5-1}$$

k is Boltzman's constant
T is the receive system noise temperature
f_m is the receiver i.f. bandwidth

For 24 channels, f_m = 100 kHz, and (I_{ch}/N_{ch}) as previously stated was assumed to be 0.1. So, for the hypothetical system considered

$$\frac{I}{kT} = 1.38 \times 10^4 \text{ or } 41.4 \text{ dB-Hz} \tag{5-2}$$

Future satellite receiver system gain/temperature (G/T) values were predicted to approach a value of 5-dB/K. The ground transmitted effective isotropic radiated power (e.i.r.p.) at 6 GHz required to produce a particular I/kT at synchronous altitude is

$$\text{e.i.r.p.} = \frac{I}{kT} - \frac{G}{T} - 29 \text{ dBW} \tag{5-3}$$

this, for the hypothetical link considered and the assumptions made, works out to 10 dBW. In this way, the maximum required sensitivity of the RFIME was determined to be such that ground based rfi sources of as low as 10 dBW could be detected.

Dynamic Range

In establishing the dynamic range requirements of the RFIME, an estimate was made of the likelihood that a radio relay beam would intersect the synchronous orbit. This estimate was based on a study for the 3.7-GHz to 4.2-GHz band conducted by American Telephone and Telegraph Co.

(AT&T)* and corrected for the narrower antenna beamwidths employed at 6 GHz. It was determined that the probability of being illuminated by more than one beam was quite small, so the RFIME dynamic range requirement was based on a single illumination by a typical equipment, the AT&T TH System (5.9 GHz to 6.4 GHz). The result of the dynamic range requirements study indicated that the power amplifier traveling wave tube (TWT) would need to be backed off by 12.5 dB from saturated power output and that the dynamic range should be 43 dB above detection threshold. The downlink e.i.r.p. of the translator at this reduced power at 4 GHz using the spacecraft ECH was taken into consideration in arriving at the necessary downlink parameters to ensure that the RFIME system sensitivity would not be degraded by downlink noise.

To arrive at the TWT back-off requirement, the following factors and assumptions were taken into consideration to ensure that any intermodulation products produced in the repeater would be below the threshold of detectability in the RFIME receiver bandwidth.

- A maximum of 8 carriers per TH link in two groups of 4, each orthogonally polarized
- A TH transmitter carrier frequency tolerance of 100 kHz, preventing the piling up of intermodulation products on specific frequencies
- A 10-kHz frequency resolution of the RFIME spectrum analysis receiver, permitting frequency resolution of the intermodulation products
- The known relationship of the magnitude of intermodulation products between the n-carrier and 2-carrier cases for signals passing through a nonlinear device
- The empirical relationship of intermodulation product amplitude versus power output back-off of prototype Intelsat IV power amplifier TWT's based on measurements.

Satellite Power Output Requirements

The minimum required saturated power output of the repeater amplifier was determined to be 3 watts. At 12.5 dB power amplifier backoff, the resulting predetection carrier-to-noise density ratio at the ground receiver is 40 dB-Hz. The factors and assumptions used in arriving at these values are as follows:

- Unity signal-to-noise ratio in the RFIME receiver predetection bandwidth
- Post-detection filtering to develop the required signal-to-noise ratio
- Detectability criterion that does not result in an unreasonably long time to perform the experiment
- Search receiver minimum bandwidth of 10 kilohertz (kHz) as determined by residual frequency modulation (FM) on the microwave relay carriers

*CCIR Document IV/32-E; October 28, 1964.

- Gain/temperature (G/T) on the Rosman terminal of 40 dB/K
- Off-axis reduction in gain of the ECH
- TWT power back-off of 12.5 dB.

Repeater Noise Figure Requirement

The maximum noise figure of the satellite receiver was established to be 12.6 dB (5000 K receive system temperature) based on the following:

- An uplink carrier-to-noise density ratio 13 dB greater than that of the downlink or 53 dB-Hz (produced 0.2 dB degradation in the overall link)
- Satellite PFF antenna gain of 51 dB at 6 GHz.

Frequency Accuracy

The frequency stability of the terrestrial microwave links set the lower bound on the useful frequency accuracy of the RFIME. A long term accuracy of 0.25 MHz was originally specified for TH equipment, and this was being improved in a retrofit program. Terminals sold by Lenkurt Electric Company provided a long term stability of ±0.005 percent or ±0.3 MHz over a 20°C ambient temperature range, and probably were stable to ±0.001 percent over a few hours. It seemed reasonable that the RFIME should contribute no more than 10 percent of the short term inaccuracy of these signals, thus an accuracy requirement of ±25 kHz was established.

Frequency Resolution

Adequate frequency resolution was important to:

- Facilitate an accurate count of separate emitters
- Facilitate identification of emitters picked up on the spacecraft antenna sidelobes
- Achieve the required measurement sensitivity.

Terrestrial radio relays operate on a relatively small number of assigned frequencies with a long term frequency tolerance of 300 kHz. Since the same frequencies may be employed by several transmitters within the same spot beam, the frequency resolution should be substantially less than a few hundred kHz to resolve the individual signals.

Since it becomes difficult to reliably detect signals of less than unity signal-to-noise ratio in the predetection bandwidth with other than complex and expensive radiometer techniques, it is necessary to reduce the predetection bandwidth as much as possible to maximize the predetection signal-to-noise ratio.

The width of the signal spectrum imposes a limit to the increase in signal-to-noise ratio by decreasing predetection bandwidth. Radio relays use a low modulation index signal, so that most of the energy is concentrated in the vicinity of the carrier. Incidental FM on the TH carriers at that time amounted to a 12 to 15 kHz frequency spread of the carrier. Older equipment operating at a 10 to 15 dB lower power level than the TH used klystrons, that perhaps had a carrier spike broadened to 40- to 50-kHz width. The newer TH systems coming into use were estimated to have a spread of 1 kHz.

Considering the factors mentioned, an RFIME resolution capability of 10 kHz was considered adequate.

Amplitude Accuracy

The ultimate objective for RFIME amplitude accuracy was a measurement capability of ±1/2 dB. This capability appeared to be consistent with the general intent of measurement accuracy called out by regulatory agencies. Furthermore, it was thought that a capability for high measurement accuracy would be an important factor in the willing acceptance of the experiment conclusions. Since the experiment measurements could very well be used as a basis for specifying future satellite system parameters, any uncertainty in the results would reflect in the increased cost of implementing hardware that would have to perform to needlessly stringent criteria.

Angular Accuracy

The 0.4 degree beamwidth of the spacecraft PFF antenna established the basic achievable angular accuracy. Strong signals entering the antenna sidelobes were recognized to be a problem, but sophisticated means, such as using a guard antenna to separate and identify such signals, would involve doubling the measurement time, and would require a 1-meter dish that would create a severe installation problem aboard the spacecraft.

Solar thermal distortion of the PFF antenna turned out to be a problem. This possibility had not been considered in the prediction of achievable angular accuracy, or as a factor in achievable amplitude accuracy.

Required Frequency Search Time

Analysis of the various factors determining the required frequency search time led to an estimate of about 600 seconds to search the entire 500-MHz band. (Actually, the spectrum analysis receiver was implemented for about 500 seconds.) The search time of course could be reduced by operating the repeater at higher than nominal gain at the risk of overloading the repeater on strong signals.

The analysis commenced with the assumption of a minimum practical predetection signal-to-noise ratio of unity with conventional detector circuitry. This is the signal-to-noise ratio for 10 dBW rfi source in a 10-kHz intermediate frequency (i.f.) bandwidth. The assumption of a 16-dB postdetection signal-to-noise ratio and the use of a square law detector yielded the 600-second estimate. It was discovered that the use of a linear detector for the same signal-to-noise ratio would reduce the

required sweep time by a factor of 4.5, but the more important question remained as to which detector would perform the best for equal sweep times taking into consideration the tolerance of the threshold decision circuits to predetection gain variations during the frequency sweep.

Signal Detection Threshold Requirements

The minimum signal-to-noise ratio required at the detector output of the spectrum analysis receiver is determined by the allowable false alarm rate and the required probability of detection. Setting the average time between false alarms equal to the frequency search time, a 90 percent detection probability, and a unity predetection signal-to-noise ratio, the permissible short term predetection gain change for a 600-second sweep was found to be ±0.54 dB and ±0.95 dB respectively for a square law and a linear detector. The corresponding postdetection signal-to-noise ratios were 16 dB and 22.5 dB, respectively. The linear detector was recommended as a consequence of this analysis.

Pulse Detection Requirements

A pulse detector mode of operation was established as a requirement for RFIME, since there was a possibility of harmonic interference in the band of interest from high power radars operating at lower frequencies.

The sensitivity of RFIME to pulse signals is considerably less than the CW sensitivity, because of the wider i.f. bandwidth required to preserve the pulse shape. On the basis of 15 dB predetection signal-to-noise required (vice 10 dB for CW signals) and a 2-MHz i.f. bandwidth (vice 10 kHz for CW signals), the minimum detectable level of rfi would be 48 dBW vice 10 dBW for CW sources. The 2-MHz bandwidth would accommodate the 1 microsecond (μsec) or greater pulse widths of most L-band and S-band radars. Improved sensitivity to 23 dBW could be obtained against radars with a greater pulse width by reducing the i.f. bandwidth to 200 kHz and increasing the repeater gain by 15 dB above nominal. It was conjectured that the increased sensitivity would be adequate to pick up the harmonics of those larger search radars (having about 70 dBW fundamental) that did not employ harmonic filtering.

A search time of about 125 seconds was estimated for an i.f. signal-to-noise ratio of 15 dB, and the tolerance to short term gain instabilities was found to be ±0.9 dB.

Repeater Requirements Summary

Repeater G/T

In considering that the RFIME should be capable of detecting sources having an e.i.r.p. as little as 10 dBW, a repeater antenna gain of 51 dB and receiver noise temperature of 5000 K (12.6 dB noise figure) for a G/T of 14.0 dB/K were postulated as being required. However, in assessing the attainable performance of the PFF antenna, it was estimated that as a practical matter, a net gain of only 47.4 dB could be realized after accounting for losses due to the feed, transmission line, and to the feed and spar blockages. To provide a measure of design safety margin, a maximum receiver

noise of 7 dB was recommended that would have yielded a G/T of 15.8 dB/K. (As a matter of interest, a preflight measured value of 14.5 dB/K and an in-orbit measured value of 11.5 dB/K were achieved.)

To meet the noise figure requirement, a tunnel diode preamplifier was required followed by a tunnel diode amplifier (TDA) stage of sufficient gain to mask the noise contribution by the power amplifier TWT driver stage that had a noise figure of approximately 17 dB.

Repeater Gain and Wideband Noise Output

As stated previously, the required carrier-to-noise density was 53 dB-Hz to establish the threshold of detection for ground sources at a level of 10 dBW e.i.r.p. The repeater input signal power at this level was -139 dBW. The repeater power output worked out to be approximately -50.5 dBW for this threshold input signal level assuming a minimum required 3 watts saturated output power, a back-off of 12.5 dB, and a dynamic range of 43 dB. Thus, the repeater gain required was -50.5 minus -139 or 88.5 dB. It was recommended that additional gain be provided in steps that could be commanded from the ground.

The repeater noise output was estimated to be -15.5 dBW, some 20.5 dB below the minimum required saturated output, based on a repeater noise temperature of 5000 K, an 88.5 dB gain, and a noise bandwidth of 600 MHz.

Ground Subsystem Requirements Summary

Spectrum Analysis Receiver and Recorder

The basic functions that were to be provided by the receiver were as follows:

- Tune across the 500-MHz wide radio frequency band of interest
- Detect and measure the characteristics of the received CW and pulse signals of such a level to meet the detection criteria discussed earlier
- Read out the results of these measurements into a suitable data format compatible with subsequent data processing
- Conduct the measurements to the accuracy required as previously developed
- Recognize and record data on special RFIME system calibration signals
- Provide a panoramic frequency display
- Provide manual control of sweep rate, sweep limits, pre- and postdetection bandwidths, threshold sensitivity, etc.

- Provide a control unit separate from the microwave receiver portion
- Provide a visual readout of the measured quantities.

In-Orbit Calibration

A number of calibration source techniques were considered, including the use of a broad spectrum signal, a comb spectrum, and a tunable signal slaved to the computer controlling the spectrum analysis receiver. The broad spectrum technique would have required about 2 kilowatts (kW) into a 25.9-meter antenna with little or no system margin. The question arose concerning whether the Rosman terminal would be legally permitted to radiate such a high e.i.r.p. The comb spectrum technique was rejected on the basis of complexity; however, it was seriously considered for the Portable Calibration Terminal, since it would not have needed to be slaved to the spectrum analysis receiver.

The third technique, the one using the tunable source slaved to the spectrum analysis receiver, was selected for both the Fixed Calibration Terminal and the Portable Calibration Terminal once a remote slaving technique had been developed.

EXPERIMENT DESCRIPTION

Figure 5-1 shows the distribution of the terrestrial 4-gigahertz (GHz) and 6-GHz point-to-point common carrier microwave relay links and terminals across the continental United States. This microwave grid was made up of a series of straight line segments, with each segment representing a link of approximately 60 kilometers (km) in length. At each end of each link was a terminal that might have as many as 16 transmitters. As a result, there were more than 80,000 such common carrier-transmitters operating in the United States and Canada. Table 5-1 lists the top thirty 6-GHz common carrier frequency assignments in the United States by transmitter density.* These terrestrial transmissions were directed parallel to the Earth, using an antenna with a gain of approximately 40 dB in the main lobe and approximately 10 dB in the side lobes. The power received from these transmissions at ATS-6, while positioned above 94°W longitude, was, therefore, the summation of the signals received from terrestrial antenna side lobe radiation and main lobe reflections. It was postulated that many such transmissions, all located within a single antenna footprint of ATS-6, would be required to have sufficient integrated signal power to be detectable at the satellite.

The experiment methodology to measure the radio frequency (rf) signals at synchronous altitude basically consisted of the following:

- Point the prime-focus feed (PFF) 9.14-meter parabolic antenna (47.5 dB gain) to a quiet area of the Earth's surface and record the Earth background noise across the 5.925-GHz to 6.425-GHz spectrum in 100-kHz increments. This procedure was designated Mode 2.
- Point the PFF antenna to center on a calibration terminal and record calibrated signals across the spectrum in 100-kHz increments. This procedure was designated Mode 3.

*1974 Electromagnetic Compatibility Analysis Center data

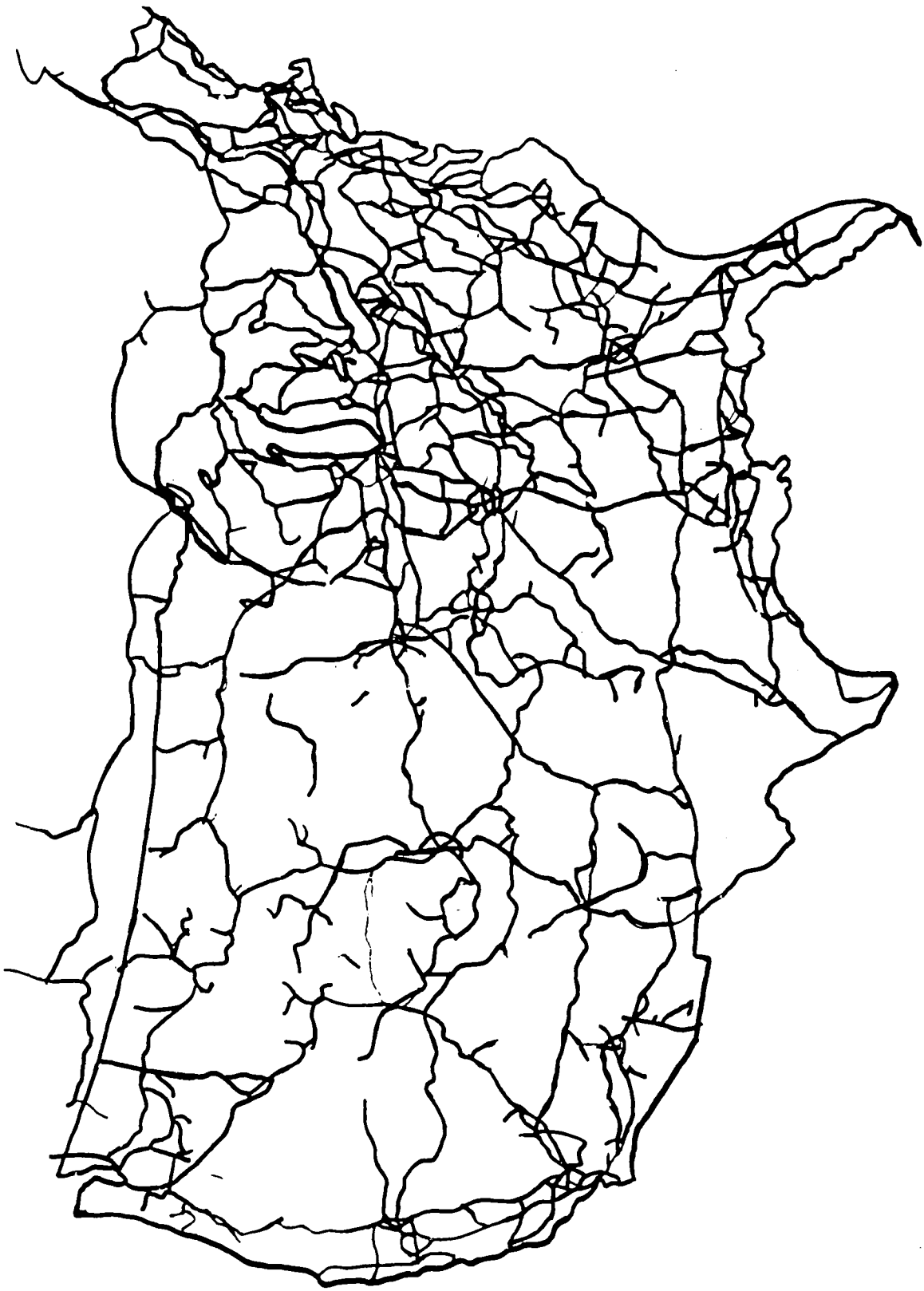

Figure 5-1. Existing Microwave Links (4 and 6 GHz)

Table 5-1
Common Carrier Frequency Assignments (5925 to 6425 MHz)
and Number of Transmitters per Frequency (Ref. 2)

Data Base: ITS Boulder, Colorado, 1974 for ConUS, Hawaii, Alaska, Canada*

	Freq. X 10^6 (Hz)	Number of Transmitters		Freq. X 10^6 (Hz)	Number of Transmitters
f_1	5925.5	3176	f_{16}	6034.2	2811
f_2	6177.5	3159	f_{17}	6123.1	2801
f_3	6226.9	3077	f_{18}	6375.2	2770
f_4	5974.8	3027	f_{19}	6424.5	2599
f_5	5945.2	2985	f_{20}	6172.5	2591
f_6	6197.2	2971	f_{21}	5930.4	706
f_7	6345.5	2921	f_{22}	6182.4	693
f_8	6093.5	2898	f_{23}	5960.0	571
f_9	6404.8	2897	f_{24}	6019.3	556
f_{10}	6063.8	2890	f_{25}	6241.7	554
f_{11}	6315.9	2881	f_{26}	6078.6	553
f_{12}	6286.2	2850	f_{27}	6108.3	546
f_{13}	6152.8	2846	f_{28}	6390.0	543
f_{14}	6004.5	2833	f_{29}	6330.7	543
f_{15}	6256.5	2813	f_{30}*	5989.7	538

*There were 469 additional frequency assignments (1974) ranging in transmitter density from 537 to 1, with the majority of the frequencies having less than 5 transmitters.

- Point the PFF antenna to a selected area to be surveyed for radio frequency interference (rfi), preferably to an area colocated or near the calibration terminal, and record the received signals and noise across the spectrum in 10-kHz increments. This procedure was designated Mode 4.

- Analyze the portions of the rfi recordings that exceed a predetermined threshold above the level of the Earth background recording.

$$\frac{\text{Mode 4}}{\text{Mode 2}} \geqslant k$$ where k is a preselected threshold (4 dB, 6 dB, etc.)

- Upon exceeding the preset threshold k, compute the detected signals' e.i.r.p. by the relation:

$$\text{Signal (dBW)} = \text{Calibration Terminal (dBW)} + 10 \log \frac{\text{Mode 4}}{\text{Mode 3}}$$

Experiment Configuration

Figure 5-2 illustrates the Radio Frequency Interference Measurement Experiment configuration. The system consisted of five principal components:

- ATS-6 spacecraft configured in the radio frequency interference (rfi) mode
- Rosman Data Acquisition Facility
- 6-GHz fixed calibration terminal colocated at Rosman Data Acquisition Facility
- 6-GHz portable calibration terminal
- Central processing facility at Goddard Space Flight Center.

Applications Technology Satellite-6

Applications Technology Satellite-6 (ATS-6) was the first NASA 3-axis stabilized synchronous satellite using momentum wheels and jets. The stabilization system made feasible the use of a deployable 9.14-meter prime-focus feed (PFF) parabolic antenna for reception of low-level rfi signals at 6-GHz; an Earth-coverage horn transmitted the rfi data signals to the Rosman Ground Station at 4 GHz.

The use of the large antenna, providing a G/T of 12 dB/K, some 28 dB higher than that generally used on geostationary communication satellites, enabled detection of 6-GHz terrestrial signals radiating as low as 10 dBW e.i.r.p. toward ATS-6. The prime-focus feed was designed to permit selection of any of four polarization modes: horizontal, vertical, right-hand circular, or left-hand circular. Most of the data taken in the RFI Experiment used the right-hand circular polarization antenna configuration to eliminate large reductions in received signal levels that might have resulted if linearly polarized rfi sources happened to be orthogonal to the PFF linear polarization.

The spacecraft rfi mode consisted of interfacing the 6-GHz rfi receiver with the 4-GHz communication transmitter. This configuration was selectable on command from the Rosman Data Acquisition Facility and when accomplished, transponded the 5.925-GHz to 6.424-GHz band to 3.7 GHz to 4.2 GHz. The rfi transponder in this configuration is shown in Figure 5-3. All of the amplifiers shown in the figure operated in a linear mode, permitting an rfi source to be translated to an output signal directly proportional to the input level. Thus, the levels of the rfi sources were measured by comparison to uplink calibration signals transmitted from the fixed or portable calibration terminals.

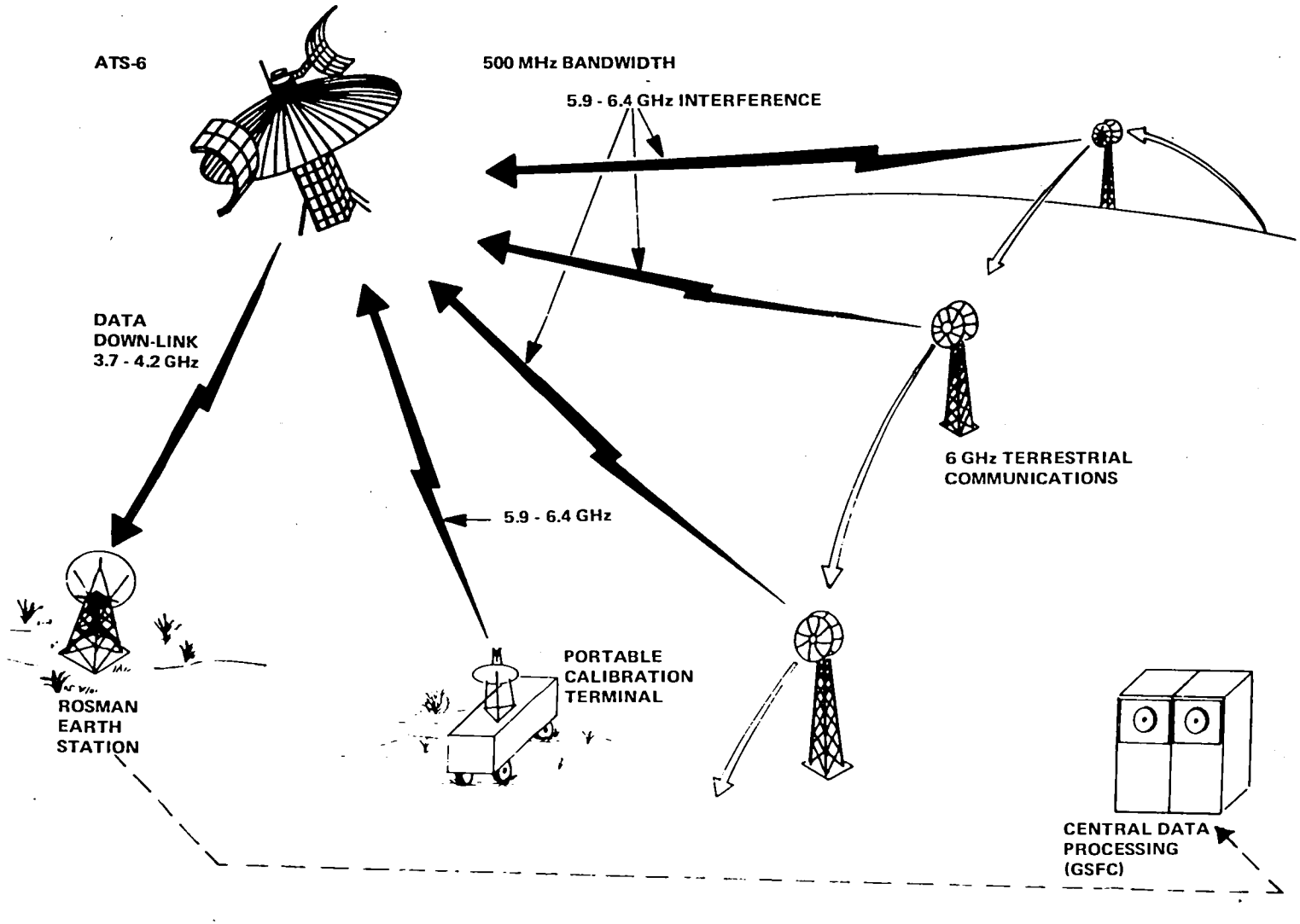

Figure 5-2. Radio Frequency Interference Measurement Experiment Configuration

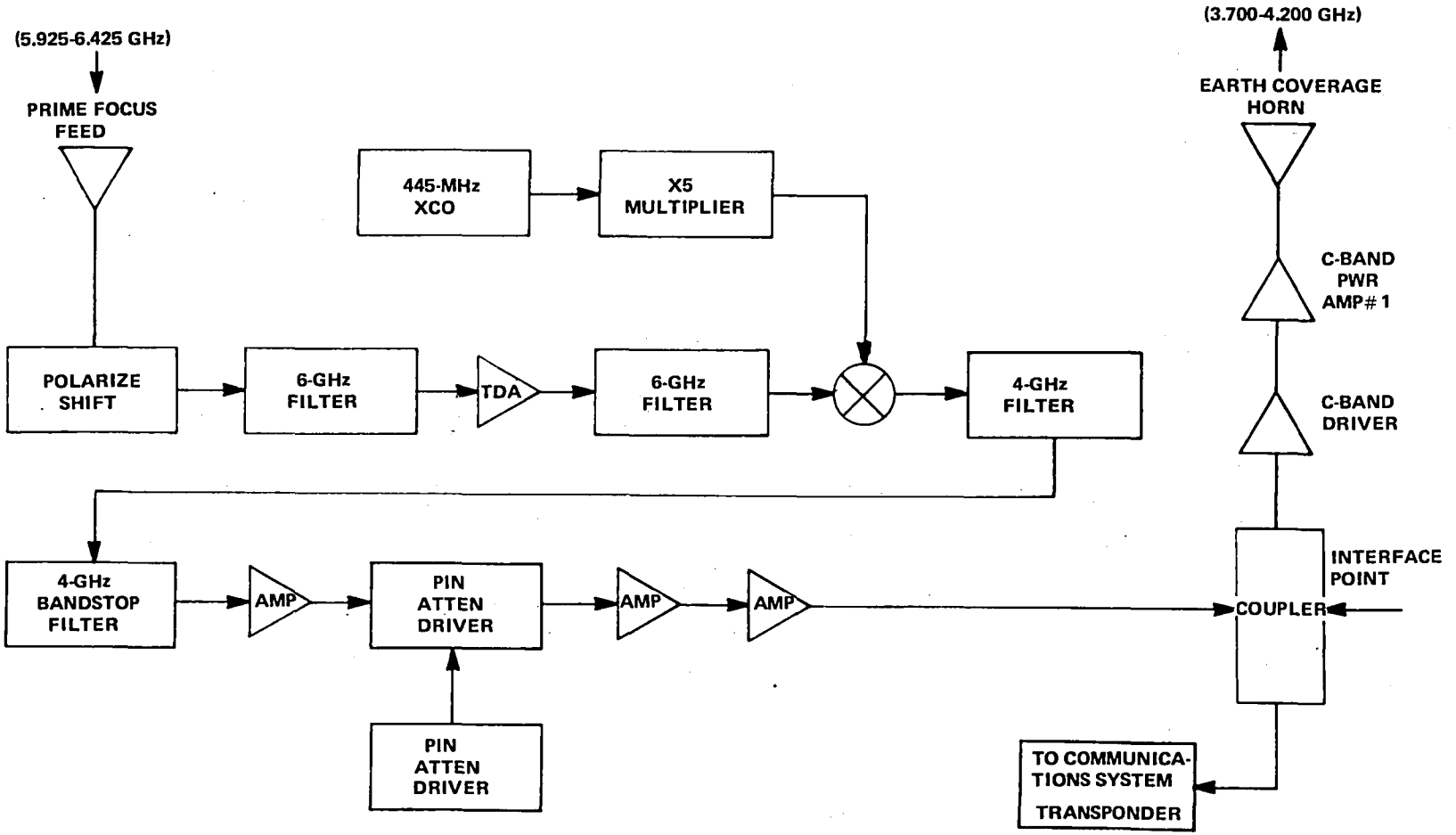

Figure 5-3. Radio Frequency Interference Measurement Experiment Transponder

The Rosman Ground Station Data Acquisition Facility (Reference 3)

The Rosman Ground Station Data Acquisition Facility (DAF) received and preprocessed the 500-MHz band between 3.7 and 4.2 GHz. The combination of the 25.9-meter antenna and low noise amplifier provided a G/T of about 39 dB/K. The downlink contributed very little noise to the experiment, so that the system sensitivity to rfi sources was virtually determined by the spacecraft receiving system.

The receiver/analyzer subsystem shown in Figure 5-4 provided the following functions:

- Generated the local oscillator frequencies used to receive rfi signals; transmitted synchronizing signals for calibration, and provided other test signals
- Downconverted the rfi signals to a fixed frequency by a stepped scan across the 500-MHz band
- Detected the characteristics of the input signals as to carrier wave, pulse-code modulation, peak values, and pulsed functions
- Detected the level of the signals in a bandwidth selectable (10 kHz and 100 kHz) linear detector (LD)
- Generated the time basis for signal conversion, signal processing, and analysis
- Provided analog-to-digital (A/D) conversion of signal data for computer interfacing and digital recording.

A PDP-11 computer system controlled the sequence of operations, analyzing and storing the signal data, and monitoring selected spacecraft telemetry items.

The Fixed Calibration Terminal

The Fixed Calibration Terminal, colocated with the rfi data acquisition equipment at Rosman Ground Station, consisted of a 1.83-meter antenna assembly and a power-calibrated 6-GHz transmitter. It was capable of transmitting signals in the 5.925-GHz to 6.425-GHz band at calibrated effective isotropically radiated power levels of 10 dBW, 20 dBW, and 30 dBW with a frequency accuracy of ±60 Hz (24-hour stability). In conjunction with the control circuitry in the rfi receiver/analyzer previously described, it could be stepped across the band in synchronization with the data acquisition timing to obtain the frequency-amplitude response of the total RFI Experiment system.

The Portable Calibration Terminal

The Portable Calibration Terminal was similar to the Fixed Calibration Terminal, but was housed in a mobile van, so that it could be moved to the center of an area to be surveyed. It provided a beacon for accurate spacecraft antenna pointing and furnished precise calibration signals. Synchronization

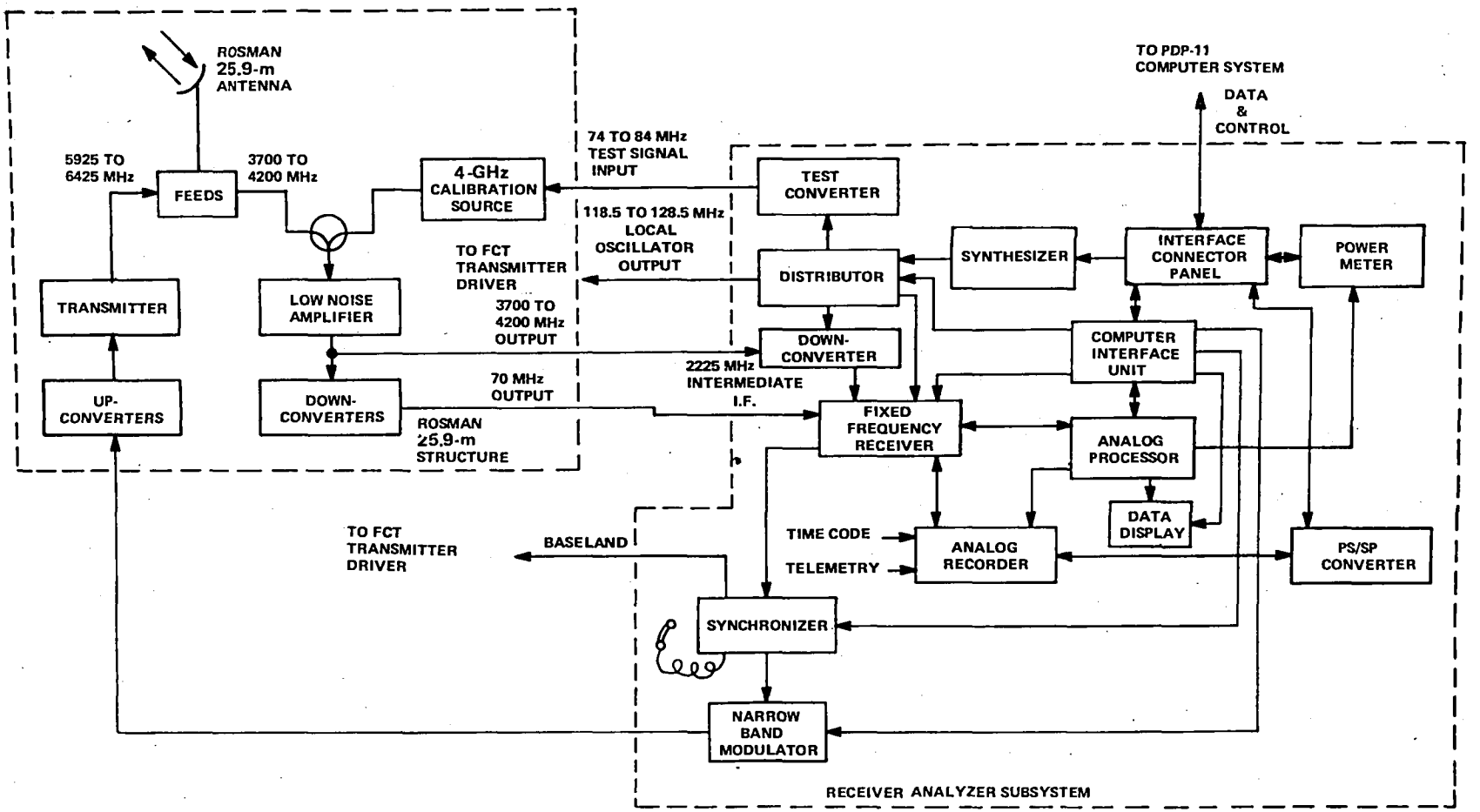

Figure 5-4. Rosman Ground Station DAF Block Diagram

with the Rosman data acquisition receiver was accomplished by a narrowband microwave link through the ATS-6 transponder.

RFIME Central Processing Facility

The RFIME Central Processing Facility was located at Goddard Space Flight Center (GSFC). Using an IBM 360/95 computer, data that were acquired at the Rosman DAF were automatically reduced to a more manageable collection of experiment measurements and converted to various formats that facilitated analysis.

RFIME digital data magnetic tapes, recorded at the DAF, were sent to GSFC where they were processed through a system of unique computer programs that produced a variety of presentations and stored results. A multiple stage processing procedure was employed, producing intermediate graphical and printed listing of various parameters of interest for analysis. The processing objective was the isolation of detected rfi radiating sources and their descriptions according to a derived set of measurement parameters. The collection of all detected sources derived from the experiment data was retained on an RFIME data base that could be automatically manipulated and accessed through a unique RFIME data base management system for further analysis and study.

Overall System Parameters

The overall RFIME system parameters are summarized in Table 5-2.

DATA COLLECTION

The following paragraphs describe the function of each of the RFIME data acquisition modes used in the experiment and the amount and type of data collected within each mode.

During each data acquisition mode, the received signal power was detected, sampled, and recorded on magnetic tape. Figure 5-5 shows the spacecraft link configuration and the data flow used throughout the experiment. In each mode, except Mode 5, the received signal power was sampled 39 times (x_i), every 10 milliseconds (msec) by the analog-digital (A/D) converter from which the mean ($\overline{x}$) and the sum of the squares (Σx^2) for each 10-msec interval was recorded. Figure 5-6 depicts the timing and recording format for the digital processing during acquisition. Mode 5 signal power was detected and analog recorded for digital processing at a later date.

ATS-6 Radio Frequency Interference Measurements Experiment (RFIME) data were recorded and collected throughout August 9, 1974 to June 11, 1975, when the satellite passed over the horizon. During this time span, approximately 1000 satellite hours were dedicated towards the collection of RFIME data, which resulted in approximately 450 hours of raw RFIME data stored on tape. All of these data were recorded by the various RFIME modes described in the following paragraphs, i.e., Modes 1A, 1B, 2A, 2B, 3A, 3B, 4, 5, 8, and 11. Table 5-3 summarizes the amount of collected data for each RFIME mode.

Table 5-2
RFIME System Parameters

System and Interface Parameters	
Receive carrier frequencies band	5925 to 6425 MHz
Transmit carrier frequencies band	3700 to 4200 MHz
Carrier modulation:	
• Relay of calibration tone and antenna pattern measurements	CW
• Relay of synchronization tone	FM
Field of view (FOV) e.i.r.p. Earth-coverage horn (saturated TWT)	26.7 dBW
Transponder rec. figure of merit	11.5 dB/K
Transponder rf bandwidth	500 MHz
Transponder gain setting (Selectable)	92.4 dB, 101.2 dB, 105.4 dB, 111.8 dB, 114.6 dB
Portable or Fixed Calibration Terminal Parameters	
Receiving system performance factors (3950 MHz, nominal):	
• Gain (1.83-m antenna)	34.5 dB
• Line losses	-1.0 dB
• Noise figure	5.0 dB
• Receiver noise power density	-204.2 dBW/Hz
• Receiver bandwidth settings	10 kHz, 100 kHz, 1 MHz
• System threshold	+10 dBW
Transmit system performance factors (6150 MHz, nominal):	
• Gain (1.83-m antenna)	38.0 dBi minimum
• E.i.r.p. (calibration tone)	30.0 dBW or 20.0 dBW or 10.0 dBW or 30.0 dBW
Rosman Ground Station Parameters	
Receiving system performance factors (3950 MHz nominal):	
• Gain 26-m (including line losses) 3700 MHz	57.5 dBi
• Gain 26-m (including line losses) 4200 MHz	58.1 dBi
• System noise temperature (45° East longitude)	89.87 K
• Noise spectral density	-209.1 dBW/Hz
• System threshold	+13.0 dB
Transmit system performance factors (6150 MHz, nominal):	
• Gain (including line losses)	29.0 dB
• E.i.r.p. (8 kW maximum)	98.0 dBW

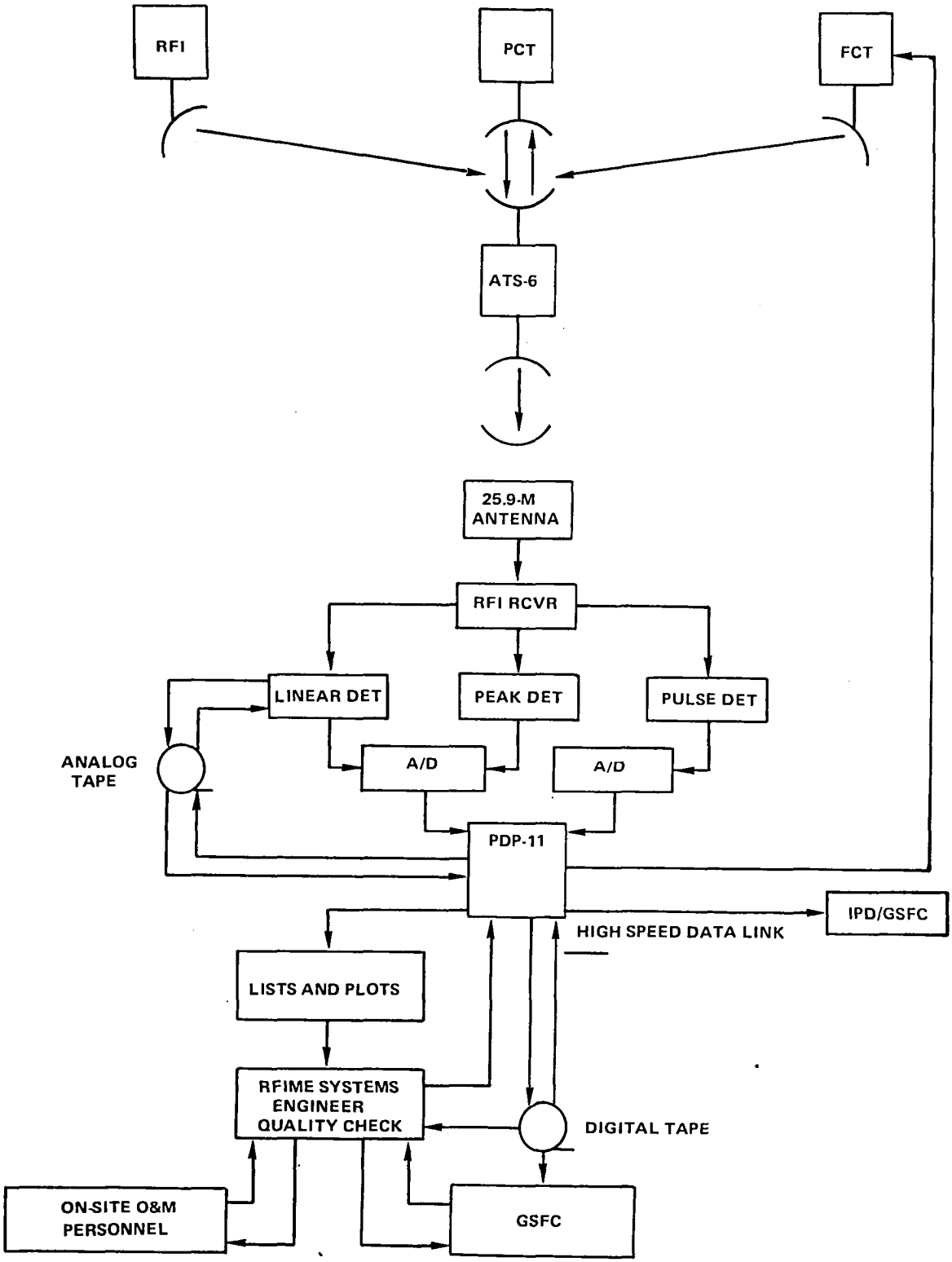

Figure 5-5. Spacecraft Link Configuration/Data Flow

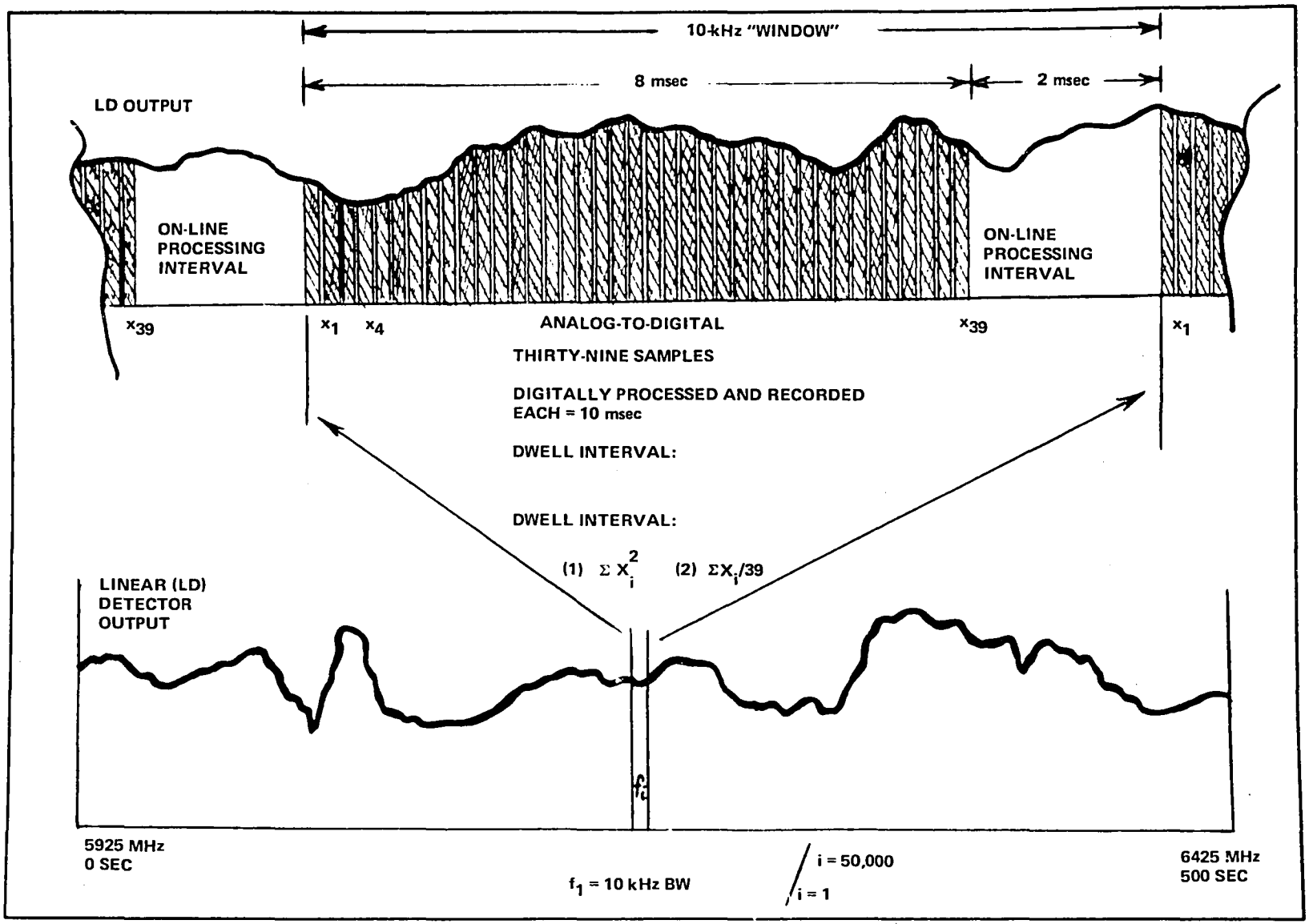

Figure 5-6. RFIME Timing and Records (Mode 4)

Table 5-3
RFIME Summary—Data Collection

Mode	Data Collected	Recording Time
Mode 1	17 files (500 sec/file)	142 min
Mode 2	115 files (50 sec/file)	96 min
Mode 3	776 files (50 sec/file)	647 min
Mode 4	2433 files (500 sec/file)	20,275 min
Mode 5	21 analog tapes	(See Mode 11)
Mode 8	68 files (500 sec/file)	567 min
Mode 11	643 files (500 sec/file)	5,358 min
	Total	27,095 min (452 hr)

Mode 1—Local RFI Measurement, 3700 to 4200 MHz

This mode was designed to determine if any detectable signals were being received in the downlink band from sources other than ATS-6. This information was needed to ensure that the power spectral density of any part of the 500-MHz band was not being biased by any other radio frequency interference (rfi) source than those observed by the satellite antenna.

A Mode 1A was used to search the 500-MHz band of the receiver to detect any rfi signals generated only by the equipment located at Rosman. This was accomplished by switching the Rosman parametric amplifier into a cold load. A Mode 1B was used to search the 500-MHz band of the receiver to detect any rfi signals received by the Rosman 26-meter antenna when ATS-6 was not transmitting to Rosman.

Only a limited amount (17 files) of Mode 1 data were collected and recorded over the data gathering period. This was because of the diagnostic function of this mode and the minimal variations encountered within the Rosman receive system that the mode was designed to evaluate. Both Modes 1A and 1B were periodically used to measure the overall system response of the Rosman receive terminal and to determine any signal interferences that could be originating or entering at Rosman. Initial and subsequent Mode 1 recordings indicated the Rosman receive terminal to be quiet and generally consistent; however, over the span of the experiment, infrequent adjustments to the antenna parametric amplifier (PARAMP) necessitated the use of this mode for diagnostic purposes.

Mode 2—System Noise Measurement

This mode was designed to measure the total noise floor or noise background of the total rfi system including the spacecraft subsystem. The noise level measured included noise from the Earth and atmosphere that was received by the satellite and transmitted to Rosman, in addition to noise from

the Earth and sky received by the 26-meter antenna at Rosman. These data were used to determine the sensitivity of the rfi receiver system and to establish detection thresholds for signal data taken in other modes. Generally, Mode 2 data were recorded when the ATS-6 9.14-meter antenna was pointed at an Earth location found to be relatively free of rfi signals.

A Mode 2A was performed to measure the noise level of the receiver system when the 10-kHz bandpass predetection filter was used. In this mode, the downconverter was stepped through the 500-MHz band in 10-kHz steps and $\bar{x}$, Σx^2, Greenwich mean time (GMT), and frequency were recorded. A Mode 2B was performed similar to Mode 2A except that a 100-kHz bandpass predetection filter was used. Thus, Mode 2A established the receiver system sensitivity during a Mode 4 data acquisition and Mode 2B established the receiver system sensitivity during a Mode 5 data acquisition.

Mode 2 data collection was also limited in scope, because it was determined relatively early in the experiment that only a very small percentage of the Mode 2 recordings could be smoothed by the smoothing software and that the off-line source determination processing would therefore be conducted with only a few selected Mode 2 files. Additionally, the operational time required to slew the spacecraft pointing axis to a quiet area, record a Mode 2, and then slew the spacecraft pointing axis back to a selected point in ConUS, was considered unjustified on a routine basis. Nearly all of the Mode 2 recordings were therefore conducted early in the data gathering phase of the experiment.

Mode 3—System Calibration

To ensure that long term fluctuations in system gains and losses did not affect the accurate measurement of unknown rfi sources, a Mode 3 calibration mode was performed before, during, and after any series of rfi data acquisitions. Thus, Mode 3 was used to measure the output of the rfi receiver system for known uplink transmitted power levels. During each Mode 3, a calibration transmitter of known effective radiated power output was stepped in 100 kHz steps through the 500-MHz band. The downconverter of the rfi receiver was also stepped in 100-kHz steps using the 10-kHz predetection bandpass filter in the rfi receiver/analyzer. The uplink transmit frequency was synchronized with the downlink detected frequency by a 4-kHz tone burst transmitted from Rosman to the calibration terminal that started the frequency step sequence. As in the other modes, $\bar{x}$, Σx^2, GMT, and frequency were digitally recorded. When the Portable Calibration Terminal (PCT) was used, the calibration mode was referred to as Mode 3A. When the Fixed Calibration Terminal (FCT) at Rosman was used, the calibration mode was referred to as Mode 3B.

Mode 3 calibrations were conducted and recorded throughout the experiment with an operational goal of recording a valid calibration at both the beginning and the end of each RFIME data tape. This goal was generally achieved except when both the FCT and the PCT were inoperative because of malfunctions. In most data gathering intervals, however, one or both of the calibration terminals were operational and Mode 3A and 3B recordings were conducted as evidenced by the 776 recorded files of Mode 3 data.

During the latter phases of data collection, the FCT was inoperative for a prolonged interval because of traveling wavetube failure and the PCT also experienced automatic sequencing problems. To acquire some form of calibration on each data tape under these circumstances, an improvised PCT

calibration was developed. This procedure consisted of the PCT radiating at eight preselected frequencies (manually operated) during a Mode 4 recording.

Mode 4—Computer Processed RFI Measurement

This mode was the primary source of rfi data for the ATS-6 RFIME. It was designed to measure the radiated power from rfi sources in the 5.925-GHz to 6.425-GHz band for specific pointings of the ATS-6 9.14-meter antenna. The timing and recording sequence was as shown in Figure 5-6. During the run of each Mode 4, the rfi receiver downconverter was stepped in increments of 10 kHz. The downconverter dwelled at each step for 10 msec, which was sufficient to acquire 39 samples from the linear detector and change frequency to the next adjacent 10-kHz band. The detector outputs represented the signal level within the 10-kHz predetection filter used during this mode. The data recorded for each 10-kHz band included $\bar{x}$, Σx^2, GMT, and frequency.

As the primary RFIME data collection mode, Mode 4 accumulated a total of 20,275 minutes of recorded data and comprised 75 percent of the total RFIME data. Because of the somewhat limited availability of ATS-6 for RFIME data collection, three major Mode 4 operational procedures were developed and implemented over the first year of ATS-6 operation. They were:

- Major metropolitan areas were periodically viewed over the life of the experiment, because these areas were considered to be likely candidates for future satelliite communication Earth terminal locations. These metropolitan areas and their associated footprints are depicted in Figure 5-7 with ATS-6 above 94°W longitude.

- A sector scan of the ConUS was conducted covering the footprint areas as depicted in Figure 5-8 with ATS-6 at 94°W longitude.

- In addition to the two operational procedures stated above, a supplemental Mode 4 operational procedure was proposed and developed for use when ATS-6 was in transit from its 94°W longitude position to its later position above 35°E. The goal of this portion of the RFIME experiment was to obtain data about selected metropolitan areas when the satellite was on the "horizon" and some of the terrestrial microwave links located within a footprint would therefore be radiating directly towards the satellite. Although the scope of this portion of the experiment was quite limited because of spacecraft operational priorities, a limited amount of horizon scan data were accumulated and the projected antenna footprints of the acquired ConUS horizon scan data are depicted in Figure 5-9 with ATS-6 drifting toward 35°E.

Table 5-4 lists the actual RFIME data recorded during August 1974 to June 1975 in support of the three procedures previously stated. This table lists the number of files of data collected by location (antenna boresight intercept). One file represents one complete 500-MHz frequency scan lasting 500 seconds.

A few selected Canadian and Mexican metropolitan areas were also periodically viewed by Mode 4 procedures during the experiment. A list of these scans is shown in Table 5-5.

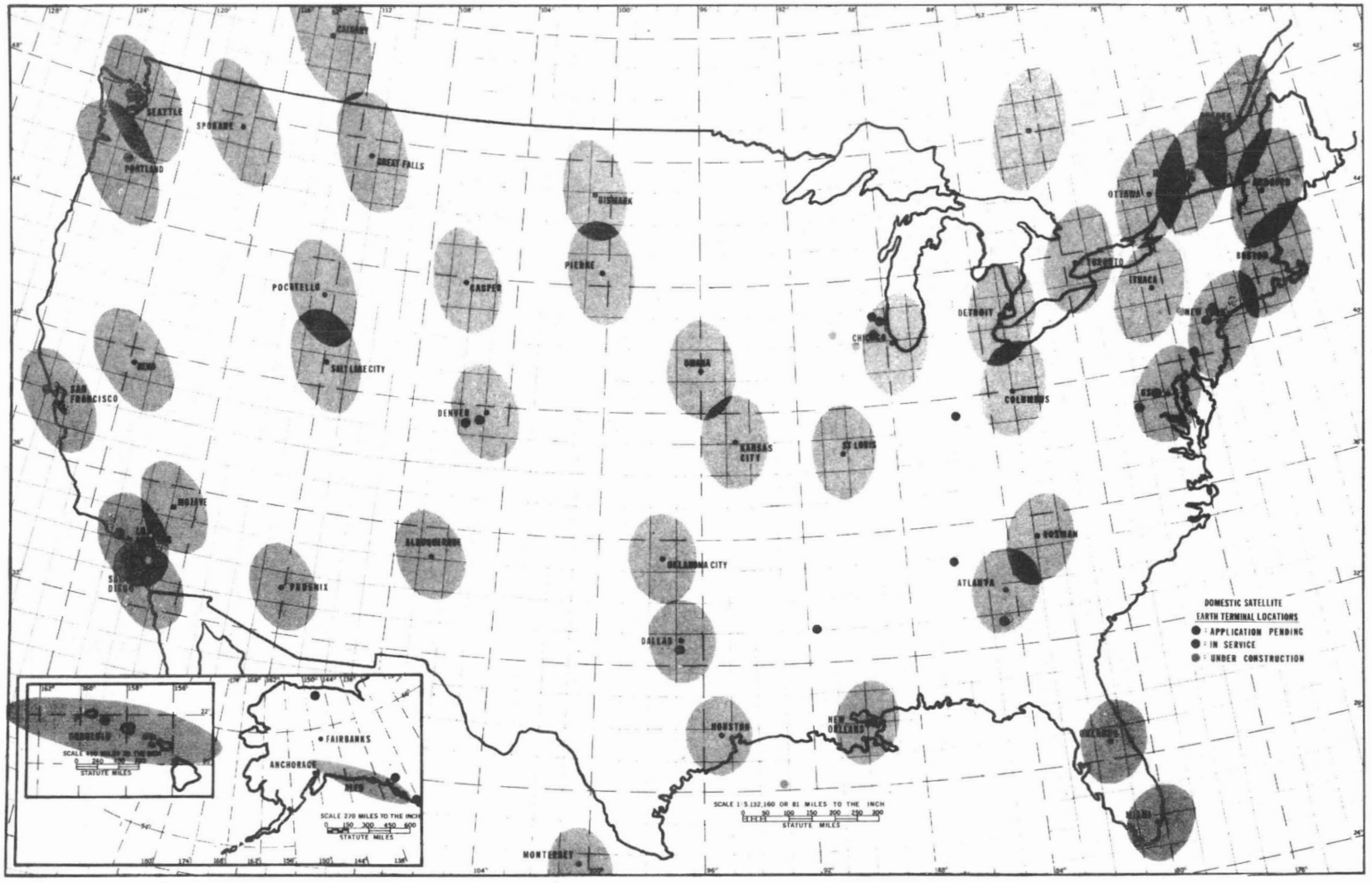

Figure 5-7. Mode 4 RFIME Antenna Footprints

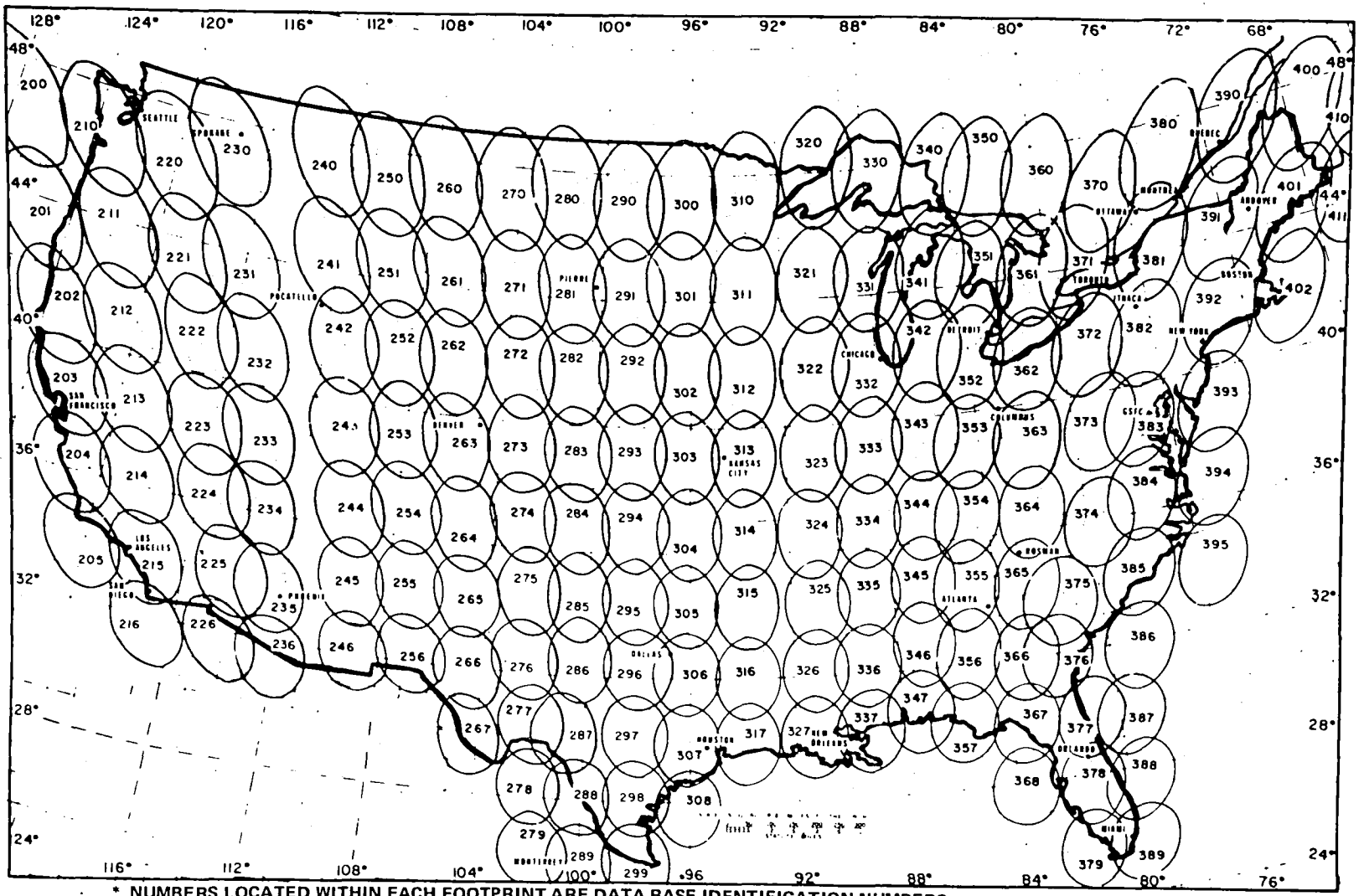

Figure 5-8. U.S. Sector Scan, Idealized 3 dB Footprints of ATS-6 9.14-meter Antenna at 6 GHz

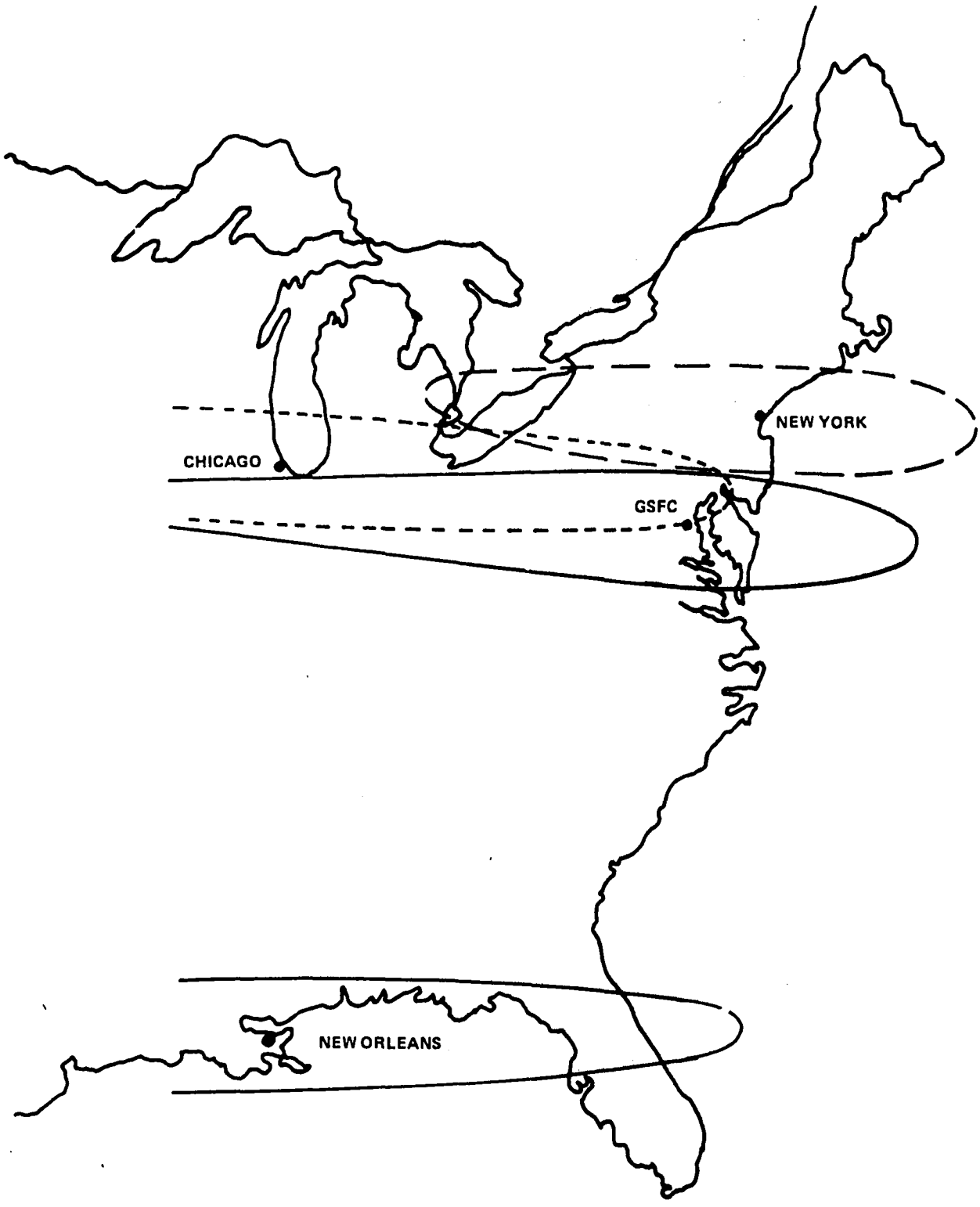

Figure 5-9. Continental U.S. Horizon Scans—Projected Antenna Footprints

Table 5-4
Mode 4 U.S. Scans

Alaska Education	12 files	Columbus, Ohio	82 files
Albuquerque, N. Mex.	17	GSFC, Md.	468**
Anchorage, Alaska	1	Dallas, Tex.	25
Andover, Maine	21	Denver, Colo.	25
Atlanta, Ga.	31	Detroit, Mich.	31
Atlantic Ocean	2	Great Falls, Mont.	12
Bismarck, N. Dak.	10	Honolulu, Hawaii	14
Boston, Mass.	92	Houston, Tex.	23
Casper, Wyo.	6	Ithaca, N.Y.	103
Chicago, Ill.	51*	Kansas City, Kans.	40
Los Angeles, Calif.	23	Portland, Oreg.	12
Miami, Fla.	22	Reno, Nev.	12
Mojave, Calif.	24	Rosman, N.C.	59
New Orleans, La.	31*	Salt Lake City, Utah	12
New York City, N.Y.	388*	San Diego, Calif.	58
Oklahoma City, Okla.	12	San Francisco, Calif.	33
Omaha, Nebr.	13	Seattle, Wash.	13
Orlando, Fla.	29	Spokane, Wash.	19
Pacific Ocean	22	St. Louis, Mo.	12
Phoenix, Ariz.	15	U.S. Sector Scans	313
Pierre, S.D.	19	Miscellaneous	103
Pocatello, Idaho	15		
			2,325 files
			19,375 min.
			(323 hr)

*Includes 2 "horizon" scans
**Includes 3 "horizon" scans

Table 5-5
Mode 4 Foreign Scans

Canada	Calgary	14 files
	Central Canada	6
	Montreal	18
	Ottawa	14
	Quebec	10
	Toronto	6
Mexico	Mexico City	10
	Monterey	14
Miscellaneous		15
	Total	107
		900 min (15 hr)

Modes 5 and 11—Analog Recorded RFI Measurement and Playback

The objective of this mode was to detect and locate rfi hot spots in the United States. This was accomplished by recording the radiated power of rfi sources and the associated frequency during a north-south or south-north sweep of a corridor of the United States by the ATS-6 9.14-meter antenna. These corridors contained the PFF antenna 3-dB beamwidth projections as the scans were systematically stepped north-south or south-north across the United States. As the spacecraft antenna was swept, the rfi downconverter was stepped 10 times through the 500-MHz band output of the linear detector recorded on analog tape. The 100-kHz predetection filter was used in this mode and allowed a step rate of 10 msec per step that retained the spectral characteristics of the detected signal. With this step rate, the rfi data for the whole corridor was scanned in 500 seconds, the same amount of time for one scan of the 500-MHz band at one location using Mode 4.

Other data were also recorded on the analog tape for use during playback that included: ATSOCC GMT, spacecraft telemetry and the latitude and longitude of the spacecraft antenna Z-axis Earth intercept.

The analog tapes produced in this mode were played back through the receiver/analyzer by Mode 11. Mode 5/Mode 11 data are therefore identical except for format. The two modes were considered as one for data collection purposes.

Mode 5 procedures were used to complete and record a total continental scan of the United States by the analog format. This United States scan was later processed into the Mode 11 digital data, as was previously listed in Table 5-3 (643 files). Each Mode 5 data tape represented a north-south or south-north scan of a section of the United States and each section was acquired by stepping the antenna boresight axis across the United States in increments of 0.3 degree in spacecraft pitch. Each step was a separate 20-minute Mode 5 recording.

Mode 8—Geographic Location

This mode was designed to assess the feasibility of locating an rfi source detected as a result of a Mode 4 or Mode 5 analysis. Two orthogonal scans, east-west and north-south, of the ATS-6 9.14-meter antenna were performed during the 500 seconds duration of each mode. The mode format for Mode 8 is the same as that for Mode 4, except that the receiver frequency was fixed (10-kHz segment) to that of the rfi source.

Off-line reduction of a Mode 8 data tape provided a line printer tabulation of the spacecraft antenna Z-axis intercept latitude and longitude, GMT, and detected power. From this tabulation, a time interval was chosen for an x-y plot of detected power versus GMT. The power maxima from the plots identified the time for the power maxima that also identified the latitude and longitude of the power maxima.

This single frequency scanning mode was used somewhat sparingly (only two files) in its designed primary function. Operational time constraints and priorities were the major reasons for the minimal use of this mode in determing rfi source locations. This function was, however, operationally tested (2 files) by using the PCT as an unknown radiator. The results of this test will be discussed later.

One important use of the Mode 8 single frequency scan over the data gathering period was to gather data (45 files) on the antenna pattern of the ATS-6 PFF 9.14-meter parabolic antenna. This portion of the experiment was dubbed the antenna pattern measurement (APM) and consisted of performing east-west sweeps that were consecutively offset in the north-south plane about the Rosman Ground Station, North Carolina. This APM procedure is depicted in Figure 5-10.

DATA PROCESSING

As with most experiments of this magnitude and nature, many phases of data processing and reduction growing pains were encountered before any meaningful results could be obtained. Most of these problems were eventually overcome, however, and a significant amount of RFIME data was reduced, evaluated, and cataloged. Some of the significant data processing problems that were encountered are briefly described.

The Source Determination Program

As noted previously, Modes 2, 3, and 4 were the primary modes used for ascertaining when a signal was present and also for determining its effective isotropic radiated power. An IBM program was developed to combine Modes 2, 3, and 4 to identify the signals detected. See Figure 5-11 wherein a Mode 4 rfi survey file was thresholded with a Mode 2 noise file and all outputs that exceeded a preset threshold were designated as valid rfi sources and were then power calibrated with a Mode 3 calibration file.

It should be noted from Figure 5-11 that the output of the RFIME system had an amplitude ripple of approximately 6 dB peak-to-peak with a periodicity of approximately 14 MHz. This was an anomaly of the system that was consistent throughout the experiment and was determined to be primarily due to the traveling wave tube amplifier in the satellite. Although somewhat detracting in appearance, its overall effects were considered negligible because, in the comparison processing, the system response characteristics were separated from the rfi signals.

One of the major problems encountered with the source determination processing was the wide range of variations in the recording sensitivities between data tapes and files. A sensitivity correction factor was therefore required, since only a very limited selection of Mode 2 noise files were available for S+N/N thresholding. A source determination preprocessing program was then conceived and developed to establish the mean background or sensitivity level for each data file. The derived sensitivity level was then compared to a selected standard* to determine a processing correction factor, delta (Δ). This preprocessing of all Mode 4 files represented a significant computer effort (2433 files) in addition to the other processing efforts required.

Another significant problem was encountered in that the overall RFIME system response underwent two unique changes during the course of the experiment because of adjustments of the parametric amplifier in the Rosman Ground Station receive system. So, three distinct overall frequency responses resulted as shown in Figure 5-12. Separate Earth background noise files were therefore required

*The selected standard was ultimately determined by empirical testing and verification to be the mean sensitivity level of file 408 of data tape 126; i.e., various processing levels and files were tested with file 408/126 providing the best overall results.

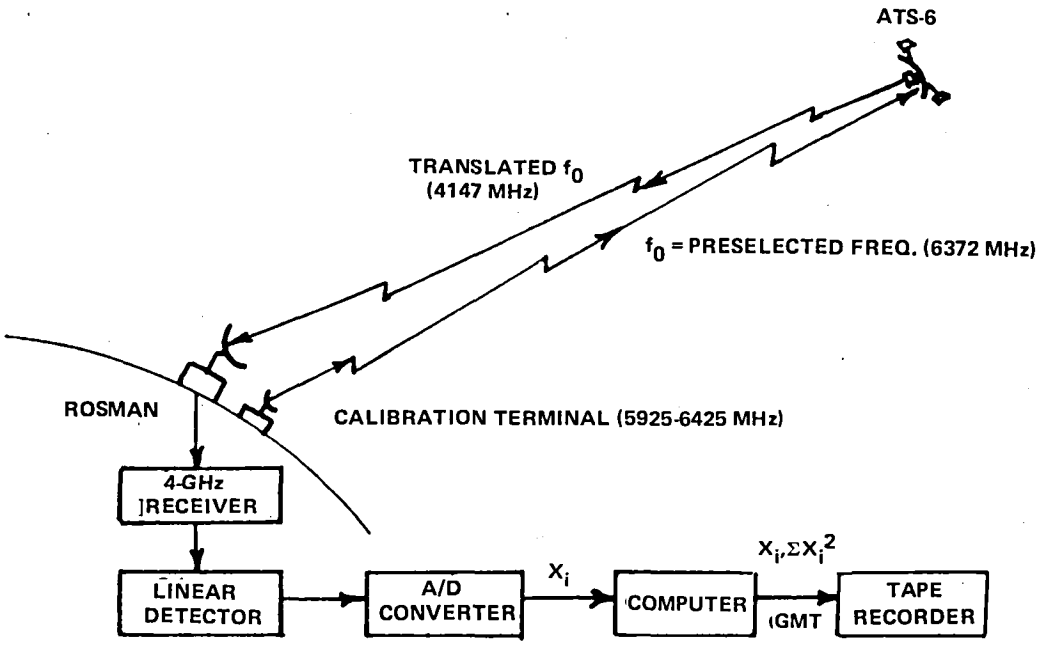

A.

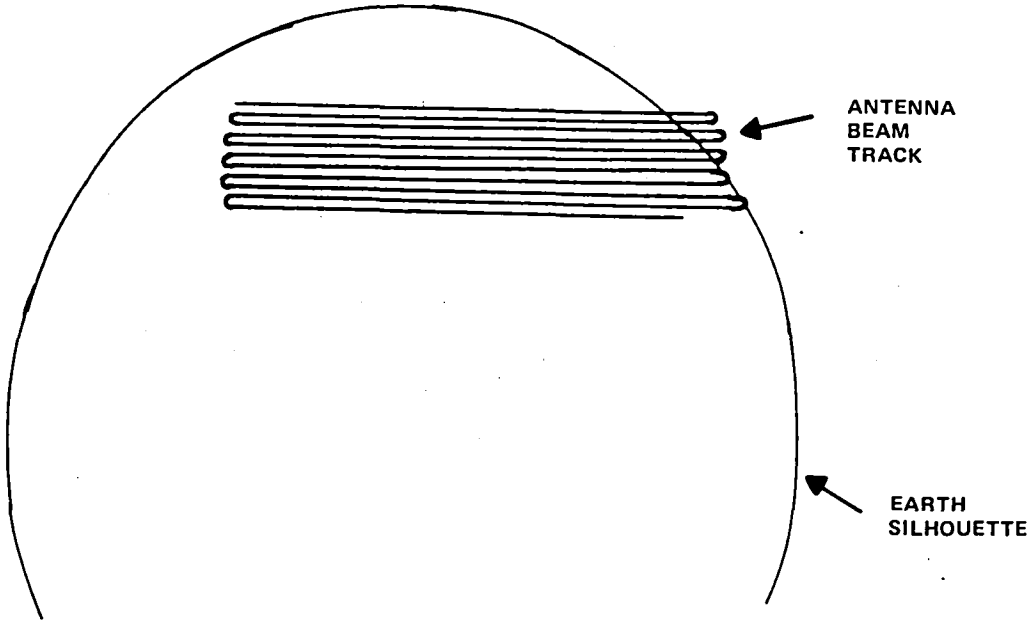

B.

Figure 5-10. Antenna Pattern Measurement Experiment

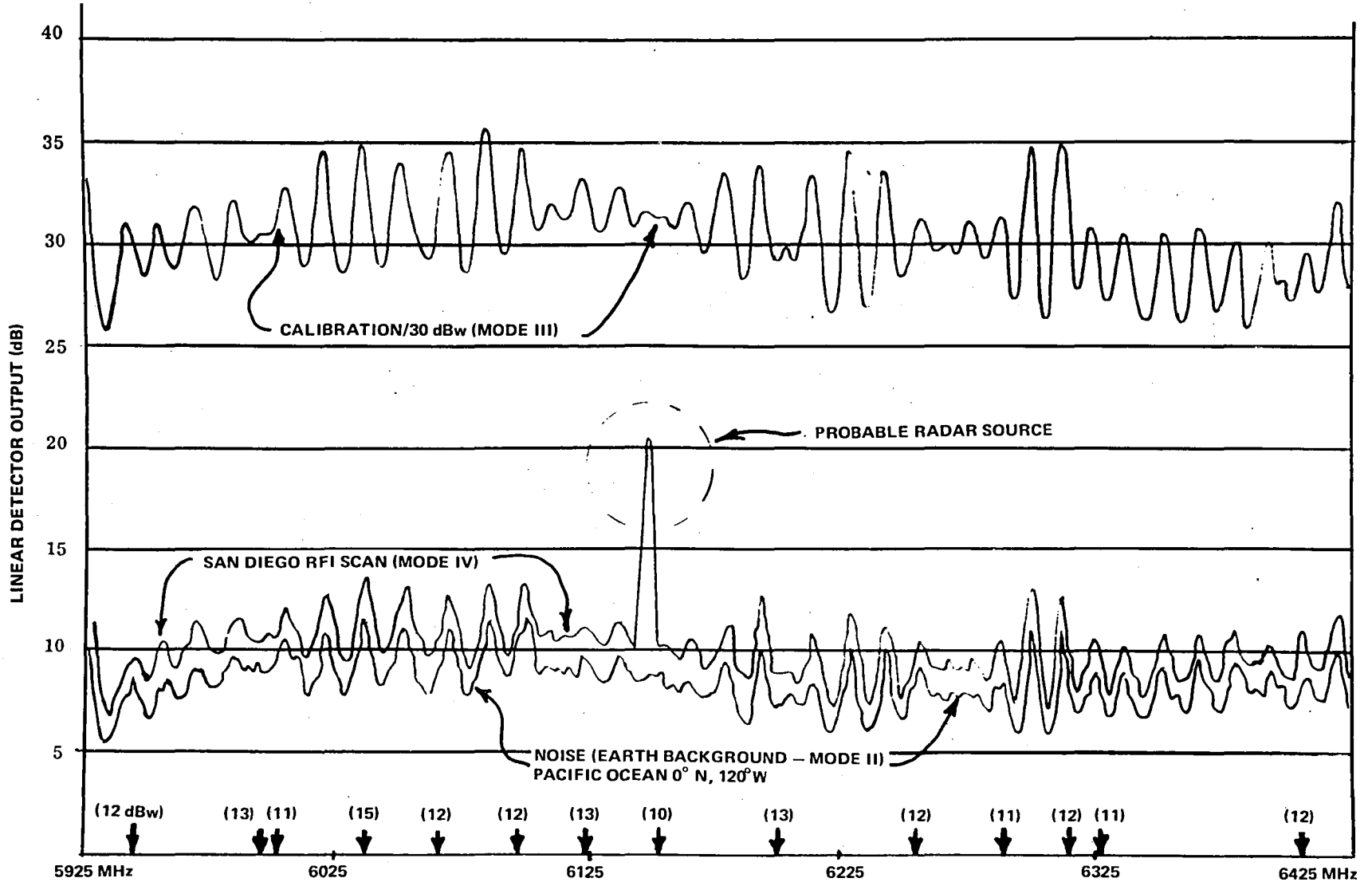

Figure 5-11. Mode 4 Processing "Source Determination"

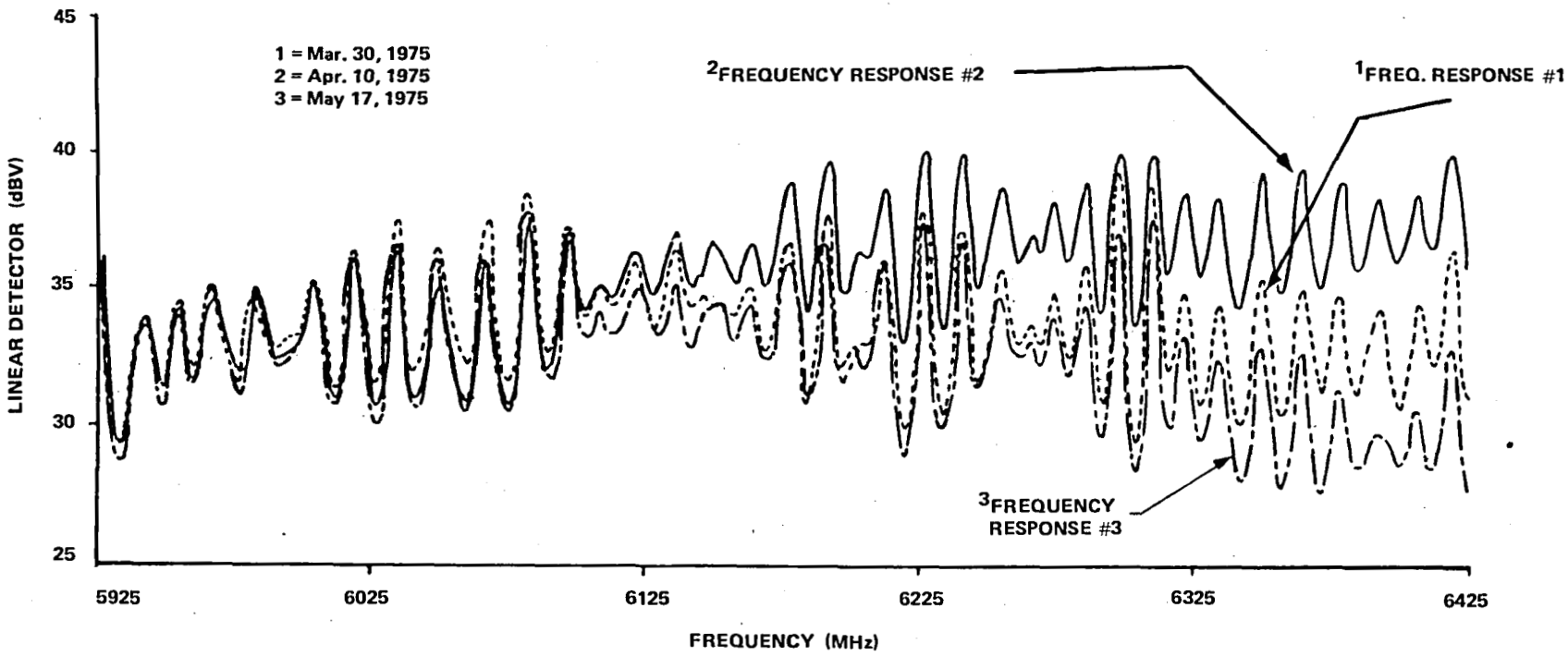

Figure 5-12. Variations in RFIME System Response, August 1974 to June 1975

to correlate with each of the response characteristics. Manual smoothing in lieu of computer smoothing of three standard Mode 2 noise files was ultimately conducted because of the 14-MHz ripple in the system and the relatively rapid rate-of-change of the oscillations.

One of the most critical problems encountered (and this was not completely determined until approximately two-thirds of the Mode 4 data had been recorded) was that the satellite 9.14-m antenna was subject to thermal warping and the antenna main beam rf boresight would drift relative to its mechanical boresight axis. This circumstance caused an uncertainty about exactly where the spacecraft axis was pointing and hence degraded the accuracy of the Mode 3 calibration recordings. A procedure was adopted whereby the Mode 3 recordings were preceded by a C-band monopulse tracking operation whenever possible. This monopulse operation used a signal radiated from the calibration terminal, so that the spacecraft antenna would align its rf axis to the calibration terminal location. However, this monopulse procedure was only occasionally successful because of operational difficulties, so that only 421 or 17 percent of all Mode 4 data recordings and their associated mode calibration recordings were preceded by a successful monopulse operation. As a consequence, it became convenient to classify all Mode 4 data files in the following manner:

- Classification A. This was data recorded on a selected site that had the PCT in the center of the ATS-6 9.14-m antenna footprint and in which the PCT had been used through C-band monopulse to boresight the ATS-6 beam on the PCT.

- Classification B. This was data recorded upon a selected site that did not have the PCT located within the antenna footprint. The PCT, however, had been previously used to boresight the beam upon the PCT, and any variation in ATS-6 antenna pointing angle between predicted and measured for the PCT locations were incorporated as an offset for all other locations (e.g., the PCT was boresighted at GSFC, the angular offset noted, and the ATS beam moved to Ithaca with the offset incorporated).

- Classification C. This was data recorded with all ATS-6 pointing conducted by computer predicts with no boresighting or offsets.

- Classification D. All files with known defects such as extremely low sensitivity, spacecraft spur not present, improper file length, etc. These data were considered to have little, if any, value and, therefore, were not processed.

Figure 5-13 shows the effect on Mode 3 recordings of boresight drift and the monopulse procedure.

Mode 5/Mode 11 Processing

The analog tapes produced by Mode 5 were played back through the rfi receiver/analyzer for analog-to-digital conversion. Each Mode 5 tape was played back through a playback frequency translator that upconverted the recorded 100-kHz bandpass to the receiver/analyzer 10-MHz intermediate frequency (i.f.). The Mode 4 detection process was used to digitize the data. This procedure allowed the computer software used for Mode 4 data to be used to process the Mode 11 digital tapes.

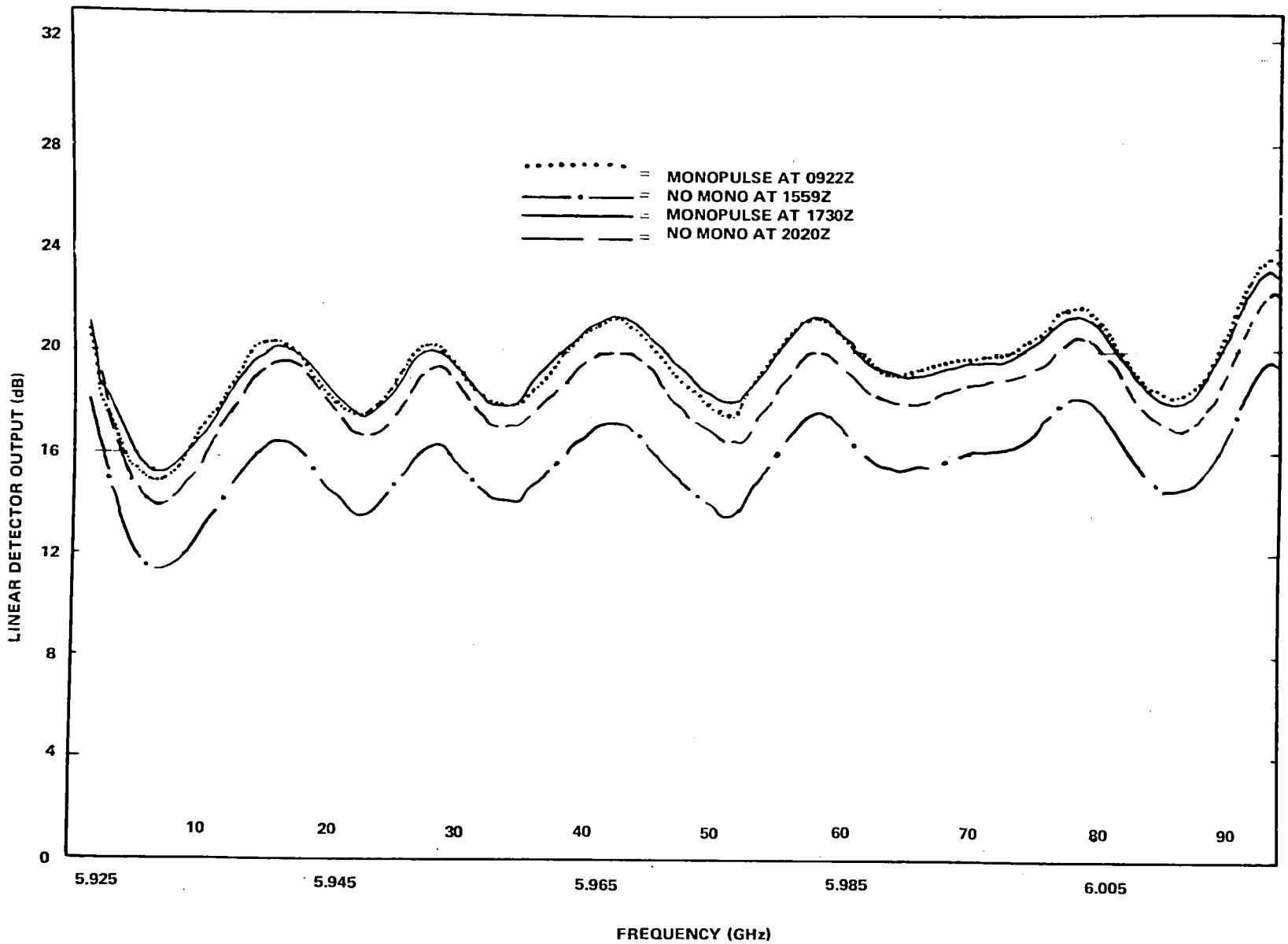

Figure 5-13. Prime-Focus Feed Boresight Drift of Mode 3A Calibrations (20 dBW)

Because the 10-kHz predetection bandpass filter was used, each 100-kHz segment of the analog tape was played back 10 times by stepping the playback translator local oscillator in 10-kHz steps, so that one of 10 adjacent 10-kHz segments of the 100-kHz band was centered at the 10 MHz receiver/analyzer i.f. during each of the 10 playback periods. The playback of the north-south antenna scan required approximately 23 minutes; thus, Modes 5 and 11 together required approximately 24 minutes of computer time or roughly 3 times the Mode 4 computer time requirement. Thus, while satellite time was conserved during a Mode 5 (approximately one-tenth the time Mode 4 would have required), the off-line processing of the data was tripled.

Playback of the analog tapes for digital recording presented a most formidable problem. Serious synchronization problems (due to mechanical slippage of the tape drives) were encountered and disk space availability. After much trial and error, frequency slippage that resulted in converting to Mode 11 digital tapes was reduced to 30 to 70 kHz.

RFIME Data Processing Completion Summary

Because of time, personnel, dollar constraints, and the processing problems described previously, only the most significant RFIME data were fully processed and analyzed. The processing effort completed was as follows:

Mode		Estimated Completion (percent)
1	(17 files)	95
2	(115 files)	95
3	(776 files)	80
4	(2433 files)	
	A. Preprocessing (level determination)	100
	B. Source Determination	
	Class A (80 files/80 completed)	100
	Class B (321 files/321 completed)	100
	Class C (1786 files/300 completed)	17
	Class D (246 files)	
	Overall (A, B, and C data)	31
5	(21 analog tapes)	100
8	(68 files)	80
11	(643 files)	
	A. Preprocessing (level determination)	8
	B. Source Determination	5

REFERENCES

1. Weinberger, H. L.; "Final Design Study Report for Radio Frequency Interference Experiment," Hughes Aircraft Co.,; NASA Contract NAS5-11657, July 31, 1969.

2. Bergman, R. R., et al., "Advanced Computer Model and Predictions for ATS-F/G Radio Frequency Interference Experiment at 6 GHz," IEEE National Telecommunications Conference 72-CHO 601-5-NTC, December 1972.

3. "Operation and Maintenance Manual, RFI Measurement Experiment, Volume II," prepared by Hughes Aircraft Co. for NASA/GSFC under contract no. NAS 5-21621, June 1975.

CHAPTER 6

RADIO FREQUENCY INTERFERENCE MEASUREMENTS TEST RESULTS

The results of the Radio Frequency Interference Measurements Experiment (RFIME) operations are grouped into nine categories: Mode 4 United States Sector Scan, Mode 4 Major Metropolitan Area Surveys, Mode 4 Horizon Scan, Mode 5/Mode 11 United States Scan, RFIME Data Base, Mode 8 Geographic Location, Prime-Focus Feed (PFF) Antenna Pattern Measurement, Mathematical Model Verification, and Postflight Gain/Temperature (G/T) Measurement.

MODE 4 UNITED STATES SECTOR SCAN

The United States continental scan resulted in an overall radio frequency interference (rfi) density plot of detectable 10-kilohertz (kHz) segments that basically correlated with the microwave link density of the major metropolitan areas as expected. Of all of the frequencies that were detected, many were not contained within the assigned common carrier frequency channels, and in some cases, these carriers were relatively high in magnitude and up to 39 megahertz (MHz) in bandwidth. The maximum detected power level of this one-time United States survey was approximately 23 dBW effective isotropic radiated power (e.i.r.p.) ground referenced or approximately -139.5 dBW/m^2 power flux density (PFD) at the satellite. The common carrier channel signals that were detected were generally near the threshold of detection. This threshold corresponded to a PFD at the satellite of approximately -150 dBW/m^2.

Due to the one-time-only nature of the continental scan, only a very general and qualitative analysis could be conducted. Additional continental scans would have been desirable for more quantitative results. Table 6-1 lists all of the signals that were detected in the continental scan data and the maximum power level detected:

- Each detected channel was normally composed of one to five 10-kHz segments and in many cases two or more detectable signals were located on adjacent 10-kHz segments.

- Detected 10-kHz segments contained within an assigned channel were normally distributed within 100 kHz of the assigned center frequency and with rare instances of up to ±200 kHz. This was well within the Federal Communications Commission tolerance of ±300 kHz.

- The detected signal strengths were relatively low and generally near the minimum detection threshold; i.e., approximately -150 dBW/m^2 PFD at the satellite. Table 6-2 lists the frequencies, locations, and number of detected occurrences for the metropolitan area data processed. The fractions listed are the number of times each frequency channel was detected versus the number of times the site was surveyed.

Table 6-1
U.S. Continental Scan Detected R.F.I. (169 Sector Scans)

Frequency (MHz)	BW	Maximum Power Level		Common Carrier Frequency	Number of Times Detected
		E.i.r.p. (dBW)	PFD (dBW/m^2)		
5925.00 - 5929.98	5 MHz	20.2	-140.3		1
5927.55 - 5966.04	39 MHz	20.0	-140.5		1
59 .11 - 5949.22	110 kHz	12.8	-149.7	5945.2	14
5959.70 - 5959.84	140 kHz	11.3	-151.2		2
5974.82 - 5974.93	110 kHz	11.8	-150.7	5974.8	18
5990.01	10 kHz	11.3	-151.2		2
6004.43 - 6004.52	90 kHz	14.5	-148.0	6004.5	18
6020.51 - 6020.99	480 kHz	9.4	-153.1		1
6032.18 - 6034.49	2.3 MHz	11.1	-151.4		5
6034.06 - 6034.23	170 kHz	17.5	-145.0	6034.2	28
6056.98 - 6057.23	250 kHz	10.4	-152.1		4
6063.74 - 6063.95	210 kHz	10.9	-151.6	6063.8	14
6064.20 - 6064.30	100 kHz	11.7	-150.8		3
6064.98 - 6064.99	20 kHz	20.7	-141.8		16
6074.68 - 6074.71	30 kHz	12.1	-150.4		1
6075.22	10 kHz	10.3	-152.2		1
6093.44 - 6093.62	180 kHz	10.0	-152.5	6093.5	14
6108.41 - 6108.42	20 kHz	11.0	-151.5		2
6123.08 - 6123.12	40 kHz	12.5	-150.0	6123.1	18

Table 6-2
Major Metropolitan Area Surveys; Number of Times Frequency Channel Detected vs. Number of Times Surveyed

		Los Angeles	San Diego	Mojave	Phoenix	San Francisco	Reno	Portland	Seattle	Alaska Education	Spokane	Calgary Canada	Great Falls Montana	Pocatello	Salt Lake City	Denver	Albuquerque	Casper	Bismark	Pierre	Omaha	Oklahoma City	Kansas City	Dallas	Houston	New Orleans	Orlando	Miami	Atlanta	Roanan	St. Louis	Chicago	Detroit	Columbus	CSTC	NYC	Ithaca	Toronto	Ottawa N.I. Canada	Montreal	Quebec	Andover	Boston	Hawaii	Monterey Mexico	Mexico City
		6	6	17	7	5	4	4	10		10	8	4	8	4	4	4	2	4	4	4	10	2	10	9	1	6	13	18	9	15	8	33	29	13	47	4	7	10	12	6	12	39	8	4	2
1	5925.01→5928.14																																1/33													
2	5925.01→5983.78																											2/13																		
1	5929→5933										1/10																																			
1	5931.25→5932.15																														1/15															
1	5931.50→5932.18																																1/33													
1	5932.38										1/10																																		
2	5936.76/0.77																																	2/29												
1	5941.78/0.84																									1/9																			
1	5941→5956																																												
186	5945.07–0.35 (5945.2)	1/6		5/17	2/7	1/5	1/4									1/4		1/2										1/13	1/18		1/15	3/6	26/33	27/29	13/13	10/47						2/12	15/39		2/4	
	5918.98																																												
1	5949.30																												1/18																
7	5960.00–0.11	2/6		8/17																									1/18					2/29										
18	5962.10–0.18	2/6	2/6	4/17		3/5	1/4	1/4					1/4		2/4				1/4				1/2											2/33											
2	5965.10→5982.61																																												
1	5969.68→5972.94	•																																											
117	5974.74–0.93 (5974.8)	6/6	2/6	3/17	3/5													2/2						1/10			2/13		14/18			2/18	24/33	26/29	12/13	7/47						1/12	12/39			
6	5975.00–0.03																														1/15		4/33										1/12				
1	5980.10																																1/33													
5	5983.14→0.81																																3/33	2/29												
1	5990.01																														1/15															
75	6000.00–0.20				2/7	1/5			2/10		2/10	2/8		1/8		1/4	4/4	2/2		4/4	2/10		2/10			2/4		2/13	2/18		4/15		14/33	2/29	5/13	6/47	2/4		6/10	5/12	2/6	6/12	7/39	3/8		2/2
105	6004.40–0.77 (6004.50)	1/6		13/17	5/7	1/5	1/4									2/4	4/4	1/2		1/4		2/2	1/10	1/3							4/15		5/33	28/29	13/13	13/47						1/12	15/39		1/4	
2	6019.34–0.85																														1/15					1/47										
4	6022.33→6027.25																																		4/13										
4	6022→6027																																			4/47									
3	6025.01–0.02																																3/33												
6	6031.45→6034.88																																		6/13										
4	6031.85→6034.52																																									9/39			
4	6032.19→6034.33																																	4/29										
4	6032→6034																																		4/47									
161	6033.99			1/17																																								
	6034.00–0.31 (6034.20)	4/6	1/6	16/17	4/7	4/5	1/4		1/10							4/4	4/4	1/2		2/4		2/2						4/13	7/18		5/15	3/8	31/33	25/29	7/13	14/47			1/10	1/12		3/12	23/39			
1	6035.08																																					1/10							
1	6054.90–0.91																																								1/39			
2	6057.22→6057.55																																	2/29										
1	6057.40→6057.74																																			1/47									
1	6057.46→6057.63																																								1/39			
126	6063.47–0.89 (6063.8)			3/17								2/8	2/4			2/4	4/4	2/2		1/4			1/10					1/13	4/18		4/15	1/8	22/33	28/29	3/13	33/47			1/10			5/12		4/4	
4	6064.02–0.97																																	2/29								3/39			
1	6064.68→6065.73																					1/2												1/29											
5	6065.00–0.71																																		4/13	1/47									
1	6066.99	1/6																																											
1	6074.96→6075.24																																			1/47									
11	6075.00–0.25	1/6	1/6	8/17			3/4																												1/29				1/12			3/39			
1	6080.84																																						1/2						

Table 6-2
Major Metropolitan Area Surveys; Number of Times Frequency Channel Detected vs. Number of Times Surveyed (continued)

		Los Angeles	San Diego	Mojave	Phoenix	San Francisco	Reno	Portland	Seattle	Alaska Education	Spokane	Calgary Canada	Great Falls Montana	Pocatello	Salt Lake City	Denver	Albuquerque	Casper	Bismark	Pierre	Omaha City	Oklahoma City Kansas	Dallas	Houston	New Orleans	Orlando	Miami	Atlanta	Roman	St. Louis	Chicago	Detroit	Columbus	GSFC	NYC	Ithaca	Toronto	N.E. Canada	Ottawa	Montreal	Quebec	Andover	Boston	Hawaii	Monterey Mexico	Mexico City
		6	6	17	7	5	4	4	10	12	10	8	4	8	4	4	4	2		4	4	10	2	10	3	9	1	6	13	18	9	15	8	33	29	13	47	4	7	10	12	6	12	39	8	4	2
78	6093.41–0.84 (6093.5)	4/6	1/6	5/17																								1/13	1/18		1/15		28/33	15/29	11/13	9/47							2/39			
2	6103.12→6107.12	2/6																																											
2	6103.74→6105.32			2/17																																								
1	6105.38				1/7																																							
106	6123.07–0.40 (6123.1)	2/6	1/6	7/17		1/5	1/4									3/4	2/4	2/2		1/4		1/2						10/13	3/18		1/15	1/8	25/33	2/29	12/13	19/47						1/12			1/2
1	6135.09–0.10																																											
2	6143.54→6147.15		2/6																																							1/39			
2	6143.85→6146.73				2/7																																							
3	6144.20→6146.41			5/17																																								
4	6144.37→6146.29																																											
1	6150.44–0.51																												1/18															
246	6152.52–0.99 (6152.8)	5/6	6/6	15/17	7/7	5/5	1/4									4/4	4/4	1/2		1/4		1/2	3/10					3/13	18/18		6/15	6/8	31/33	19/29	13/13	11/47			3/10	4/12		4/12	1/39			
2	6167.50–0.60																														2/15														
1	6172.30–0.34								1/10																																				
1	6174.98					1/5																																						
1	6179.66–0.67								1/10																																				
2	6185.03																																			1/47	1/4								
1	6189.77																																												
4	6190.40→6193.06																																									1/39			
129	6197.11–0.31 (6197.2)		1/6	9/17	4/7	3/5	2/4					2/8			1/4	2/4	3/4	1/2					6/10							3/18		2/15	5/8	21/33	21/29	12/13	21/47							16/39			
6	6200.00–0.01	2/6																										1/13					3/33												
2	6215.03																																												
1	6220.79																																									1/12	1/39			
12	6220.23→6230.32																																									1/12				
11	6220.37→6229.53																																		12/13										
6	6221.32→6229.56																																										11/39			
12	6221.45→6228.81																																									6/12				
6	6222.13→6227.29																																								12/12					
5	6222.82→6227.07																																						6/10							
23	6222→6227																																	5/29											
6	6224.30→6226.18																																			23/47										
3	6224.88																																								3/6					
1	6225.00–0.16																																									6/12				
173	6226.72-6227.03 (6226.9)	3/6	4/6	16/17	5/7	5/5	3/4										3/4	2/2										1/13															2/39			
1	6242.18																											9/13	9/18		4/15	4/8	30/33	22/29	13/13	19/47						3/12	24/39			
117	6256.51–0.79 (6256.5)			16/17	7/7	2/5	4/4		2/10		1/10						2/4	1/2																		1/47										
7	6261.41→6269.91																														4/15		1/33	51/29	19/13	15/47						3/12	21/39		1/4	
9	6264.89–6265.00								1/10																						7/15														
1	6365.67								1/10																										1/13	2/47			1/10	2/12	2/6					
5	6271.34											5/8																																	
2	6275.00					2/5																																							
175	6286.02–0.29 (6286.2)	5/6	4/6	11/17	3/7	1/5	4/4							1/8			3/4											10/13	8/18		6/15	5/8	31/33	28/29	13/13	12/47					1/6	12/12	32/29			
2	6269.08–0.65																												3/18															
3	6303.86→6306.88																											9/13																	
2	6304.12→6306.63																												3/18															
1	6304.49																											1/13																	
2	6306.81–0.53																											1/13			1/15														

Table 6-2
Major Metropolitan Area Surveys; Number of Times Frequency Channel Detected vs. Number of Times Surveyed (continued)

		Los Angeles	San Diego	Mojave	Phoenix	San Francisco	Reno	Portland	Seattle	Alaska Education	Spokane	Calgary Canada	Great Falls Montana	Pocatello	Salt Lake City	Denver	Albuquerque	Casper	Bismarck	Pierre	Omaha	Kansas City	Oklahoma City	Dallas	Houston	New Orleans	Orlando	Miami	Atlanta	Roanan	St. Louis	Chicago	Detroit	Columbus	GSFC	NYC	Ithaca	Toronto	N.E. Canada	Ottawa	Montreal	Quebec	Andover	Boston	Hawaii	Monterey Mexico	Mexico City
		6	6	17	7	5	4	4	10	12	10	8	4	8	4	4	4	2	4	4	4	10	2	10	3	9	4	6	13	18	4	15	8	33	29	13	47	4	4	10	12	6	12	39	8	4	2
2	6306.11–0.44																															2/15															
5	6308.16–0.81				1/7																		1/2						1/13							2/47										
7	6309.04–0.64	1/6						1/4							1/4			1/2														1/15			1/29									1/39			
2	6310.02–0.61							1/4							1/4																																
38	6315.52–0.87 (6315.9)	1/6		2/17	2/17	1/7						2/8	2/4			1/4	1/4															1/15		2/33	5/29	4/13	6/47							1/39			
42	6326.57–0.58																													5/18		5/15	5/8	4/33	4/29		8/47							6/39			
1	6331.72																													1/18																
49	6332.72																													6/18		5/15	5/8	5/33	10/29		6/47							12/39			
61	6333.72																													6/18		6/15	6/8	7/33	14/29		9/47							22/39			
7	6343.85→6346.77																							7/10																						
2	6344.35→6346.29																								2/3																						
11	6344.97																																4/8	2/33			1/47										
70	6345.42–0.64 (6345.5)	4/5	5/6	11/17	1/7	2/5	3/4										1/4												4/13	2/18	2/4			4/33	13/29	6/13	3/47							3/39			
2	6348.68–0.91						1/4																									1/15															
1	6349.02														1/4																																
1	6361.51																					1/2																								
1	6363.85																					1/2													2/29		2/47							2/39			
8	6369.29–0.26				1/7							1/8																																		
1	6374.41																					1/2																								
81	6375.05–0.34 (6375.2)	3/6	4/6	12/17	2/7	1/5	4/4								3/4														5/13		1/4	1/15		6/33	11/29	13/13	13/47						1/12	4/39			
1	6378.79																					1/2																								
1	6379.34																					1/2																								
1	6380.15																					1/2																								
3	6385.42–0.98							1/4							1/4							1/2																								
1	6386.72																					1/2																								
	6387.59–0.90																											1/13		1/4					1/13										
3	6388.60																																		1/29										
2	6389.28–0.38							1/4																												1/13										
23	6390.42–0.87																													6/18		1/15	2/8	3/33	4/29		5/47							2/39			
3	6391.10–0.91																														1/4				1/29	1/13									
1	6392.62																																		1/29										
1	6396.02																						1/2																						
1	6397.41																						1/2																						
1	6398.15																														1/4														
2	6402.56–0.57																													2/18															
1	6403.74																													1/18															
1	6404.02																						1/2																						
237	6404.21-0.99 (6404.8)	5/6	6/6	16/17	7/7	5/5	4/4								1/4	1/4	2/4						1/2		1/2				13/13	18/18	1/4	7/15	3/8	26/33	28/29	13/13	35/47			1/10	3/12	3/6	12/12	23/39			
2	6405.00–0.03																																		2/29										
1	6406.45																						1/2																						
1	6409.21																						1/2																						
1	6415.48–0.78																						1/2																						
1	6416.39																						1/2																						
68	6417.65–0.91			1/17																			1/2						11/33	9/18		4/15	7/8	11/33	4/29	6/13	3/47	3/4	1/4					11/39			
2	6418.39–0.44																																			2/13										
7	6420.05–0.39							1/4															1/2													2/29		1/47							2/39			
49	6421.49–0.37																						1/2						10/13	9/18		3/15	8/8	3/33	1/29	7/13		2/4					6/39			

MODE 4 HORIZON SCAN

Since the majority of the C-band interference to be detected at ATS-6 was expected to emanate from terrestrial microwave common carrier transmitters, concentrated areas of these transmitters (i.e., major metropolitan areas) were viewed as the satellite was moved toward 35°E longitude as these areas approached the horizon of the Earth (1 degree to 3 degree elevation angle from the Earth location). Some of the main beams of these terrestrial transmitters were expected to be radiating directly towards the satellite with a resultant substantial increase in detected power level. These data were used for comparison and validation of previously detected and processed data from the 94°W longitude satellite position.

Four U.S. metropolitan areas were ultimately horizon scan surveyed: New York City, Chicago, New Orleans, and Washington, D.C./Baltimore (Goddard Space Flight Center). (These horizon scan footprints were previously shown in Figure 5-10, Chapter 5.) Processing of this horizon scan data by semiautomatic methods revealed consistent and expected results.

MODE 4 MAJOR METROPOLITAN AREA SURVEYS

The results of periodically surveying the major metropolitan areas were consistent with that expected relative to the size of the metropolitan area and also with the results obtained in the one-time continental scan. The majority of the detectable rfi was centered about the major metropolitan areas and was significantly greater in the Pacific southwest and along the northeastern seaboard. However, there were many instances of rfi that were not within the assigned common carrier channels. These detectable rfi signals were not always present at a particular location, but when present, represented a potential source of interference of up to 10 MHz in bandwidth and a power flux density at the satellite of as great as -128 dBW/m^2. Figure 6-1 shows frequencies versus geographic location of some of these unidentified rfi signals. The contour lines within Figure 6-1 contain four distinct wideband interference areas, whereas the symbols represent narrowband interference. This figure includes both continental scan and metropolitan scan data.

The detected common carrier frequency usage was generally consistent with that expected:

- Sixteen of the top 20 frequency assignments listed in Table 6-1 were readily detectable. Each of these frequency assignments had a transmitter population of greater than 2500 transmitters. Five additional common carrier channels were also detected at various times and locations and had a transmitter population of approximately 500 transmitters. This observation confirmed the original postulate that many common carrier transmitters would have to be located within one single antenna footprint to produce a detectable rfi signal at satellite altitude.

- The common carrier channels detected for each area were consistent with those previously detected from 94°W longitude. There were a few instances of additional common carrier channels detected by the horizon scan data, but examination of Figure 5-10 (Chapter 5) also reveals a large increase in the Earth viewing area for a single horizon scan.

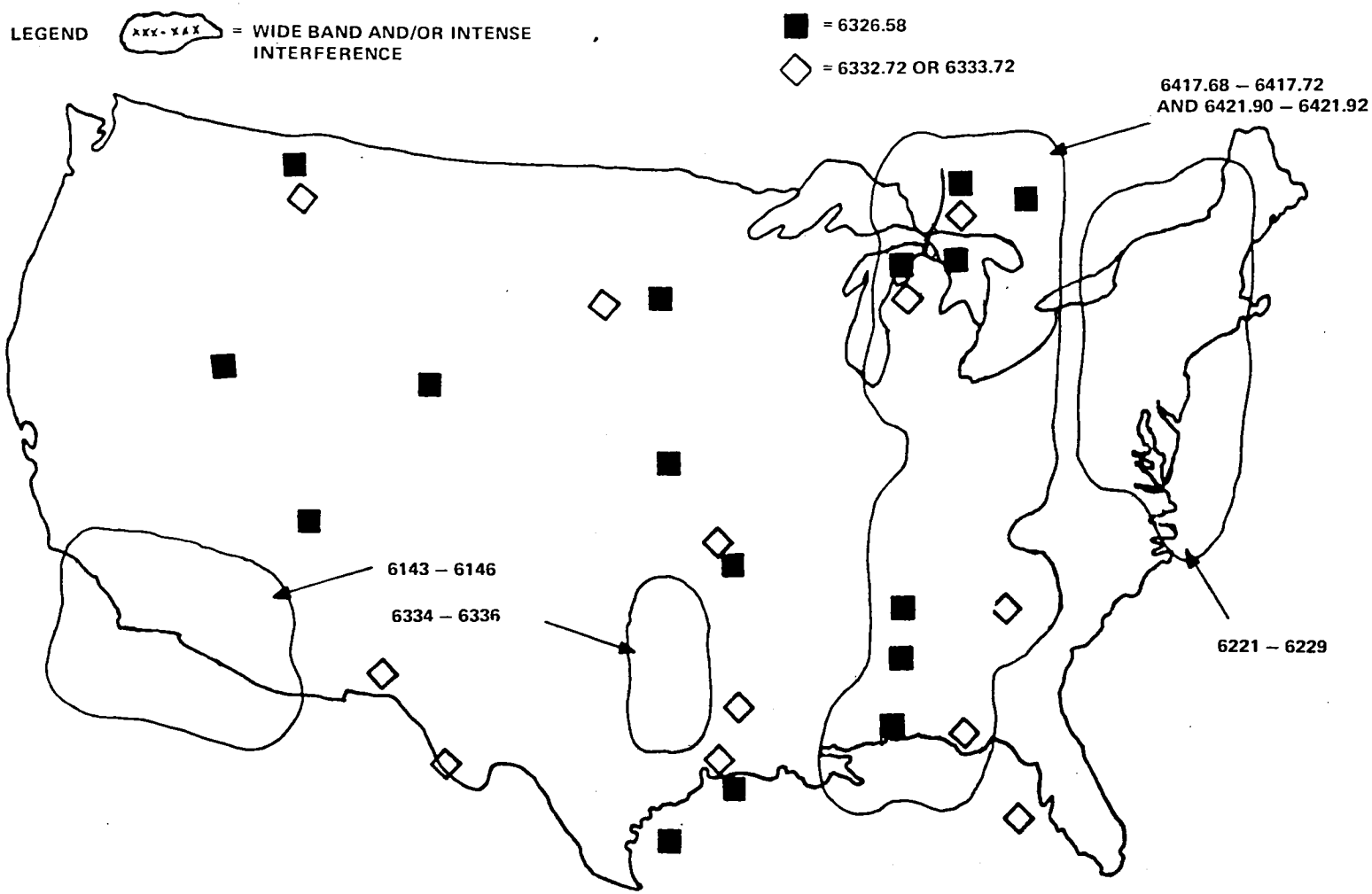

Figure 6-1. Some Unidentified RFI

- The magnitudes of the detected power level were greatly increased with some determined to be in excess of 30 dBW e.i.r.p.

- The spectral distribution about the common carrier channel assignments as detected with the horizon scan was consistent with the data previously detected and processed from 94°W longitude, i.e., ±200 kHz of assigned center frequency.

Figures 6-2 and 6-3 show raw horizon scan data plots of the Goddard Space Flight Center (GSFC) areas as recorded June 11, 1975. Shown are 4 of the 16 common carrier channels detected (6093.5, 6404.8, 6004.5, and 6256.5 MHz). The levels shown in the figures are linear detector (LD) output levels with 0 dB equals 0.1 volt and not e.i.r.p. power levels. These LD levels were later compared to calibrate levels contained on the same recording to ascertain signal power levels in dBW e.i.r.p.

MODE 5/MODE 11 UNITED STATES SCAN

Because of time and priority constraints, only one signal Mode 11 tape, tape No. 250, was processed by the Mode 4 source determination program for validity comparison of Mode 5/Mode 11 to Mode 4. The file from this tape, that corresponds approximately to a pointing intercept in the area around Goddard Space Flight Center, Greenbelt, Maryland, was compared to the frequency statistics from that area derived from Mode 4 analysis and was found to be in excellent agreement. Shown in Table 6-3 are some of the results from this processed Mode 11 file, indicating the detected frequency and the common carrier assignment from which it resulted. An offset of approximately -80 kHz from the detected value was caused by conversion errors in transposing from analog to digital tape and was taken into consideration. This was not a standard offset and varied somewhat from file to file; normal offset was ascertained to be approximately -70 kHz. Power levels are also listed, but these only represent relative power levels, because valid calibration was not available. These relative listed power levels were noted to be approximately 4 dBW high when compared to calibrated Mode 4 from the same area.

Although the processing of the Mode 5/Mode 11 United States scan was not completed, the limited amount of processing conducted demonstrated that this mode can produce limited but usable results. However, from the experience gained, the magnitude of time and effort involved in acquiring and processing the Mode 5/Mode 11 data minimized the usefulness of this mode as a primary operational procedure. The time lag involved between the Mode 5 recording and Mode 11 processing was lengthy and the information available from Mode 11 files was degraded as compared to Mode 4 data files.

RFIME DATA BASE

The product of the RFIME effort, the RFIME data base, was a compilation of 10-kHz bandwidth signals in the 5.925 to 6.425 GHz frequency band that were identified and characterized with respect to location, time, frequency, and power level. The collection and storage of these data on magnetic tape was accomplished semiautomatically, and the data were transferred to punched cards.

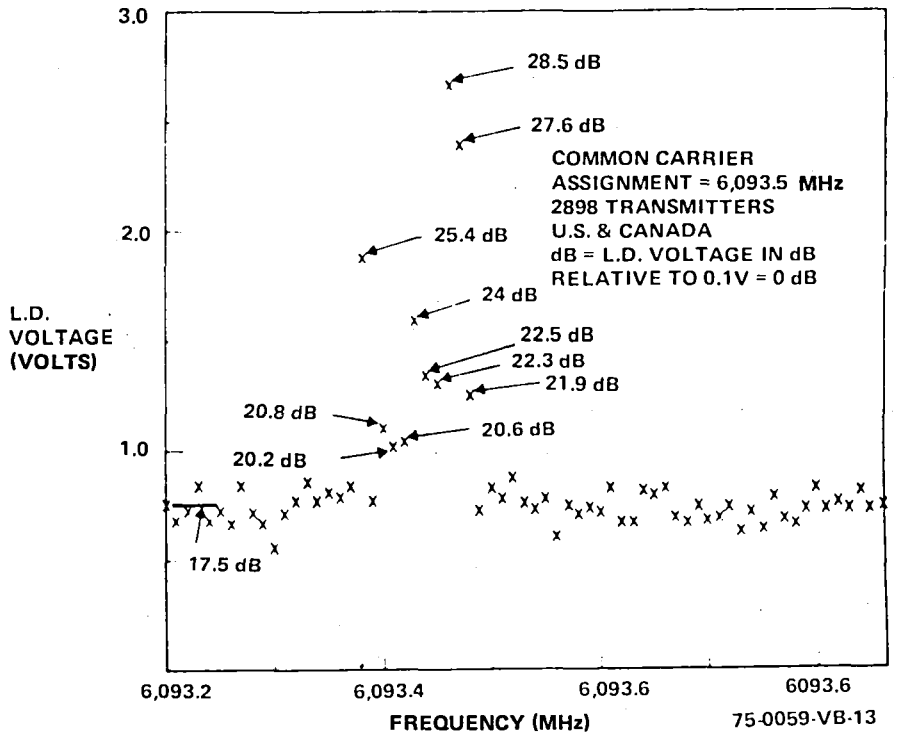

A

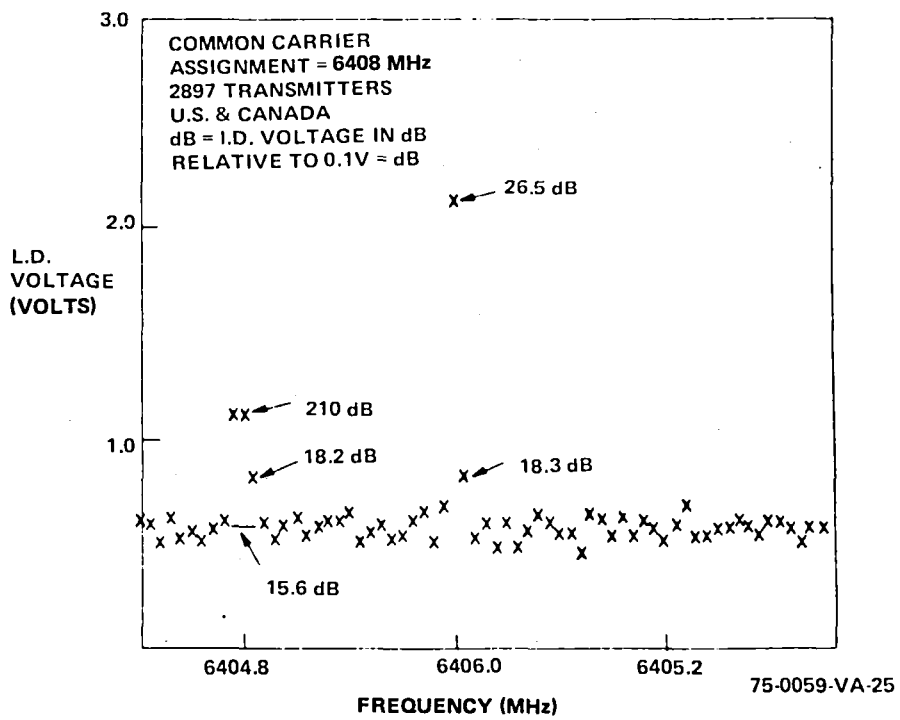

Figure 6-2. Horizon Scan GSFC, June 11, 1975, (6093.5 and 6404.8 MHz)

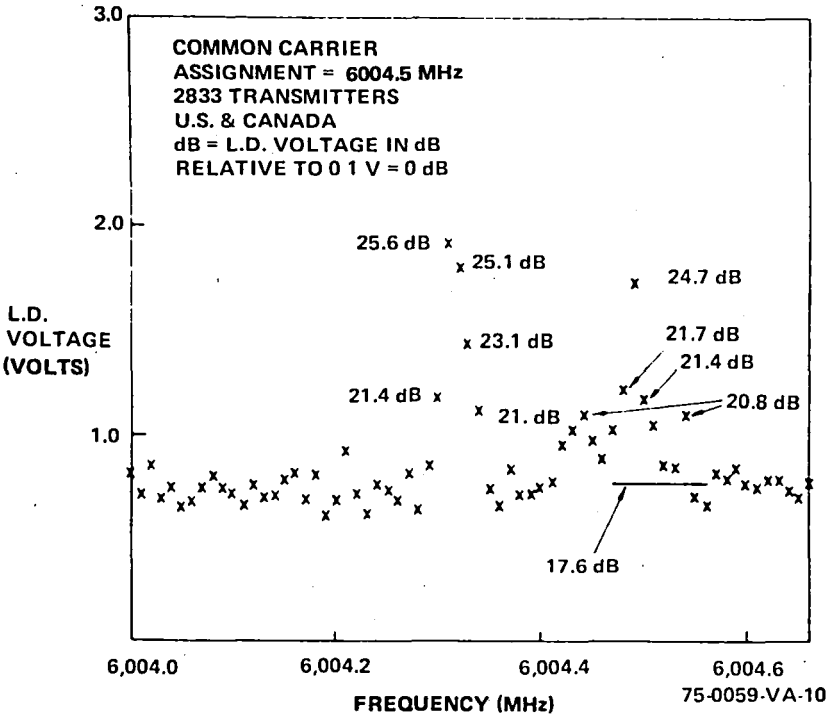

A

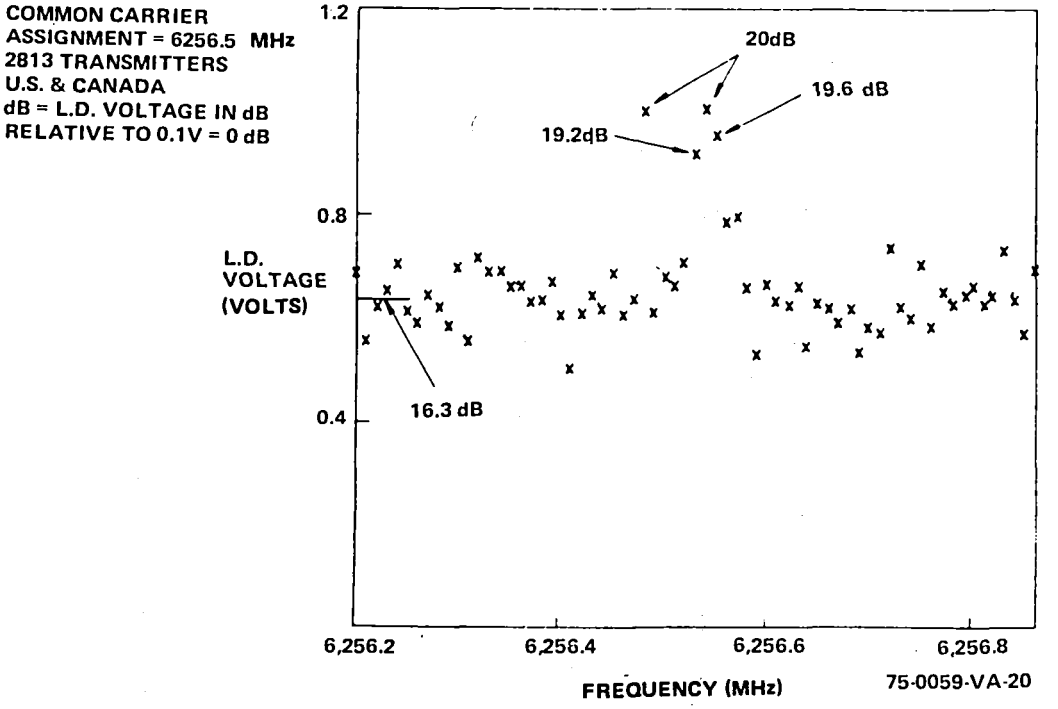

Figure 6-3. Horizon Scan, June 11, 1975,
(6004.5 and 6256.5 MHz)

Table 6-3
Detected Frequencies and Common Carrier Frequency Assignments

Frequency (MHz)	RFI (dBW)	R Ratio*	Common Carrier Assignment
5945.05	14.9216	0.8339	
5945.14	17.5935	0.7874	5945.20
5945.15	16.0029	0.8455	
5974.70	17.2096	0.7855	
5974.72	15.5564	0.7982	5974.80
5974.89	15.7607	0.8215	
6004.44	16.2374	0.8214	
6004.45	15.4299	0.8082	6004.50
6004.46	15.3902	0.7628	
6010.92	16.6910	0.6452	Unknown
6034.00	18.2651	0.7925	6034.20
6034.19	17.8086	0.7709	
6063.50	17.3135	0.7930	
6063.73	17.8993	0.7574	6063.80
6063.74	17.4132	0.7392	
6063.75	16.9591	0.7826	
6093.70	20.2396	0.8675	6093.50
6123.04	17.9975	0.7807	6123.10
6123.05	15.9214	0.8041	
6152.60	21.6112	0.7715	6152.80
6152.79	19.3274	0.7133	
6197.10	18.0997	0.7416	6197.20
6222-6229	Unidentified source that was also normally detected throughout the New England area by Mode 4.		
6256.40	19.5477	0.8538	
6256.42	19.8983	0.8296	6256.5
6256.43	18.5958	0.7444	
6308.80	16.8344	0.8285	Unknown
6375.00	19.6632	0.8663	6375.20
6404.75	19.7054	0.7769	6404.80
6404.76	19.9820	0.7396	
6424.92	17.6239	0.8027	
6424.93	17.8670	0.7982	6424.5
6424.96	17.0896	0.8111	

*The R ratio is the statistical quantity

X_i^2 i = 39 where X_i are the analog/digital samples recorded

ΣX_i^2 i = 1 during a 20-kHz recording interval

The quantity is useful in identifying single carrier wave sources.

MODE 8 GEOGRAPHIC LOCATION

The Mode 8 geographic location procedure was designed to access the location of rfi sources previously detected and isolated by frequency during Mode 4 RFIME measurements. The portable calibration terminal (PCT) was used as the rfi source during the Mode 8-geographic location test. Since its exact location was known, it provided a convenient reference with which to establish the accuracy of locating an rfi source from the ATS-6 geostationary orbit.

The Mode 8 configuration consisted of two orthogonal, east-west and north-south scans of the ATS-6 9.14-meter antenna about the general area of the portable calibration terminal. Power levels were recorded for each scan using the same data format as Mode 4, with the exception that the frequency of the receiver remained constant. The satellite roll and pitch angles were also recorded during each scan. Thus, a correlation between the time of occurrence of power maxima and the time of occurrence of a change in roll and pitch provided an estimate of the portable calibration terminal's location in terms of the satellite antenna roll and pitch angles. These estimates of roll and pitch were converted to an Earth intercept latitude and longitude and compared with the known location of the portable calibration terminal. Figure 6-4 illustrates the procedure used.

The analysis showed that the portable calibration terminal's location could be estimated to an accuracy of 133 to 153 kilometers. The primary source of error was caused by misalignment of the prime-focus feed (PFF) antenna Z-axis and its boresight axis. Increasing the location accuracy of this technique could have been accomplished by including the effects of the misalignment of the spacecraft boresight axis with the spacecraft Z-axis. However, further data would have been required to model the alignment characteristics, because the data obtained were dispersive and thereby inconclusive.

PFF ANTENNA PATTERN MEASUREMENT

Figure 6-5 shows the relative on-axis power measurement of the PFF antenna as recorded during the Antenna Pattern Measurement (APM) experiment. (The APM experiment was previously shown in Figure 5-11, Chapter 5.) The spacecraft Earth-coverage horn (ECH) receive antenna was also used briefly at the beginning and the end of each APM recording for comparison purposes. It should be noted that all of the dB values given in Figure 6-5 are relative values in which 0.1 volt output from the linear detector is represented as 0 dB.

From comparisons of Figure 6-5 and other similar APM recordings to the prelaunch antenna pattern measurements shown in Figures 6-6 (ECH receive), 6-7 (ECH transmit), and 6-8 (PFF receive), the following observations were noted:

- An in-orbit degradation of the satellite antenna system was evident. Prelaunch gain differential between the PFF receive and the ECH receive antennas was 28.3 dB. The APM recorded post-launch differential between these antennas (after ECH transmit off-axis correction) was approximately 21.3 dB. This apparent degradation is believed to have been caused, at least in part, by thermal deformation of the PFF antenna.

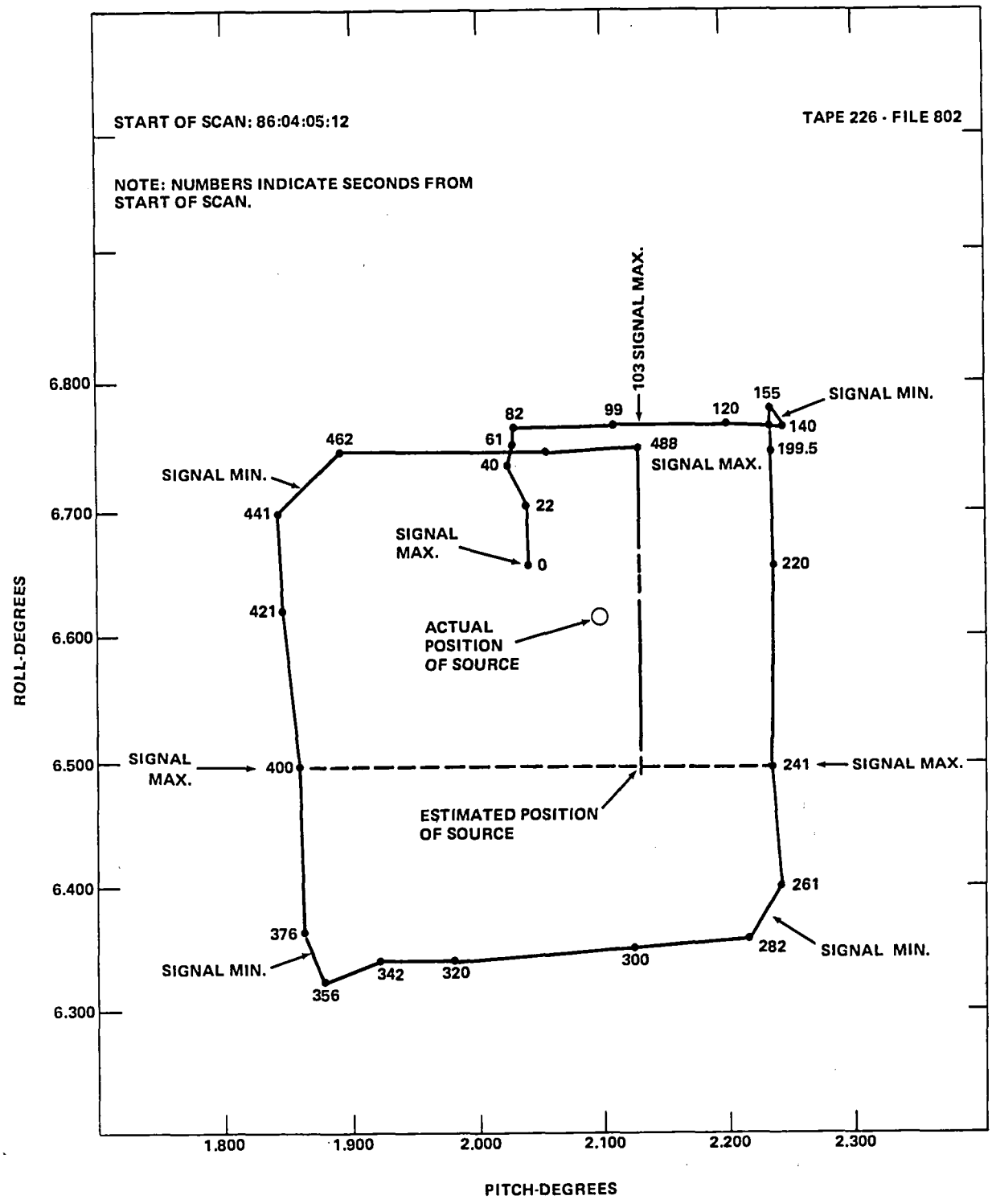

Figure 6-4. Mode-8 Scan Plotted in Roll and Pitch

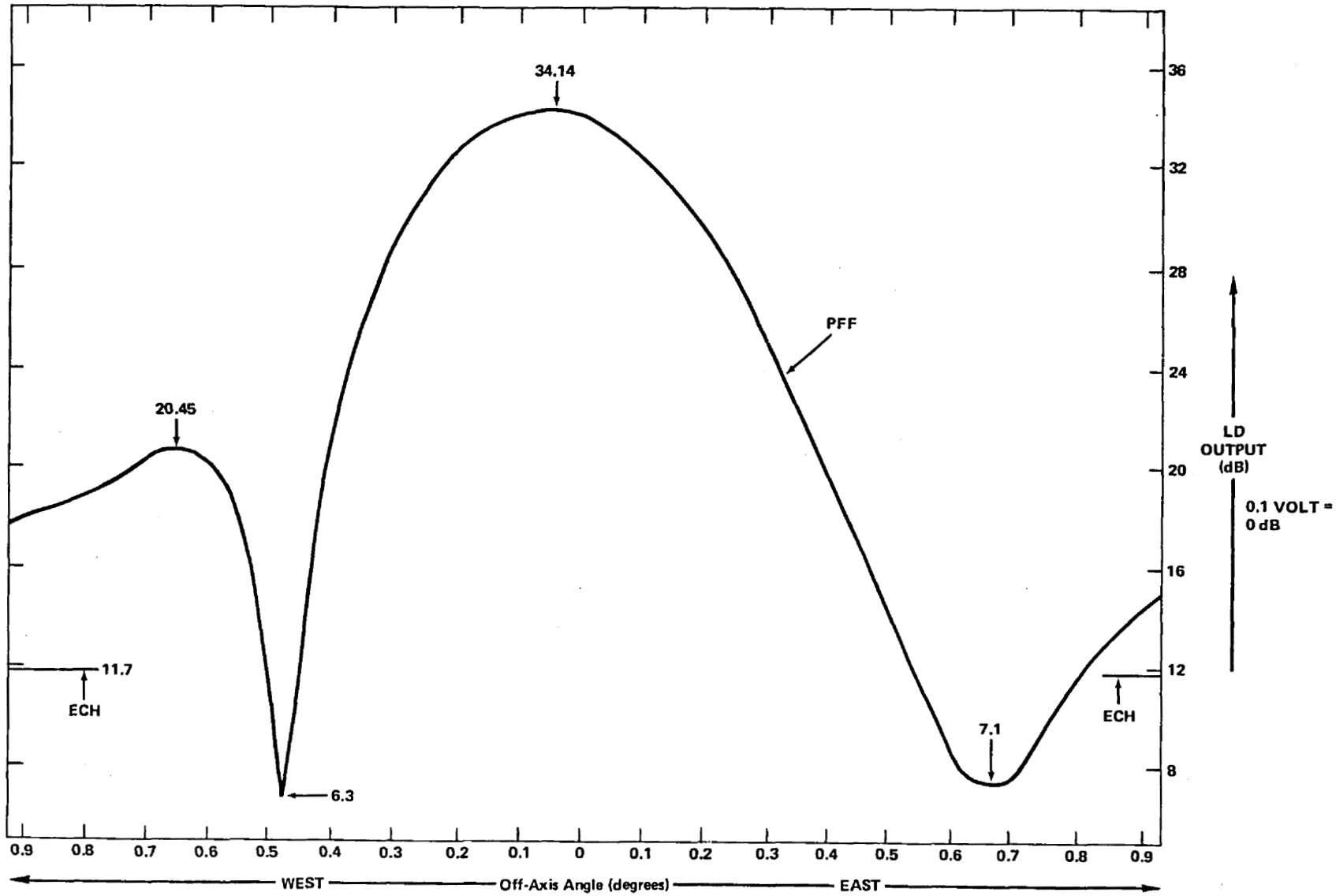

Figure 6-5. Prime-Focus Feed Antenna Pattern Measurement

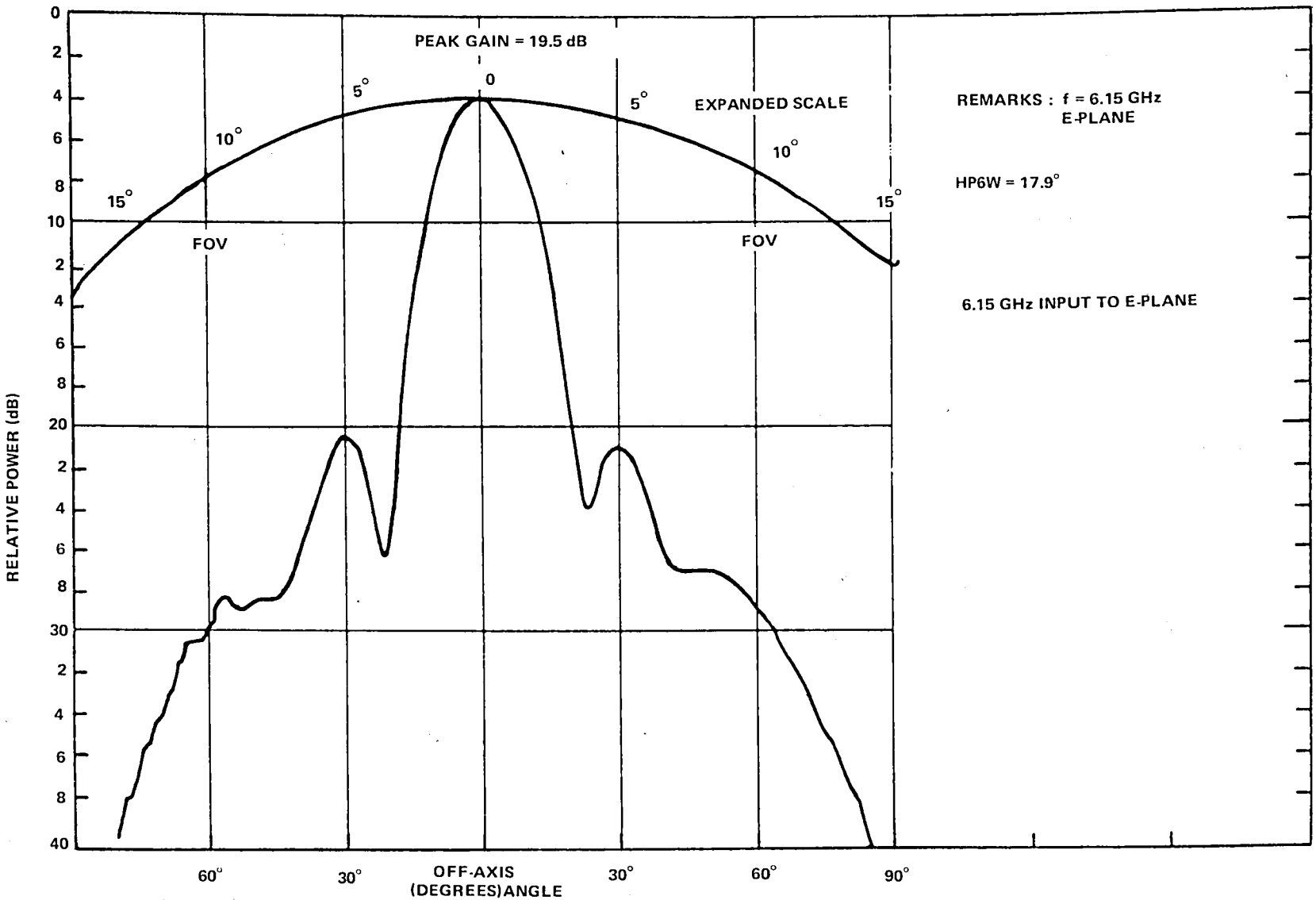

Figure 6-6. Receive Earth-Coverage Horn Antenna Pattern (E Plane) Prelaunch

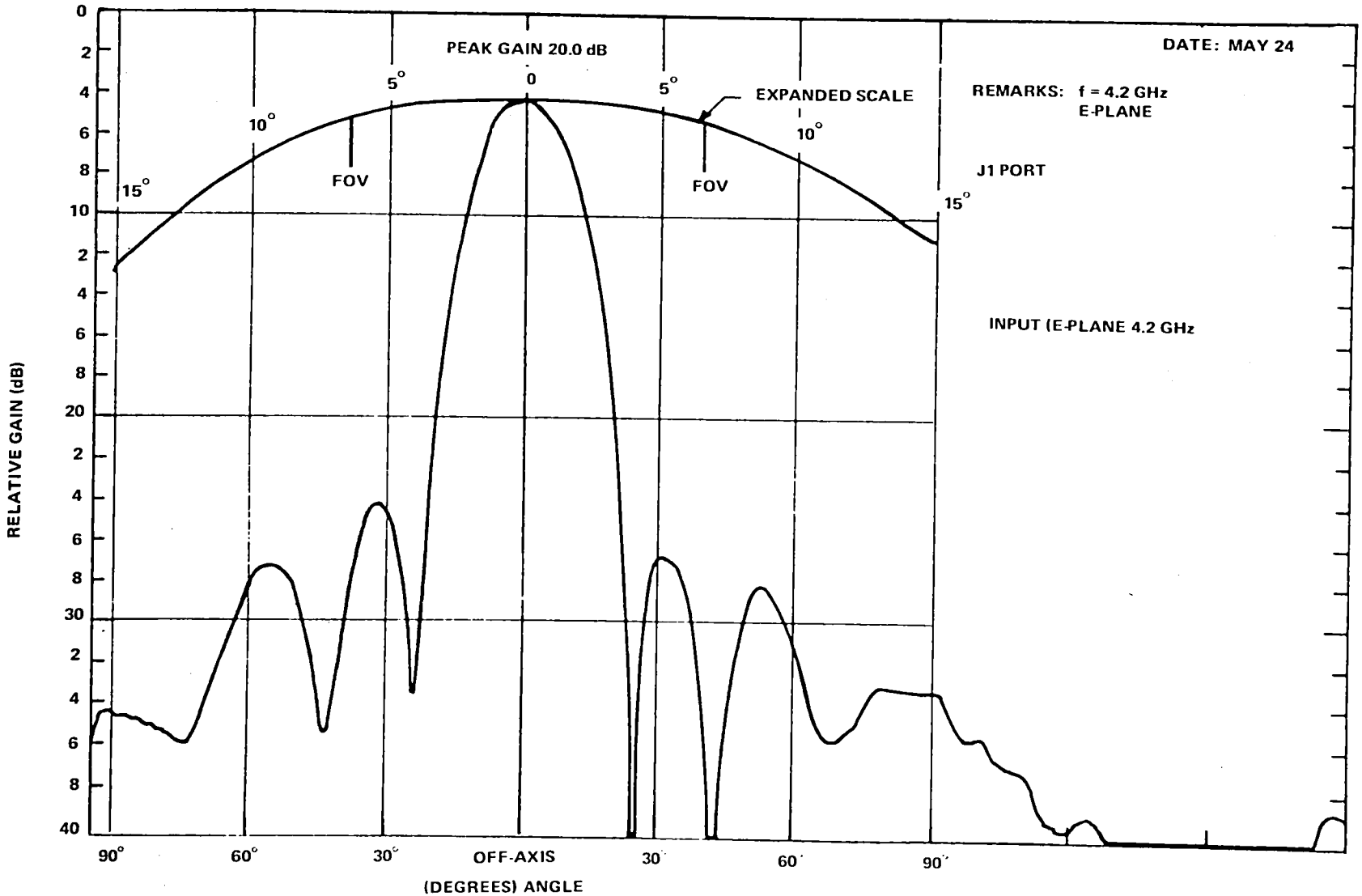

Figure 6-7. Transmit Earth-Coverage Horn Antenna Pattern (E Plane) Prelaunch

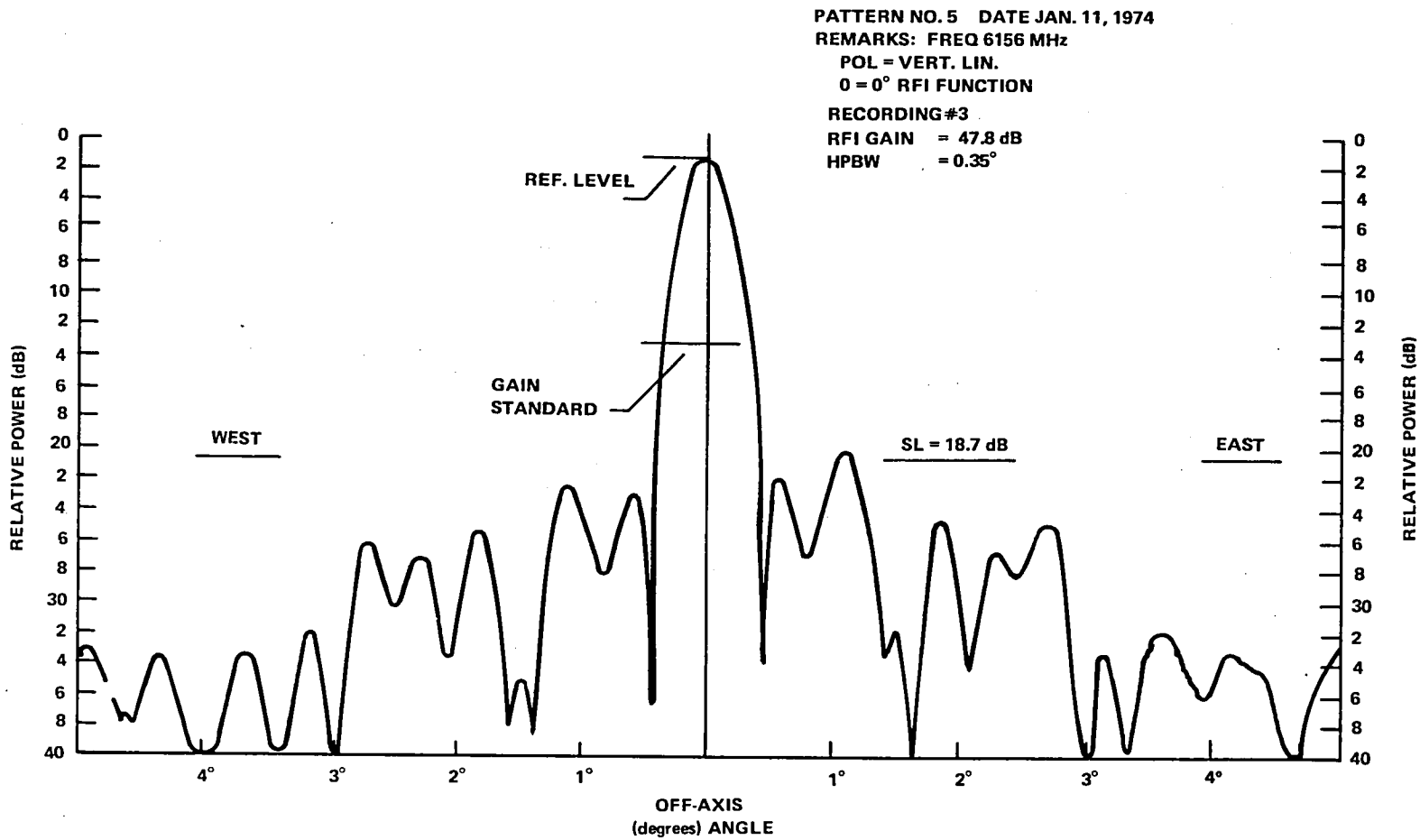

Figure 6-8. Prime-Focus Feed Receive East-West Plane Prelaunch

- The in-orbit half power beamwidth (HPBW) of the PFF antenna was approximately 0.38 degree compared to the preflight HPBW of 0.35 degree.

- The prelaunch and in-orbit PFF measurements were somewhat inconsistent concerning location and depth of the main side lobes indicating a possible PFF deformation.

- The main lobe of the PFF pattern appeared to have drifted from west to east as noted from examining a series of APM recordings.

VERIFICATION OF THE MATHEMATICAL MODEL

Selected files of processed RFIME data on Ithaca, New York, and Columbus, Ohio, were shipped to the Institute of Telecommunications Sciences (ITS) within the Office of Telecommunications U.S. Department of Commerce at Boulder, Colorado, for verification of the ITS math model. See Figure 6-4, "Mode-8 Scan Plotted in Roll and Pitch." Preliminary and limited comparisons of the processed data to ITS RFIME predictions for certain areas indicated the following:

- Favorable frequency comparison of the predicted common carrier channels (Tables 6-4 and 6-5).

- Power level predictions were normally 4 to 6 dB higher than those measured (Tables 6-4 and 6-5).

The departure in power levels between the predictions and the empirical data is somewhat understandable, because the RFIME determination of power level was estimated to have a root-mean-square (rms) accuracy of -3.5 dB to +1.0 dB for data collected under monopulse procedures and 3.5 dB to +6.0 dB for data collected without monopulse procedures. The estimated error budget is listed as follows:

Calibration terminal error (system)	±0.5 dB
Calibration terminal antenna pointing	+0.25 dB
PFF boresight error (with monopulse)	+0.5 dB
PFF boresight error (without monopulse)	+6.0 dB
RFIME system gain stability	±0.5 dB
ECH alignment error	±0.5 dB
Polarization error	-3.0 dB
Integrated source distribution error	-1.5 dB
Total rms error	-3.46 dB, +1.03 for monopulsed operations -3.46 dB, +6.07 for nonmonopulsed operations

Table 6-4
Institute of Telecommunications Sciences RFIME Predictions
for New York City

ATS-6 Longitude = 90.00°W
Main Beamwidth (first null to first null = 1.5 degrees)

Target is New York City

Target Latitude = 40.708°N
Target Longitude = 74.000°W

		Maximum Predicted Levels		
	Frequency MHz	Signal Power Density dBW/10 kHz	Main Lobe Contribution	Side Lobes Contribution
1	6226.90	-145.6	-146.2	-154.3
2	5974.80	-145.8	-146.4	-154.2
3	6197.20	-146.0	-146.6	-154.7
4	5945.20	-146.0	-146.6	-154.6
5	6345.50	-146.0	-146.6	-155.1
6	6093.50	-146.1	-146.7	-154.9
7	6034.20	-146.2	-146.8	-154.8
8	6315.90	-146.3	-146.9	-155.1
9	6063.80	-146.3	-147.0	-154.9
10	6256.50	-146.3	-147.0	-154.9

IN-ORBIT G/T MEASUREMENT

In developing a technique for in-orbit measurement of the rfi transponder gain/temperature (G/T), the standard method employed to measure the G/T of a communications transponder was first examined to determine its applicability. This technique makes use of the assumption that the communications transponder contains a hard limiter and is easily saturated by the uplink transmitter. The method is to saturate the transponder with a carrier-wave (CW) signal and measure the output of the downlink receiver. Then the uplink signal is reduced until the measured downlink receiver level decreases exactly 3 dB. At this point, the uplink transmitter power is measured. By assuming that (at this point) the spacecraft transponder is transmitting half its power in noise and the other half in a CW signal, the uplink received signal power would then equal its input noise power. From these measurements, one should be able to determine the G/T.

Table 6-5
Spacecraft Pointed at New York City, December 17, 1974

Common Carrier* Frequency Assignment	Frequency	0552Z	G.M.T.: dBW/10 kHz 0602Z	0652Z	0702Z	0752Z	0802Z	0350Z	0901Z	ITS Predictions dBW m^2 /10 kHz	dBW /10 kHz
	5,945,110,000	9.678	10.784	11.006	10.389		10.897				
	5,945,120,000				10.251						
5,945,200,000	5,945,200,000	9.908				12.739	11.061		12.563	-146.0	16
	5,945,220,000			8.505							
	5,960,000,000			11.281						Portable calibration terminal generated	
5,974,800,000	5,974,860,000				12.355				13.172	-145.8	16.2
	6,004,420,000			9.316							
6,004,500,000	6,004,470,000				9.262	11.380	9.427				
	6,004,500,000						12.441			2833 transmitters	
	6,004,510,000			13.441				11.714			
	6,034,130,000						13.871	13.842			
	6,034,150,000		14.272					9.971		-146.2	15.8
6,034,200,000	6,034,170,000						11.502				
	6,034,330,000		11.044	10.661							
	6,046,350,000		7.144								
	6,048,080,000	10.974	11.267	12.151	11.947	11.795	12.299	13.008	12.424	Spacecraft generated	
	6,048,090,000	13.481	12.975	11.462	13.174	11.689	11.613	11.610	11.531		
	6,057,590,000	20.678									
	6,057,620,000	25.464									
	6,057,650,000	21.434								Believed to be pulse source (radar)	
	6,057,700,000	14.529									

Table 6-5
Spacecraft Pointed at New York City, December 17, 1974 (continued)

Common Carrier* Frequency Assignment	Frequency	G.M.T.: dBW/10 kHz 0552Z	0602Z	0652Z	0702Z	0752Z	0802Z	0850Z	0901Z	ITS Predictions dBW m^2 /10 kHz	dBW /10 kHz
	6,063,660,000			9.858							
6,063,800,000	6,063,670,000			8.700	9.818						
	6,063,800,000			14.503						-146.3	15.7
	6,063,810,000				12.595						
	6,064,980,000							8.716			
	6,075,150,000	18.074								Believed to be pulse source (radar)	
	6,075,180,000	20.371									
	6,075,200,000	21.053								Believed to be pulse source (radar)	
	6,075,210,000	18.462									
	6,075,230,000	16.919									
	6,093,470,000			8.605							
6,093,500,000	6,093,800,000				6.062						
	6,093,810,000	9.607	9.551	9.483	11.350	7.675		9.645	9.880	-146.1	15.9
6,123,100,000	6,123,120,000					10.110					
	6,123,160,000			10.294						2801 transmitters	
	6,152,700,000		7.637								
6,152,800,000	6,152,750,000			12.102							
	6,152,760,000				8.988						
	6,152,770,000		6.534							2846 transmitters	
	6,152,790,000					8.209					
6,197,200,000	6,197,260,000							10.644		-146.0	16
	6,226,830,000				13.296	13				-145.6	16.4
6,226,900,000	6,226,840,000				11.582						
	6,230,000,000	14.302	14.644	14.330	14.787	14.780	15.092	16.350	15.607		

Table 6-5
Spacecraft Pointed at New York City, December 17, 1974 (continued)

Common Carrier* Frequency Assignment	Frequency	G.M.T.: dBW/10 kHz								ITS Predictions	
		0552Z	0602Z	0652Z	0702Z	0752Z	0802Z	0850Z	0901Z	dBW m^2 /10 kHz	dBW /10 kHz
	2,230,010,000	19.760	20.068	19.961	20.229	19.992	19.926	29.596	20.296	Spacecraft generated	
	6,233,060,000			9.303							
	6,233,420,000				9.158						
6,256,500,000	6,256,530,000							13.081			
	6,256,550,000			10.708						-146.3	15.7
	6,256,560,000	9.000			7.667						
	6,296,460,000	7.074									
6,315,900,000	6,315,840,000						10.109			-146.3	15.7
	6,332,720,000		7.721								
6,375,200,000	6,375,160,000								12.244	2770 transmitters	
	6,404,780,000				12.255		7.397				
6,404,800,000	6,404,840,000		9.368							2897 transmitters	

*FCC tolerance for newly installed equipment after 1975 = 0.005 percent nearly equal to ±300 kHz

This technique was not considered useful because of the linearity of the rfi transponder, making it impractical to saturate it. Instead, a technique was devised that is similar to that used to measure the noise figure of a receiver. With this method, the uplink transmitter was used as a calibrated noise source and the downlink receiver was employed as a power meter to measure the increase in noise power (due to the uplink noise) in the same manner that a noise figure meter is used. This method was considered to be highly accurate using an uplink signal consisting of a flat spectrum of white noise. Also, the technique lent itself to using a CW signal as long as the detector in the downlink receiver was a true power measuring device rather than an envelope detector.

A special G/T measurement test was conducted on May 30, 1975 as shown in Figure 6-9. This test measured the G/T in three configurations:

- PFF used on both uplink and downlink
- PFF used on uplink and ECH used on downlink
- ECH used on both uplink and downlink

The two methods of measurement were employed, one using a noise uplink signal and one using a CW uplink signal.

From these measurements and data reduction, the following G/T's were postulated for the rfi transponder:

PFF: 11.5 dB/K
ECH: -18.8 dB/K

These values were about 3 dB below the G/T calculated from prelaunch information. The predictions prior to launch of ATS-6 showed the PFF G/T to be 15 dB/K (G = 48 dB) while prelaunch measurement of the rfi transponder noise figure and the values of PFF gain (47.5 dB) used during flight placed the G/T at 14.5 dB/K. This degradation in the postflight system gain was also noted during the PFF Antenna Measurement experiment and was therefore consistent.

CONCLUSIONS

Based upon the in-orbit measurement of PFF G/T ratio, the RFIME met its design minimum source e.i.r.p. detection capability of 10 dBW. Since the measured ratio of PFF to ECH antenna gains dropped several dB from the preflight to the in-orbit condition, the in-orbit measurements were conducted with some PFF electrical boresight error at the time of measurement due to solar thermal distortion of the spacecraft antenna dish. This is reflected in the +6.0 dB budget error item in Table 6-6 attributed to nonmonopulse PFF boresight error.

The experiment objectives of measuring the rfi power density at geosynchronous attitude and of measuring the geographical and frequency distribution of rfi sources was met during the first year

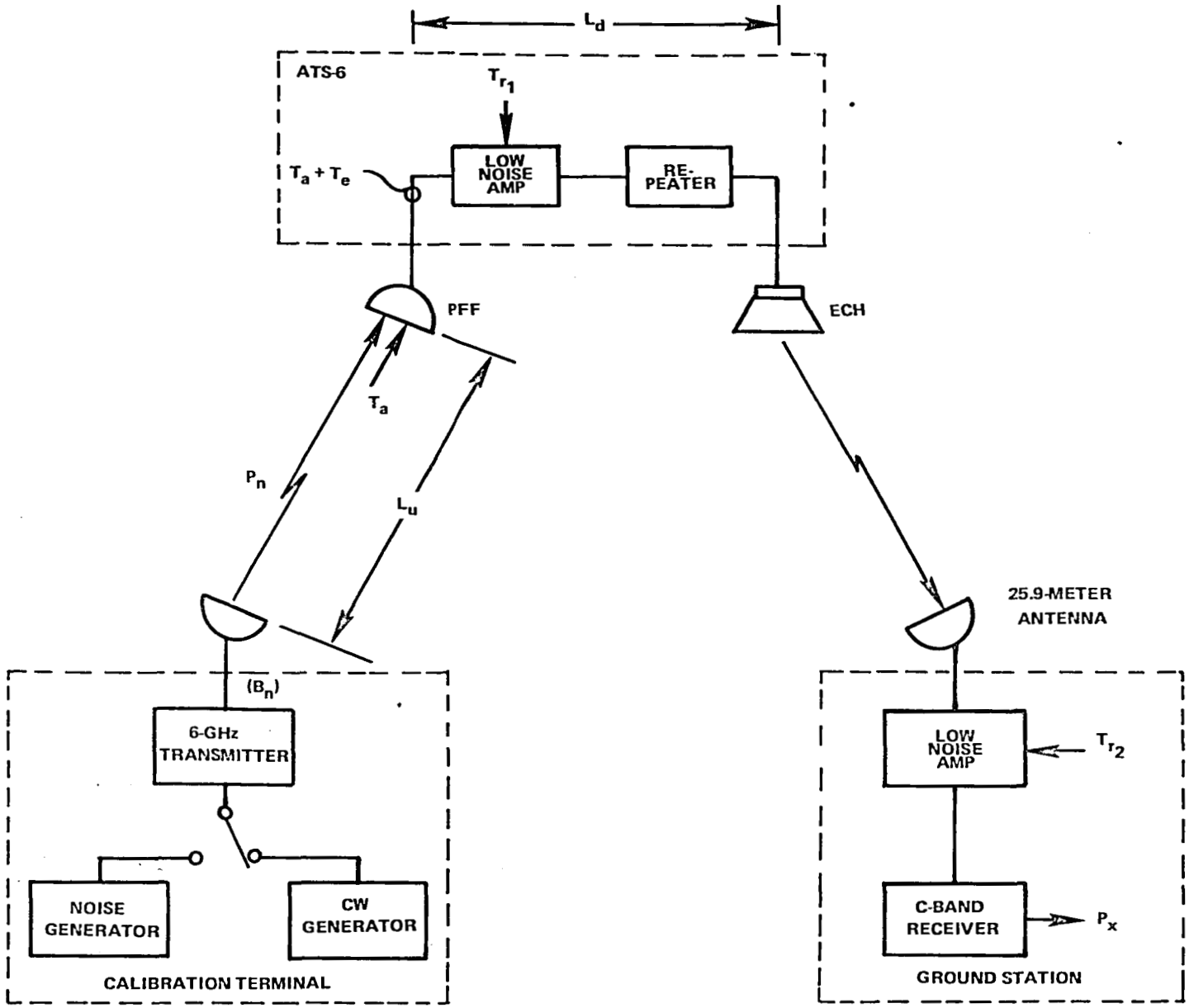

Figure 6-9. Radio Frequency Interference G/T Measurement System Model

that ATS-6 observed the continental United States and adjacent areas. The goal of measuring the incident flux to within 0.5 dB was ambitious, but at least the sources of error in power level measurement were identified and assigned reasonable values based on the experimental results and the calibrations through the mechanization of the source determination program described previously.

The RFIME data were supplied to the cognizant agencies. The impact of these data in determining the RFIME goals of establishing maximum satellite G/T ratios and minimum downlink e.i.r.p. power required of satellite systems is unknown.

The objective of establishing model utility was not accomplished because of circumstances beyond NASA's control. Preliminary analyses of RFIME data about Ithaca, New York, and Columbus, Ohio, resulting from an effort by the Institute of Telecommunications Sciences of the Office of Telecommunications, U.S. Department of Commerce at Boulder, Colorado, indicated a favorable frequency comparison with the predicted common carrier channels, but a modeled power level of 4 to 6 dB higher than measured.

CHAPTER 7

EARTH STATION ANTENNA EVALUATIONS

INTRODUCTION

Earth station wide angle pattern measurement was implemented and successfully accomplished by the cooperative efforts of the Communications Satellite Corporation (Comsat) and the National Aeronautics and Space Administration (NASA) by use of the geosynchronous communications satellite, ATS-6. These measurements were made during the period August 6 through October 29, 1976. ATS-6 was made available for this experiment while it was drifting from its easterly position of 35°E longitude to the westerly station of 140°W longitude. The Applications Technology Satellite (ATS) instrumentation at the NASA Rosman Ground Station near Brevard, North Carolina, was used. The radiation pattern of high-gain antennas at angles in excess of 90 degrees off the antenna boresight was measured. To achieve this, it was necessary to develop a measurement system that had a dynamic range greater than 75 decibel (dB). The method developed permitted radiation measurements of 90 dB below the peak of the antenna pattern. The experiment made use of two distinct steps in the measurements technique to accomplish the unusually large dynamic range.

EXPERIMENT DESCRIPTION

Experiment Configuration

The configuration of ATS-6 with its 9.14-meter parabolic antenna, a wideband linear radio frequency interference (rfi) transponder, and Earth-coverage horn to transmit, was ideally suited to make the antenna pattern measurements. It was a three-axis stabilized satellite that employed inertia wheels and jets. The stabilization system permitted the 9.14-meter parabolic antenna to be pointed to a designated ground station with an accuracy of 0.1 degree. The spacecraft with its large antenna provided a gain/temperature (G/T) of 12 dB/K that permitted reception of signals radiating from the ground with an effective isotropic radiated power (e.i.r.p.) of 10 dBW. The design of the spacecraft permitted the selection of any one of four polarization modes; namely, linear east-west, linear north-south, right-hand circular or left-hand circular.

The rfi transponder had the capacity to receive signals in the 5925-megahertz (MHz) to 6425-MHz range and transpond them directly to the 3700-MHz to 4200-MHz range. The gain of the transponder was selectable in five steps over a 20-dB range. A simplified block diagram of the rfi transponder of the spacecraft is shown in Figure 7-1. All the amplifiers were linear; thus the level of the transmitted 4-gigahertz (GHz) signal was directly proportional to the level of the 6-GHz signal.

The Rosman Ground Station was used to receive and record data from ATS-6 because it had a 26-meter parabolic antenna, a cooled paramp, and the ATS ranging receiver (ATSR). The ATSR was

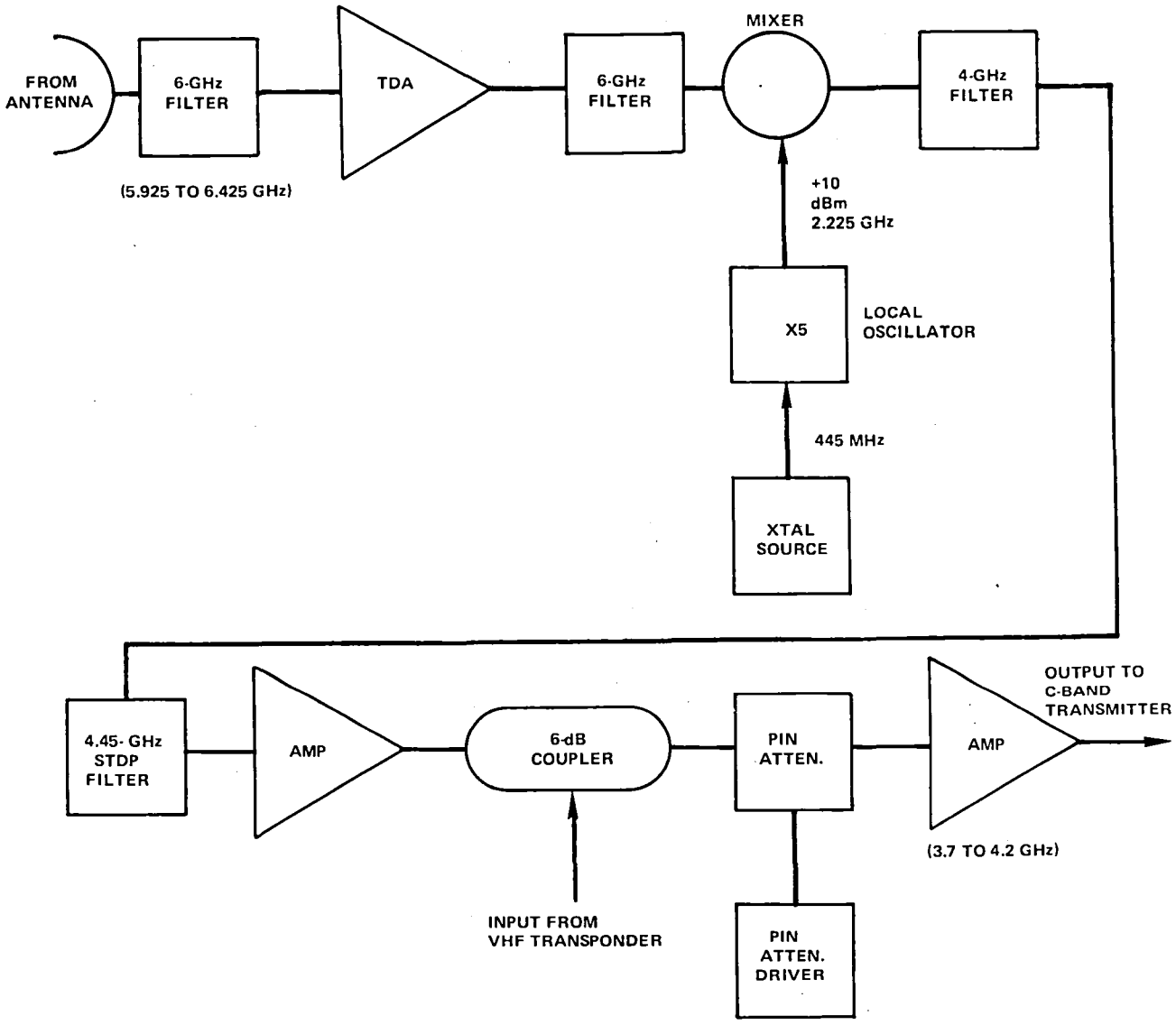

RF 1 TRANSPONDER
GAIN MODES: 48, 56, 60, 66, 70 dB
GAIN OUTPUT MODES WITH THE C-BAND TRANSMITTER
LINEAR GAIN OF 44 dB
G1 = 114 dB
G2 = 110 dB
G3 = 104 dB
G4 = 100 dB
G5 = 92 dB

Figure 7-1. Simplified RFI Transponder Block Diagram

designed to operate within 2 dB of its noise threshold of -148 decibels, referred to 1 milliwatt (dBm). The signal levels actually recorded were in the range of -86.5 dBm to -145 dBm. A block diagram of the data acquisition configuration is shown in Figure 7-2.

Experiment Operation

The far field pattern measurements were made with the spacecraft antenna pointed at the Earth station under test. Then, by rotating the ground antenna in elevation or azimuth, a recording was made of the spacecraft antenna received signal versus time at the Rosman Ground Station.

To achieve the needed dynamic range, the initial step in the measurement process was to have the antenna under test transmit sufficient power to cause the spacecraft transmitter to be near saturation while it provided the acquisition of linear data. This was accomplished at an e.i.r.p. of approximately 55 decibels, referred to 1 watt (dBW). Operating at this level, an accurate measurement was made of the main lobe and near side lobes (on either side of the main lobe); however, the far side lobes descriptive data was within the noise of the ground receive system.

To obtain the wide-angle data, the test ground transmit power was increased by 40 dB that accentuated the received far side lobe levels. At this level the main lobe and the first three side lobes saturated the spacecraft transmitter. This saturated data was discarded during the data analysis process. The data analysis process combined the data from both steps to generate a continuous antenna pattern. To ensure continuity, a comparison was made of the initial unsaturated side lobes taken in Step 2 with the reference that was the same spatial side lobes in Step 1.

TESTING

The schedule of the tests is shown in Table 7-1.

Seven basic tests were scheduled for each participating Earth station. The tests were scheduled in a way to minimize ground station operations and were limited to four or five hours. Consequently, all tests were not completed in a number of cases.

The first test evaluated the transmit gain of the Intelsat Earth Station by a direct comparison technique to the Rosman Ground Station transmit gain.

The second and third tests consisted of making narrow angle (±5 degrees) antenna patterns by performing elevation and azimuth scans of ATS-6 while it was configured in Earth-coverage horn (ECH) for both receive and transmit.

The fourth and fifth tests were a repeat of the second and third tests with the major difference being that the high-gain spacecraft antenna (prime-focus feed) was used for receive and the Earth station transmit power was reduced. An example is shown in Figure 7-2.

The sixth test was principally an elevation scan. In some cases, where it was appropriate, an azimuth scan was performed. The high-gain antenna was used for receive, as in the fourth and fifth tests, and

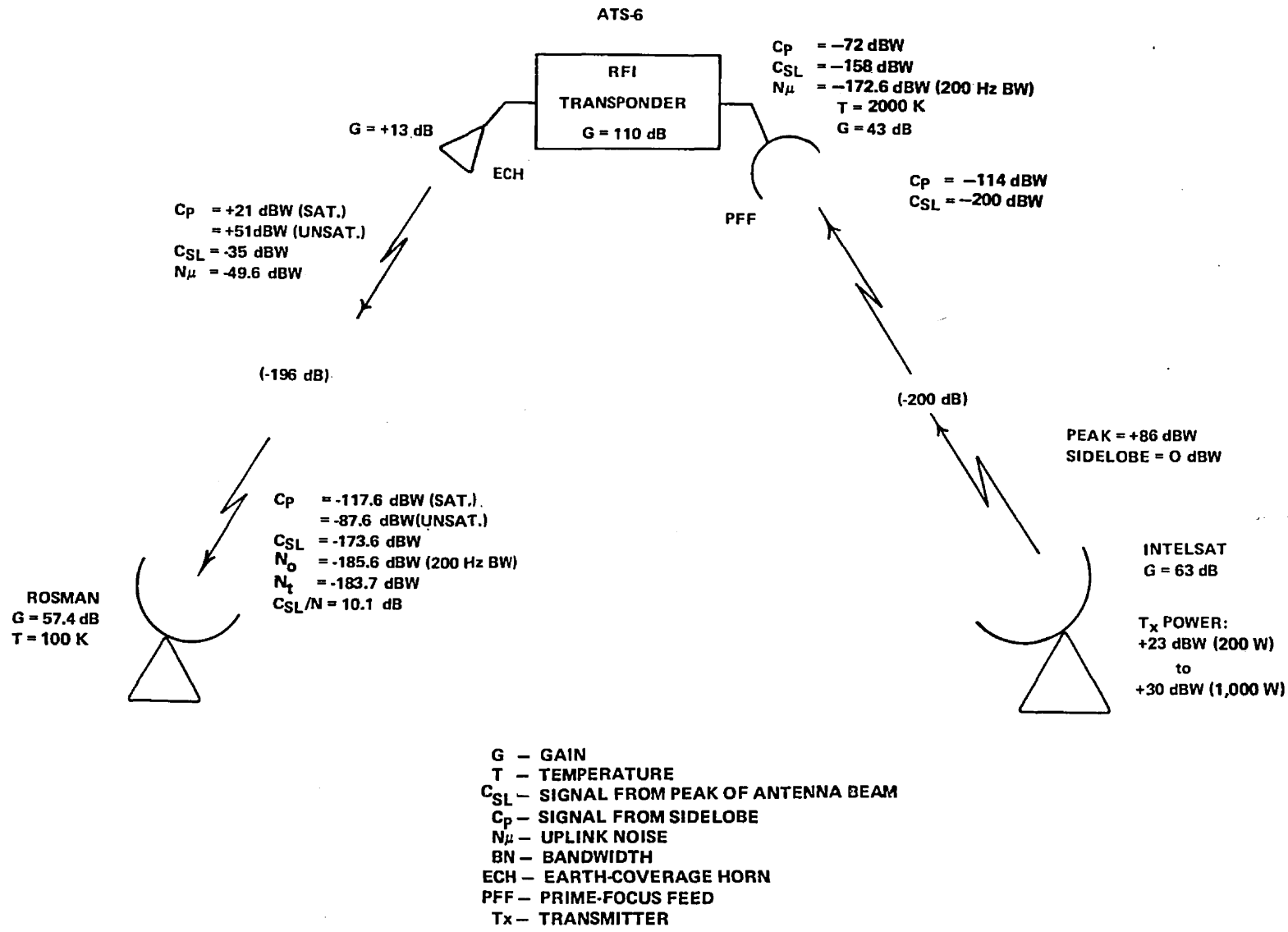

Figure 7-2. Antenna Pattern Measurement Test Configuration

Table 7-1
Test Schedule

Test No.	Date (1976)	Earth Station	Comments
1	August 6	Lario, Italy	Test to qualify experiment procedure
2	September 5	Taif, Saudi Arabia	(1)
3	September 7	Pleumeur-Bodou 3, France	(1)
4	September 8	Emeq Ha'ela, Israel	(1)
5	September 22/23	Baqa, Jordan	No test results due to communication difficulties
6	September 23/24	Lario, Italy	No test results due to technical difficulties
7	September 24/25	Tanum, Sweden	Limited elevation pattern obtained due to mispointing of satellite antenna
8	September 23/30	Thermopylae, Greece	(1)
9	October 1	Lario, Italy	(1)
10	October 2	Goonhilly 3, United Kingdom	(1)
11	October 2/3	Goonhilly 2, United Kingdom	Elevation and azimuth pattern obtained
12	October 4	Lakhdaria 1, Algeria	Azimuth pattern obtained
13	October 6	Aguimes, Spain	(1)
14	October 12	Barbados, B.W.I.	(1)
15	October 13	Balcarce 1, Argentina	(1)
16	October 14	Matura Point, Trinidad	(1)
17	October 15	Prospect Pen, Jamaica	(1)
18	October 18	Tulancingo 1, Mexico	(1)
19	October 19	Longovilo, Chile	(1)
20	October 20	Tangua 1, Brazil	(1)
21	October 29	Cambita, Dominican Republic	(1)

(1)Elevation pattern obtained

the Earth station raised its transmit power to typically 200 to 1000 watts. Overlapping the data from the low power runs with the data from the high power runs resulted in the dynamic range of nearly 90 dB. An example of this test is shown in Figure 7-3.

Finally, a calibration test on the saturation characteristics of the satellite traveling wave tube (TWT) was performed only if there was sufficient time. The entire procedure required four to five hours and was performed at times when Earth station traffic was at a minimum.

Applications Technology Satellite-6

ATS-6 was capable of operating in the communication satellite band with the same 6/4-GHz translation used by Intelsat. Through appropriate switching it was arranged to receive and transmit on either its Earth-coverage horn, or its high-gain prime-focus feed 9.14-meter diameter reflector antenna (gain was approximately 42 dB), or any combination of them. The rfi transponder was used for these tests. It was a 500-MHz transponder with a large linear gain whose range could be commanded over a 22-dB range in five steps. The output was used to drive a 10-watt (TWT) transmitter. A simplified block diagram of the transponder is shown in Figure 7-1.

Recording Earth Stations

Two Earth stations were used to record the transponded test signals. These were the 26-meter NASA ATS-6 terminal at Rosman Ground Station and the 10-meter United Kingdom Goonhilly Research Station.

The Rosman Ground Station was the principal recording station. The ATSR receiver system was used. It had a detection threshold of approximately -176 dBW level. The signals detected by this system were recorded on both 10-inch wide chart recorders and backup 8-channel chart recorders.

The Goonhilly Earth station was used primarily to make on-site recordings of their antenna patterns and as back-up, and to monitor test conditions for a number of other tests. Processed results of the antenna patterns, recorded by them, were in excellent agreement.

Test Configuration

To obtain these measurements at large scan angles, a dynamic range of greater than 75 dB was required.

The test configuration used the high-gain satellite antenna, high-power transmission at the Intelsat Earth stations and the high-gain receive antenna at the Rosman Ground Station in the United States. This configuration, with accompanying signal levels, is shown in Figure 7-2.

As can be seen from the values given in Figure 7-2, a dynamic range of 86 dB can be achieved, assuming the station under test transmits an e.i.r.p. of +86 dBW and that the detection threshold at Rosman is a carrier-to-noise ratio (C/N) of 10.0 dB. The Earth station first transmits a low-power signal (0.1 watt, typically) then a high-power signal (approximately 200 watts to 1000 watts) for measuring at large scan angles.

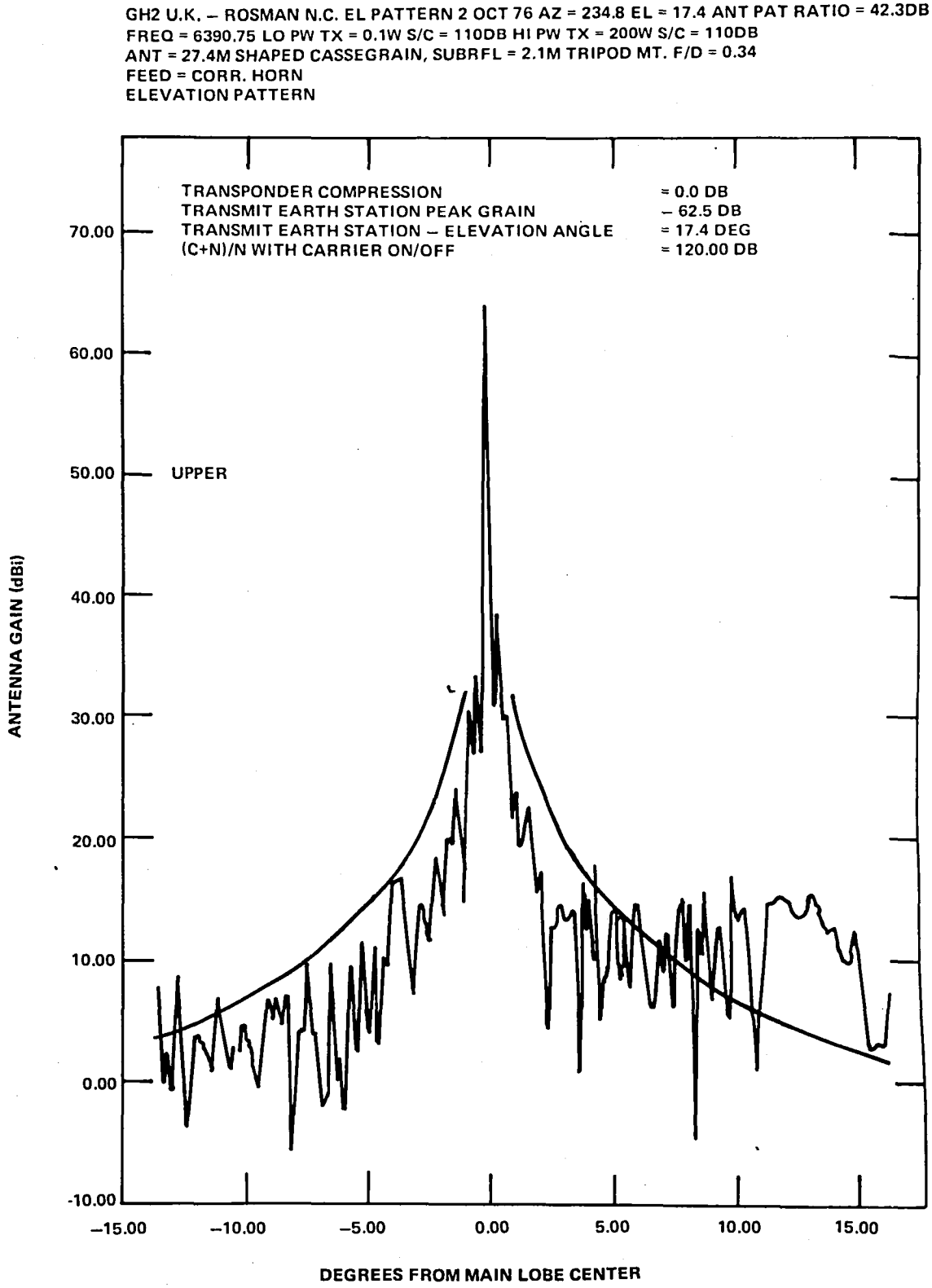

Figure 7-3. Elevation Pattern for 27.4-meter Goonhilly 2

Test Results

Of the 21 tests conducted, 18 produced useful data and one of them, Goonhilly 2 (United Kingdom), resulted in both an elevation and azimuth pattern. The plotted results for Goonhilly 2 are given in Figures 7-3 and 7-4, while Figure 7-5 is the plotted results for an azimuth pattern produced by the Lakhdaria 1, Algeria, 32-meter antenna. The remainder of the patterns are given in a paper "Far Field Large Angle Antenna Pattern Measurement," by Moore.*

Data Processing Procedure

The objective of the data reduction was to provide a profile of the peaks of the antenna lobes. This was obtained by merging both antenna patterns taken by means of the high-transmitter power and low-transmitter power modes. These patterns were merged by correlating off-axis lobes that were not in saturation on the high-power patterns. A dBi (gain relative to an isotropic antenna) scale was obtained by referring the peak of the low-power patterns to the gain of the antenna under test. The scale obtained was then used to measure the peak of every identifiable lobe. This resulted in a data reading at an average of every 0.2 degree. All the data points and their angles, referred to the main-beam axis, were entered into a computer file. The file was then used to produce the patterns shown as graphs in the figures. No other processing of the data was performed. A curve of the equation, $dBi = 35 - 25 \log.\theta$ for the range, $1° \leqslant \theta \leqslant 48°$, has been superimposed on the graphs. Other information concerning the characteristics of the antenna tested and pertinent test values were also included on each figure.

When using the graphs, a number of cautions should be noted. These are:

- The patterns obtained are single-plane scans, either an elevation scan or an azimuth scan.
- Except for Earth stations near or on the equator, they are not scans along the geostationary arc, which would be a more worthwhile scan but nearly impossible to obtain with operational antenna.
- The subreflector support spars probably played a major role in the shape of the profile of the lobe peaks. The orientation or the effects of these spars are still an unknown.
- Great care was exercised in attempting to maintain accuracy by using pre- and post-chart calibration. The data reduction procedure chosen does not relay on absolute values but on readings relative to beam peak. It is felt that an overall accuracy of 3 dB was maintained.
- An error of 1 dB in choosing the antenna gain, at the measurement frequency, will shift the profile up or down by the same amount.
- Because the satellite was constantly moving at 0.05 degree per hour and the beamwidth of the 9.14-meter antenna was approximately 0.2 degree, a change in pointing of this antenna at the Earth station under test caused an apparent change in the pattern profile.

*Moore, R. L., et al., prepared for Antennas and Propagation Society IEEE International Symposium, June 1977.

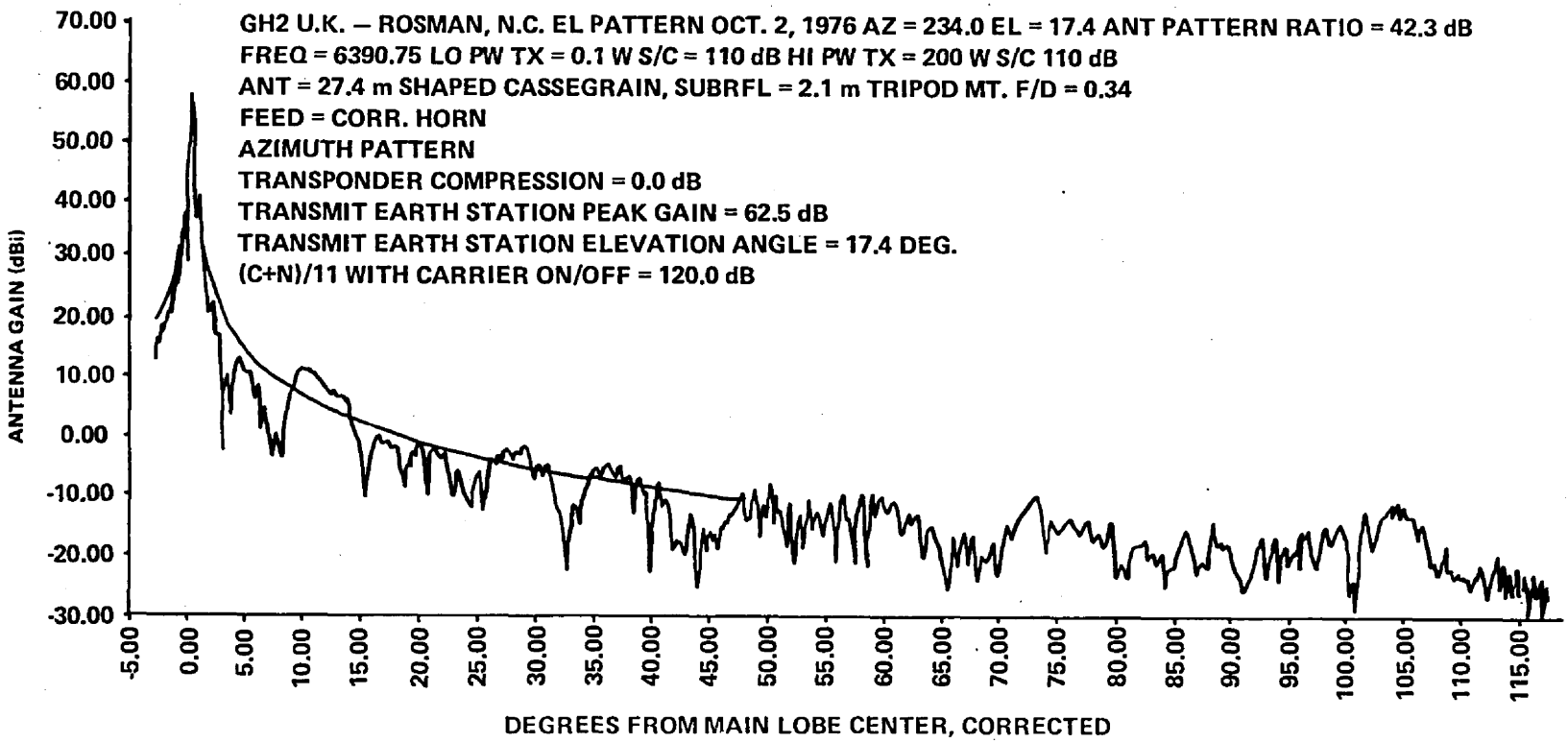

Figure 7-4. Azimuth Pattern for 27.4-meter Antenna, Goonhilly 2, United Kingdom

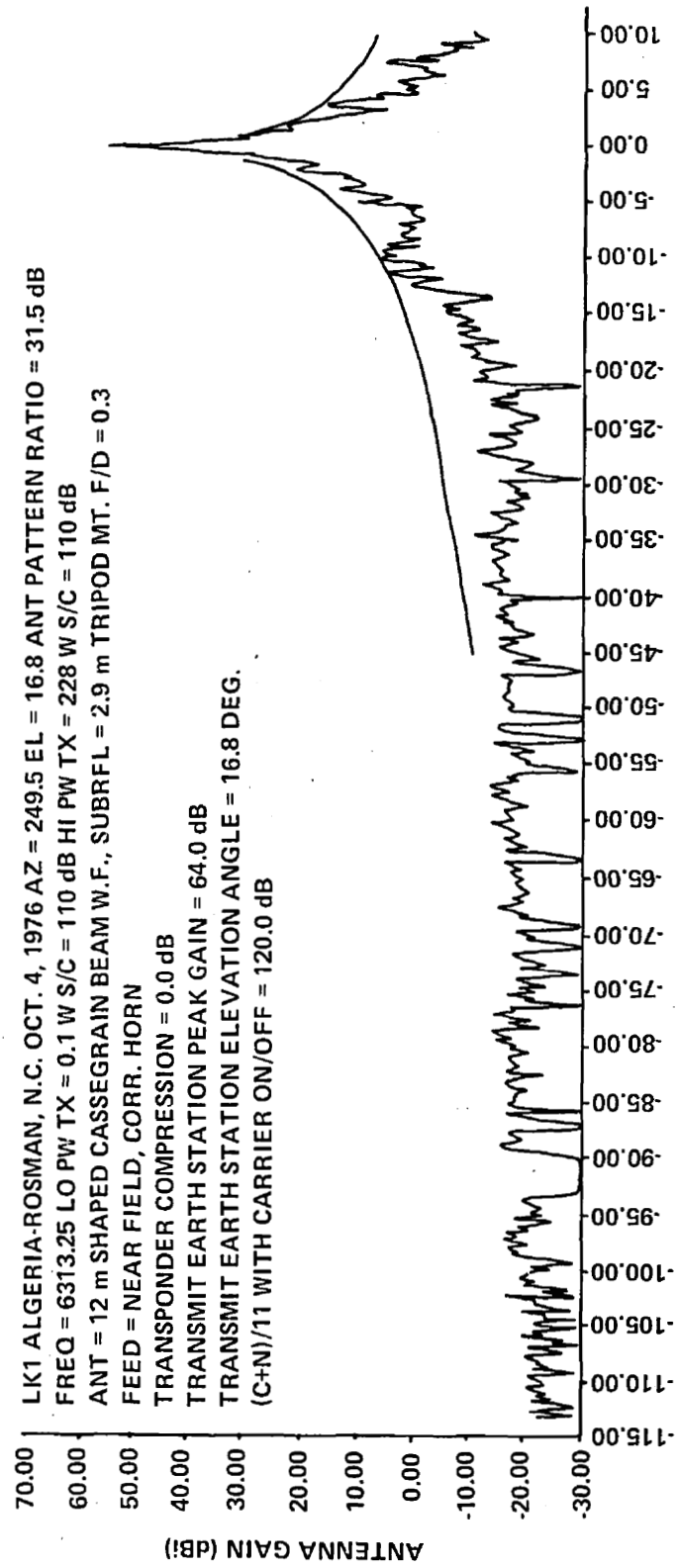

Figure 7-5. Azimuth Pattern for 32-meter Antenna, Lakhdaria 1, Algeria

This change was always in a direction to reduce the received signal level (since each run was begun after maximizing the signal) resulting in an apparent improvement of the profile.

- For plotting convenience, whenever a significant gap of measured data occurred, data values of -29.9 dBi or other appropriate values were synthesized to drive the plotting pen to the bottom of the graph.

CONCLUSIONS

The objective of the experiment was met and illustrated by the resulting wide-angle antenna patterns. These results should prove useful in improving large Earth station antenna design.

Part C
Experiments Above 10 GHz

CHAPTER 8

COMSAT MILLIMETER WAVE PROPAGATION EXPERIMENT

INTRODUCTION

The ATS-6 Comsat Millimeter Wave Propagation Experiment was designed to gather statistical rain and snow attenuation at 13 and 18 gigahertz (GHz). The purpose of this data was to determine system design and future parameters for communications satellite systems above 10 GHz.

The experiment used a total of 39 ground stations located in the eastern part of the United States and in Europe to uplink either 13 or 18 GHz or both to ATS-6. A linear transponder on ATS-6 translated these carriers to C-band (4150 MHz) and transmitted the composite signals to ground stations located at Andover, Maine, or Buitrago, Spain. These ground stations received the C-band signal and processed the data by calibrating and recording each carrier once per second.

Objective of Experiment

The purpose of the Comsat Millimeter Wave Propagation Experiment was to collect sufficient long-term data on atmospheric attenuation for a large number of locations in the eastern United States or Europe to permit determination of system power margins needed in satellites operating at frequencies about 13 and 18 GHz. In addition, space diversity was used as a technique on the uplink stations to provide a solution to attenuation due to intense localized rain cells typical of thunderstorms.

The duration of the Comsat propagation experiment was sufficiently long to permit a statistical comparison between measured attenuation at a site and general meteorological parameters that are routinely collected by the Weather Bureau, such as rainfull rate, number of thunderstorm days, total precipitation, and weather radar information.

The low power consumption (15 watts) allowed the experiment to be operated continuously 24 hours a day, 7 days a week with the exception of the eclipse periods and special tests that required large amounts of power.

U.S. Operations

Fifteen dual-frequency ground terminals transmitted signals in the 13.19 to 13.20-GHz and 17.79 to 17.80-GHz range and were located throughout the eastern half of the United States. These dual-frequency terminals were located at Andover, Maine; Detroit, Michigan; Philadelphia, Pennsylvania; Washington, D.C.; Wallops Island, Virginia; Atlanta, Georgia; New Orleans, Louisiana; Miami, Florida; Boston, Massachusetts; Columbus, Ohio; and Starkville, Mississippi. In addition, nine single-frequency terminals (17.79 to 17.80 GHz) were included for diversity study.

ATS-6 linearly translated the 13.19 to 13.20-GHz uplink to a 4.140 to 4.150-GHz C-band downlink and the 17.79 to 17.80-GHz uplink signal to a 4.160 to 4.170-GHz downlink for reception at the central receiving facility at Andover, Maine.

The ground station at Andover received the signals at 4.1 GHz, separated the 39 individual carriers and recorded them for further analysis. This facility also served as a control center for the experiment to monitor performance of all uplink stations and to conduct and control the experiment. Uplinks were provided at 13 and 18 GHz to permit automatic tracking of the C-band antenna and to provide clear sky calibration for the overall system during the experiment.

The experiment was operated continuously between July 1974 and May 1975, with the exception of the eclipse periods and the special tests that used large amounts of power or special spacecraft pointings that were incompatible with the Comsat propagation experiment. On May 20, 1975, the satellite was drifted to 35°E longitude to begin European operations. Later, when the satellite was drifting to 140°W longitude (August 28 to September 7, 1976), measurements were made from Clarksburg, Maryland, and Baltimore-Washington International Airport (Westinghouse), Baltimore, Maryland, by uplinking a 13.2-GHz signal to ATS-6 at low elevation angles (3.6° to 14°). The C-band downlink was received and recorded at Buitrago, Spain.

European/Indian Operations

In May 1975 ATS-6 began a drift to 35°E longitude to begin a second year of operation in Europe and India. In August 1976 the drift back to 140°W longitude was begun to complete the European phase of ATS-6 operations.

Receive (C-band) and processing equipment were relocated from Andover, Maine, to Buitrago, Spain, and installed using a 42-foot (12.8-meter) C-band antenna that had previously been used with Intelsat service. Buitrago, Spain, is a small town about 80 kilometers (km) north of Madrid that was the location of the Intelsat ground station operated by CNET, the Spanish telephone/television company.

By August 1975 most of the European transmit stations had been installed using relocated 13- and 18-GHz stations that were used during the first year's operation in the United States.

The transmit terminals were located as follows: Dual-frequency (13 and 18 GHz) stations were located in Leeheim, Germany; Plymouth, England; Gratz, Austria; Eindhoven, Holland; Fucino, Italy; and at the C-band receive station, Buitrago, Spain. This station provided the calibration signals, as was done at Andover, Maine.

Single-frequency (18-GHz) diversity stations were located at: Slough, England; Leeheim, Germany; and Darmstadt, Germany. The European experiment was operated 10 hours per day.

Indian operations, which were coordinated under the Indian Space Research Organization (ISRO), began between March and April 1976 due to delays in procurement and engineering problems with

the transmitting terminals. High temperatures also caused excessive failures of the transmitters. Buitrago provided the C-band receive equipment for the 12-hour per day Comsat propagation experiment for India. ISRO built some of the 13- and 18-GHz transmit terminals but little else is known of the results or problem areas as no ISRO final report on the experiment has been received.

SYSTEM DESCRIPTION

General System Description

The Comsat Millimeter Wave Propagation Experiment was divided into three main parts:

1. The ground transmit terminal (GTT) (13 and 18 GHz) in a transportable shelter that provided an uplink to ATS-6.

2. The transponder, located on ATS-6, that received 13 or 18 GHz and translated these frequencies to the 4-GHz downlink.

3. The C-band receive station that received the composite 4-GHz signal from ATS-6, down-converted this signal to 70 megahertz (MHz) and separated it into the separate carriers and recorded them on magnetic tape and strip charts. These data were then reduced later by Comsat Corporation and compared with a calibration signal provided by the station. Tables 8-1 and 8-2 give performance parameters for the system.

Ground Transmit Terminal

Fifteen dual-frequency (13/18-GHz) and ten single-frequency (18-GHz) ground transmit terminals were produced. These terminals were housed in a fiberglass enclosure that was transportable and self-contained. A typical dual-frequency ground transmit terminal is shown in Figure 8-1. The dual-frequency terminals had 28-watt traveling wave tube amplifiers (TWTA) and the single-frequency terminals had a 6-watt TWTA (18 GHz).

Both terminals contained a power monitor, antennas, a rain gauge, and a strip chart recorder to record power level and rain rate. The antenna had a 4-degree beamwidth and did not require repeaking to correct for inclination of the satellite.

Comsat Propagation Experiment Transponder

The Comsat propagation experiment transponder used on ATS-6 is shown in Figure 8-2. This transponder translated the received frequencies of 13.19 to 13.20 GHz to 4.14 to 4.15 GHz and the 17.79 to 17.80 GHz to 4.16 to 4.17 GHz.

The 13/18-GHz receive antenna on ATS-6 was a dual-frequency, linearly polarized parabolic reflector with an elliptical pattern (4 degrees × 8.5 degrees) designed to cover the entire continental United States. This allowed the Comsat propagation equipment to be used for all normal pointings

Table 8-1
Uplink Performance Parameters

Parameters	Attenuation Experiment		Diversity Experiment
	13 GHz	18 GHz	18 GHz
Transmitter			
Power (dBW)	+14	+14	+7
Antenna gain (dB)	32.5	32.5	32.5
E.i.r.p. (dBW)	46.5	46.5	39.5
Free-Space Propagation Loss (dB)	-206.2	-209.8	-209.8
Average Antenna Misalignment			
Transmitter (dB)	-1.5	-1.5	-1.5
Satellite receiver (dB)	-0.7	-1.5	-1.5
Total (dB)	-2.2	-3.0	-3.0
Satellite			
On-axis antenna gain (dB)	25.7	28.6	28.6
Receive power (dBW)	-136.2	-137.7	-144.7
Noise power density (dBW/Hz)	-194.5	-194.5	-194.5
Uplink Performance			
C/N_o (dB-Hz)	58.3	56.8	49.8

in the United States. The C-band transmit antenna was an Earth-coverage horn that was integrated with the communications package horn and was polarized linearly east and west. The power consumption of the Comsat propagation experiment was 14 watts, thus the transponder did not impose power constraints on the spacecraft in normal conditions. Most hardware was off-the-shelf space qualified hardware such as the C-band TWTA that had been used as an intermediate power amplifier aboard previous Intelsat satellites. New technology developed for the Comsat propagation package was the 4-GHz microwave integrated circuit tunnel-diode amplifier that survived the orbital elements without serious degradation.

It can be seen from Figure 8-2 that both the 13- and 18-GHz frequency translator and the C-band downlink had redundant systems that could be switched in the event of a failure. The normal telemetry points were monitored through the telemetry and command (T&C) subsystem.

The Comsat propagation experiment transponder was designed and built by Dr. Christopher Mahle of Comsat Laboratories.

Table 8-2
4-GHz Downlink Performance Parameters

Parameter	Attenuation Experiment		Diversity Experiment
	13 GHz	18 GHz	18 GHz
Satellite			
Transponder gain (dB)	101	109	109
Power/carrier (dBW)	-35.2	-28.7	-35.7
Antenna gain (less loss) (dB)	16.0	16.0	16.0
E.i.r.p. (dBW)	-19.2	-12.7	-19.7
Free-Space Propagation Loss (dB)	-196	-196	-196
Antenna Misalignment (dB)	0	0	0
Earth Terminal G/T (dB/K)	37	37	37
Downlink Performance			
C/N (dB-Hz)	50.4	56.8	49.9
System Performance			
C/N_o total (dB-Hz)	49.7	53.9	46.8
Receive system bandwidth (dB)	20	20	20
Minimum C/N for retaining phase lock (dB)	3	3	3
Measurement dynamic range (dB)	26.7 +1.2 to -2.4	30.8 +1.9 to -2.7	23.8 +1.9 to -2.7

Ground Receive and Data Acquisition Station

In the U.S. operations between July 1974 and May 1975, the ground station was located at Andover, Maine. This was the location of the first American Earth station and, as a matter of historical fact, the antenna used in the experiment was the old cornucopia horn antenna used with the Telstar experiments with the research center at Goonhilly, England.

The block diagram for the ground receive station is shown in Figure 8-3. The system was a dual-conversion receiver (40 + 2 spare in all) with carrier processors that were phase locked. The output of these processors were recorded on magnetic tape by the online computer. Once a week tapes were forwarded to Comsat Laboratories for subsequent processing. These tapes combined telemetry data, orbital data, pointing data, rain gauge data from each of the transmitter sites with calibration data from the power monitors on each transmitter.

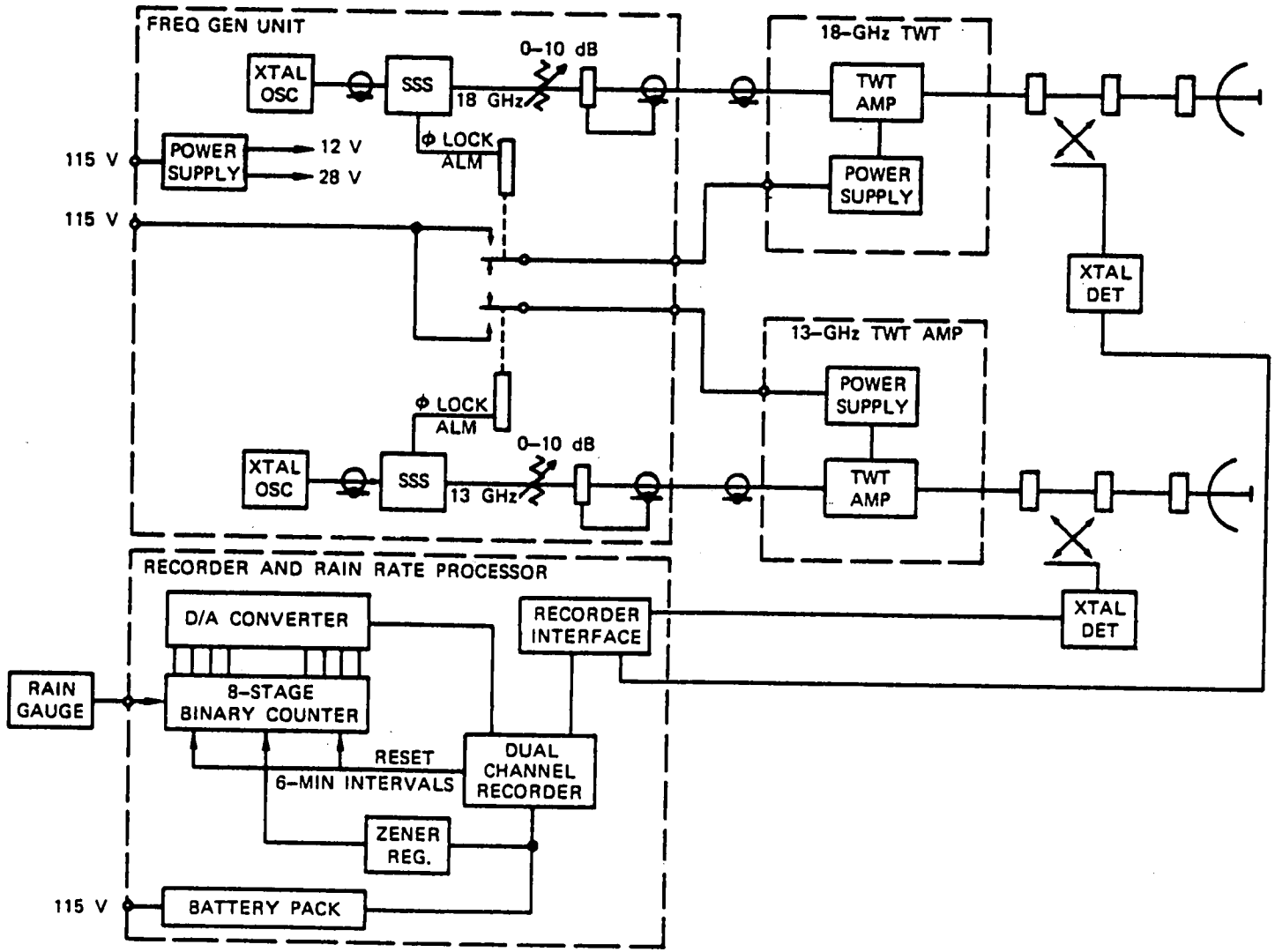

Figure 8-1. Ground Transmitter Terminal

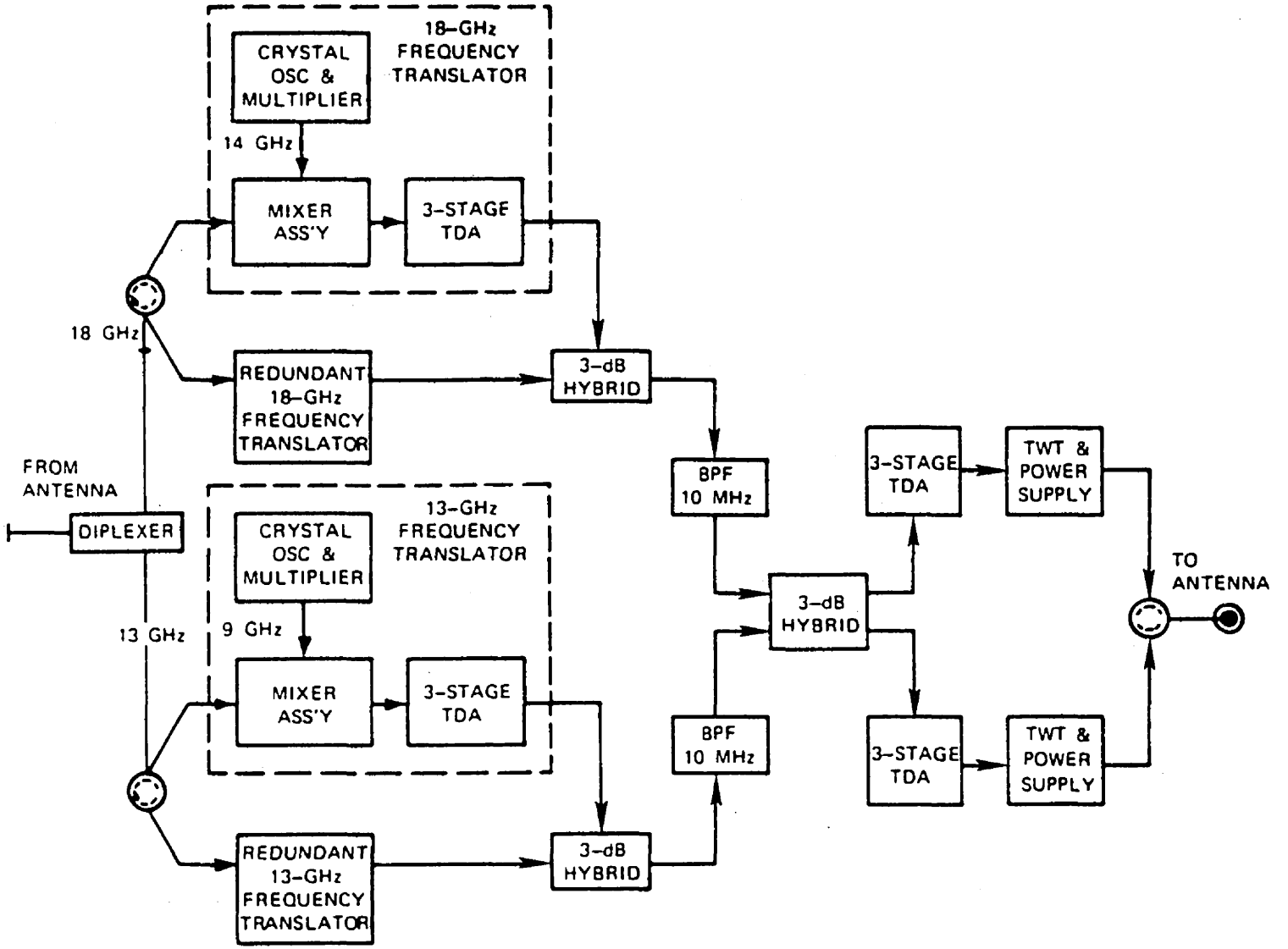

Figure 8-2. Overall Repeater Block Diagram

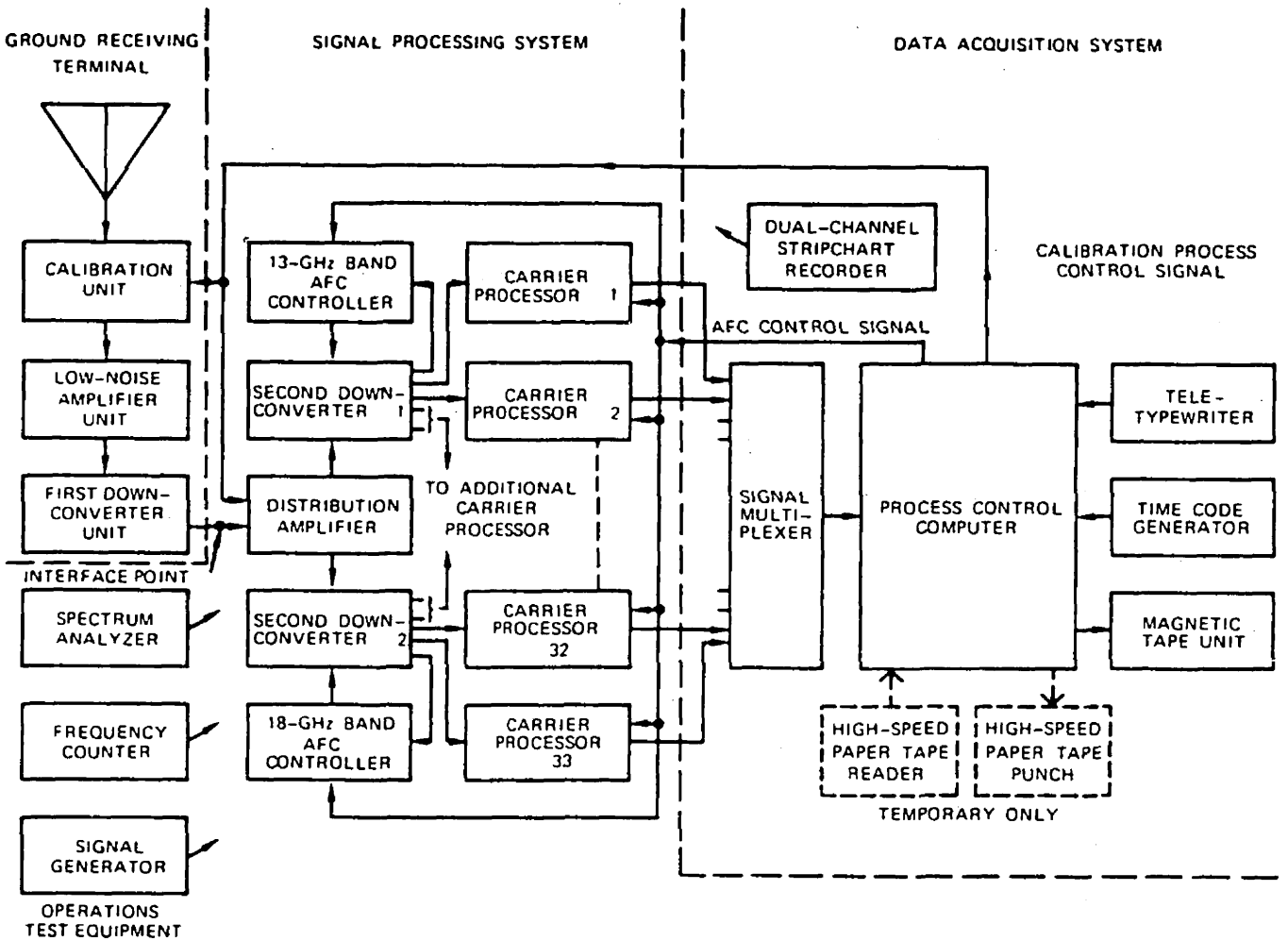

Figure 8-3. Receiving System Block Diagram

At Andover, two 1.8-meter antennas (13 and 18 GHz) for calibration transmitters were mounted on the horn antenna (C-band) to provide autotrack and phase-lock references. This was replaced with a standard dual-frequency ground transmit terminal at Buitrago, Spain, for the European operations.

Calibration signals were also inserted into the front end of the C-band receiver for a reference.

EXPERIMENT RESULTS AND DATA REDUCTION

U.S. Operations 13 and 18 GHz/Diversity Attenuation

The data were processed in 7-day blocks and accumulated in 4-week blocks. Monthly, quarterly, half-year, and total data statistics were obtained. The following series of figures (Figures 8-4 to 8-14) represent a typical sample of data obtained from various sites as indicated with diversity, 13 and 18 GHz and 13 GHz attenuation versus the percent of time exceeded. These data were collected during August, September, and October of 1974.

U.S. Operations

Using ATS-6 enroute west, measurements of 13-GHz fading at low elevation angles were made to 140 watts at the completion of European operations in 1976. Measurements were made of signal fluctuations at 13.2 GHz for elevation angles of 3.6 to 14 degrees along low elevation angle slant paths from Clarksburg, Maryland, and Baltimore-Washington International Airport (BWI) (Westinghouse) in Baltimore, Maryland, to ATS-6 during the period August 28 to September 7, 1976. Signal fluctuations of up to 15 dB peak-to-peak were encountered under heavy overcast conditions at elevation angles between 3.5 to 4.5 degrees. Fluctuation amplitudes decreased sharply with elevation angle to small values above 7 degrees.

Figures 8-15 and 8-16 illustrate received signal strength versus elevation angle for Clarksburg and BWI (Westinghouse) respectively.

European/Indian Operations; 13 and 18 GHz/Diversity Attenuation

European Space Agency (ESA) data were reduced by Comsat Laboratories and a report was written by ESA. Copies were not available from NASA or Comsat Laboratories. It was understood that the lowest rainfall in 50 years occurred in Europe during the 1975-1976 year.

The ISRO data were delivered to India and were reduced by ISRO. To date no report has been received from ISRO.

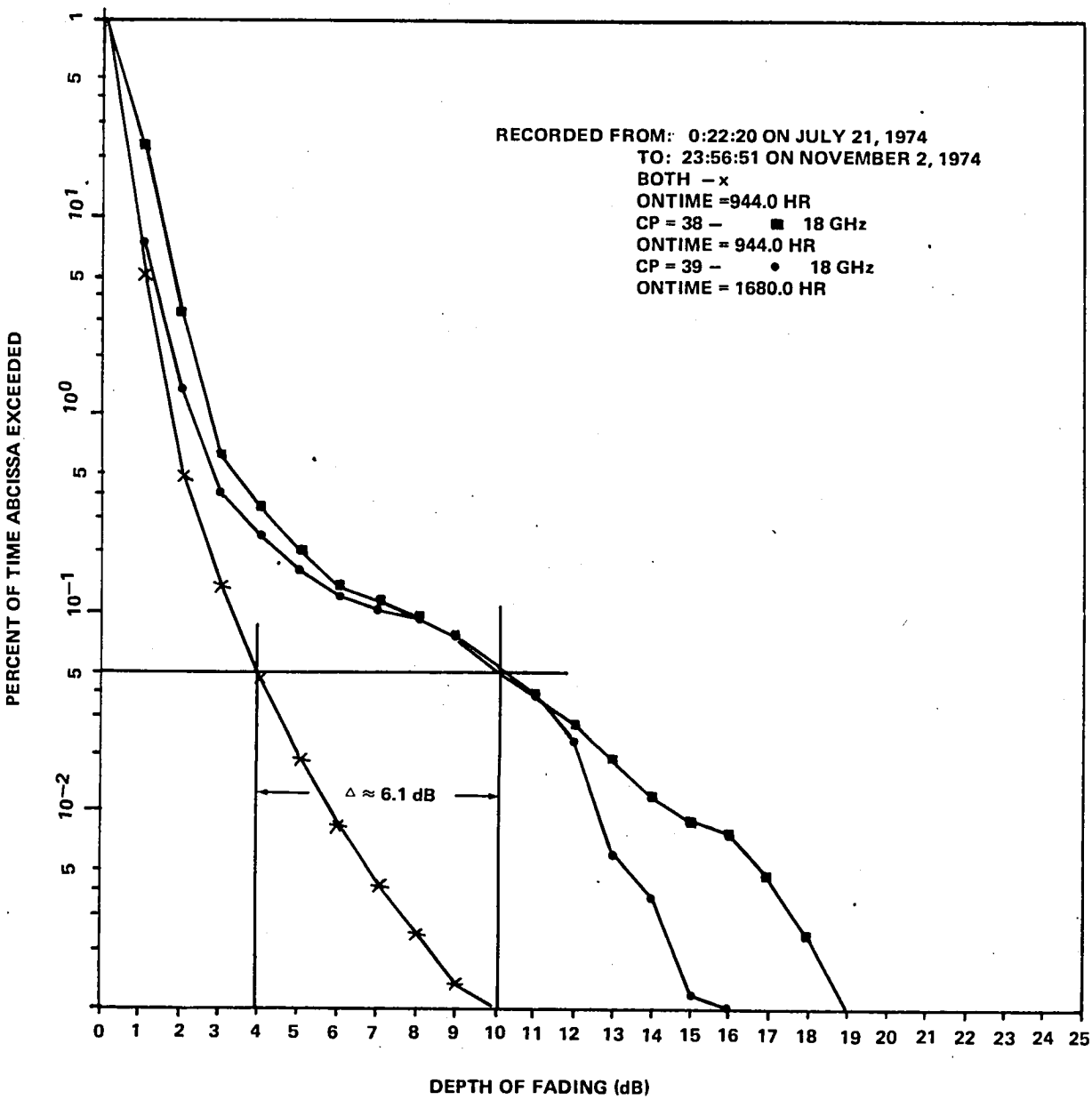

Figure 8-4. Fading Distributions Using Diversity for Boston: 17.8 Mile Separation

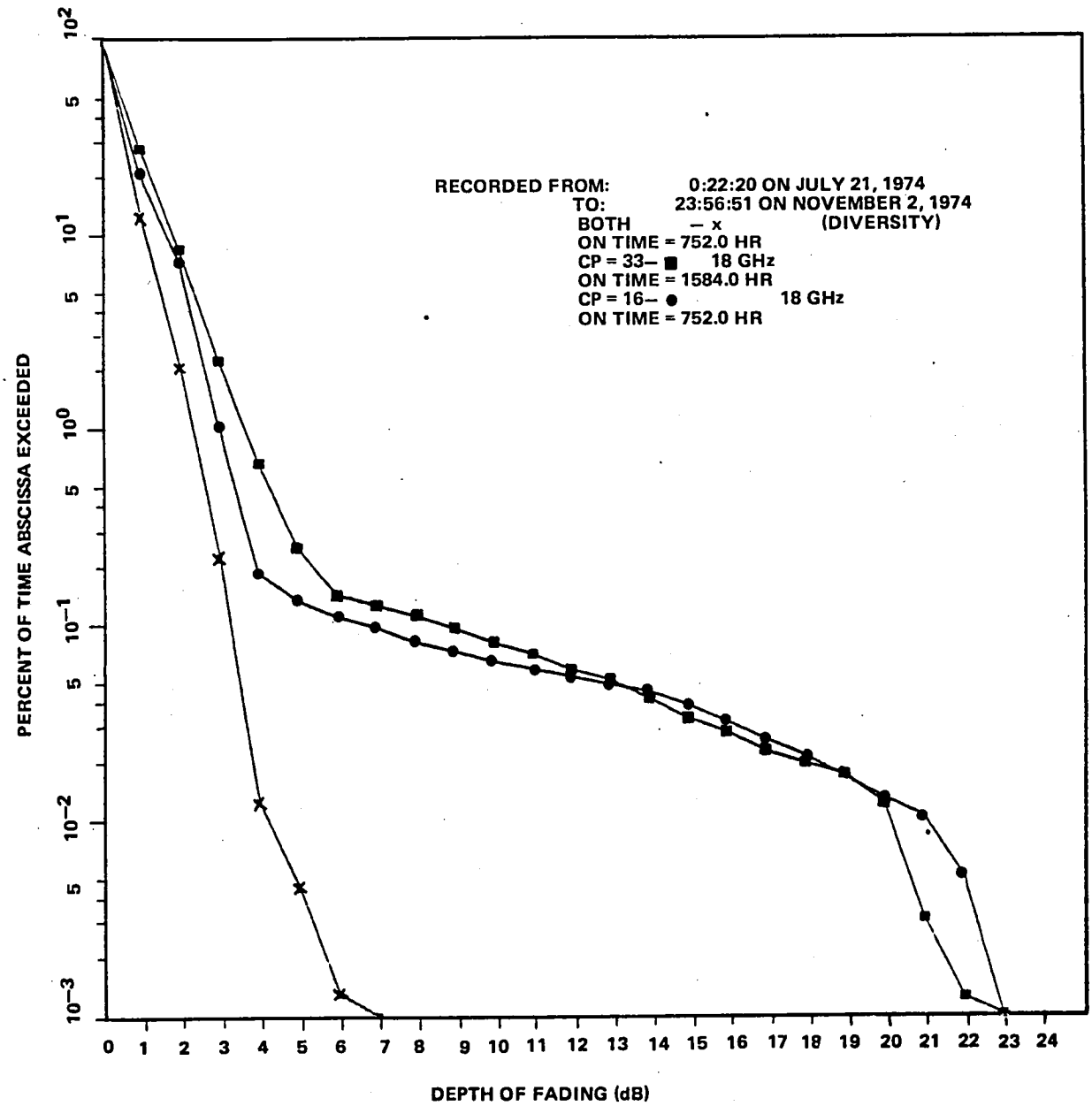

Figure 8-5. Fading Distribution Using Diversity for Starkville: 19.8 Mile Separation

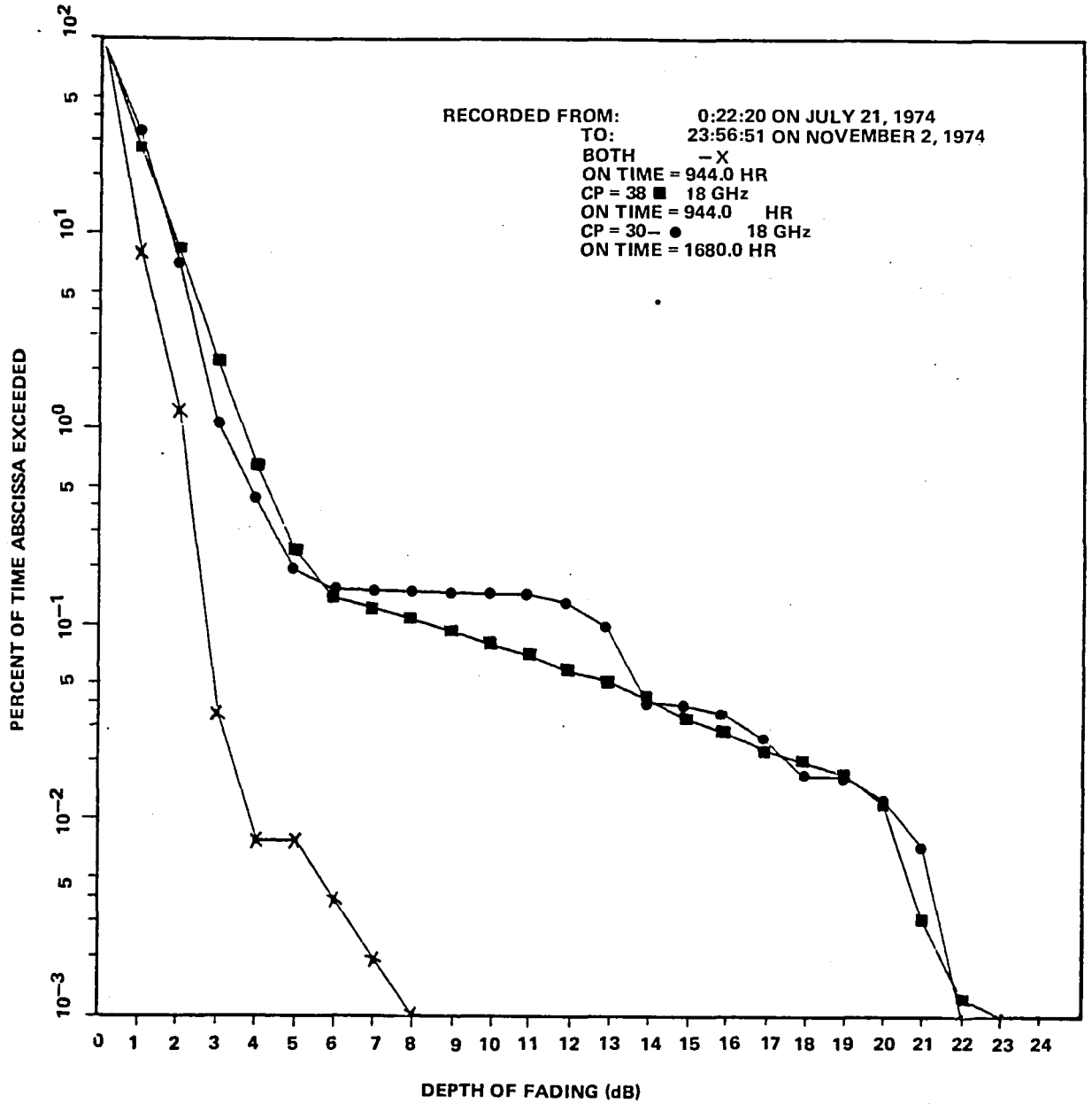

Figure 8-6. Fading Distribution Using Diversity for Starkville: 8.8 Mile Separation

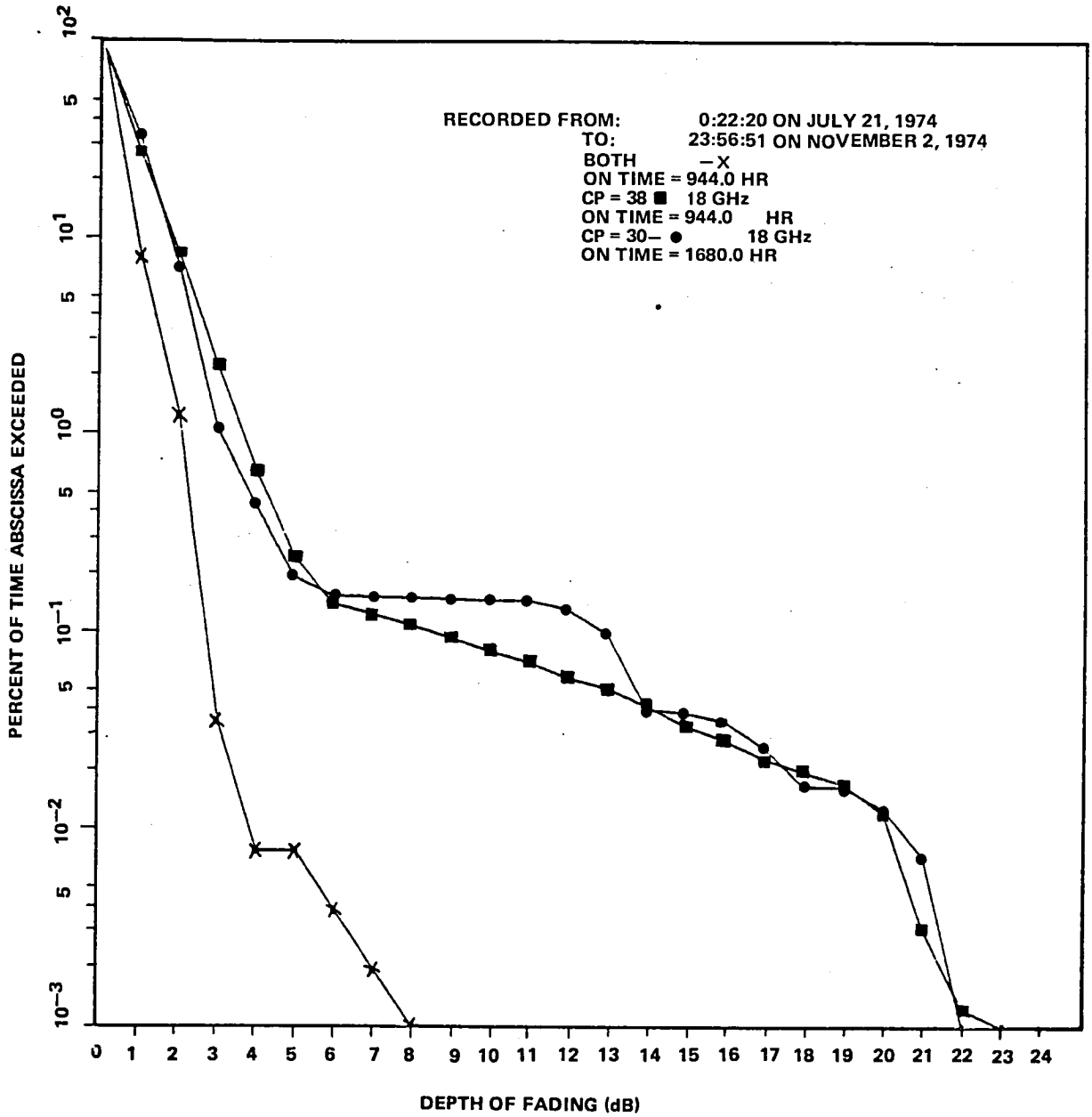

Figure 8-6. Fading Distribution Using Diversity for Starkville: 8.8 Mile Separation

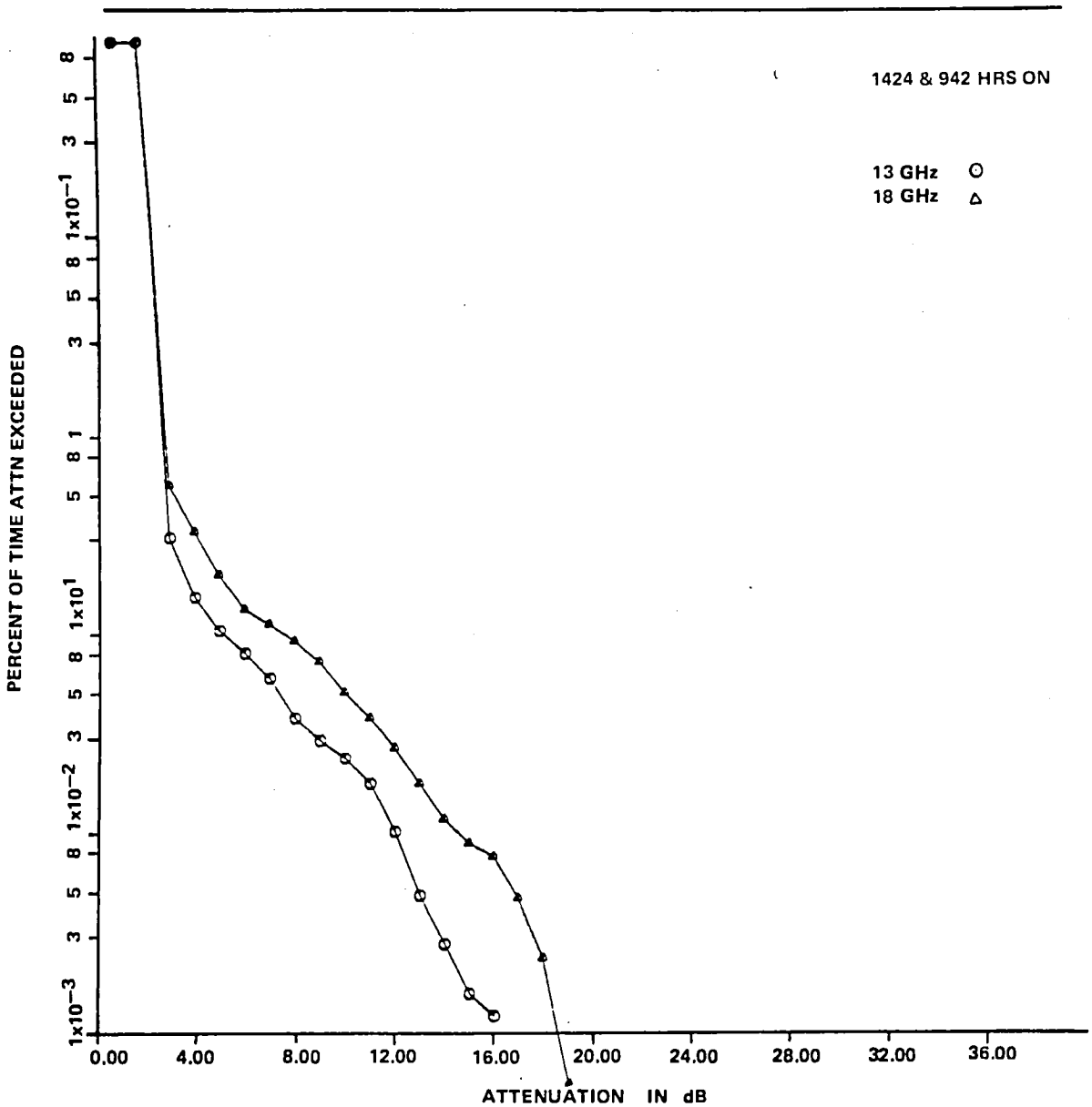

Figure 8-7. August 1, 1974 to October 31, 1974—Boston Cambridge

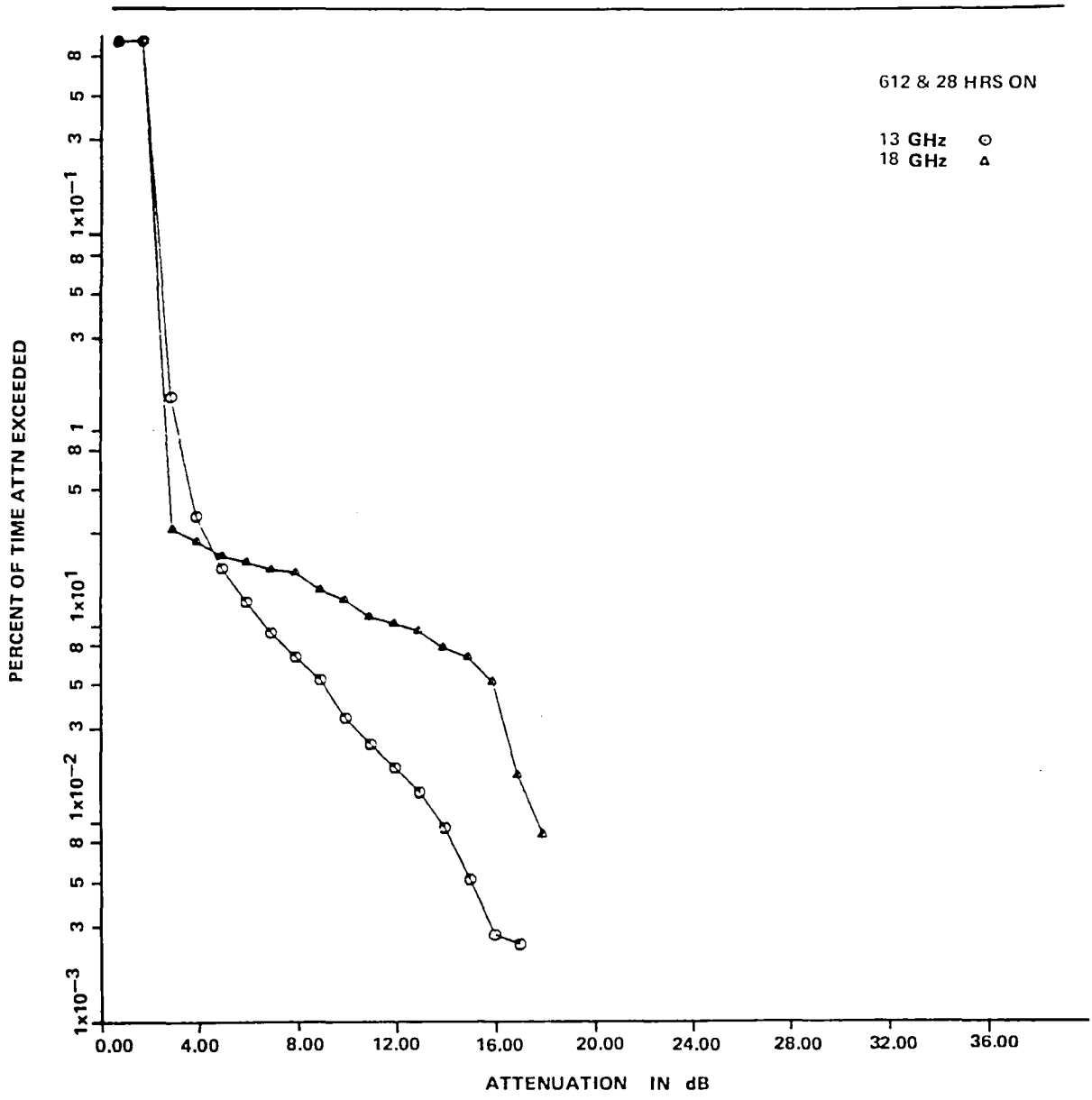

Figure 8-9. August 1, 1974 to October 31, 1974—Miami

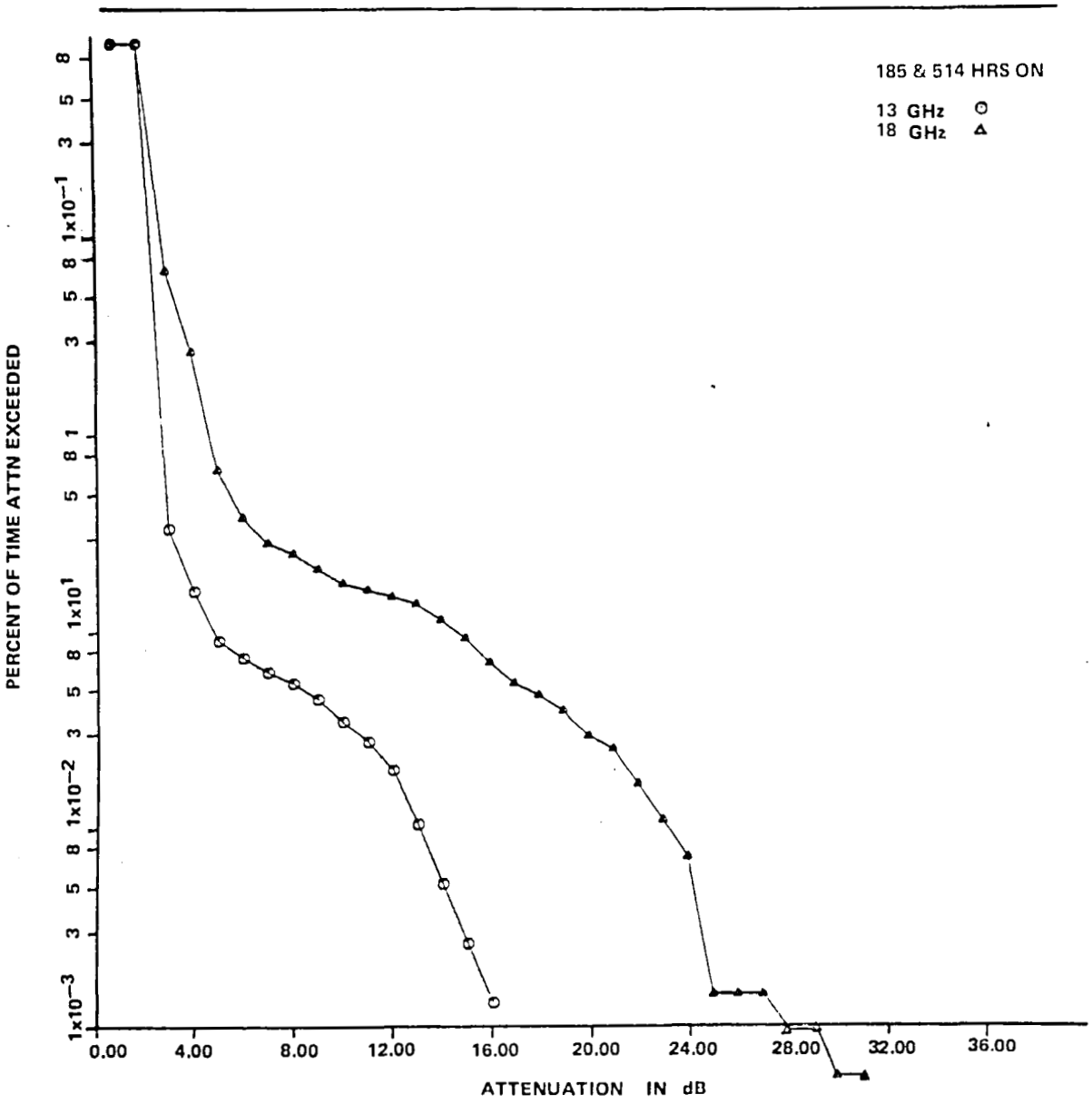

Figure 8-10. August 1, 1974 to October 31, 1974—New Orleans

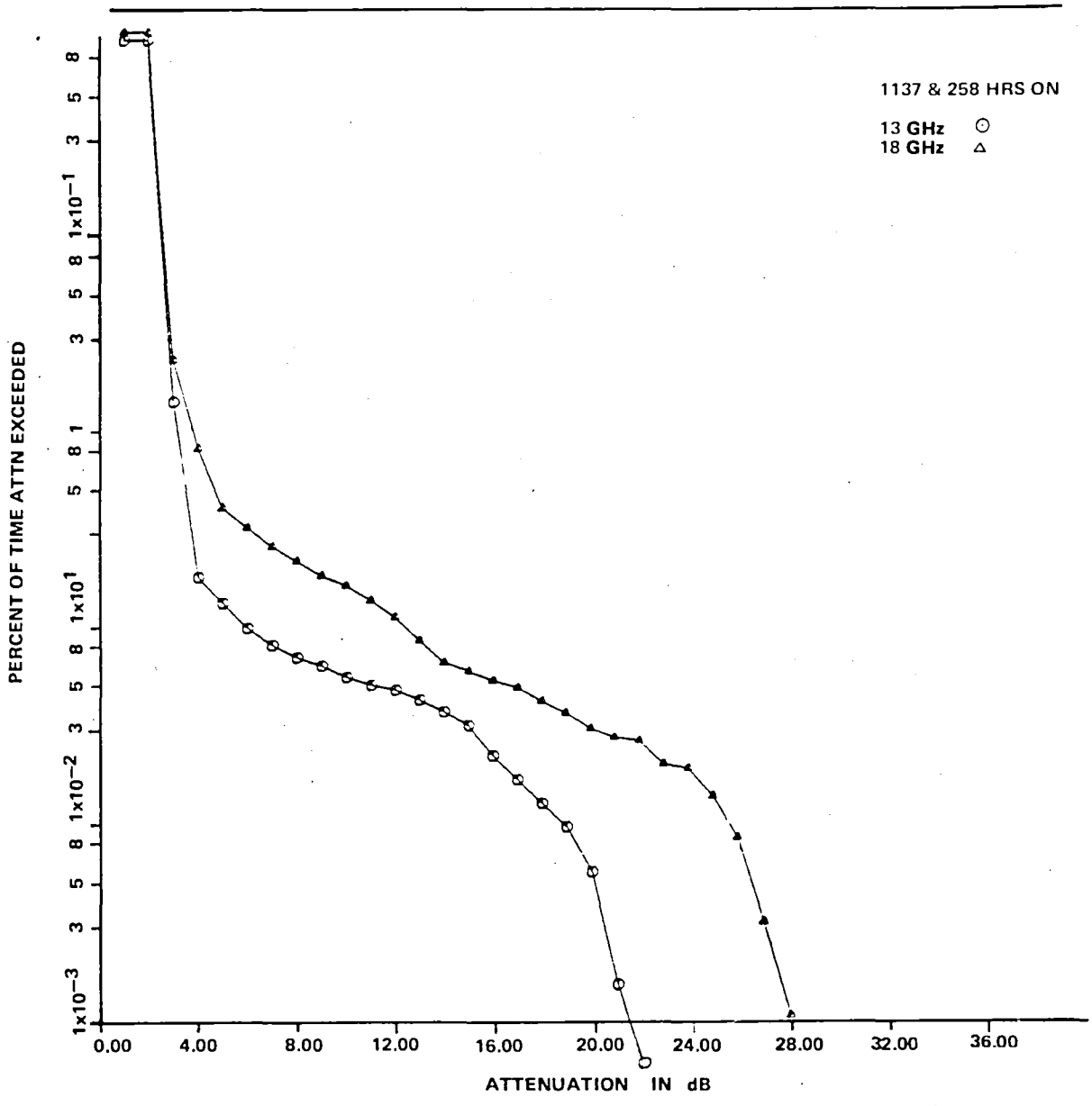

Figure 8-11. August 31, 1974 to October 31, 1974—Atlanta

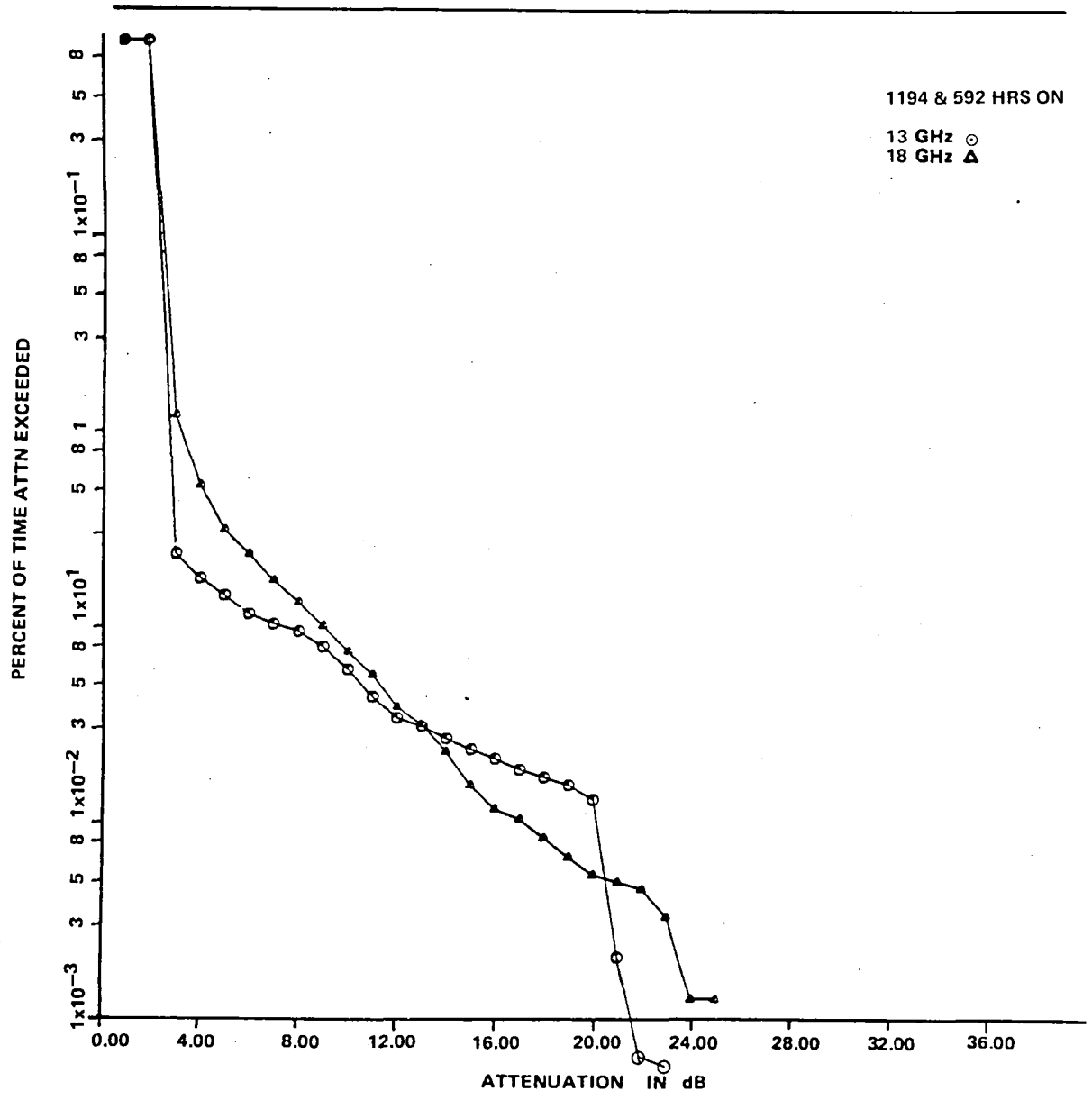

Figure 8-12. August 1, 1974 to October 31, 1974—Fayettesville

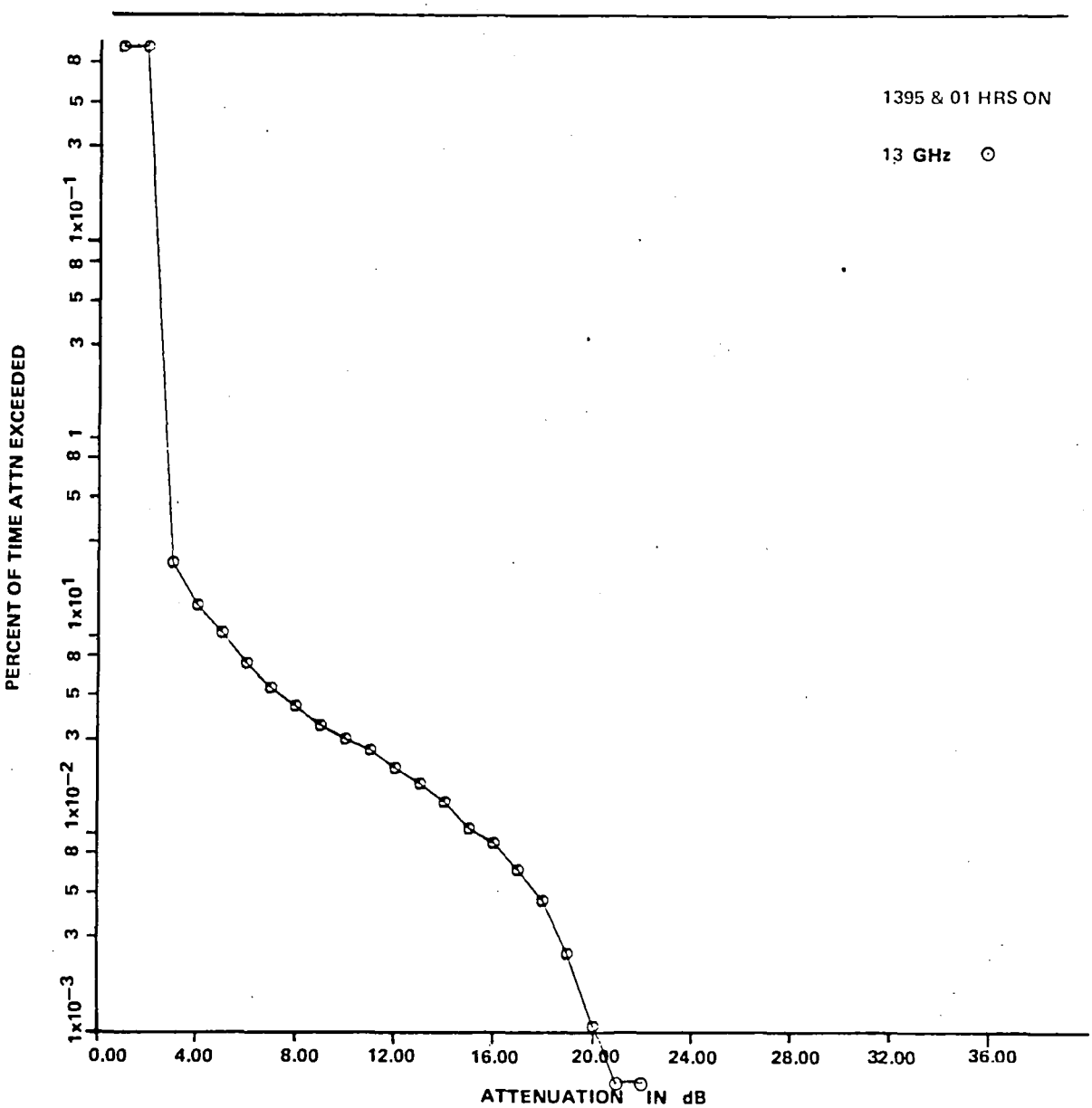

Figure 8-13. August 1, 1974 to October 31, 1974—Washington

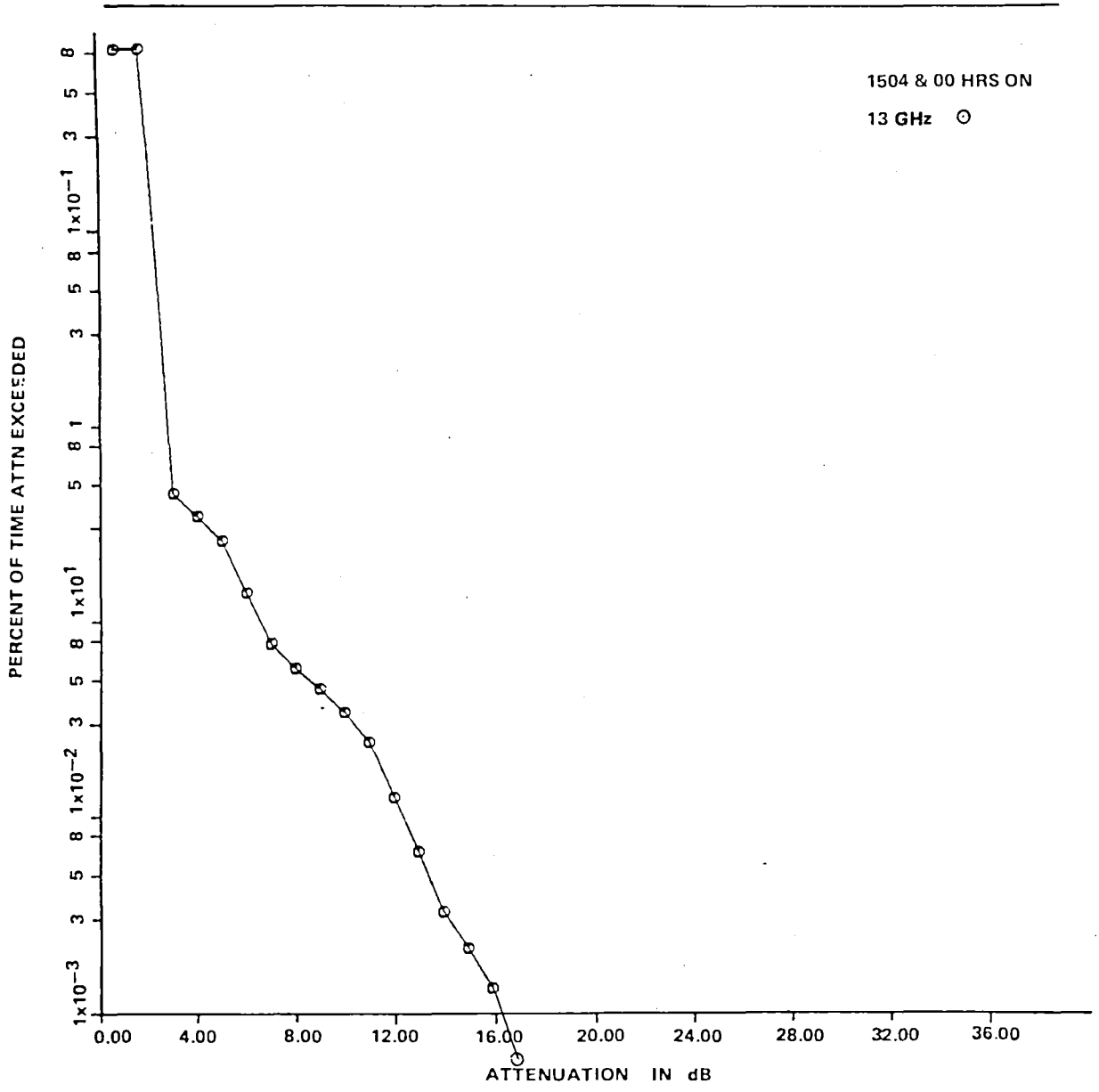

Figure 8-14. August 1, 1974 to October 31, 1974—Philadelphia

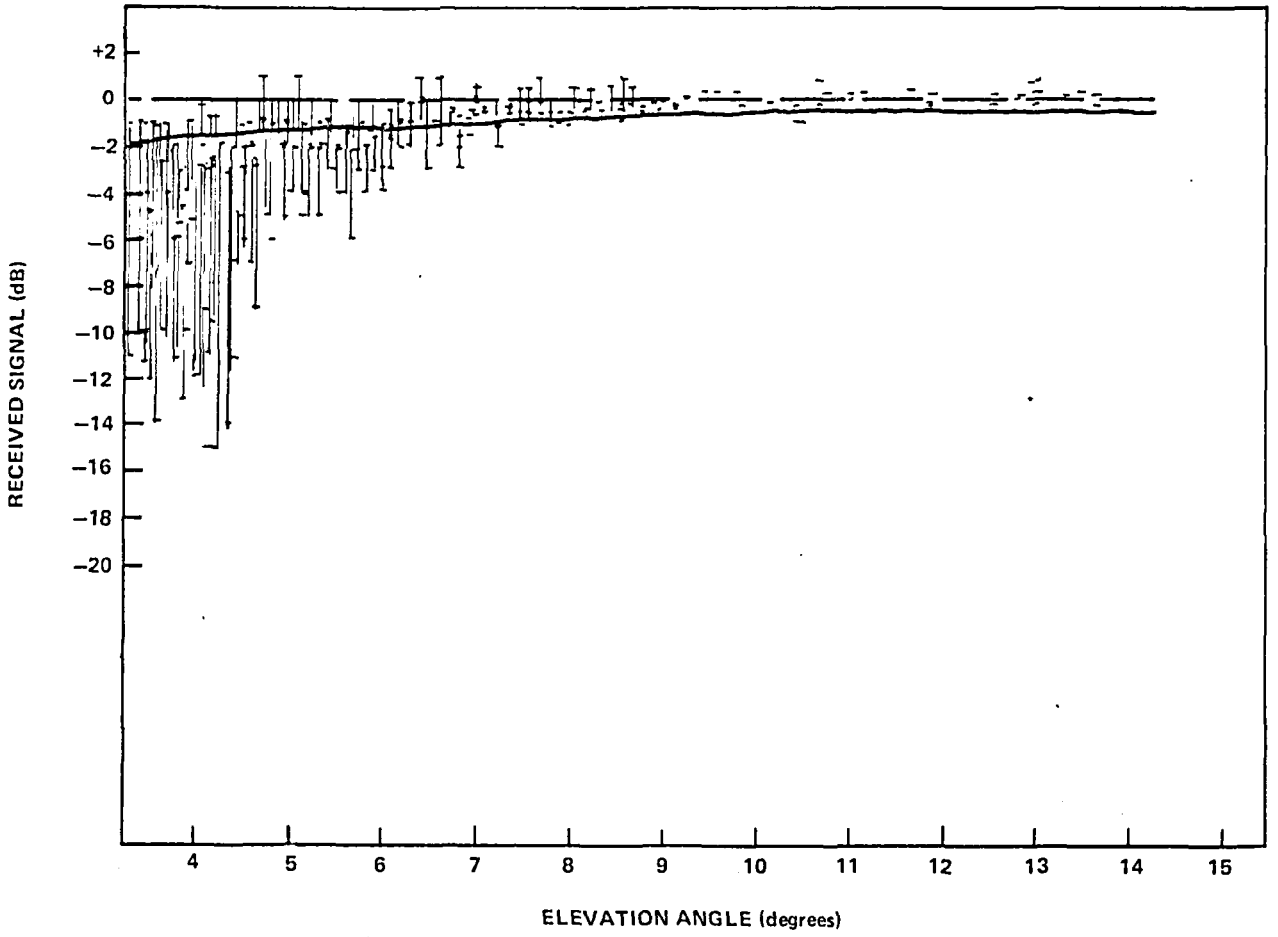

Figure 8-15. Clarksburg Carrier Median Signal Level (X) and Fluctuation (I) of the Received Signal as a Function of the Elevation Angle

SIGNIFICANT EXPERIMENT RESULTS AND SUMMARY

Rainfall Attenuation 13 GHz, United States

By taking an average of the data for the 8 cities shown in the preceding pages, a reasonable assumption could be made that an attenuation of 8 dB would not be exceeded 99.95 percent of the time, with a maximum attenuation for all cities of 22 dB.

Rainfall Attenuation 18 GHz, United States

An average of 6 of the 8 cities shown in the results were calculated and a similar assumption could be made that 13.3 dB would not be exceeded 99.95 percent of the time, with a 28.0 dB maximum recorded attenuation due to rain (Atlanta, New Orleans).

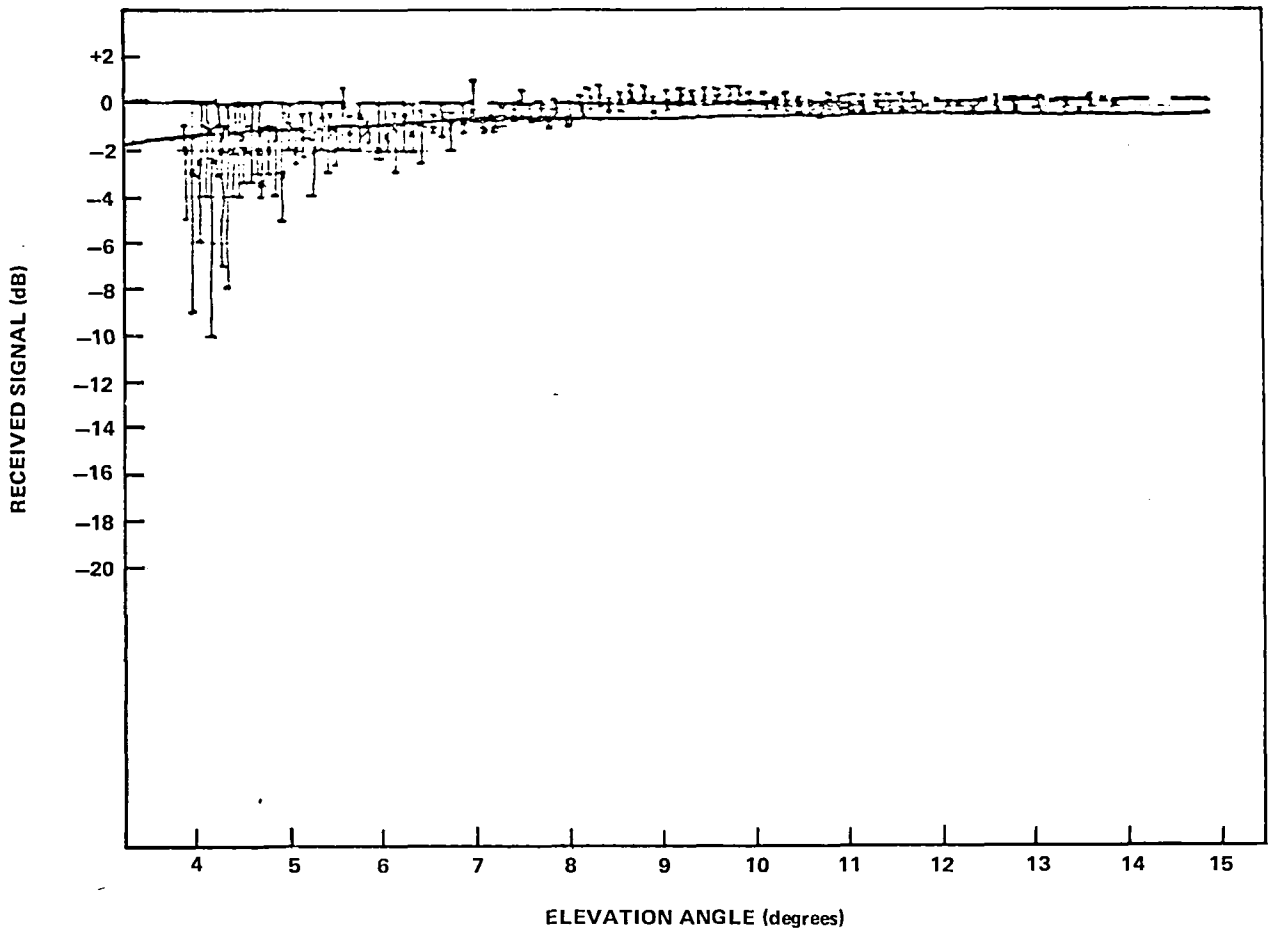

Figure 8-16. Baltimore Carrier Median Signal Level (X) and Fluctuation (I) of the Received Signal as a Function of the Elevation Angle

Diversity Improvement 18 GHz, United States

The improvement due to diversity of 18 GHz with a 17.8 mile separation at Boston did not exceed 6.1 dB 99.95 percent of the time.

In Starksville, Mississippi, a 19.8 mile separation provided a 10 dB improvement 99.95 percent of the time, while an 8.8 mile separation produced an 11 dB improvement.

These attenuations should be used in the design of new satellite systems to provide sufficient margins for reliable communications for the cities involved.

Equipment Development and Reliability

The 13- and 18-GHz ground transmit stations experienced a reliability problem with the traveling wave tube amplifier, power supply, and solid-state source having higher failures than predicted. The

European phase had the same problems with the terminals that were on loan. In addition, India reported a temperature related failure problem with their uplinks.

The data acquisition facility (C-band receive station) was very reliable with the only downtime due to maintenance and repair. One problem that did arise in Spain was that the autotrack system did not function as expected and the 40-foot antenna had to be manually repeaked. This caused extra perturbations in the data that had to be corrected.

FINAL IN-ORBIT TEST

Introduction

As part of the ATS-6 Comsat Millimeter Wave Propagation Experiment (Reference 1) a 13/18/14-GHz transponder (Reference 2) was designed, fabricated and tested during 1971 and 1972. ATS-6 was launched in May 1974 and in-orbit tests of the transponder were performed on June 13 to 15, 1974; and April 22, 23, 1975. The transponder was operated continuously for two years and subsequently turned on for 1- to 2-day periods every few months. Telemetry data obtained from these periodic turn-ons indicated that the transponder was still operating normally.

NASA generously provided an opportunity to test the transponder a last time before final turn-off of the spacecraft during July 1979. Although the meteorological conditions were unfavorable, the test results indicated that the transponder was still fully operational and had not suffered any failures.

Testing

NASA provided use of the Rosman Ground Station, North Carolina, as the Earth station facility during the test. Comsat Laboratories provided the uplink signal source, transmitter, and 13/18-GHz antenna mounted on a trailer. Initially, an effort was made to find a useable 13- or 18-GHz traveling wave tube amplifier (TWTA) out of the ATS-6 propagation experiment ground terminals. However, out of a large number of TWTA's, only two 13-GHz units with deteriorated performance could be located. A frequency synthesizer was used as a signal source and a standard 1.8-meter parabolic antenna with exchangeable feeds (13 and 18 GHz) mounted on a trailer was used as the uplink antenna. A power meter was used to measure uplink power by a directional coupler. Unfortunately, one of the feeds did not have the proper mounting hardware and, therefore, all measurements were made with the same feed. After the test, the antenna gain for this configuration was measured at Comsat Laboratories. The downlink used the 25.9-meter parabolic antenna receiving system as calibrated by NASA personnel; a 70-MHz signal, from the 4-GHz/70-MHz downconverter output, was provided by cable to a spectrum analyzer located at the uplink antenna. Calibration was accomplished by switching the low-noise amplifier input to a -110 dBm calibration signal at 4155 MHz and noting the level and gain setting of the spectrum analyzer. Gain drift over the measurement period was measured to be less than 1 dB. Absolute accuracy of the calibration signal power was estimated at ±2 dB. A schematic of the overall test setup is shown in Figure 8-17.

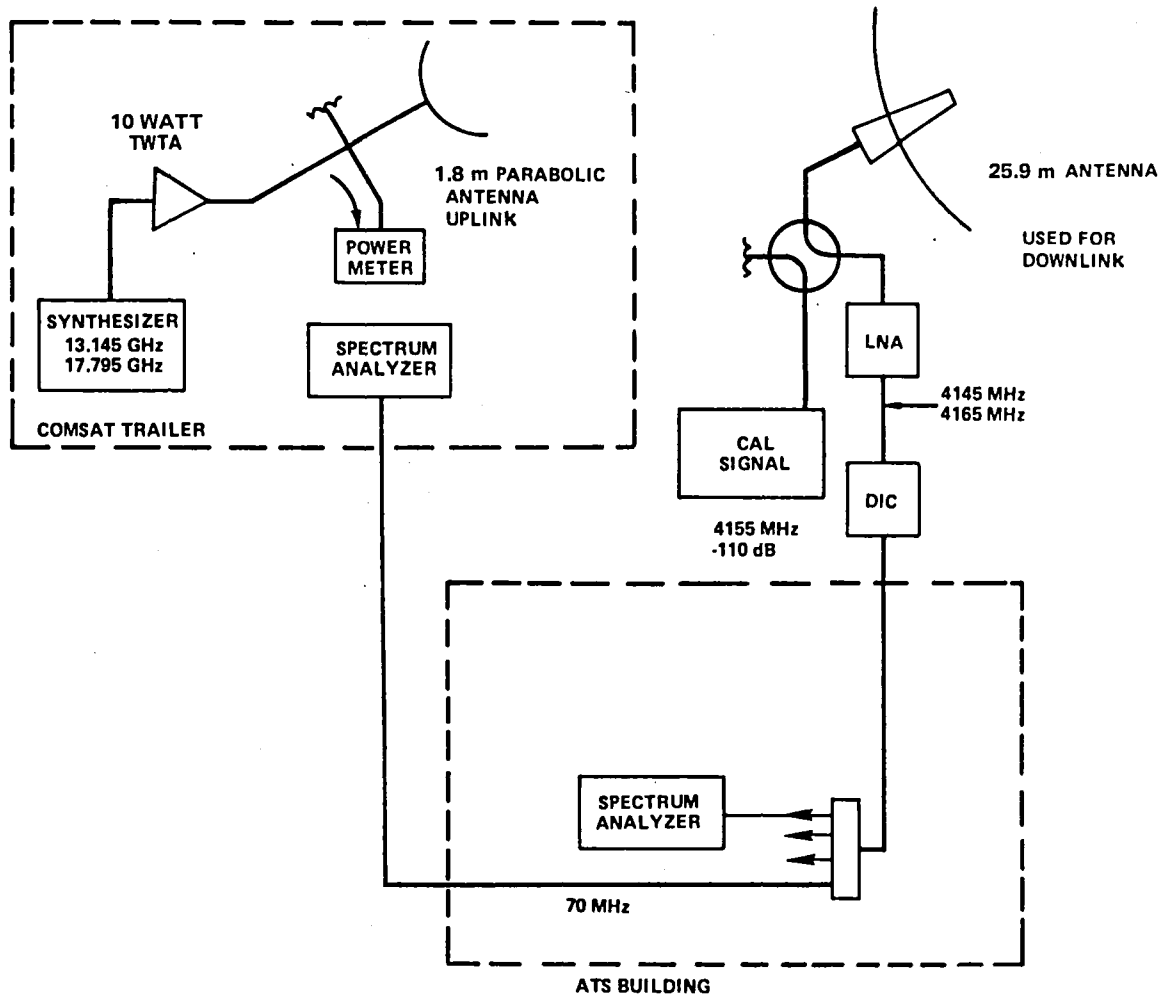

Figure 8-17. ATS-6 C-Band Equipment Test Schematic, Rosman Ground Station

The equipment was set up during the afternoon of July 23, 1979. The spacecraft was available in the morning of the 24th. The 25.9-meter antenna was pointed by using a 6-GHz uplink signal transmitted by this antenna and adjusted for maximum AGC voltage telemetered from the satellite receiver. Thereafter, program track was used. Earth station pointing was 20.01 degrees elevation and 247.72 degrees azimuth during the test. The spacecraft was located at 137.45° West longitude. Earth station location, as seen from the spacecraft, was 5.33° north and 6.19° east. The spacecraft Z-axis was pointed to 8.2° east and 6.6° north from the subsatellite point which brought the propagation experiment receive antenna within 0.1 dB of beam peak at Rosman. After adjusting the receive (25.9-meter) and transmit (1.8-meter) polarization for maximum signal, a series of measurements were taken. Unfortunately, during the morning a heavy cloud cover with some rain showers was present, and the received signal at 17.795 GHz/4165 MHz varied over a 10-dB range within a few minutes. Nevertheless, all redundant transponder paths were measured. A normal traveling wave tube turn-on (70 to 80 seconds) was observed for both "A" and "B" transmitters. Also, the transponder local oscillator frequency difference between "A" and "B" chains was measured.

The following day, July 25th, the weather continued to be rainy, although the cloud cover was more stratiform and the rain continuous. Measurements of all redundant paths were repeated after the spacecraft became available. The Z-axis was pointed at 8.19° north and 6.75° east during this set of measurements. Again normal traveling wave tube turn-on and the same local oscillator frequency differences as before were observed. Since the weather continued to be poor (southerly flow of very moist, unstable air encountering the slope of the Great Smokey Mountains) and no improvements were predicted for the next few days, the testing had to be terminated without a set of clear sky measurements.

Transponder temperatures were in the 24° to 27°C range throughout the testing and all transponder power monitor telemetry appeared to be normal. Commanding of the spacecraft was handled by Cooper Chapman who functioned as test coordinator.

Table 8-3 shows a link budget for the tests and provides equations to calculate the transponder gain given the received (4-GHz) power in dBm. It should be pointed out that only "standard atmosphere" losses due to oxygen and water vapor have been taken into account.

Table 8-4 summarizes the measurements of both days. The scatter in the data from May 24th for the 18-GHz path is believed to be caused by propagation losses. The data of May 25th suffers obviously from some attenuations due to rain and clouds; however, conditions were steady during the 30-minute testing time.

Table 8-5 presents a transponder gain summary starting with prelaunch data and all three in-orbit tests. For the July 1979 test, only the data measured on May 25th were used. During the prelaunch period, the transponder gain varied typically 1 to 2 dB over a period of several months as evidenced by various measurements. The repeatability and accuracy of the measurements were estimated to be 0.1 dB and 0.5 dB for the prelaunch data. For the in-orbit data repeatability over a short period of time was estimated at 1 dB. Overall accuracy of the in-orbit measurements was difficult to estimate due to the many factors involved; 4 dB was estimated for the previous tests. For the July 1979 tests, this number was larger.

In addition, for the July 1979 tests significant clouds and rainfall were present in the propagation path. Unfortunately, no direct estimates of these losses could be made. Assuming a rainfall rate sufficient to cause a 3-dB loss at 13.195 GHz, the corresponding loss at 17.795 would be approximately 6 dB. This might at least partially explain the low gain measured for the 18-GHz paths. On the other hand, it can reasonably be presumed that the traveling wave tube gain had decreased a few dB due to cathode degradation; however, this would show as a degraded gain in both 13- and 18-GHz paths.

Another way to quantify changes in the transponder is to look at the gain differences when switching, for instance, from "A" to "B" chains. Since this is a relative measurement, the accuracy is superior to a gain measurement. Table 8-6 summarizes these gain differences. Compared to prelaunch and previous in-orbit tests, the gain differences measured in July 1979 look quite reasonable and it can be concluded that no particular path had changed more than 1 or 2 dB with respect to the redundant path.

Table 8-3
Link Budget for May 24 and 25, 1979 Measurements

	May 24th	May 25th	
Transmitted Power	+41.3 dBm	+38.8 dBm	Measured
Antenna gain	46.0 dB	47.0 dB	18 measured 13 estimate
Path loss	-206.8 dB	-209.4 dB	Calculated
Atmospheric Absorption $O_2 + H_2O$ Standard Atm.	-0.45 dB	-1.05 dB	Ref. graph
Spacecraft antenna correction	-0.1 dB	-0.1 dB	From pattern
Spacecraft antenna gain	+26.5 dB	+29.1 dB	Measured by F.I.
Waveguide loss	-0.5 dB	-0.8 dB	Estimate
Transponder gain	X_{13}	X_{18}	
Coax 4 GHz	-0.5 dB	-0.5 dB	Estimate
Spacecraft antenna gain (4 GHz)	+17.0 dB	+17.0 dB	Estimate
Spacecraft antenna correction	-0.2 dB	-0.2 dB	From pattern
Path loss	-196.7 dB	-196.7 dB	Calculated
E/S antenna gain	58.0 dB	58.0 dB	Estimate
$P_{received}$ (dBm) =	$-216.5 + X_{13}$ (dB)	$-218.9 + X_{18}$ (dB)	
or transponder gain	X_{13} (dB) = $P_{received}$ (dBm) +216.5		
	X_{18} (dB) = $P_{received}$ (dBm) +218.9		

CONCLUSIONS

From the measured data it was clear that the transponder was still fully functional and no malfunctions had occurred. Although no clear weather was available during the tests, it appeared that the transponder gain may have decreased by as much as 2 to 3 dB compared to prelaunch. Such a trend was also evident from the power monitor telemetry gathered over the past few years during the periodic turn-on. Table 8-7 presents data provided by C. Chapman that shows about 1 dB degradation in power output from 1976 to 1979.

Overall, it was clear that the technology developed during 1971, especially the 4-GHz MIC tunnel diode amplifiers, survived the orbital environment for 5 years without serious degradation.

Table 8-4
Measurement Results

Transponder Setting			Received (dBm) 7/24		Received (dBm) 7/25		Received Frequency Change (kHz) Both Days, Same Data	
13	18	Tx	13 GHz X 4145 MHz	18 GHz X 4165 MHz	13 GHz X 4145 MHz	18 GHz X 4165 MHz	13 GHz	18 GHz
A	A	A		-118 . . . -130	-119	-118		
A	B	A		-128		-117 . . . -118		-15
A	B	B		-134		-118		
A	A	B	-118 . . . -119	-134	-118	-118.5		+15
B	A	B	-118		-118	-118	-2	
B	A	A	-120		-120	-119		
A	A	A	-120	-120	-120.5	-119	+2	
Weather condition			Cumulus clouds, no rain	Variable heavy cumulus clouds, some rain	Steady rain, heavy cloud cover			

Table 8-5
Transponder Gain Summary (dB)

Transponder Setting			Prelaunch 1972 and 1973		June 1974 In-Orbit		April 1975 In-Orbit		July 1979 In-Orbit	
13	18	Tx	X_{13*} (dB)	X_{18*} (dB)	X_{13*} (dB)	X_{18*} (dB)	X_{13*} (dB)	X_{18*} (dB)	X_{13*} (dB)	X_{18*} (dB)
A	A	A	101.3 100.0	109.4 110.9	101.2 100.8	109.3 112.2	102.5	109.9	97.5 96.5	100.9
A	B	A								101.9
A	B	B	101.6 100.5	108.8 109.9	–	–	100.1	109.8	–	100.9
A	A	B	101.6 100.5	108.5 109.8	–	107.5	102.9	108.7	98.5	100.4
B	A	B	101.9 101.2	108.5 109.8	–	–	103.3	108.7	98.5	100.9
B	A	A	101.8 100.5	109.4 110.9	–	–	103.0	109.7	96.5	99.9

*GHz

Table 8-6
Gain Differences in dB Observed When Switching From A to B

Switching Action	Prelaunch		June 1974		April 1975		July 1979	
	T_xA	T_xB	T_xA	T_xB	T_xA	T_xB	T_xA	T_xB
13A → 13B	+0.5	+0.7, +0.3	–	+0.2	+0.5	+0.3, +0.4	+0.5	+1.0
18A → 18B	+0.1	+0.1	–	0	+1.9	+1.1	+1.5, +0.5	–
	R_x		R_x		R_x		R_x	
	A	B	A	B	A	B	A	B
T_xA → T_xB 13-GHz Channel	+0.5	+0.7	–	+0.8	+0.4	+0.3	–	+2
T_xA → T_xB 18-GHz Channel	-1.1	-1.1	–	-4.8	-1.2	-1.8	–	-2

Table 8-7
Comsat Propagation 24-Hour End-of-Life Test 13, 18, and 4 GHz

End-of-Life Test, Times (Z)	13 GHz A or B	18 GHz A or B	4 GHz A or B	V (LIC) (volts)	Temperature (°C)					Po (dBW)				
					13 GHz	18 GHz	4 GHz	Recvr	Xmitter	7/21/79	7/2/78	Xmit 1/2/78	10/14/77	6/13/76
21 July 1979														
1800	A	A	A	27.9	23.6	23.0	23.0	24.8	23.0	17.4	17.7	17.7	17.5	17.6
2100/2153	A	B	A	27.9	20.5	19.8	19.5	22.0	19.5	15.9	15.9	16.1	16.2	16.7
22 July 1979														
0000/0058	B	A	A	27.9	17.0	16.7	16.7	18.3	16.7	17.3	17.6	17.5	17.5	–
0300/0408	B	B	A	27.9	16.7	15.8	16.7	17.3	16.4	16.1	15.8	16.1	16.3	16.7
0600/0706	B	B	B	27.9	17.3	17.6	17.6	17.6	17.3	15.2	15.4	15.5	16.0	16.2
0900/1001	A	B	B	27.9	22.3	22.6	23.0	23.6	23.0	15.1	15.3	15.4	15.7	–
1200/1258	B	A	B	27.9	24.8	25.8	25.5	27.0	25.2	16.7	17.2	17.3	17.0	17.5
1500/1555	A	A	B	27.9	26.1	26.1	26.4	27.3	26.4	16.7	17.3	17.2	16.8	17.2
$\bar{X}$ (AVE)										16.3	16.5	16.61	16.63	16.98

CHAPTER 9

ATS-6 MILLIMETER WAVE PROPAGATION AND COMMUNICATION EXPERIMENT AT 20 AND 30 GHz

SYSTEM PARAMETERS

The ATS-6 Millimeter Wave Experiment (MWE), developed and implemented by the National Aeronautics and Space Administration (NASA) Goddard Space Flight Center (GSFC), has provided the first direct signal measurements of space-Earth links from an orbiting satellite. It was designed to measure and evaluate the propagation characteristics of space-to-Earth links centered at 20 and 30 gigahertz (GHz). ATS-6 was the second NASA flight experiment to evaluate propagation effects above 10 GHz. The first experiment launched on board ATS-5 in July 1969, provided measurements at 15.3 and 31.65 GHz.

Studies at 11 locations (Table 9-1) in the continental United States were directed at an evaluation of rain attenuation effects, scintillations, depolarization, site diversity, coherence bandwidth, and analog and digital communications techniques. In addition to direct measurements on the 20- and 30-GHz links, methods of attenuation prediction with radars, rain gauges, and radiometers were developed and compared with directly measured attenuation.

All stations, except Holmdel, New Jersey, measured signal attenuation at 20- and/or 30-GHz test frequencies. Also, three separate diversity experiments were conducted: (1) a short baseline experiment using 3 terminals at Columbus, Ohio; (2) another relatively short baseline system experiment conducted at Austin, Texas; and (3) a long baseline experiment using four terminals, Goddard Space Flight Center, Westinghouse Electric Corporation, Comsat Laboratories, and the Naval Research Laboratory that completely ringed the metropolitan area of Washington, D.C.

The quantity and quality of data obtained from the overall experiment were affected by two factors. An important constraint on the entire experiment was the lack of availability of the beacon transmission during periods of precipitation. Since many experiments were conducted on ATS-6, priorities were set up to accommodate all experimenters. Unfortunately, the ATS-6 Millimeter Wave Experiment did not have a high priority; therefore, on numerous occasions at the eleven stations, the satellite was not available during most periods of precipitation. Regular weekly times were assigned that averaged 1 hour per day.

The 20- and 30-GHz horn antennas were used on the spacecraft to obtain simultaneous coverage of the entire United States for the eleven participating stations. A 20/30-GHz parabolic reflector antenna was also employed to produce a narrow spot beam when link conditions called for high spacecraft effective isotropic radiated power (e.i.r.p.). Unfortunately, the 20-GHz horn traveling wave tube amplifier (TWTA) failed to operate; so, wide angle coverage at this test frequency was not available from the beginning of the experimental test period.

Table 9-1
ATS-6 MWE Participants

Location Organization	Elevation Angle (deg) (Antenna diameter)	Major Areas of Investigation
Rosman, North Carolina NASA GSFC	47 (4.6 m)	Prime facility 20- and 30-GHz attenuation, coherence bandwidth, differential phase effects, scintillation, communications links, radars, radiometers, rain gauge network
Greenbelt, Maryland NASA GSFC	41 (3 m)	20- and 30-GHz attenuation, site diversity,** radiometers
Austin, Texas Univ. of Texas (Ref. 2)*	54 (1.5, 3 m)	30-GHz attenuation, 2-terminal site diversity, radiometer
Blacksburg, Virginia VPI and SU*	45 (1.2 m)	20-GHz attenuation, depolarization
Clarksburg, Maryland (Comsat (Ref. 2)*	41 (3, 4.6 m)	20- and 30-GHz attenuation, site diversity,** radiometers
Columbus, Ohio Ohio State Univ. (Ref. 3)*	42 (3, 4.6 m)	20- and 30-GHz attenuation, 3-terminal site diversity, scintillation, radars, radiometers
Holmdel, New Jersey	39 (3.7 m)	20-GHz depolarization
Baltimore, Maryland Westinghouse	41 (3.7 m)	20-GHz attenuation; site diversity**
Waldorf, Maryland Naval Research Laboratory	42 (18.3 m)	20- and 30-GHz attenuation; site diversity,** radiometers
Richland, Washington Battelle N.W.*	31 (9.1 m)	20-GHz attenuation, radiometer
Ft. Monmouth, New Jersey USASCA	39 (4.6 m)	30-GHz attenuation

*GSFC supported participation
**Washington, D.C. area diversity experiment

In June of 1975, ATS-6 was moved to 35° E longitude where its primary mission was an experimental demonstration of an educational satellite television system in India. Since these transmissions only lasted for 8 hours a day, the satellite was available for the remainder of the day. As a result, the English, Dutch, German, and French experimenters became participants in the millimeter wave propagation experiment. The European experiment lasted from August 1975 to October 1976. At this time, the satellite sank below the horizon on its path to a new position at 140° W longitude.

A listing of the European stations that participated in the experiment is shown in Table 9-2. Also listed are the various measurements performed by each station and their respective antenna size and operational elevation angle. The main consideration for most of the European stations was signal depolarization. Of the seven stations listed, four were English and they performed the largest variety of propagation measurements.

During the course of the European experiment, a number of system problems arose that affected the propagation data. They were:

- The Polaris sensor on the satellite failed in September 1975 resulting in reduced satellite stability in yaw. Roll and pitch instabilities occurred occasionally as well. These instabilities had a degrading effect on signal depolarization measurements.
- Problems in program track of the ground antennas were encountered.
- The second 20-GHz satellite transmitter failed in June of 1976.
- Scheduling problems were also encountered during test periods when valuable data could have been obtained.

GROUND TERMINALS SYSTEM

It would be impractical to present detailed descriptions of all the ground stations that participated in the millimeter wave experiment. These descriptions can be found in the references that follow this chapter. Therefore, only a functional description of NASA's prime facility, the Rosman Ground Station in North Carolina, will be presented. In addition, general operational parameters of the remaining stations will be given, so that a good grasp of the system requirements necessary for operating at 20- and 30-GHz frequencies for a spacecraft can be obtained.

The experiment had three modes of operation: (a) the continuous wave (CW) mode in which the 20- and 30-GHz carriers only were transmitted; (b) a multitone mode in which nine spectral lines spaced 180 megahertz (MHz) apart were transmitted, centered at 20 and 30 GHz; and (c) a communication mode, in which frequency modulated communication uplink signals received on the spacecraft transponder were retransmitted at 20.15 and 30.15 GHz.

The CW mode was used mainly to obtain rain attenuation statistics at the 20- and 30-GHz test frequencies. This was the main mode of operation for all participants in the experiment. The

Table 9-2
MWE European Experimenters

Participating Stations	Antenna Size (Meters) Elevation Angle (Degrees)	Test Measurements
University of Birmingham, England	6 21°	Signal depolarization 35-GHz sky temperature, 30-GHz attenuation measurements, 5.6-GHz meteorological radar
University of Bradford, England	3.6 20°	20-GHz attenuation measurements, 9.4-GHz radar returns, 20-GHz depolarization measurements
SRC Appleton Lab, Slough, England	3 22.4°	30-GHz attenuation measurements, path diversity measurements, 30-GHz sky temperature measurements, 30-GHz depolarization measurements, 9.4-GHz radar returns
British Post Office Research Center, Ipswich, England	6.1 23°	20- and 30-GHz signal depolarization measurements, 20- and 30-GHz attenuation measurements, signal scintillation measurements, 20- and 30-GHz sky temperature measurements
Technical University of Eindhoven, Holland	3 25°	30-GHz depolarization measurements, 30-GHz sky temperature measurements, 30-GHz scintillation measurements, 30-GHz attenuation measurements
Centre National d'Etudes de Télécommunications, Moulineaux, France	9 25°	20-GHz signal depolarization measurements, 20-GHz sky temperature measurements
Bundespost FIZ, LeeHeim, Germany	3 27.5°	30-GHz signal depolarization and phase measurements, 30-GHz attenuation measurements, 11.4-GHz sky temperature measurements

multitone mode was employed by the Rosman Ground Station to determine the wideband frequency characteristics of the 20- and 30-GHz spacecraft channels. The nine tones produced a bandwidth of 1440 MHz at both test frequencies. The communication mode was used by the Rosman Ground Station to test links consisting of a 6-GHz uplink frequency and a variety of downlink frequencies of either 4 GHz, 20 GHz or 30 GHz. These links were used to transmit and receive both analog and digital data.

All participants, excluding the Rosman Ground Station, had a receive-only capability. A general functional description that would apply to a station instrumented to receive the 20- and/or 30-GHz signals will be given. This description can apply to any of the participant stations with slight variations.

The station employed a parabolic antenna with a Cassegrain type feed. The output of the feed assembly was connected to a diplexer that separated the 20- and 30-GHz receive signals. Each signal was fed to its own respective front-end unit. This unit consisted of a mixer, assorted filters, and an amplifier following the mixer. If sky temperatures were being measured, one of the filters would be used to separate the temperature signal from the spacecraft received signal. The mixer frequency translated the received signals to a common intermediate frequency of 1.05 GHz. This signal was fed to a signal processor that converted the received signal to a direct current (d.c.) voltage within the limits of zero to five volts. The strength of the received signal was proportional to the output voltage. Signal attenuation was measured by comparing the received signal level with a level that represented a clear sky weather condition with the use of receiver calibration curves.

The noise figure for the above receiver configuration was about 13 decibels (dB). Inclusion of a parametric amplifier preceding the mixer unit would reduce the noise figure to about 5 dB. A pictorial representation of this station is shown in Figure 9-1.

SATELLITE SYSTEM

The major elements of the MWE satellite system are shown in Figure 9-2. The experiment had three modes of operation: continuous wave (CW), multitone (MT) and communication, selectable at 20 and/or 30 GHz. In the CW mode, a 10-GHz signal was developed by multiplication from the 5-MHz master oscillator, then doubled for the 20-GHz carrier, and tripled for the 30-GHz carrier. The carriers were used to drive four 2-watt traveling wave tube amplifiers to transmit through either of two antenna systems to the Earth. The parabolic antenna was used when a narrow spot beam was required, and the horn antennas were used for wide coverage of the continental United States. The TWTA's were permanently connected to antennas.

In the multitone mode, a 180-MHz signal was developed from the 5-MHz master oscillator to phase modulate the 10-GHz carriers in the 20- and 30-GHz channels. A combination of nine tones was generated, four on either side of the carrier spaced 180 MHz apart, resulting in a total spectrum of 1440 MHz.

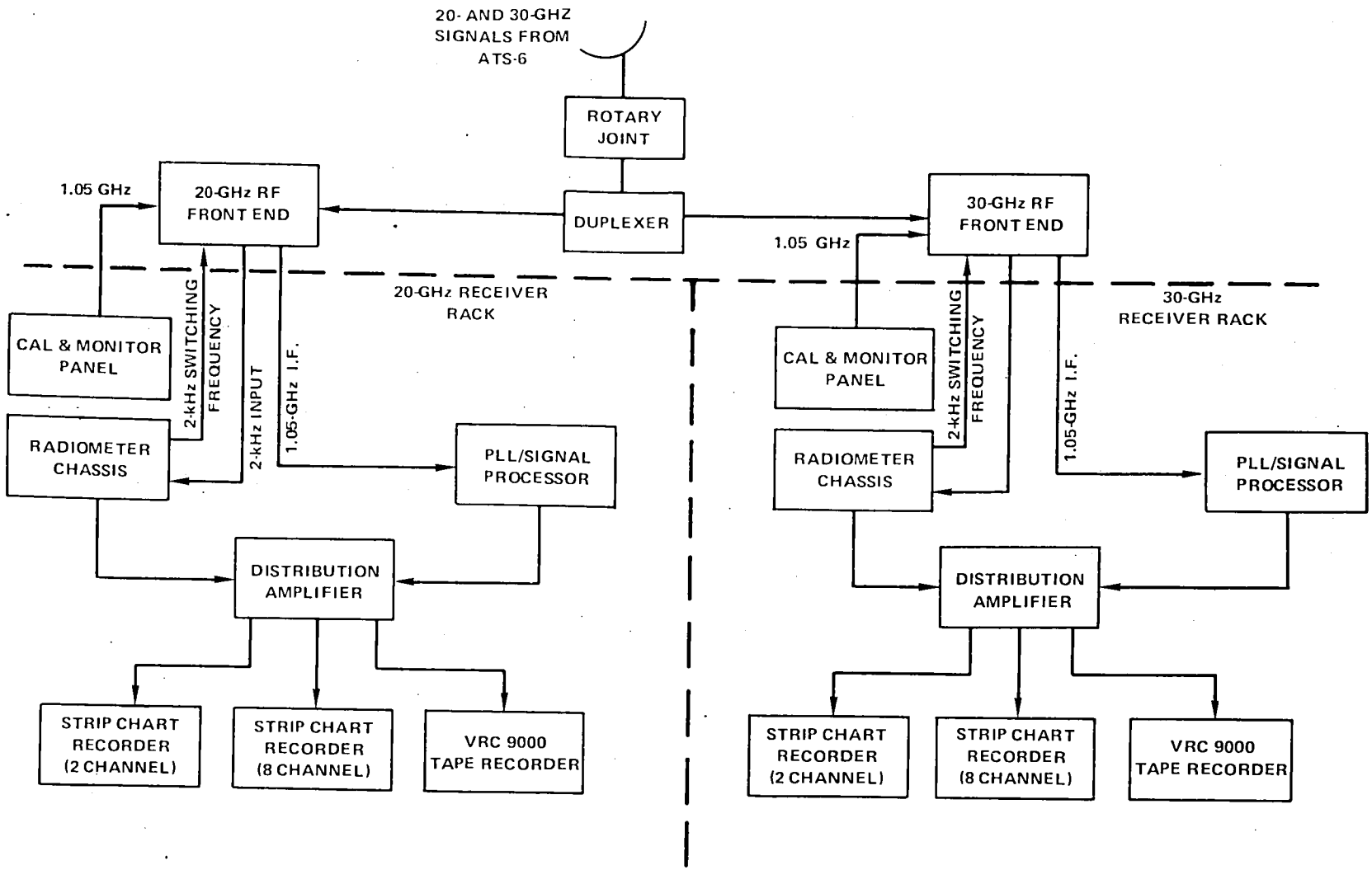

Figure 9-1. Typical Millimeter Wave Ground Station

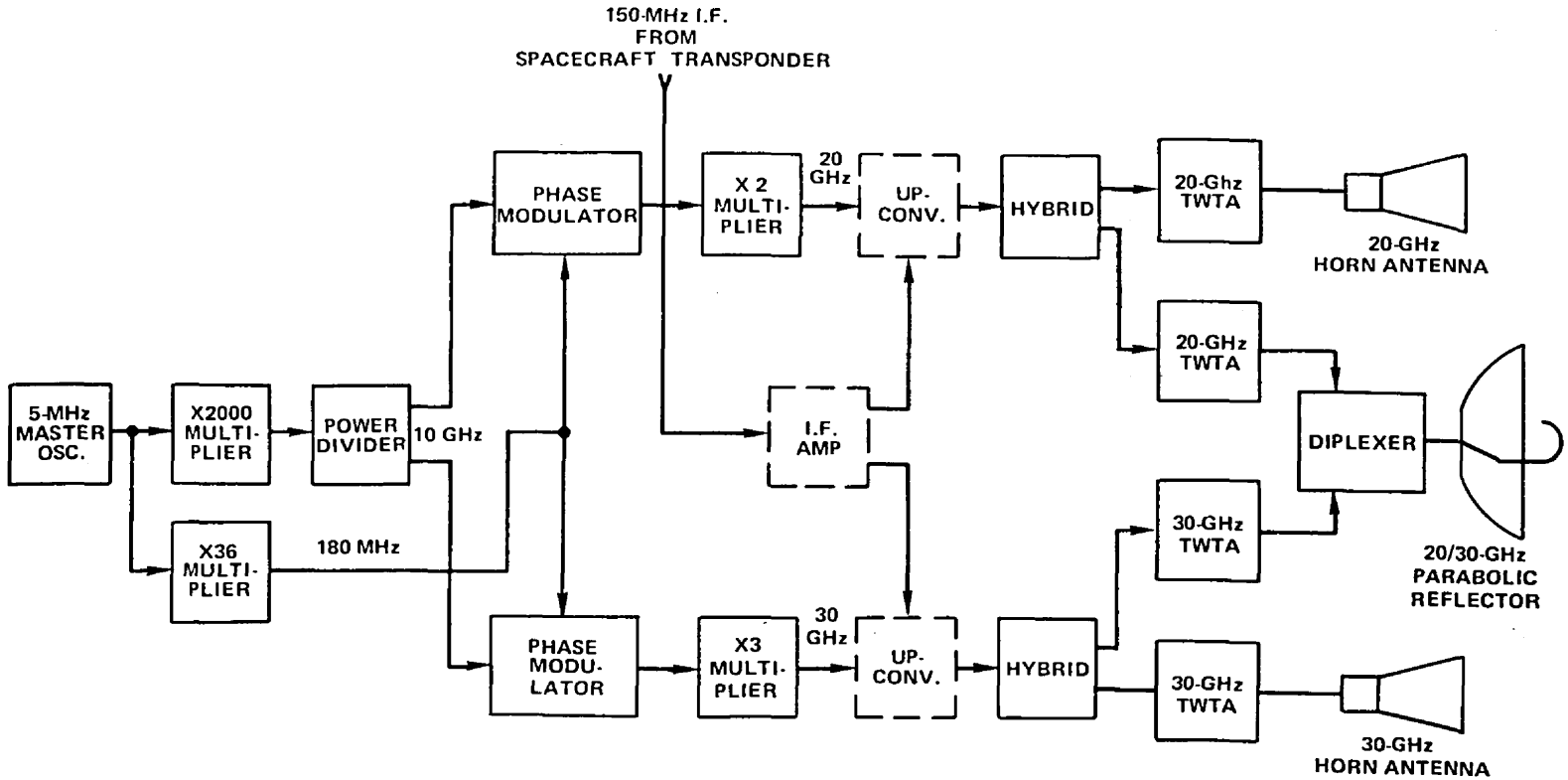

Figure 9-2. Millimeter Wave Experiment Flight Hardware Elements

In the communication mode, the 150-MHz intermediate frequency (i.f.) from the spacecraft was used to drive an upconverter that produced a 30.15-GHz or 20.15-GHz transmitted signal for communication tests. Bandwidths of 40 MHz or 12 MHz were available on command for the 150-MHz i.f. signal. The uplink frequency of the spacecraft transponder was one of three in the 6-GHz band, and the C-band downlink was one of three in the 4-GHz band.

Three antennas were provided in the experiment: a 20-GHz horn antenna, a 30-GHz horn antenna, and a 20/30-GHz parabolic antenna. In each case, the radiated radio frequency (rf) was linearly polarized with the plane of the E-vector aligned to the north-south axis of the spacecraft. For both horn antennas, the 3-dB beamwidths were approximately 6 degrees in the north-south direction and 8 degrees in the east-west direction. For these antennas, an e.i.r.p. of about 60 decibels referred to 1 milliwatt (dBm) was obtained for all three modes. The parabolic antenna provided a 3-dB beamwidth of 2.3 degrees at 20 GHz and 1.6 degrees at 30 GHz. For the 20-GHz frequency, an e.i.r.p. of 70.6 dBm was obtained, and for the 30-GHz frequency, an e.i.r.p. of 73.6 dBm was obtained.

PARTICIPATING GROUND STATIONS

The prime facility of the 11 ground terminals was the NASA Rosman Ground Station near Brevard, North Carolina, that was equipped to measure 20- and 30-GHz attenuation, coherence bandwidth, communications link characterization, and prediction techniques with radars and rain gauges. A second NASA terminal, located at Goddard Space Flight Center, Greenbelt, Maryland, performed 20- and 30-GHz attenuation measurements and scintillation studies. A major element of the MWE involved the participation of a number of organizations with unique specialities in the millimeter wave propagation area. Nine organizations with 13 ground terminals participated in the experiment, their locations and major areas of measurement are summarized in Table 9-1.

All terminals were equipped to measure attenuation at 20 or 30 GHz, or both; and all, except for Bell Laboratories, could do rain gauge measurements as well. The Washington, D.C., area diversity experiment consisted of four terminals in the Washington metropolitan area that jointly observed 20-GHz attenuation events from which site diversity statistics were developed.

Out of 11 ground terminal locations, no information concerning the system configuration or experimental results was obtained from three of the participants. These were, Bell Laboratories at Holmdel, New Jersey, Naval Research Laboratory at Waldorf, Maryland, and U.S. Army Communications Agency at Fort Monmouth, New Jersey.

University of Texas at Austin, Texas

This station was instrumented to measure 30-GHz attenuation due to rain, sky temperature using a radiometer, and site diversity statistics using two ground terminals spaced 11 kilometers (km) apart. The 30-GHz data were obtained by radiometric means. Space diversity measurements were accomplished with 20-GHz radiometers and 30-GHz receivers, located at each of the separated sites.

The northern site, Balcones Research Center, used two 3-meter parabolic antennas attached side by side to a mount. The pointing of these antennas were controlled by an observer with a setting accuracy of 0.03 degree. The antenna for the second site (on the main campus of the University of Texas) was a 1.5 meter converted searchlight. Its pointing accuracy held within 0.02 degree. For simultaneous operation at 20 and 30 GHz, the feeds were placed into the focus side by side.

The 30-GHz satellite receivers had superheterodyne front ends with a 1.05 GHz i.f. This signal was fed to a phase-locked loop receiver in which the downconverted carrier was locked to a 10-MHz crystal oscillator. The noise bandwidth of these receivers was 50 to 100 hertz (Hz). The single sideband noise figure of the receiver was 12 dB. With the horn antenna pointed at Rosman, North Carolina, fade margins better than 33 dB were possible for both receivers.

The 20-GHz sky-noise radiometers were Dicke switched receivers. Their local oscillator frequency was chosen to correspond with the first lower sideband frequency of the 20-GHz satellite transmitter at 19.82 GHz. For additional isolation, the radiometers were approximately cross-polarized to the satellite signal. The sensitivity of the radiometers was approximately 1 kelvin (K) with a one-second integration time.

Ohio State University at Columbus, Ohio

The main objective of the experiment for this location was to determine the improvement in reliability resulting from the use of the path diversity on millimeter wavelength, satellite Earth communication links.

This was accomplished by measuring the path attenuation observed on 20- and 30-GHz ATS-6 downlinks at two spatially separated ground terminals. Radiometric noise emission at 20 and 30 GHz along these same propagation paths was also recorded for correlation with the attenuation data. A third remote terminal recorded 20-GHz radiometric noise emission along the propagation path directed toward the position of ATS-6 to provide an additional estimate of path attenuation and diversity. Measurements of radar backscatter and radiometric noise emission at 3, 9, and 15 GHz over the regions through which the propagation paths to the remote terminals pass was made using the Ohio State University (OSU) high resolution radar/radiometer system and the OSU low resolution radar system. Finally, a cooperative experiment with the Comsat Corporation provided uplink attenuation on four spatially separated propagation paths at 17.8 GHz and one path at 13.2 GHz.

The relative position of these four terminals along with the measured parameters are shown in Figure 9-3.

The fixed and transportable terminals consisted of the same 20/30-GHz front ends. The outputs consisted of the two-frequency satellite signal levels and radiometric noise levels. These signals were fed into quadruple superheterodyne phase-locked loop receivers that converted the input 1.05-GHz signal to the final 2.5-kilohertz (kHz) signal. The computed dynamic range for both terminals was about 55 dB for the satellite 20-GHz CW/parabolic antenna mode. For the 30-GHz CW/horn it was about 35 dB. Both terminals used a 4.6-meter parabolic antenna with a square corrugated feed horn.

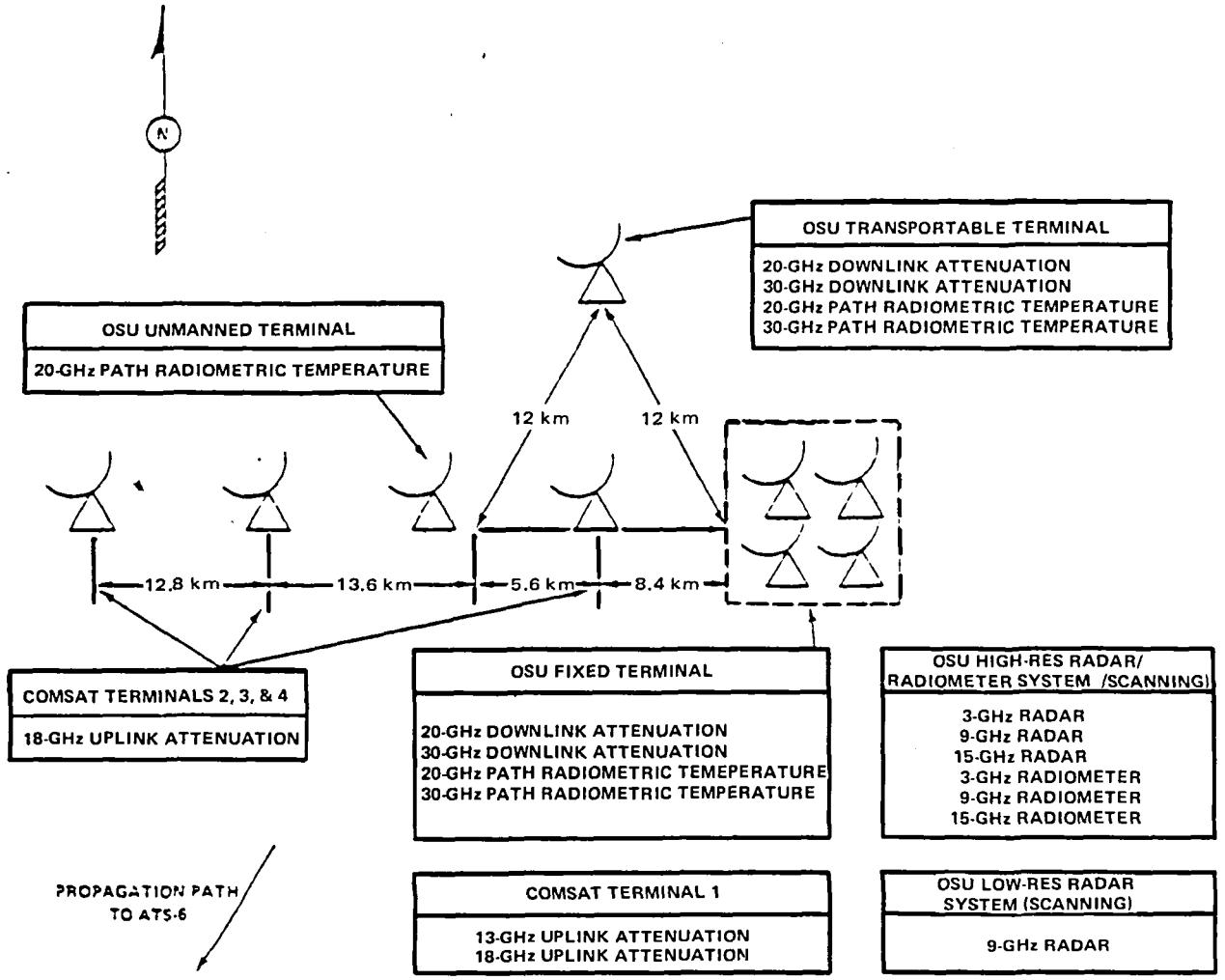

Figure 9-3. ATS-6 Diversity Experiment, Electro-Science Laboratory
Ohio State University, Columbus, Ohio

Comsat Laboratories in Clarksburg, Maryland

The Comsat terminal was instrumented for the purpose of collecting propagation data using the ATS-6 20/30-GHz beacons and also in obtaining data for the long baseline diversity experiment jointly with NASA/GSFC and Westinghouse. The measuring equipment for these tasks consisted of: (1) A 3-meter diameter antenna receiver system for accepting 20-GHz satellite continuous wave signals and a radiometer system at 11.6 GHz for monitoring sky-noise temperature, (2) a 4.6-meter diameter antenna receiver system capable of receiving 20- and 30-GHz main CW signals and radiometer at 20 and 30 GHz, (3) rain gauges along the boresight path toward the satellite for recording instantaneous rainfall rates, and (4) a weather radar at 5.4 GHz for detecting the motion pattern of the rain cloud in large scale.

Tunnel diode and uncooled parametric amplifiers were used in the 20-GHz front-ends of the 3- and 4.6-meter systems, respectively. The 30-GHz system had a low-noise mixer front end. Signal processors, which detected the downconverted signals by individual narrowband phase-locked receivers, gave output amplitudes that were proportional to the satellite beacon signal attenuation levels. Performance parameters for both systems were as follows:

3-meter Antenna System

	11.6 GHz	20 GHz
Antenna gain	48.7 dB	53.5 dB
Pointing accuracy	±0.1 degree	±0.1 degree
Noise figure	5 dB	8 dB
Radiometer sensitivity	1 K	–
Radiometer bandwidth	100 MHz	–
Receiver bandwidth	–	10 kHz

4.6-meter Antenna System

	20 GHz	30 GHz
Antenna gain	57 dB	60.5 dB
Pointing accuracy	±0.01 degree	±0.01 degree
Noise figure	4 dB	8 dB
Radiometer sensitivity	1 K	1 K
Radiometer bandwidth	100 MHz	100 MHz
Receiver bandwidth	10 kHz	10 kHz

Virginia Polytechnic Institute Terminal at Blacksburg, Virginia

The Virginia Polytechnic Institute and State University ATS-6 Experiment was primarily concerned with the depolarization effects of precipitation at millimeter wavelengths. The system was instrumented to receive and measure the linearly polarized 20-GHz spacecraft signal. Two signals were involved in this measurement process: the incoming power in the copolarized and cross-polarized components of the incident signal.

The antenna employed in the experiment was a 1.2-meter parabolic reflector with a dual polarized prime-focus feed to receive the two distinct polarized signals. The receiver was switched between the cross-polarized and copolarized antenna feeds once every 2 seconds. The measured antenna gain was 45.8 dB and port-to-port isolation for the two signals was 48 dB. The maximum measurable difference between the two dissimilar polarized signal components was 40 dB.

Battelle-Northwest Laboratories at Richland, Washington

The system instrumented by the Battelle-Northwest Laboratories was used to measure attenuation on a space-to-Earth link of a 20-GHz signal. Sky temperature, using a radiometer, was also measured concurrently with the above attenuation. A 9.14-meter diameter Cassegrain antenna was employed for the measurement.

The major instrument used was a 20-GHz receiver-radiometer system that measured the 20-GHz carrier level and simultaneously measured the radiometric sky temperature in the same antenna pattern. A single balanced diode mixer was used for both purposes. The mixer-input port was switched between the antenna and an ambient temperature wave guide termination at a 1 kHz rate. The computed fade margin was about 50 dB for the above configuration assuming a unity signal-to-noise ratio.

Westinghouse Station at Linthicum Heights, Maryland

The Westinghouse station was instrumented to receive the 20-GHz spacecraft signal for measurement of rain attenuation for its locale and also to be a part of the long baseline diversity experiment. A 3.6-meter parabolic reflector was employed at this station. The 20-GHz receiver had an effective noise figure of 13 dB that produced an overall system dynamic range of 51 dB when the CW mode was employed on the spacecraft. This range was computed on the basis of a minimum hold-in lock range of -115 dBm for the phase-locked loop receiver and the measured clear weather i.f. signal level of -64 dBm.

Goddard Space Flight Center Station at Greenbelt, Maryland

The Goddard Space Flight Center station was instrumented to receive the 20- and 30-GHz spacecraft signals, and, in addition, to measure the corresponding sky temperatures near these frequencies. A 3-meter parabolic antenna with a Cassegrainian feed was employed in the system. For the receive system, the single sideband noise figure was 13 dB.

For the 20-GHz CW mode, the measured i.f. received signal level was -68.5 dBm. Also the measured hold-in threshold of the phase-locked loop receiver was -112 dBm. It follows that the overall system dynamic range was 43.5 dB.

NASA Prime Station at Rosman, North Carolina

The prime NASA Millimeter Wave Experiment ground terminal was located at the NASA Rosman Ground Station, near Brevard, North Carolina. The system used a 4.6-meter parabolic reflector antenna with a dual-frequency feed and an rf front-end mounted at the antenna. The system was capable of measuring the 20- and 30-GHz received signals in the CW mode and also of measuring the multiple signals at 20 or 30 GHz in the multitone mode. In this mode, at one frequency, nine separate tones were transmitted by the spacecraft. They included a carrier and four sidebands at

±180 MHz, ±360 MHz, ±540 MHz, and ±720 MHz. The received-signal levels of these nine signals were measured, along with the phase of each sideband pair.

Sky temperatures at 20 and 30 GHz were measured in the receiver-radiometer units. The radiometer used a 100-MHz bandwidth centered at 20.270 GHz. The radiometer had a T_{min} sensitivity of 0.0240 and 0.870 K for a 10-second integration time at 20 and 30 GHz, respectively. These sensitivities were achieved at the Rosman site with the parametric amplifier. In the communications mode, signals were transmitted by Rosman to the spacecraft at a 6-GHz frequency. They were then translated to an i.f. of 150 MHz and fed to the millimeter wave unit as shown in Figure 9-2. Spacecraft signals were received at frequencies of 30.15 or 20.15 GHz at the ground terminal. Bandwidths of 40 or 12 MHz were available, on command. Communication signals were processed through the system and were frequency translated to 70-MHz i.f. where they were then fed to their respective demodulators.

The receiver noise figure for the 20-GHz system was 4.6 dB and for the 30-GHz system it was 5.6 dB without the radiometer in the system. Inclusion of the radiometer would have increased the noise figure due to the effect of signal losses from passive units placed before the parametric amplifiers. With this system, fade margins of 33 dB were attained from actual signal measurements.

In addition to the above measurements, a number of other functions were measured and recorded. This included outputs from a 3- and 8-GHz meteorological radar, 10 rain gauges, and meteorological data. All parameters were recorded on a single 8-track digital tape with the aid of a PDP-11 computer system.

Relative placement of the main ground terminal, meteorological radar, and the 10 rain buckets are shown in Figure 9-4. The buckets and radar were located on a line that was approximately defined by the pointing vector of the main antenna to ATS-6. A radar return at a specific frequency was obtained from 255,100-meter range bins in a 2-second time interval. With this type of range resolution, it was possible to determine the intensity and range extent of the precipitation causing the 20- and 30-GHz attenuation along the elevated beam.

Wind turbulence was one of the main factors in causing divergence between the rain-rate factors that exist in the elevated beam and what was actually measured in the rain buckets. To determine if a correlation existed between the wind turbulence and the measured rain rate, three anemometers were installed at various points near the test antenna to measure wind speed and direction.

In attempting to obtain data in the carrier-wave (CW) and multitone (MT) modes, various equipment problems became evident. As a result, very limited sky temperature and MT measurements were obtained during the test period.

The ground hardware problems centered around the 20- and 30-GHz ATS-6 Millimeter Wave Experiment receiver. Four main problem areas were discovered during the course of the experiment: (1) inability to obtain reliable and accurate calibrations, (2) radiometer drift, (3) problems with 20- and 30-GHz parametric amplifiers, and (4) beat frequency problems when operating in the MT mode. The main causes of the problems associated with calibration were the frequency selective

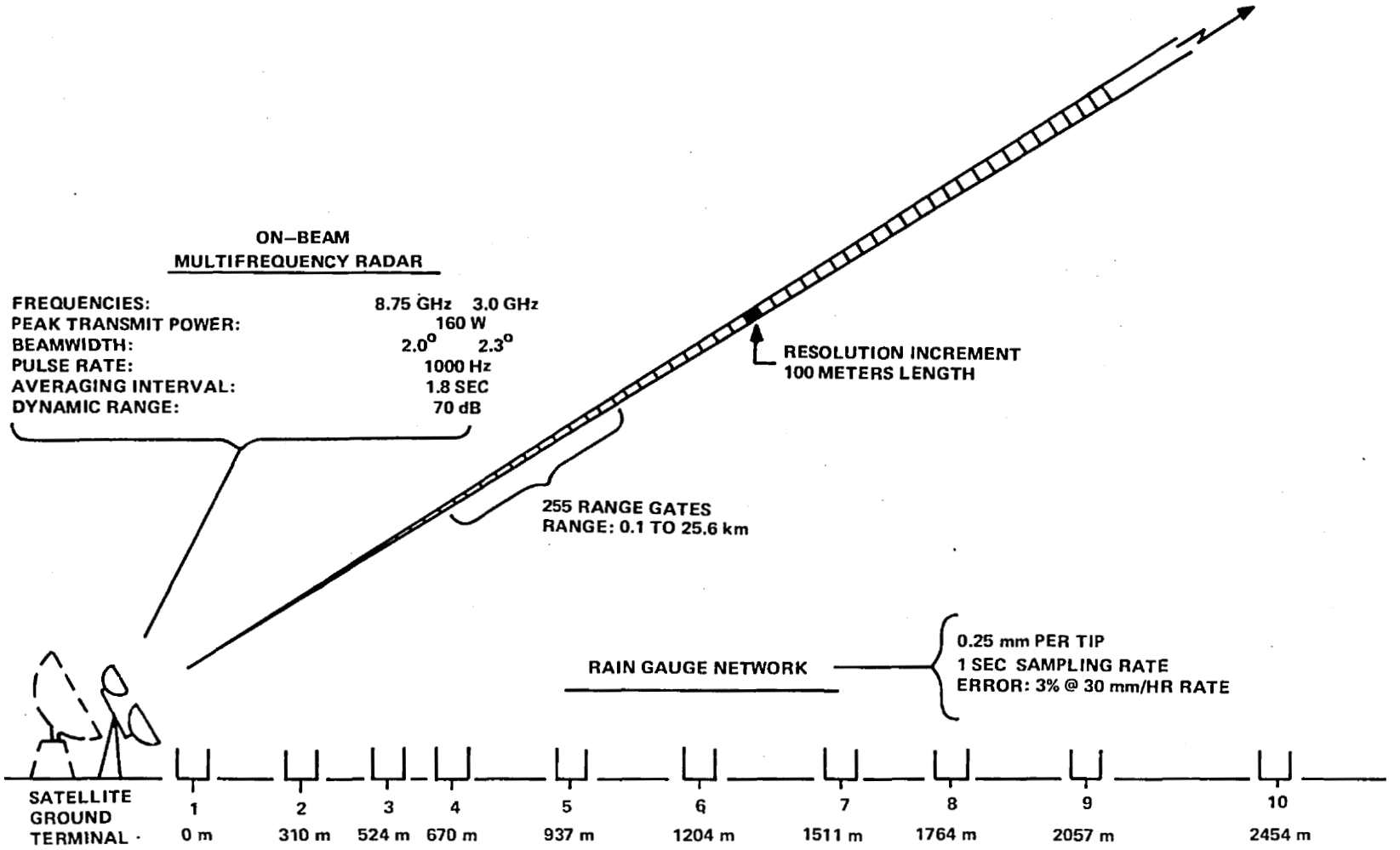

Figure 9-4. Radar and Rain-Gauge Measurements at Rosman Ground Station

characteristics of the 200 feet of cable between the front end of the receiver and the signal processor. Also the lack of a uniform response from the various mixers contributed to the problems. The main cause of the radiometer drift was the instability in the noise source. For the parametric amplifiers, design deficiencies in the high-voltage beam supply transformer caused problems until it was corrected. Also, the units required too much warmup time and drifted initially so as to make them impractical for use in propagation tests. When operating in the MT mode, it was necessary to adjust the 5-MHz frequency standard. This adjustment caused a definite beat frequency to appear on the carrier and sidebands that affected the accuracy of the recorded data.

European Ground Stations

Seven European ground stations participated in the experiment. Of these, four were English and one each was French, German, and Dutch. The respective antenna sizes, elevation angles, and types of test measurements for the seven stations are listed in Table 9-2. All the stations used their own equipment and had antenna sizes that ranged from 3 to 9 meters. The high satellite e.i.r.p. enabled experimenters to measure attenuation and cross polarization with a very large dynamic range using rather simple receiver equipment.

University of Birmingham at Birmingham, England

This station used a 6-meter asymmetrical parabolic antenna with a unique offset feed to minimize the effect of aperture blockage. The computer controlled tracking system could maintain a tracking accuracy of ±0.01 degree for 4 hours.

A dual-frequency feed system was employed to obtain simultaneous operation at 30 and 5.6 GHz. The receiver had three stages of fixed frequency downconversion to an i.f. of 65 kHz, where a phase-locked loop was used to track the signal. The dual channel 30-GHz receiver had maximum copolar and cross-polar sensitivities of -135 dBm, and -155 dBm respectively. For a clear sky signal level of -95 dBm, the resulting dynamic ranges were 40 and 60 dB.

The 30-GHz radiometer operated in the Dicke mode. It achieved a resolution of ±5 K with an integration time of 5 seconds.

University of Bradford at Bradford, England

This station used a 3.6-meter symmetrical Cassegrain antenna for reception with a two-channel, phase-locked receiver. Programmed tracking, using a PDP-8 minicomputer, gave 0.022 degree resolution with 5-minute updates.

A 9.4-GHz meteorological radar was also operated with a fixed beam directed along the satellite path. This radar employed 62 range bins over a range of about 10 km. Special features of this radar (Reference 1) included a high calibration stability (~0.25 dB) and a short near-in range of 60 meters. The principal purpose of the radar was to locate rain cells within the elevated radio path.

British Post Office Research Center Station at Ipswich, England

This station also used a 6.1-meter offset Cassegrain antenna. The antenna had 3-dB beamwidths of 0.18 degree and 0.13 degree at 20 and 30 GHz, respectively. The tracking accuracy was ±0.01 degree and was achieved by using pointing data read from a paper tape at 4-minute time intervals. Phase locked receivers were employed having a loop bandwidth of 200 Hz. Each had a calibrated dynamic range of 30 dB.

Radiometers at 20 and 30 GHz were also employed at the station. They were of the unbalanced Dicke switching type and their 0.6-meter antennas had 3-dB beamwidths of 1.8 and 1.2 degrees at 20 and 30 GHz, respectively. The radiometers had minimum detectable input temperature increments of 1 K with a time constant of 1 second.

The SRC Appleton Laboratory Station at Slough, England

At this station, a three-site network was employed to determine space diversity gain at 30 GHz. The diversity network consisted of a station at the main Appleton laboratory and two small stations located at Langley and Winkfield. The two outstations had 1-meter antennas while the central station had a 3-meter antenna. All the antennas were front fed. The station spacings were 2 km (Appleton and Langley) and 10.3 km (Appleton and Winkfield). Standard phase-lock techniques were used to track the satellite signal. Radiometers at 30 GHz were also employed at the outstations. These units measured the total power in a 6-MHz bandwidth with bandstop filters inserted to prevent detection of the satellite signal.

A 9.4-GHz meteorological radar was also employed at the Appleton station. Its antenna had a 1 degree beamwidth and range bins from 500 meters in length to 22.5 km. The radar and cross-polarization data were recorded at a rate of 2.5 seconds.

Station at The Technical Institute of Eindhoven, Holland

This station used a 3-meter Cassegrain reflector antenna. At 30 GHz, the antenna gain was 56 dB and the 3-dB beamwidth was 0.28 degree. Phase-locked loop receivers at 30 GHz were employed to receive the copolar and cross-polar signals. The loop bandwidths of the copolar and cross-polar receivers were 200 and 20 Hz, respectively. A 30-GHz Dicke type radiometer was also employed at the station.

Centre National d'Etudes de Télécommunications Station at Moulineaux, France

This station employed a 9-meter Cassegrain antenna with a beamwidth of 0.11 degree at 20 GHz. The phase-locked loop receivers used at this station were capable of obtaining 40 dB isolation between the copolar and cross-polar signal channels. The received signal levels were recorded at a 0.1-second rate and averaged over a 2-second time interval by a computer. A 20-GHz radiometer was also employed at the station to measure sky temperature.

Bundespost FTZ Station at Leeheim, Germany

A 3-meter antenna with a prime-focus feed was employed at this station. A half wave plate was inserted in the feed to aid in the assessment of the measurement errors for the cross-polarized signal level. This dielectric plate was located in the feed system in front of the orthomode transducer and turned the polarization of the incoming wave into the main axes of the feed.

Phase-locked loop receivers were employed for measuring the amplitude of the copolar and cross-polar signal levels. Sky temperature measurements using an 11.4-GHz radiometer were also performed.

THEORETICAL CONSIDERATIONS RELATED TO MEASURED PARAMETERS

Introduction

Propagation effects on the signal that was transmitted over a space-Earth link were defined by measuring various signal parameters that were produced by meteorological effects. Experimenters found four parameters that effectively defined the propagation effects of 20-/30-GHz signals. These effects were as follows: (1) signal scintillation, (2) effects of rain, (3) bandwidth restrictions, and (4) depolarization effects. The various theoretical and/or empirically derived expressions that describe the above phenomena are presented in the following paragraphs.

Signal Scintillation

The amplitude, phase, and angle-of-arrival of a microwave signal passing through the troposphere varies according to inhomogeneities in the refractivity (clear air), clouds, and rain. The effects occur on time scales shorter than a minute and on spatial scales shorter than a kilometer. The phenomena of amplitude and angle-of-arrival fluctuations combine to form received signal amplitude fluctuations. Figure 9-5 shows a model (Reference 2) depicting these effects on the received signal. This model uses the concept of incident plane-wave decomposition.

Signal effects due to the above phenomenon are usually expressed in terms of a signal variance, S^2, with an assumption of weak turbulence. This log-amplitude variance (weak turbulence) is invoked for a plane-wave incident on a region of turbulence, propagating distance L (km) and impinging on a circular aperture of diameter d.

Measurements made at the Ohio State University of ATS-6 20- and 30-GHz beacons, were used to derive empirical constants for a model with an effective turbulence height of 6 km (typical), and a mean-Earth radius of 6377 km.

A plot of average variance, S^2, as a function of elevation angle is shown in Figure 9-6. It is known that peak-to-peak variations of 30 N-units in the refractive index are expected on a time scale of days and hours. The corresponding fluctuations in received signal amplitude variance expressed in dB would be expected to be about 20 dB peak-to-peak for a fluctuation of 30 N-units out of an average of 345. The effect on S^2 of this variation about the mean is also shown in Figure 9-6.

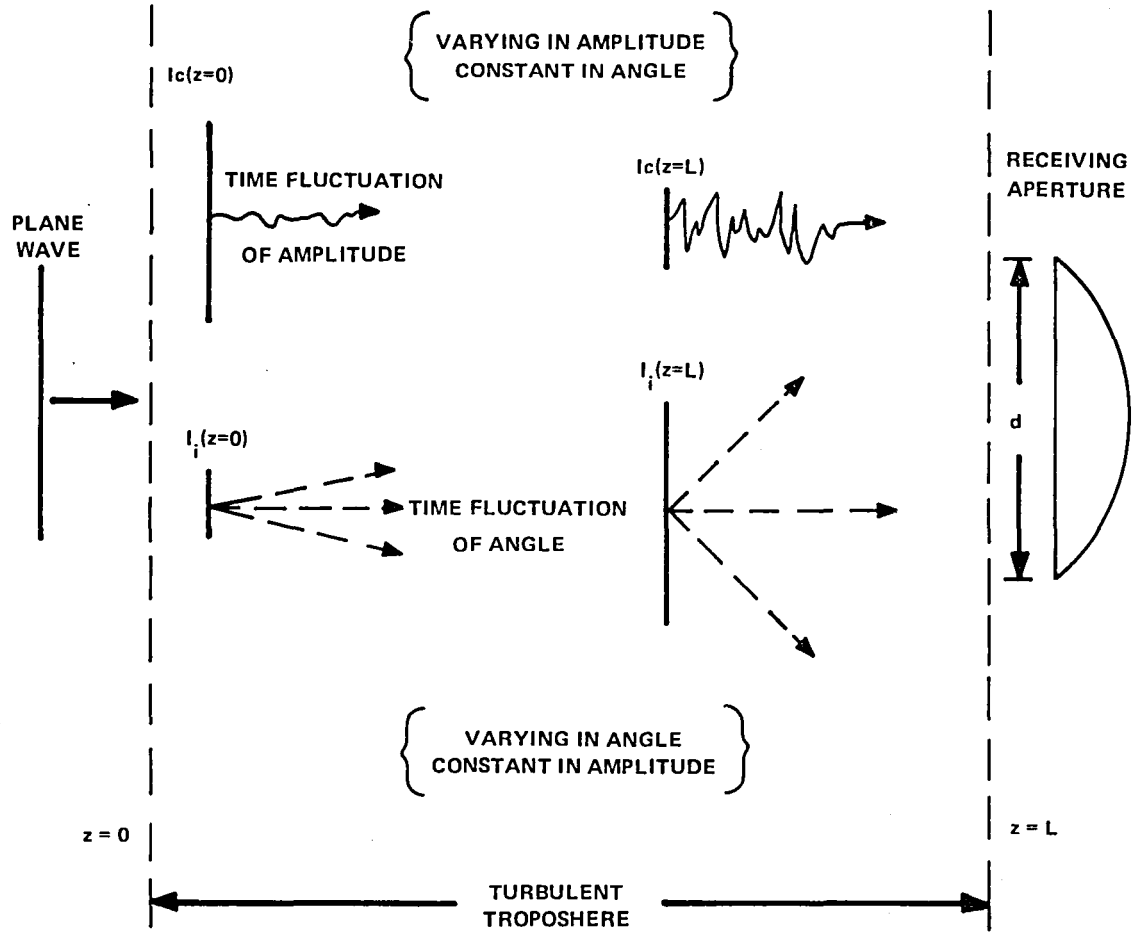

Figure 9-5. Decomposition into Coherent and Incoherent Components

Wavefront tilt on angle-of-arrival variation results in time-averaged gain degradation; and phase incoherence results in instantaneous gain loss, excluding the atmospheric loss.

Tropospheric effects on the signal are defined by the magnitude of the gain reduction R and S parameters. To apply them to a link design, they must be incorporated in a long-term cumulative probability distribution like that shown in Figure 9-7. For turbulence induced fluctuations, it was assumed that they followed a log-normal distribution with the mean and median being equal. The R and S factors were computed where the R factor defined the median point and the S factor the corresponding standard deviation σ_v for the distribution, as shown in Figure 9-7. These long-term turbulence effects predominate down to a percentage time of about 1 percent. Below this value, adverse attenuation effects due to rain and abnormal refraction effects tend to predominate.

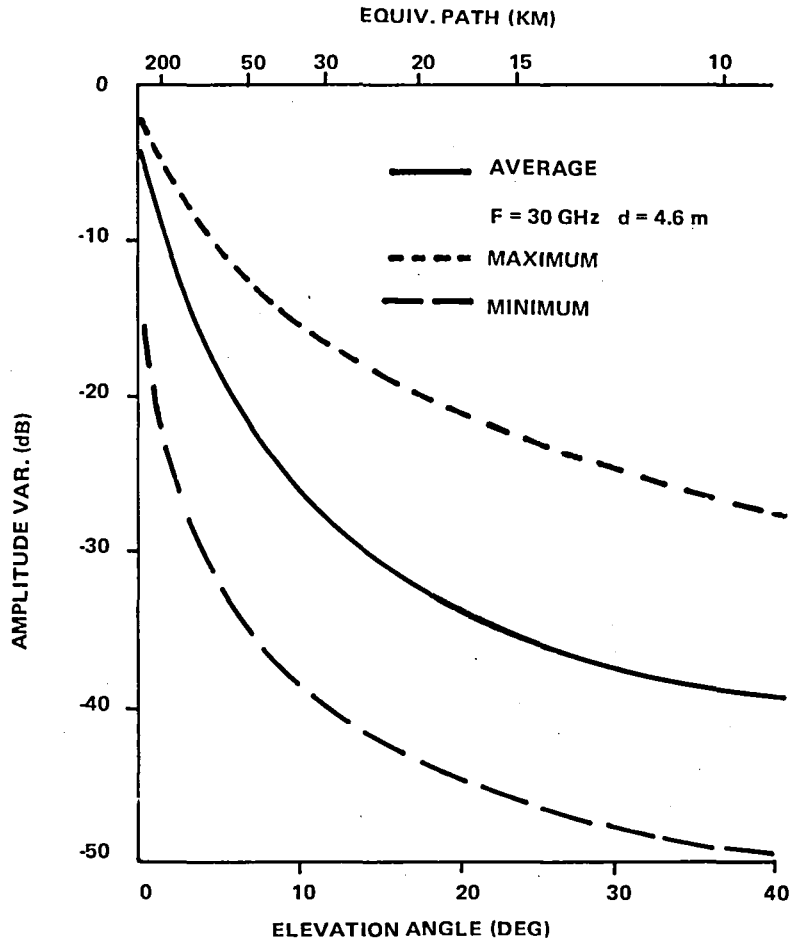

Figure 9-6. Effect of 20-dB Peak-to-Peak Variation on Amplitude Variance

Rain Effects

Attenuation of a signal passing through rain is the product of the fractional loss due to absorption and the fractional loss due to scattering of the microwave signal away from its direction of travel. The magnitude of these deviations is a function of temperature of the drops, the size and number within the elevated beam, the frequency of the transmitted signal, and the dielectric properties of the rain water. Since the absorption and scatter cross sections of the raindrops are functions of drop size and wavelength, the attenuation rate A (dB/km) can be written as (Reference 4):

$$A = \int_{\cdot}^{\cdot\cdot} N(D)\, Q_t(D, \lambda)\, dD \qquad (9\text{-}1)$$

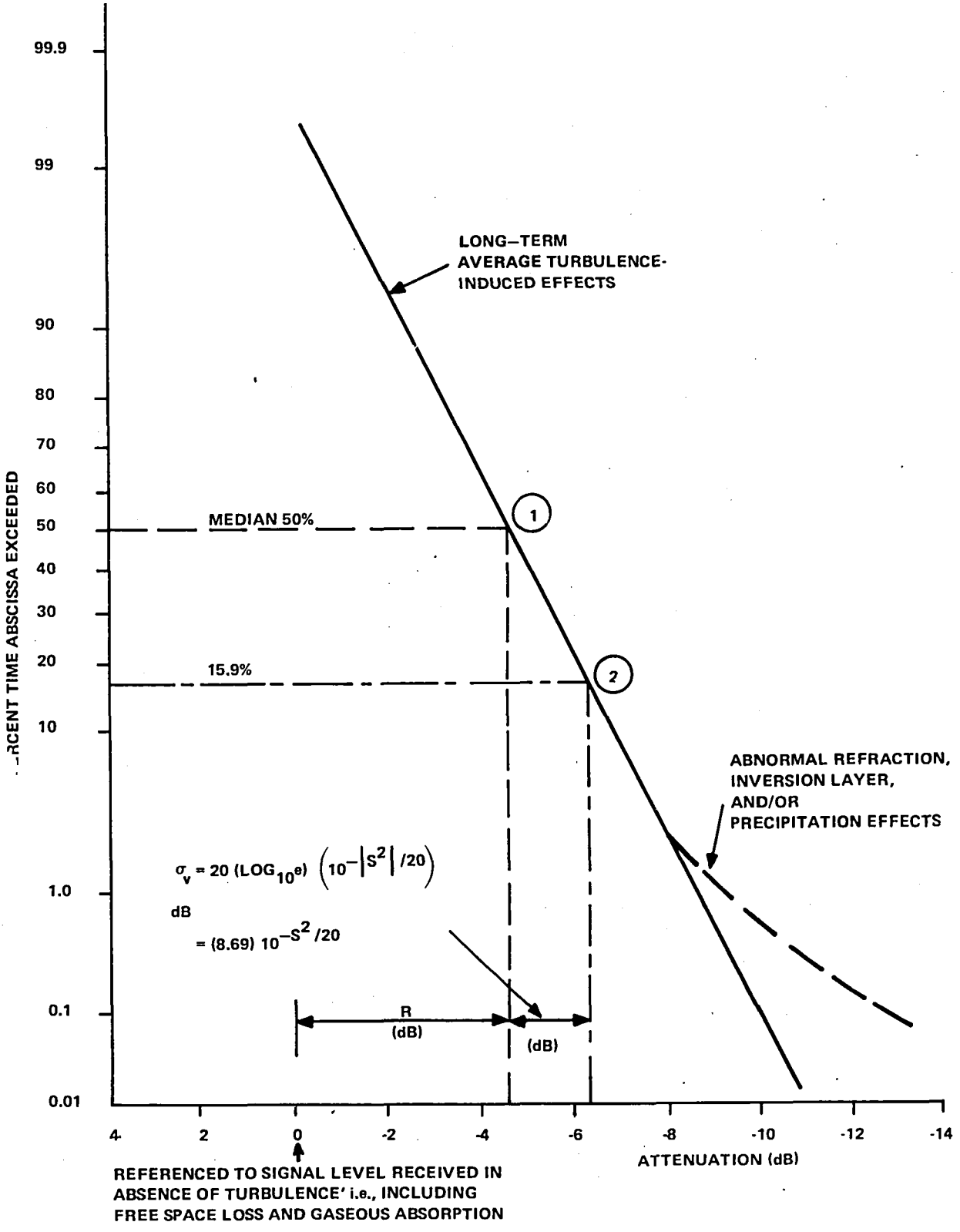

Figure 9-7. Hypothetical Fade Distribution Function

where Q_t is the sum of the absorption and scatter attenuation cross section of a rain drop of diameter, D, and N (D) is the number of drops of each diameter per unit of D.

From various measurements (Reference 3) of the rain-drop size distributions, it was determined that the size and number of drops are related to the rain-rate parameter (RR). The rain-drop sizes generally vary from about 0.5 mm to 6 mm with a median value of 1.5 mm. As RR increases, the number of drops in the size range of 3 mm to 6 mm also increases.

Since N (D) is a function of RR, the A factor can be computed as a function of RR from Equation 9-1. Results (Reference 4) of this computation shows that A is related to RR by the relation,

$$A\ (dB/km) = a\ (f)\ (RR)^{b\ (f)} \tag{9-2}$$

where the coefficients a and b are functions of frequency. For test frequencies of interest, 20 GHz and 30 GHz, the values of these factors for a rain temperature of 0°C are as follows:

20 GHz	30 GHz
$a = 7.134 \times 10^{-2}$	$a = 0.195$
$b = 1.053$	$b = 0.987$

Total attenuation along an Earth-space path can be computed by using Equation 9-2 and knowing the path average rain rate and the effective path length, L, for the elevated path.

Sky Temperature—It has been found that the sky temperature, T_s, is directly related to the total attenuation, A_t, along the space-Earth path. This is because T_s is determined by the magnitude of the signal energy absorption process for the conditions of both clear sky and precipitation. The attenuation mechanism due to scattering only becomes important at drop diameters in the 4- to 6-mm range. Since most of the raindrops are less than these values, absorption predominates and a close relationship between total attenuation and sky temperature exists. It can be shown from measurements that the finite predictable limit for total attenuation, A_{pt}, is about 10 dB.

Frequency Scaling—Frequency scaling is the technique of predicting the attenuation (A) at one frequency from the measured attenuation at another frequency. For this experiment, this would involve predicting the attenuation (A) at 30 GHz from the measured attenuation at 20 GHz or the opposite. Three different techniques have been developed for this scaling procedure. Because both 20- and 30-GHz signal measurements were obtained from the same antenna, the storm-path length for both frequencies will be spatially identical. The three technique descriptions follow:

- Empirical Scaling

  An empirical relationship has been developed through the use of concurrent radar data at 11 and 19 GHz. The relationship is as follows:

$$\frac{A(30)}{A(20)} = \frac{(30)^{1.72}}{(20)} = 2.10 \tag{9-3}$$

- Specific Attenuation Scaling

  With this technique, the use of the attenuation rate of the form a $(RR)^b$ can be employed to develop A ratio values, from the a and b values given from Equation (9-2). The A ratio for the frequencies of interest are as follows:

$$\frac{A\,(30)}{A\,(20)} = 2.66\,(RR)^{-0.066} \tag{9-4}$$

  For path average rain-rate values of 10, 25, and 50 mm/hr, the corresponding A ratio values are computed to be 2.285, 2.15, and 2.055. As the rain increases, the A ratio decreases and appears to be approaching a value of 2. This limit corresponds to the value obtained from the empirical approach.

- Gaussian Rain Distribution Scaling

  In this technique, it is assumed that each rain cell is spatially distributed along the Earth-space path according to the relation,

$$RR\,(s) = (RR)_o\, e^{-s^2/\ell_o^2} \tag{9-5}$$

  where s is along the path, ℓ_o is the characteristic rain cell dimension, and $(RR)_o$ is the peak rain rate in the cell.

  A (30) relates to A (20) for an ℓ_o of 4 km by the following expression:

$$\frac{A\,(30)}{A\,(20)} = 2.703\,A\,(20)^{0.063} \tag{9-6}$$

  For an A(20) of 3, 10, 20, and 30 dB, the corresponding A ratio values are 2.52, 2.34, 2.24, and 2.182. In this technique, the ratio limit also seems to be approaching a limit of 2.

Path Diversity—Rain attenuation often degrades space-Earth paths operating above 10 GHz so seriously that the requirements of economical design and reliable performance cannot be achieved simultaneously. To overcome this problem, Hogg (Reference 5) proposed the use of path diversity of space-Earth paths to achieve the desired level of system reliability at a reasonable cost compromise. This proposal was based on the hypothesis that rain cells and, in particular, the intense rain cells that cause the most severe fading are rather limited in spatial extent. Furthermore, these rain cells do not occur immediately adjacent to one another. Thus, the probability of simultaneous fading on two paths to spatially separated Earth terminals would be less than that associated with either individual path.

Placement of the diversity terminals with respect to the expected movement of the intense rain cells is shown in Figure 9-8.

The parameters used to specify the space diversity improvement are the diversity gain, E, and the diversity improvement, I. These factors are defined in Figure 9-9, which shows the distribution of rain attenuation exceeded on a single path A (t), for a given percentage of time, t, and the rain attenuation, A_{div} (t), exceeded jointly on two separated paths for the same percentage of time. E can be interpreted as the reduction in the required system margin at a particular percentage of time. I can be interpreted as the factor by which the fade time is improved at a particular attenuation level.

An empirical model was used to relate E to the site separation distance, d, and the attenuation level, A, obtained at a single site. For A less than 20 dB, the following empirical expressions were derived:

$$E = m\,(1\text{-}e^{-nd}) \tag{9-7}$$

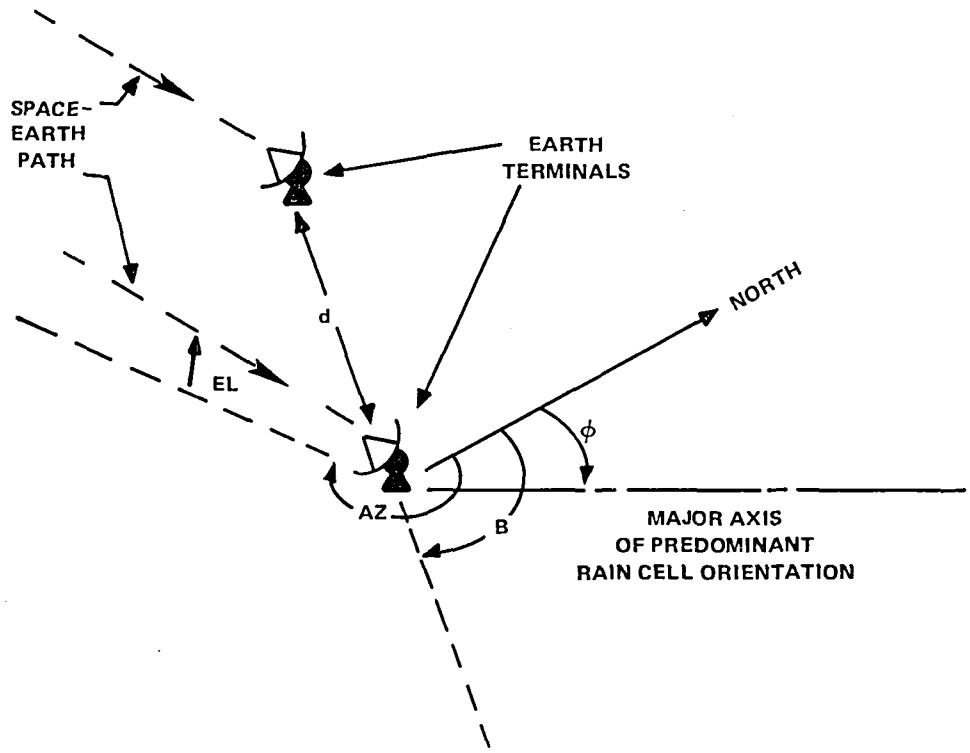

Figure 9-8. Path Diversity Configuration and Parameters

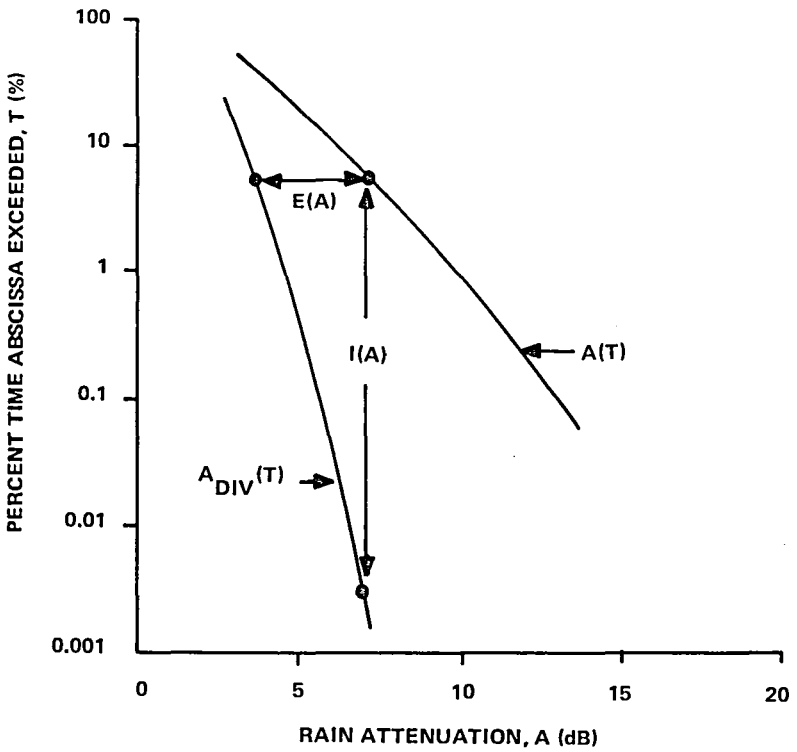

Figure 9-9. Hypothetical Rain Attenuation, A (dB)

where

$$m = A - 3.6\,(1 - e^{-0.24A})$$

$$n = 0.46\,(1 - e^{-0.26A})$$

E will increase as d increases up to a value of about 10 km. Past this distance, the E factor tends to approach its limit asymptotically. This upper limit on site separation corresponds to the distance at which uncorrelated fading at the individual Earth terminals occur. Possibly, negatively correlated rainfall along the separated paths could produce higher values of diversity gain.

To determine if higher diversity gains are possible, a long baseline diversity experiment was developed. Four stations that enclosed a large metropolitan area (Washington, D.C.) were involved in the experiment. The location and names of the participants are shown in Figure 9-10. As shown, the distances were large enough to obtain some measure of the ability to maintain a high service time for communication systems that must operate in an area that is being inundated by severe thunderstorms.

Meteorological Radar Considerations—A multifrequency meteorological radar operating at frequencies of 3 and 8.75 GHz, was developed to measure the meteorological conditions that exist in

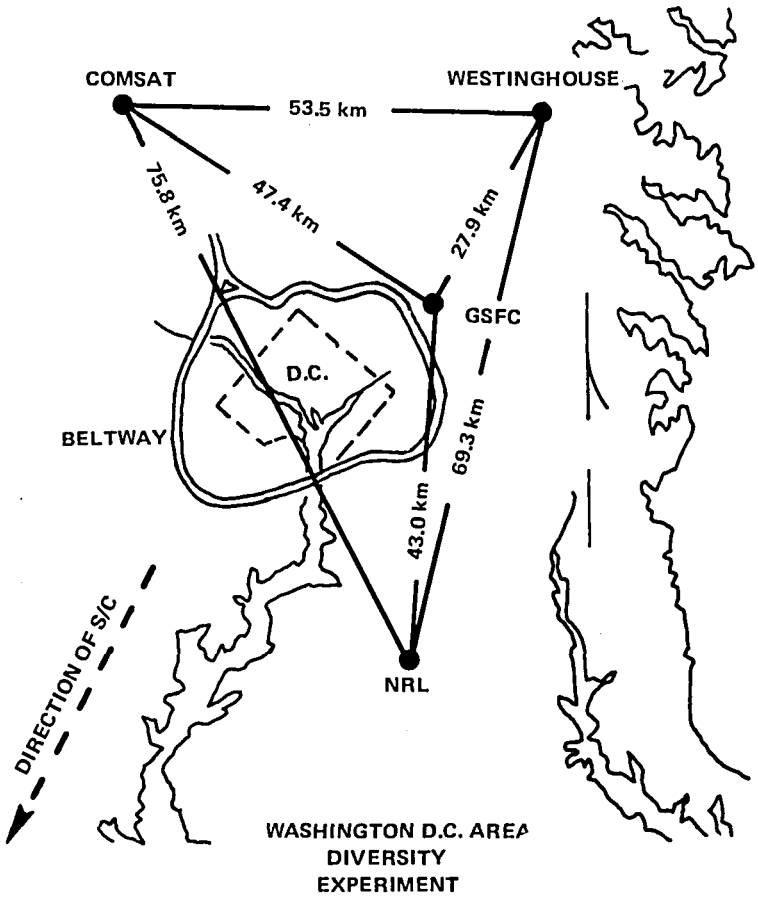

Figure 9-10. Washington, D.C. Area Diversity Experiment

an elevated path at the time rain attenuation measurements were being performed. The radar data, consisting of returns from 100-meter range increments, were used in three different investigations: (1) radar computed rain rate compared with ground measured rain rate, (2) radar reflectivity plots to show how rain rates are distributed both spatially and in time, and (3) use of the radar data to predict attenuation.

To use radar return to determine various meteorological and system parameters, it is necessary to relate the receive power to some parameter that is a function of the size and number of raindrops being illuminated by the radar. The factor employed is the reflectivity, η, that is defined as the sum of the raindrop radar cross sections per unit volume. Using the basic radar equation where the reflectivity factor, Z, is a function of the drop-size distribution, it has been found that Z is empirically related to the rain rate (RR) parameter according to the relation:

$$Z = W(RR)^{\alpha} \tag{9-8}$$

The constants W and α are related to the type of precipitation that is present during the test. For continuous rain, W = 200 and α = 1.6. By combining these equations, it is possible to derive the following experession that relates received radar power, P_r, to RR:

$$\bar{p}_r = \frac{(\text{Radar Constant})\,(RR)^{\alpha}}{r^2} \tag{9-9}$$

This equation forms the basis for measuring the rate of rainfall as a function of the radar return at a given range, r.

Rain attenuation at the 20-GHz and 30-GHz frequencies can be computed from the radar return by using Equation 9-8 and the derivation of an expression that relates A to Z. For the 255 one hundred-meter range bins, the total attenuation A_t can be computed after determining Z_i for the ith range bin as a function of the radar return P_{ri}. By summing all the radar returns from the respective range bins, the total attenuation can be obtained.

Communication Parameters

The ATS-6 communication experiment provided the first operational millimeter wavelength communication link from an orbiting satellite. A 40-MHz noise bandwidth channel, a 6-GHz uplink and 4-, 20-, and 30-GHz downlinks were employed for both analog and digital test transmissions.

For the digital test, a two-channel (four-phase) unbalanced direct mode with one channel at a rate of 10 megabits per second (Mbps) and a second channel at a 1 Mbps rate was tested. In addition, a 15-Mbps biphase (differentially encoded) and 20 Mbps/200 kbps two-channel, quadriphase S(t) signal transmission was also tested.

An optimum coherent detection scheme was employed in the system. This consisted of regenerating the coherent carrier reference by using a carrier extraction loop. After demodulation, an integrate and dump circuit was employed followed by a bit sampling circuit.

In a digital system, the measure of its operational efficiency is the magnitude of the resulting average bit error rate (BER). This factor is mainly a function of the energy per bit, E_b, divided by the noise spectral density N_o. The BER is always plotted as a function of E_b/N_o, which is actually the signal-to-noise ratio in a bandwidth equal to the bit rate.

Coherence Bandwidth

If the dispersive properties of the propagating medium is sufficiently high, the phase and/or amplitude of wide bandwidth transmissions may be selectively altered in frequency. It is therefore necessary to determine if the troposphere does have an upper limit to the bandwidth it can support. This bandwidth limitation is determined by noting if any frequency selective properties to the amplitude fading across the wide bandwidth exist and if any phase nonlinearities across the bandwidth of interest are present.

For rain, the frequency dependence of the attenuation rate $\partial A/\partial f$ can be computed. For example, at 20 GHz and an RR of 25 mm/hr, A = 2.18 dB/km so $\partial A/\partial f$ = 0.23 dB/km-GHz. For an effective storm path length of 5 km $\partial A/\partial f$ = 1.5 dB/GHz; therefore, for a bandwidth of 1 GHz, the amplitude variation due to rain is estimated at 1.15 dB. For the test band of 1.44 GHz, the expected amplitude variations would be 1.7 dB for a path length of 5 km.

The relative differential phase output, V_ϕ, is proportional to ϕ_u, ϕ_L, and ϕ_c which are the phases of the upper tone, lower tone, and carrier with respect to an arbitrary reference. This function provides a measure of the linearity of the channel frequency-phase characteristics. In an ideal system, V_ϕ would be zero; however, system noise and bandwidth limitations in a practical system cause a residual value of V_ϕ.

Another approach in determining the coherence bandwidth limitation due to propagation was to record the analog data directly on an analog tape and analyze it on a special purpose multichannel spectrum analysis-correlation processor called the ubiquitous spectrum analyzer. The objective was to determine the short-term channel characteristics by using multitone correlation functions derived from the multitone data. This overall function involved the autocorrelation function of the carrier and the crosscorrelation function of the sideband pairs. From this overall function, such important channel parameters as coherence bandwidth, time spread, and fading bandwidth could be determined. However, time spread and fading bandwidth parameters were not applicable to line-of-sight satellite-Earth links at 20 and 30 GHz.

Signal Depolarization

Depolarization or changes in the polarization sense of a transmitted signal will result from the nonspherical shape of raindrops, snowflakes, and ice crystals that are present in the propagation path. Also multipaths and adverse refractive effects produce the phenomena. Depolarization is described quantitatively by two related variables; these are illustrated in Figure 9-11. The cross polarization ratio (CPR) is the decibel ratio of the cross-polarized component of the received electric field to the copolarized component.

Because it is directly related to the electric field, the CPR is more frequently used by investigators studying the scattering process itself. Communicators are more concerned with cross talk, and the relevant parameter here is the cross-polarization isolation (CPI). In a two-channel communication system, the CPI is the decibel ratio of the power received from the copolarized transmitter to the power received from the cross-polarized transmitter. In practice, the CPI value is essentially the negative of the CPR value, and the terms and numerical magnitudes are often interchanged.

The mechanism by which a raindrop causes the depolarization process of the transmitted signal is directly related to its elliptical shape as an oblate spheroid. The oblate particle through its different phase and differential attenuation properties provides the key mechanism in the depolarization process. This process occurs because the incident electric field component along the major axis experiences more attenuation and phase shift than the component along the minor axis. This effect causes the depolarization of incident fields that are not linearly polarized along one of the *principal*

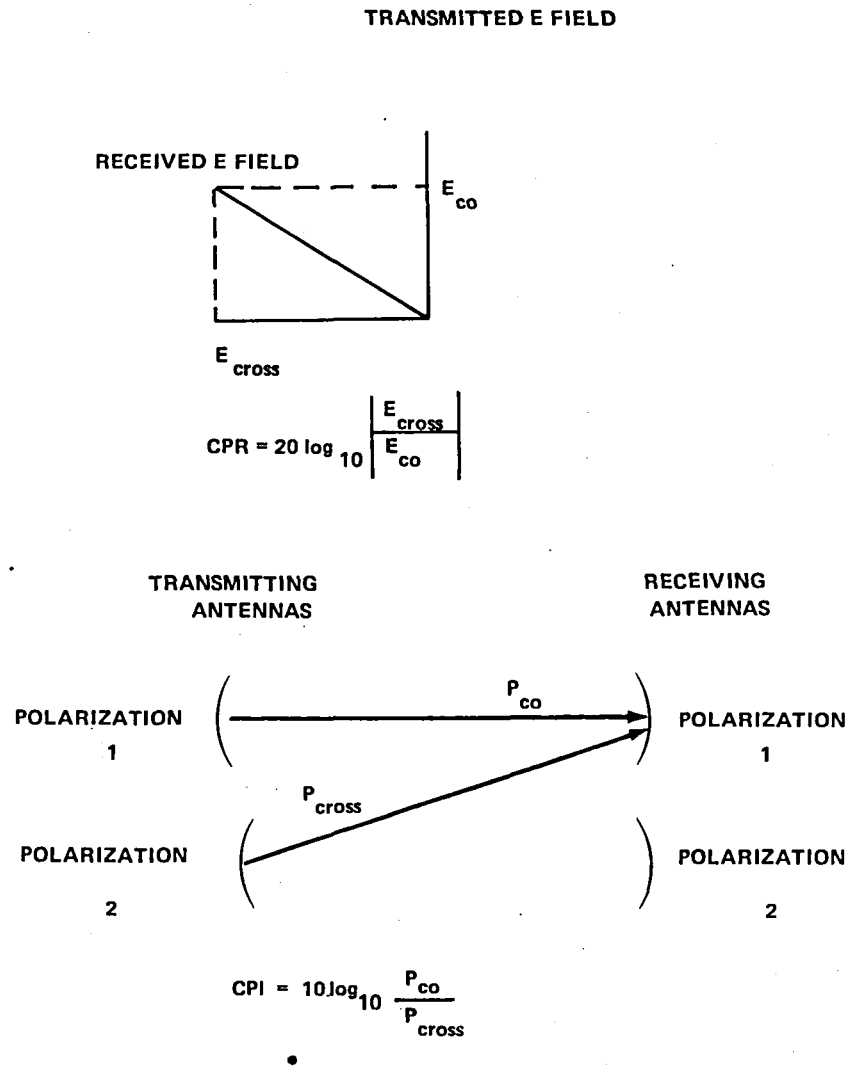

Figure 9-11. Definition of Depolarization Parameters

axes. The extent of the depolarization depends on the angular orientation of the plane or polarization relative to the axes of the oblate spheroid. Circular polarization suffers the greatest amount of depolarization, because on the average its polarization angle is oriented about 45 degrees from the major and minor axes of the oblate spheriod.

Depolarization on a ground-to-satellite path may be different from depolarization along a ground path for three reasons: (1) differences in size and shape distributions of the raindrops; (2) presence of snow and ice in the freezing layer of the troposhere; and (3) influence of cirrus cloud ice crystals. Correlation of the CPI factor with rain rate has not been possible because of the difficulty in obtaining a representative value of rain rate for an elevated path. However, depolarization can be related to the total attenuation level, A_T, measured along an elevated path. The relationship is,

$$CPI = f - g \log^{10} A_T \qquad (9\text{-}10)$$

where CPI and A_T are expressed in dB. Approximate values of the f and g factors are 40 and 20, respectively.

The International Radio Consultative Committee (CCIR) has proposed a relationship of the "f" factor as a function of frequency, f, elevation angle, θ, and the polarization tilt, τ, with respect to the horizontal. The "f" factor is minimized for a τ of 45 degrees, which corresponds to circular polarization. The depolarization effect varies inversely with the magnitude of the "f" factor.

REFERENCES

1. McEwan, N. J., et al., "A Self Calibrating 9.4 GHz Meteorological Radar" Bradford University Electrical Engineering Technical Report 231, December 1976.

2. Theobold, D. M., et al., "Gain Degradation and Amplitude Scintillation Due to Tropospheric Turbulence," The Ohio State University Electro-Science Lab., Tech Report 784229-6, Revision A.

3. Laws, J. O., et al., "The Relation of Raindrops Size to Intensity," Trans. AM Geophys. Union, Vol. 24, October/November 1943, pp. 452-460.

4. Olsen, R. L., et al., "The aR^b Relation in the Calculation of Rain Attenuation," IEEE Trans. Ant. and Prop., Vol. AP-26, March 1978, pp. 318-329.

5. Hogg, D. C., (1968) "Millimeter Wave Communications Through the Atmosphere," Science Vol. 159, p. 39.

CHAPTER 10

EXPERIMENTAL DATA–MILLIMETER WAVE PROPAGATION AT 20 AND 30 GHz

INTRODUCTION

Signal degradation on a space-Earth link due to meteorological conditions, can be defined by four different effects: (1) signal scintillation; (2) rain effects; (3) coherent bandwidth restrictions; and (4) depolarization effects. Cogent examples of these four propagation effects will be presented in the following paragraphs. The data were obtained from the active participants in the experiment. Common examples will not be presented from all the participants, because all stations did not measure the same parameters (Tables 9-1 and 9-2, Chapter 9) and, it would be redundant.

Signal Scintillation

Signal scintillations are caused by the variation of the amplitude, phase and angle-of-arrival of the signal as it propagates through the troposphere. This is because of the variations in the refractive index of the propagating medium. The strength of this scintillation varies directly with frequency and the magnitude of the path length through the troposphere; therefore, it varies inversely with the magnitude of the elevation angle. Scintillation effects are minimized for theta (θ) greater than 10 degrees and clear weather conditions where no abnormal refractive index conditions exist.

During the normal experimental test period, the operational elevation angle for the majority of active U.S. participants was 40 degrees or greater. Thus, it would be expected that the scintillation effects would be minimal during this period. Some scintillations were noted when various types of clouds intercepted the elevated beam. An example of this phenomenon is shown in Figure 10-1 as recorded at the Goddard Space Flight Center (GSFC) station. These scintillations were 2 decibels (dB) peak-to-peak and lasted for approximately 3 minutes. The elevation angle at the time of the recording was 41 degrees.

After the onset of the drift of ATS-6 toward India on May 10, 1975, the elevation angle decreased steadily until the horizon was reached on June 14, 1975. During this period, signal fluctuations increased both in magnitude and in frequency of occurrence because of the increasing path length through the troposphere.

During this period, scintillation activity increased significantly during periods when water-laden clouds and rain intercepted the elevated beam. Figure 10-2 shows the extreme contrast in the nature of the scintillation recorded during rain and during early morning clear skies at the Comsat station in Clarksburg, Maryland.

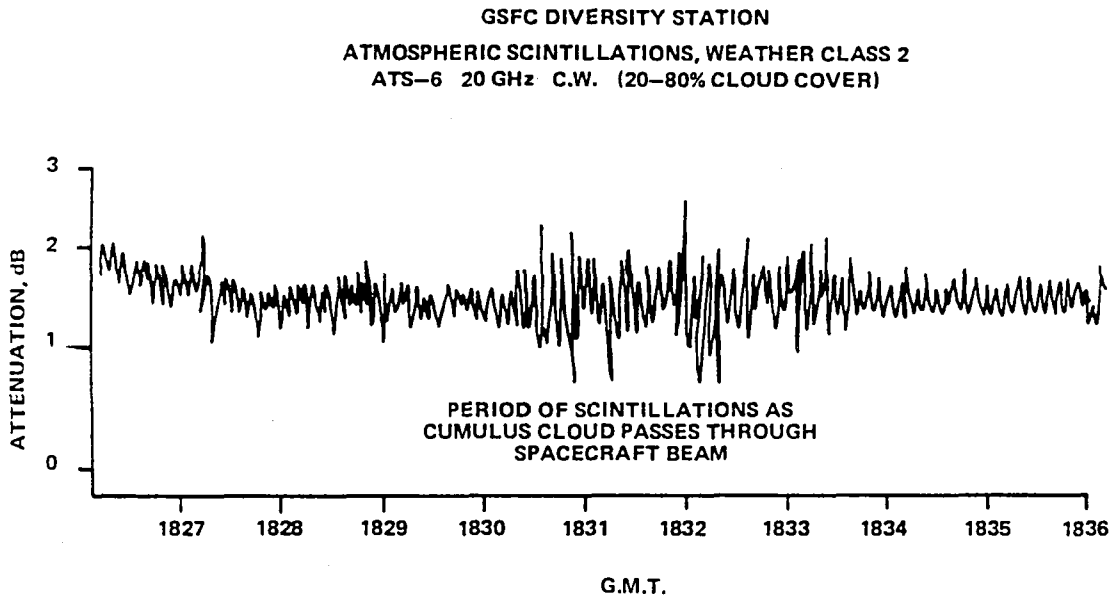

Figure 10-1. Amplitude Scintillations During Cloud Movement, GSFC

Scintillation activity at 30 gigahertz (GHz) was always higher than that measured at 20 GHz. Also, the signal perturbations tended to track each other thus showing a strong correlation. The main factors in determining the magnitude of the scintillation were the extent and amount of moisture within the elevated beam and the magnitude of the path length of the volume of moisture.

Ohio State University also observed the descent of ATS-6 from 42 to 2 degrees elevation angle. The variances of the signal scintillation for 20- and 30-GHz test frequencies are shown in Figure 10-3. The trend of the variance values can be compared to the theoretical trends as shown in this figure. Variance values were computed at each elevation angle by using the data from discrete time intervals. The dispersion of the variance values tended to be higher at higher elevation angles. The curves were computed for a minimum mean square fit of the data.

It has been stated that the magnitude of signal scintillation increases with increasing frequency. A quantitative measure of this trend can be obtained from the ratio value of the 30-GHz variance to the 20-GHz variance. The value for this ratio variance was 4.4 dB with a tendency for it to decrease as the elevation angle increased.

European experimenters also recorded the signal scintillation phenomenon at lower elevation angles. At the University of Birmingham station, it was found that clear weather scintillation at 30 GHz rarely exceeded 0.5 dB peak-to-peak. With heavy clouds passing through the antenna beam, the fluctuation increased to about 2 or 3 dB peak-to-peak. Scintillation during rain was generally less than that caused by clouds alone. Spectral measurements of the scintillation indicated that the majority were confined below a frequency of 2 hertz (Hz). Examples of the measured scintillation at 30 GHz for rain and clouds are shown in Figure 10-4.

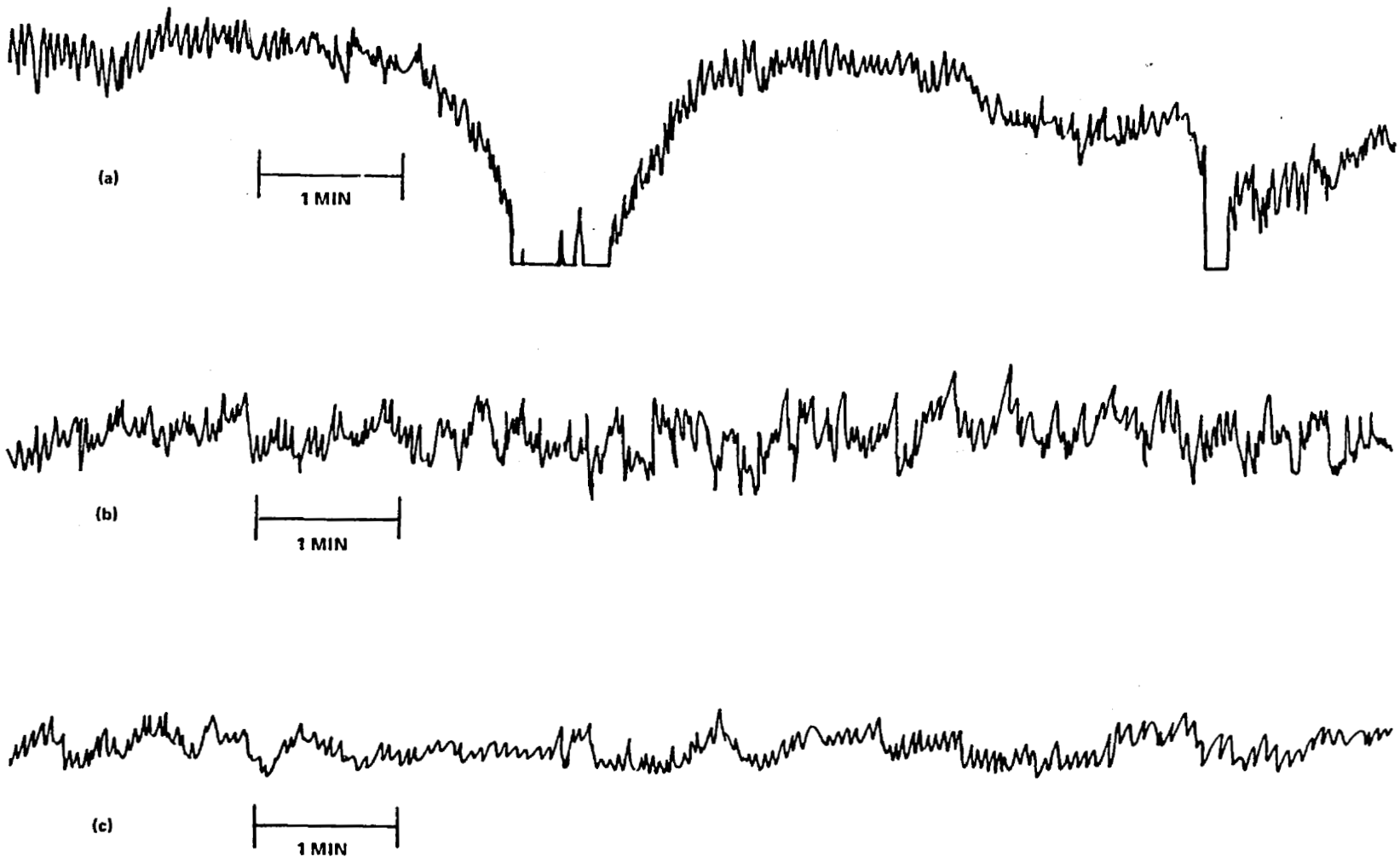

(a) RAPID SCINTILLATIONS DURING MODERATE RAINFALL AT ~6° ELEVATION ANGLE.
(b) STRONG SCINTILLATIONS DURING HEAVY LOCAL CLOUD COVER AT ~6° ELEVATION ANGLE.
(c) SLOW SCINTILLATIONS DURING OVERCAST SKIES AT ~3.5° ELEVATION ANGLE.

Figure 10-2. Scintillation Activity for Various Conditions

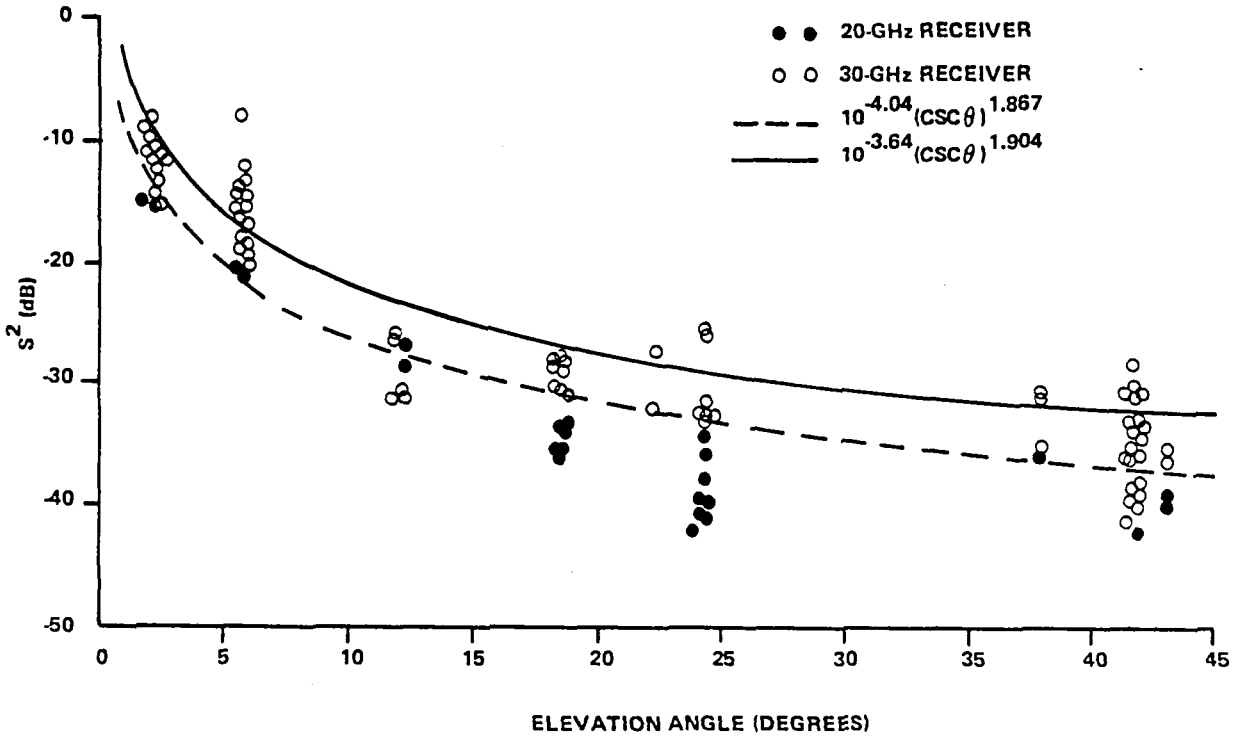

Figure 10-3. Measured Amplitude Variance vs. Elevation Angle (Columbus, Ohio)

During a drift phase of ATS-6 in 1976, the University of Birmingham ground station tracked the satellite down to elevation angles on the order of 0.5 degree. During clear weather conditions, the main signal level remained reasonably constant and exhibited typical scintillation behavior for elevation angles above 3 degrees. However, the excess signal attenuation relative to the reference attenuation at 21 degrees elevation, and the excess scintillation amplitude increased with decreasing elevation angle. The excess attenuation above 3 degrees followed the cosecant law according to theory. Below 3 degrees, the excess attenuation was greater than that predicted by theory and there was evidence of Rayleigh fading where fades in excess of 20 dB occurred.

Rain Effects

Introduction

The presence of rain in an elevated beam of an Earth-space link perturbs the signal through the processes of absorption and scattering. Absorption predominates for low and intermediate rain rates where sky temperature closely track the resultant rain attenuation. At high rain rates (RR), the scattering process tends to increase, relative to the absorption process, so that the radar return, which depends on the scattering process, tends to increase.

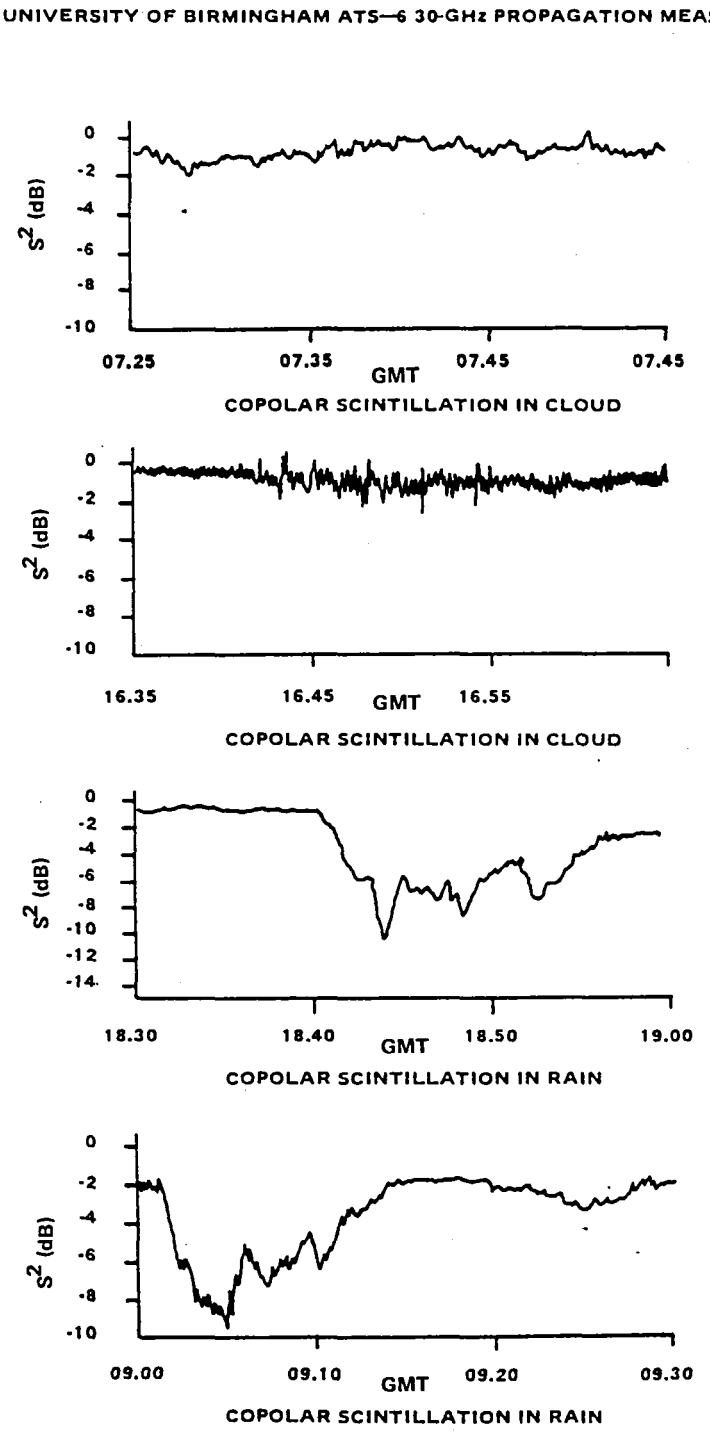

Figure 10-4. Examples of Various Scintillation Activity in Europe

Signal attenuation is mainly a function of the amount of water in the elevated beam (and the distribution of drop sizes), rather than the rate at which rain passes through the beam volume. However, since RR is easily measured, this parameter is used for predicting the resultant signal attenuation as shown in Equation 9-2 (Chapter 9) along with the effective path length, L, through the storm. Experimental results of the rain effects on the propagation signal and the other factors that are closely related to the signal attenuation such as sky temperature, frequency scaling, radar return, diversity considerations, and RR measurements will be presented.

Signal Attenuation and Sky Temperature

Measured signal attenuation (A_t) due to rain is usually presented in the form of real-time plots for an individual rain event. A_t data accumulated over a given time period is usually presented in the form of a cumulative probability distribution. Examples of the time plots are shown in Figures 10-5, 10-6, and 10-7. The 30-GHz data for the first figure was obtained from the University of Texas station. The latter two figures were obtained from the NASA Rosman Ground Station in North Carolina. These figures show computer plots of the minutely mean value versus time of the 20- and 30-GHz attenuation.

The figures show the characteristics of a rain fade. High A_t values are characterized by a limited time period, which shows that these fades were due to intense rain cells of limited extent that traversed the elevated beam. Because of this limited extent of intense rain cells, the storm path length, L, varied inversely with the RR for an elevated path.

Examples of cumulative distributions for the above stations over the same time period are given in Figure 10-8 and 10-9. Figure 10-10 shows the cumulative distributions obtained from NASA's Greenbelt stations for concurrent 20-GHz and 30-GHz total attenuation (A_t) values for 11 hours of rain data. For the Rosman Ground Station, the highest measurable values of A_t for 20- and 30-GHz were 16 and 33 dB, respectively. The highest fade depth measured at the University of Texas station was 35 dB for the 30-GHz test frequency. Higher A_t values were not measured, because the data from some rain events were not recorded because of time scheduling problems.

To supplement direct A_t measurements, sky temperature measurements, (T_s), were also made. Since this is a passive measurement, it could be made even if the time schedule did not permit direct A_t measurements. A good example of the excellent correlation obtained between T_s and A_t is shown in Figure 10-5. This correlation permitted a prediction of A_t by computation. It has been shown that excellent prediction accuracy results up to a total attenuation A_t value of about 10 dB. At this point the prediction accuracy for A_t is very poor. Therefore, it is generally accepted that a maximum prediction limit of only about 10 dB is possible. Using the T_s measurements over the overall test period, and an attenuation ratio value of 2.5 for the 30-GHz attenuation over the 20-GHz attenuation, a corrected cumulative distribution was determined as shown in Figure 10-8.

Measured values for the Greenbelt GSFC station exceeded 14 dB for 20 GHz and 38 dB for 30 GHz. For 0.9 percent of the measurement period, the attenuation value exceeded 14 dB for 20 GHz. For only 0.08 percent of the measurement period, the attenuation value exceeded 38 dB for 30 GHz. Therefore, these high attenuation values due to rain attenuation can be classified as rare.

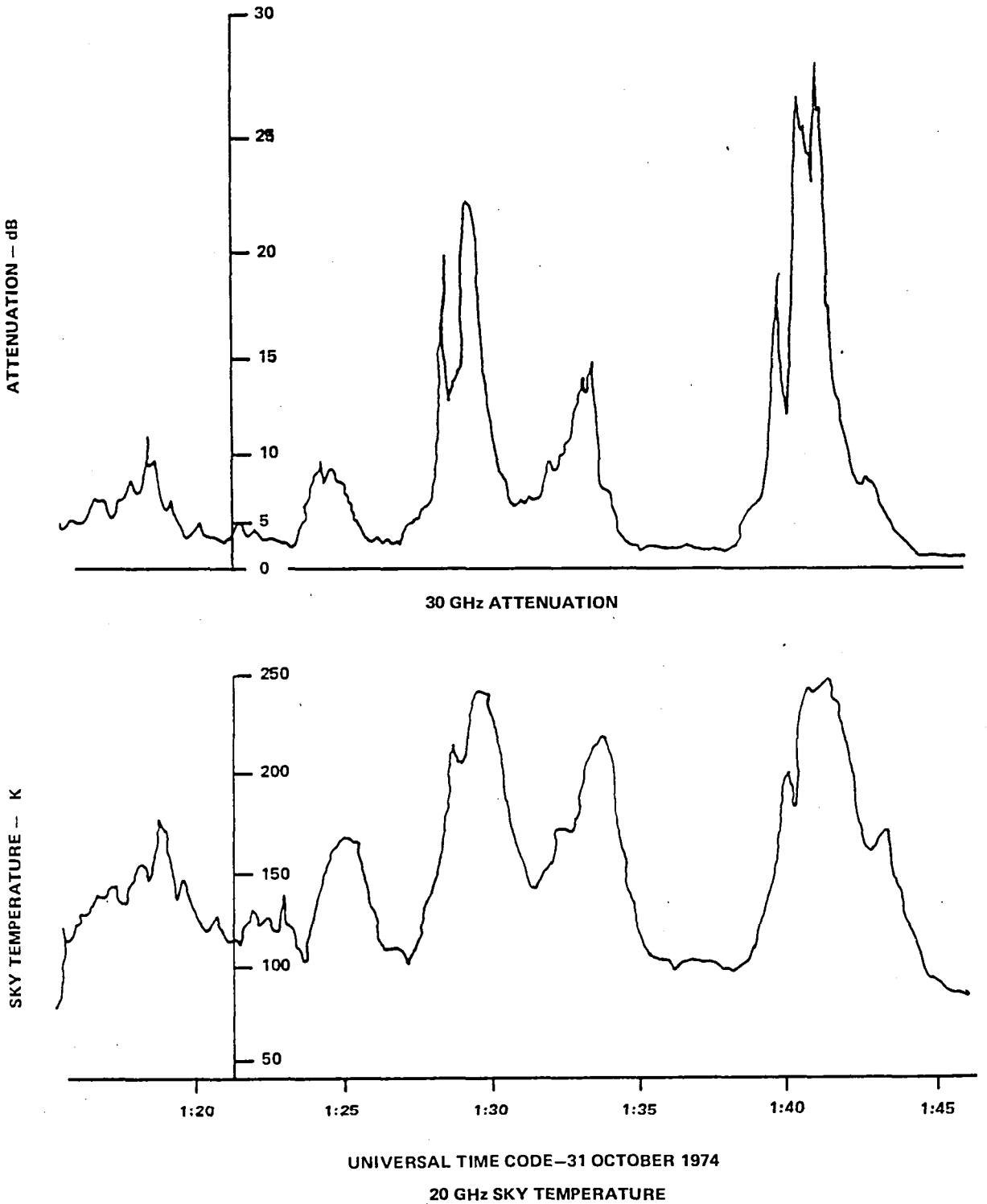

Figure 10-5. Attenuation at 30-GHz and Sky Temperature at 20-GHz

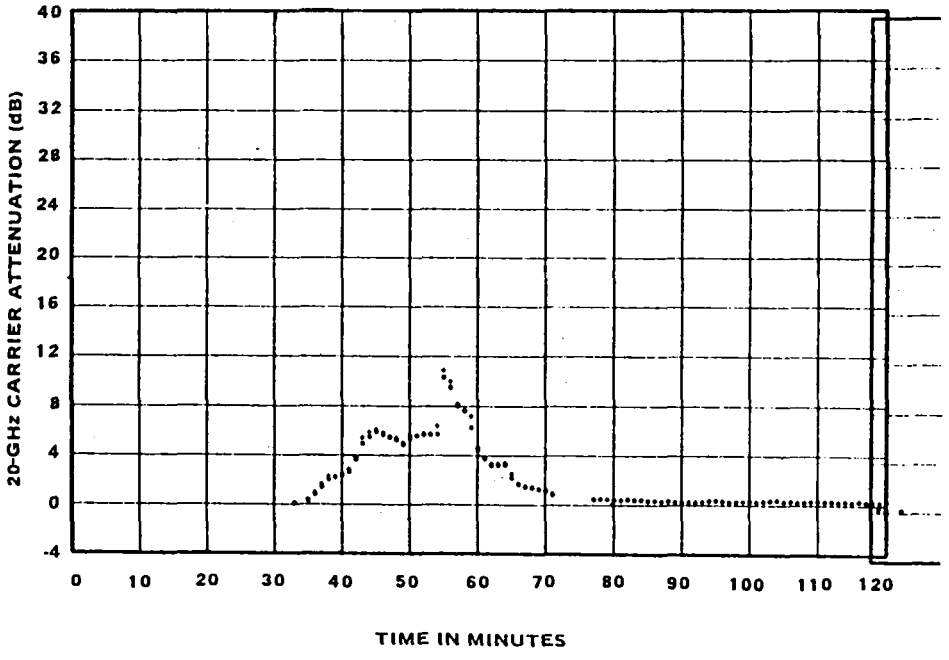

START TIME			STOP TIME		
YEAR	=	1974	YEAR	=	1974
DAY	=	185	DAY	=	185
GMT	=	2100	GMT	=	2350

	20-GHz	30-GHz
TEST MODE	CM	CM
PARAMP	OFF	OFF
S/C ANT. GAIN	HI	LO
MULT. CHAIN	A	A

Figure 10-6. Minutely Mean 20-GHz Attenuation Values vs. Time

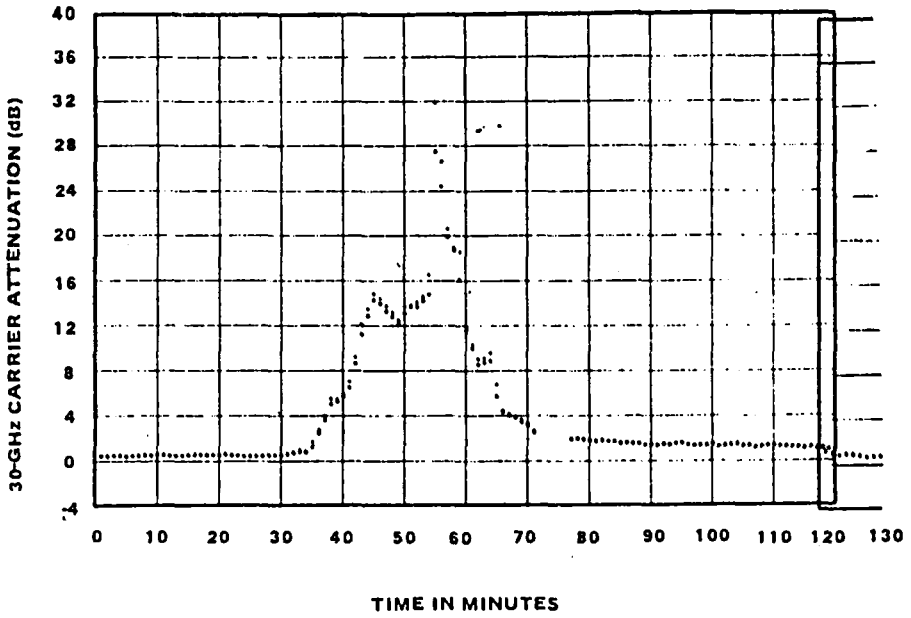

START TIME		STOP TIME	
YEAR = 1974		YEAR = 1974	
DAY = 185		DAY = 185	
GMT = 2100		GMT = 2350	
	20-GHz		30-GHz
TEST MODE	CM		CM
PARAMP	OFF		OFF
S/C ANT. GAIN	HI		LO
MULT. CHAIN	A		A

Figure 10-7. Minutely Mean 30-GHz Attenuation Values vs. Time

An example of the measured functional relationship between point rain rate and the 20-GHz attenuation value is shown by the four second mean computer plot of the values in Figure 10-11. The rain-rate values were obtained from a tipping bucket placed near the main receiving antenna. As shown, on the basis of one storm, it appears that no functional relationship existed between the two parameters. However, over a long-term basis (e.g., all precipitation within a year), a functional relationship could exist.

Representative attenuation rain rate pair values could be obtained from long-term cumulative distributions of attenuation and rain rate normalized over a common time period. The values were chosen for constant values of the probability of occurrence of rain rate and attenuation. Performing a least mean square fit of the pair values to the function $c(RR)^d$, it was possible to obtain a functional relationship between path length, L, and rain rate, RR. An example of the results of this computation is shown in Figure 10-12. Also shown are plots of A_t versus rain rate for a constant path length

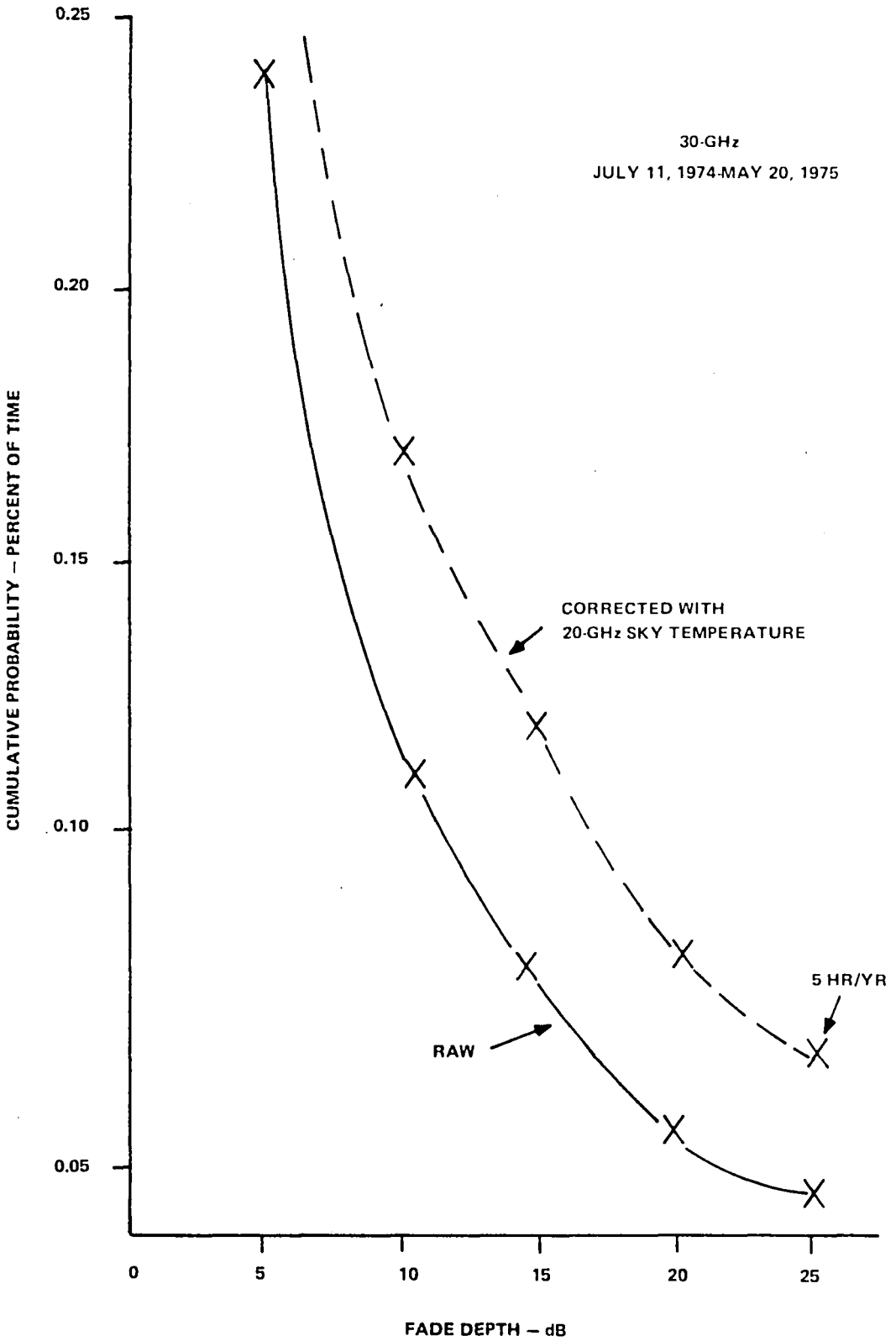

Figure 10-8. Cumulative Fade Probabilities at 30 GHz

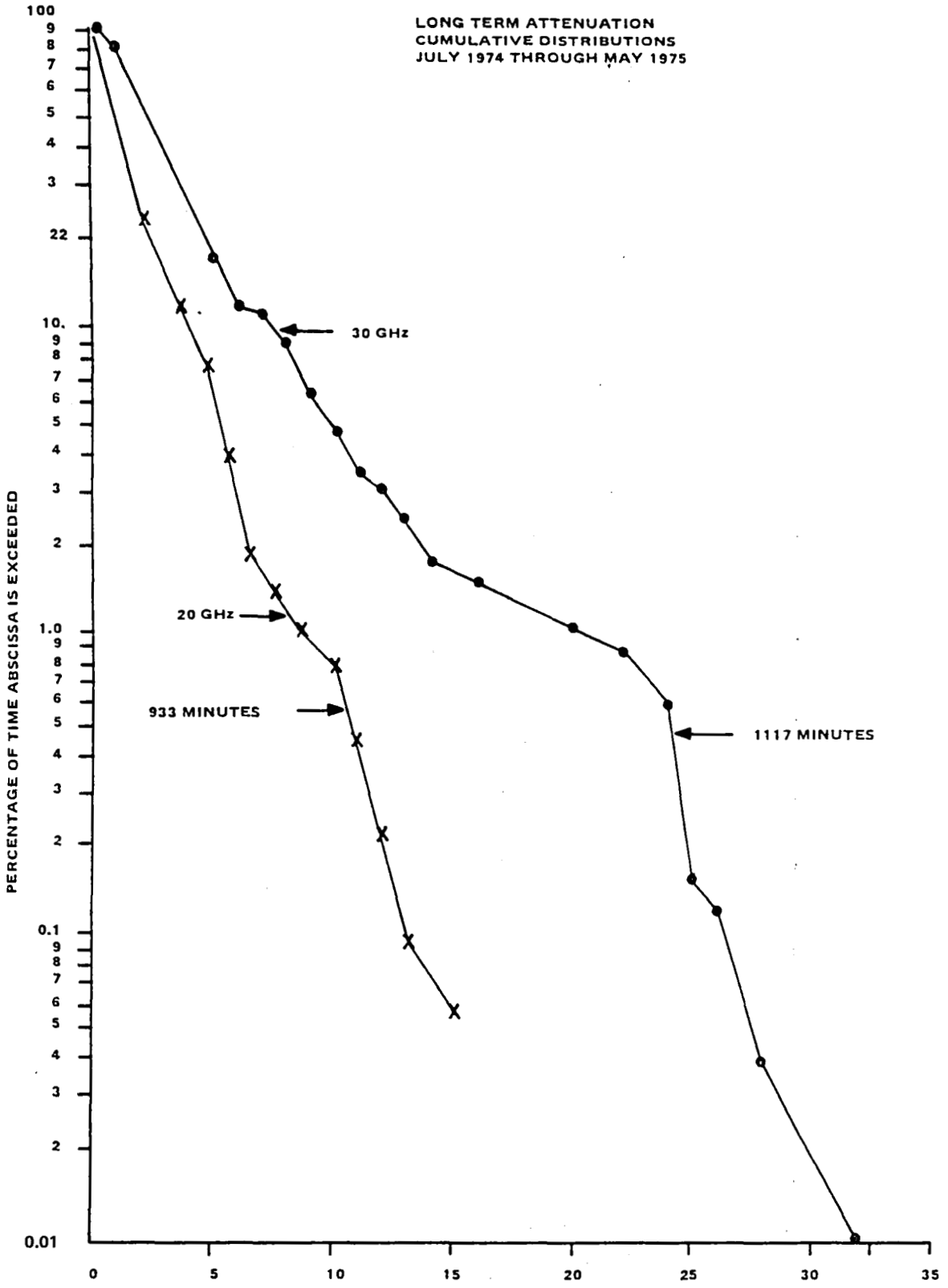

Figure 10-9. Long-Term Attenuation Cumulative Distributions

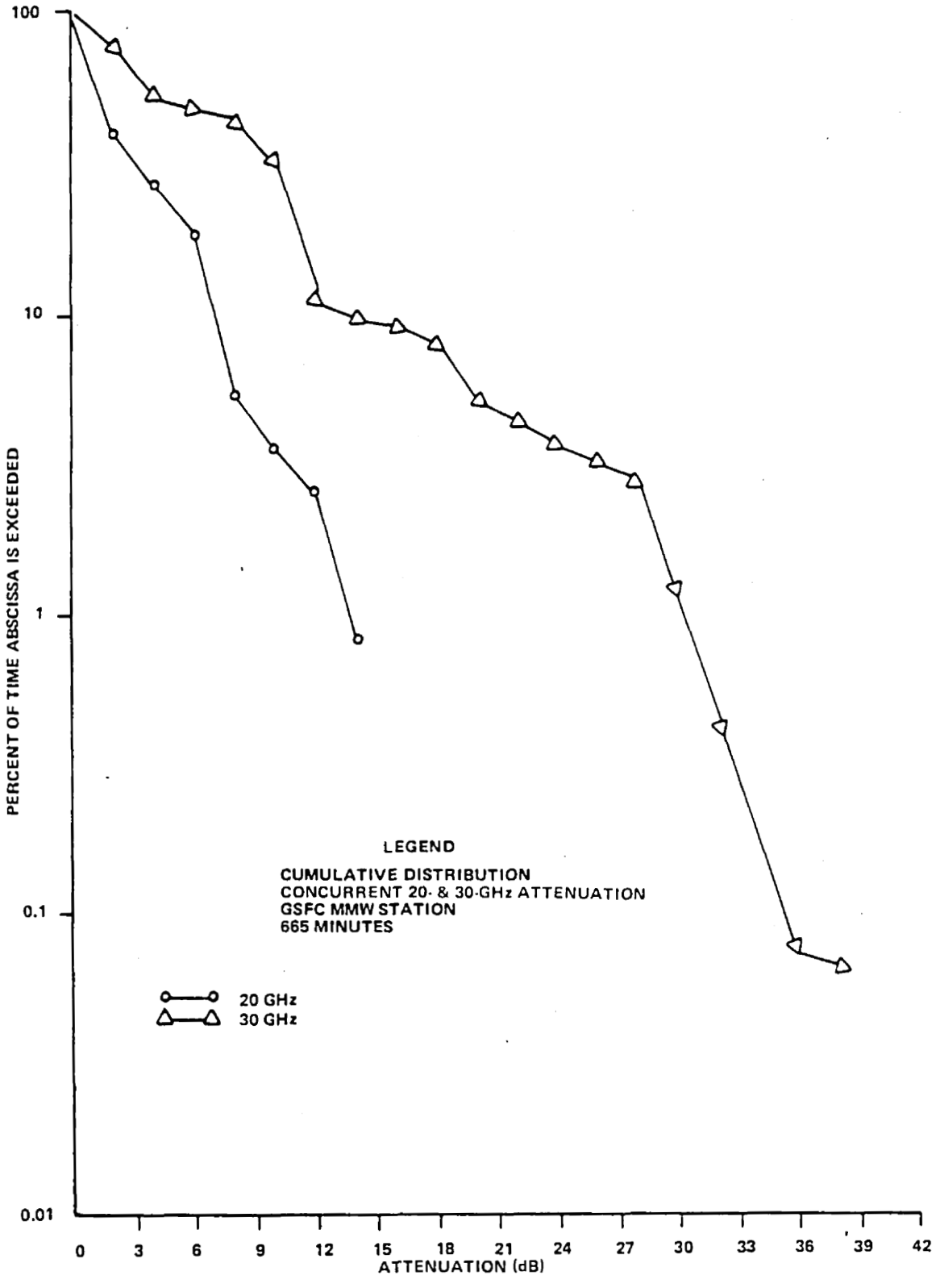

Figure 10-10. Concurrent 20- and 30-GHz Attenuation Cumulative Distributions

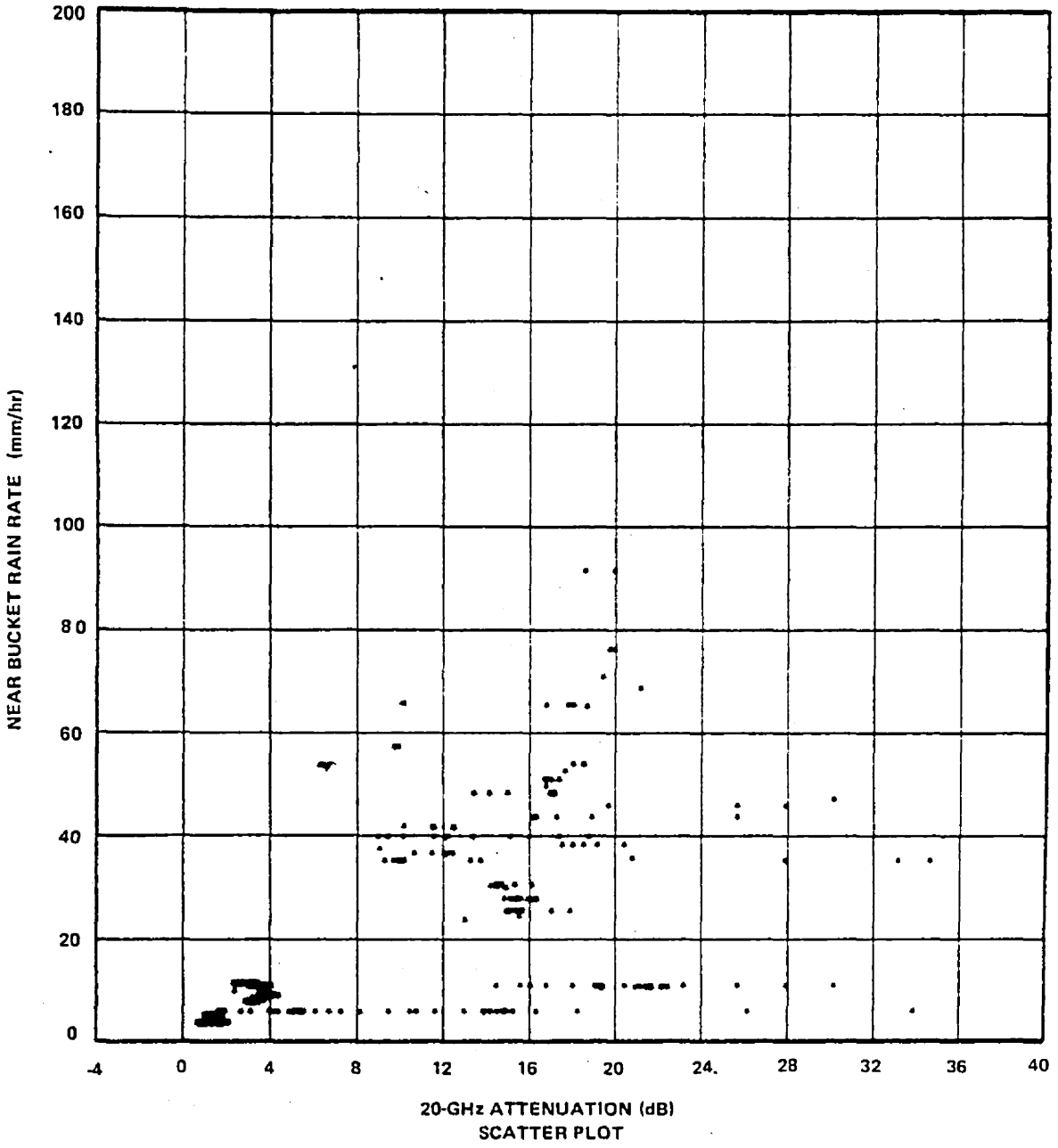

START TIME			STOP TIME		
OUTER INTERVAL					
YEAR	=	1975	YEAR	=	1975
DAY	=	09	DAY	=	09
GMT	=	113	GMT	=	300
INNER INTERVAL					
DAY	=	09	DAY	=	09
GMT	=	220	GMT	=	249

	20-GHz	30-GHz
TEST MODE	CM	CM
PARAMP	OFF	OFF
S/C ANT. GAIN	HI	NA
MULT. CHAIN	A	A

Figure 10-11. Near Bucket Rain Rate vs. 20-GHz Attenuation

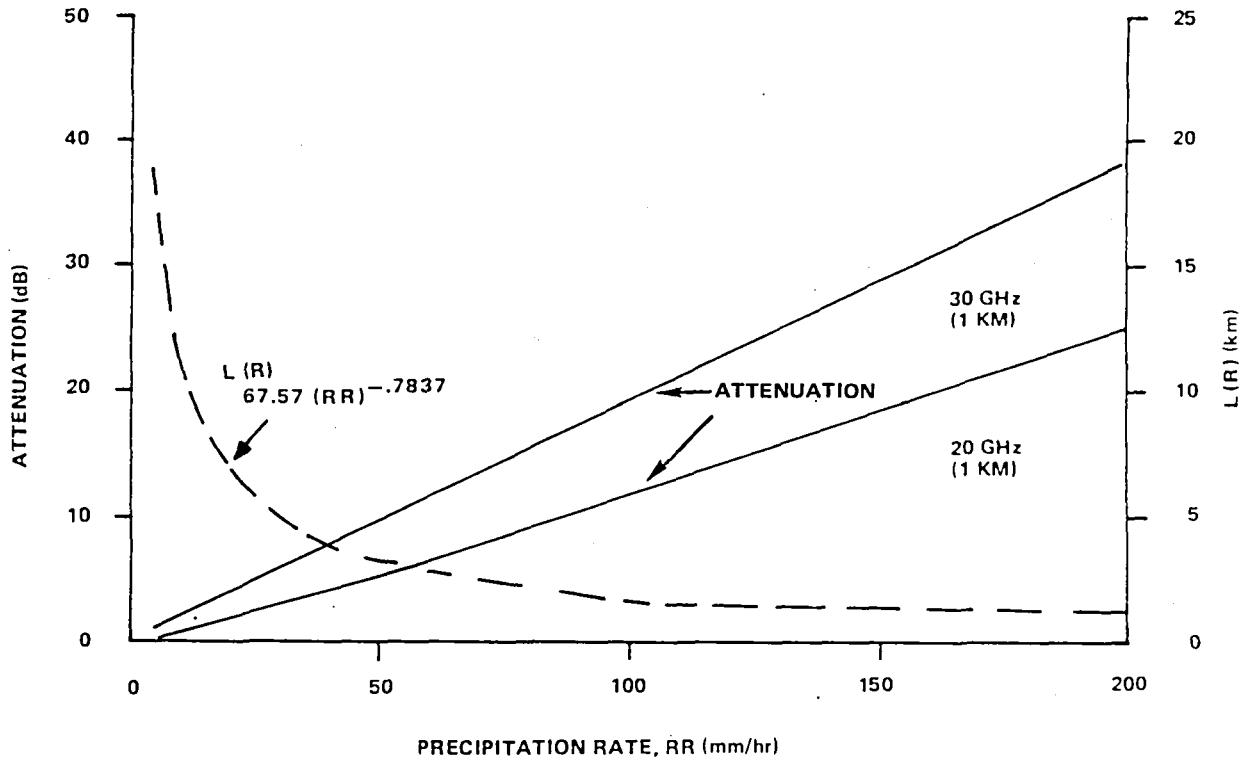

Figure 10-12. Predicted Path Attenuation and Measured Effective Path Length for Rosman Ground Station

of 1 km at 30- and 20-GHz frequencies. Data for the L(R) values were obtained from the ATS-5 Propagation Experiment conducted at a frequency of 15.3 GHz (Reference 1). The functional trend of the L(R) value shows that the attenuation at low values of rain rate is a critical function of path length. As the rain rate and attenuation increases, the path length factor tends to approach a limiting value and A_t becomes a critical function of rain rate.

European experimenters also developed 20- and 30-GHz attenuation statistics. Results for the University of Bradford in England are shown in Figure 10-13 and in Figure 10-14 for the British Post Office located in Ipswich, England. The elevation angle for the European ground stations was about one-half of what it was for the U.S. stations; therefore, the path length through the rain environment should have been doubled. This would have implied higher attenuation values for the same type of precipitation; however, as shown in Figure 10-13, lower values of attenuation were measured over a yearly period at Bradford University. As shown in the monthly histogram, there was only one fade of 9 dB that lasted for 5 minutes in May 1976. All other fades are of the order of 5 dB or less. One explanation offered for these low attenuation values was that the path length through the rain environment was reduced because of the height of the site. This height was 450 meters above sea level.

The cumulative 20- and 30-GHz attenuation distributions and the distribution for concurrent rain-rate measurements for the Ipswich station are shown in Figure 10-14. Peak measured attenuation

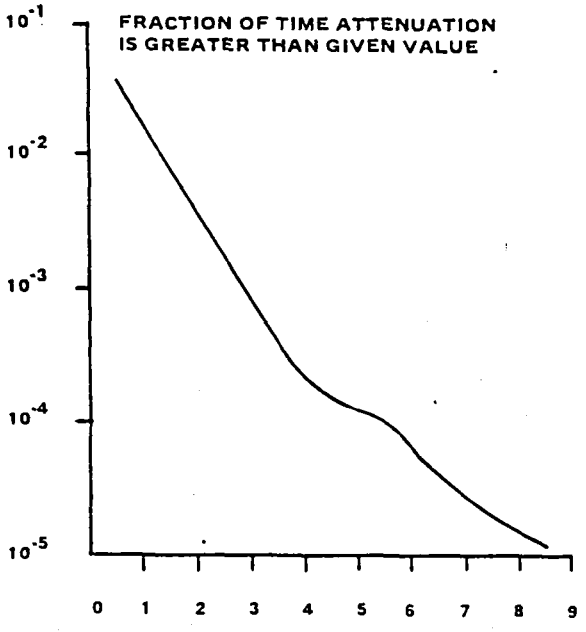

Cumulative statistics of 20-GHz attenuation
Bradford University ATS-6 observations,
September 1975 — July 1976. Total hours 926.

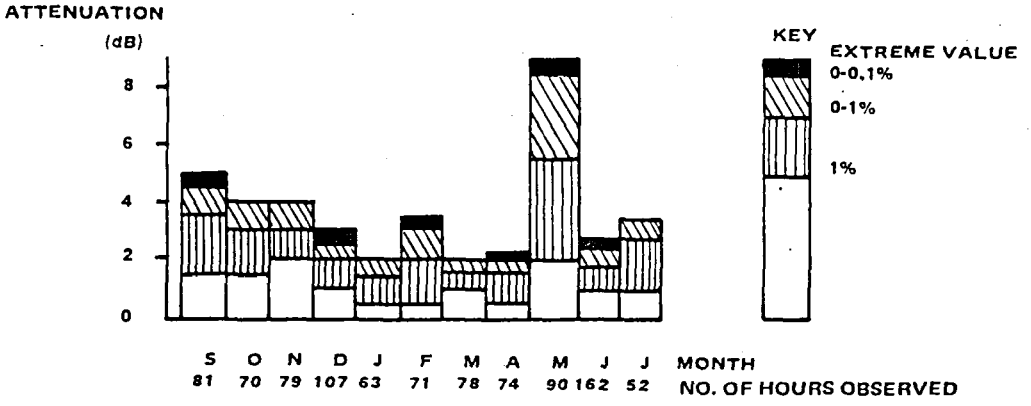

Figure 10-13. Monthly Statistics of 20-GHz Attenuation, September 1975 to July 1976

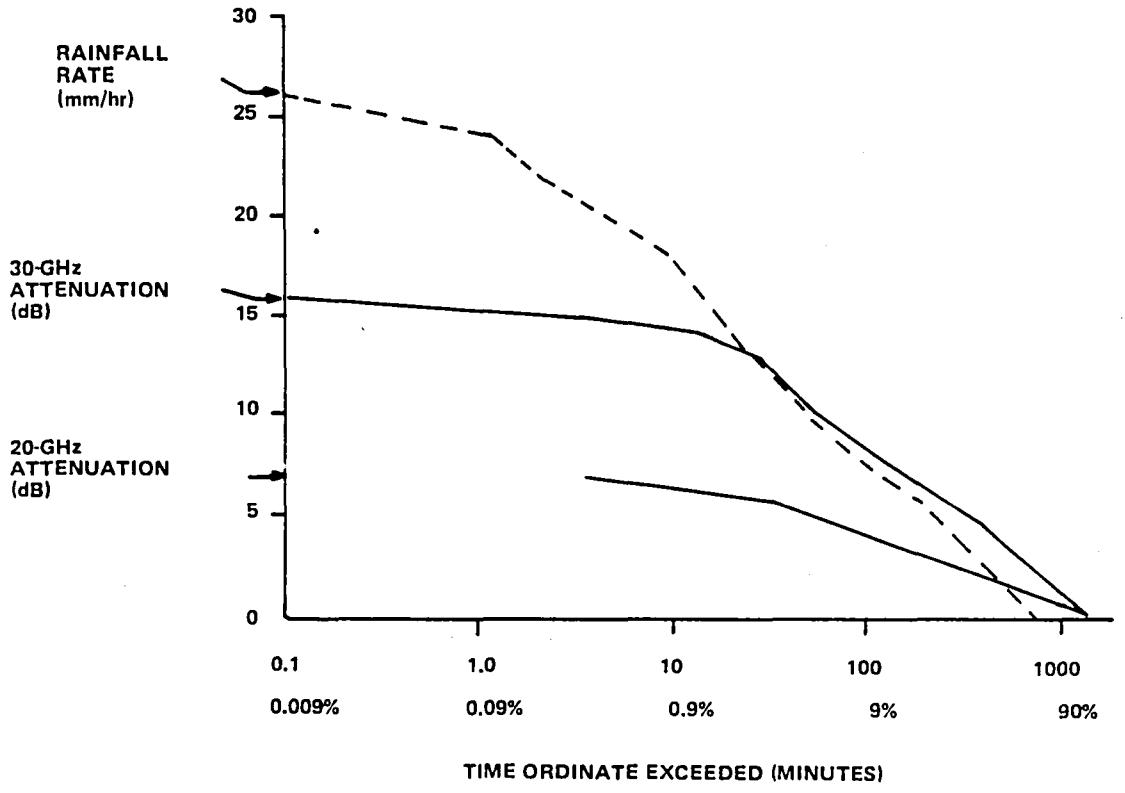

Figure 10-14. Cumulative Distributions for Concurrent 20- and 30-GHz Attenuation and Rainfall Rate (1156 hours total time)

values of 16 and 7 dB for the 30- and 20-GHz frequencies were obtained. The main differences between these attenuation statistics and the U.S. stations were in the peak attenuation values measured at very low percentages of time (0.1 percent). For this station, it was 16 dB and for the U.S. station, attenuation values greater than 25 dB were obtained. These high attenuation values are a strict function of the type and frequency of the thunderstorm activity within the measuring locale. If the thunderstorm activity in England is less severe than it is in the continental United States, the lower peak attenuation values would follow.

These low peak attenuation values for 30 GHz were also obtained from the German station located in Leeheim, Germany. Resulting percentage values for various attenuation levels are shown in the following tabulation:

30-GHz Attenuation (dB)	Percentage of time during which attenuation was exceeded
2	1.4
4	0.38
6	0.22
8	0.18
10	0.089

In addition to the differences in thunderstorm activity mentioned previously, another factor causing the low attenuation results would be satellite scheduling times. If various thunderstorms were missed because the satellite was unavailable, reduced attenuation measurements would logically result. Without a better controlled experiment, correct conclusions regarding the differences in attenuation statistics between Europe and the United States cannot be obtained.

Frequency Scaling

From the three empirically derived methods of frequency scaling shown previously, the expected frequency ratio of 30-GHz attenuation to 20-GHz attenuation should fall in the interval of 2 to 2.5. Concurrent measured 20-GHz and 30-GHz values of A_t, obtained from the Rosman Ground Station, is shown in Figure 10-15, which is a computer plot of the four second mean values of A_t. As shown, the dispersion of the points is quite low, and the slope value of the scatter plot is 2.45.

A minutely mean scatter plot for the attenuation values is shown in Figure 10-16 from data obtained from the University of Texas. In this case, the slope value was about 2.65. A higher dispersion of points was obtained relative to scatter from the test run at Rosman, North Carolina.

A scatter plot of the concurrent A_t values obtained at the Comsat station is shown in Figure 10-17 for one rain event. As shown, the slope value limits fall within 3.5 and 2 with a majority of the points near the limit.

Data obtained from the NASA GSFC station for nine rain events is shown in Figure 10-18. The slope values for this scatter plot show that a majority of the points fall between the 2 to 1 and 3 to 1 range.

The measured data described shows good correlation with the prediction techniques described. Most of the measured data falls within a slope interval of 2.5 to 3, whereas the specific attenuation and empirical scaling methods predict values in the 2 to 2.5 region. The Gaussian rain distribution technique does predict slope values greater than 2.5 for low values of A_t. It is interesting to note that the slope values are a function of the attenuation values. It varies inversely with attenuation. For the latter scaling technique in which 1_o = 4 km, the slope value approaches a value of 3 as attenuation at 20 GHz approaches the limit of 0 dB. Increasing 1_o to a higher value will result in a larger slope value for a given attenuation at 20 GHz (A [20]). Actually from the effective path-length considerations, it can be argued that 1_o is also a function of the attenuation values.

The ground station located at Ipswich, England, performed concurrent 20-GHz and 30-GHz attenuation measurements that produced ratio values between 2.1 to 2.29 for attenuation at 30 GHz (A [30]) values of 2 to 16 dB. Figure 10-19 shows the attenuation ratio values derived from long-term attenuation cumulative distributions using values of attenuation exceeded for equal percentage times. As shown, the ratio values ranged from 2.1 to 2.3. The theoretical curves plotted in the figure assume uniform rain along the given path length. These curves were based on calculations carried out by Oguchi and Hosoya (Reference 2) using the Laws and Parsons drop-size distribution. The curves show that attenuation ratio is a direct function of the drop-size distribution along the elevated path. Variations in the parameter during a rain event would cause the ratio value to vary also.

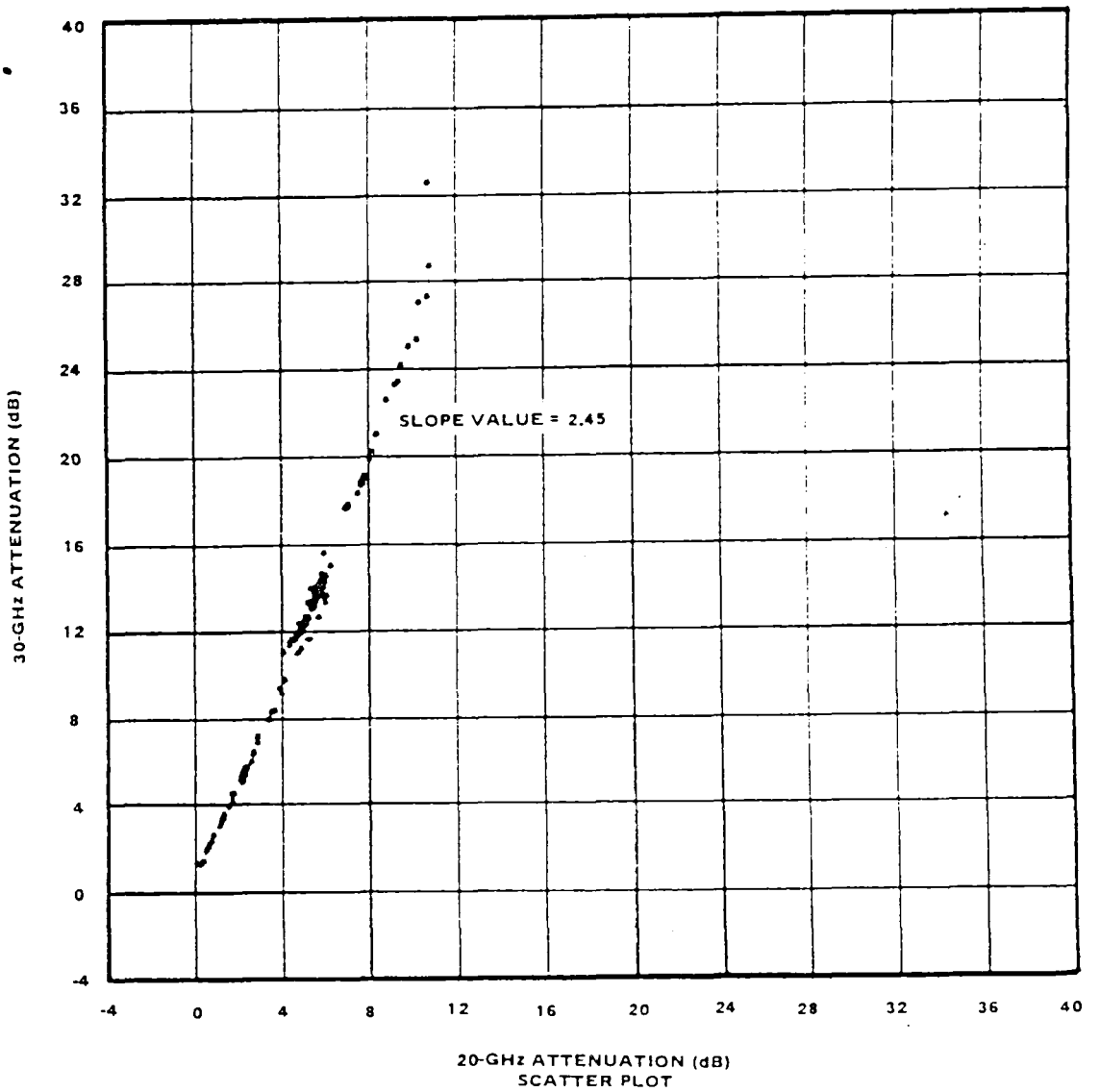

START TIME			STOP TIME				20 GHz	30 GHz
YEAR	=	1974	YEAR	=	1974	TEST MODE	CW	CW
DAY	=	185	DAY	=	185	PARAMP	OFF	OFF
GMT	=	2100	GMT	=	2159	S/C ANT. GAIN	HI	LO
						MULT. CHAIN	A	A

Figure 10-15. Four Second Mean 30-GHz Attenuation vs. 20-GHz Attenuation

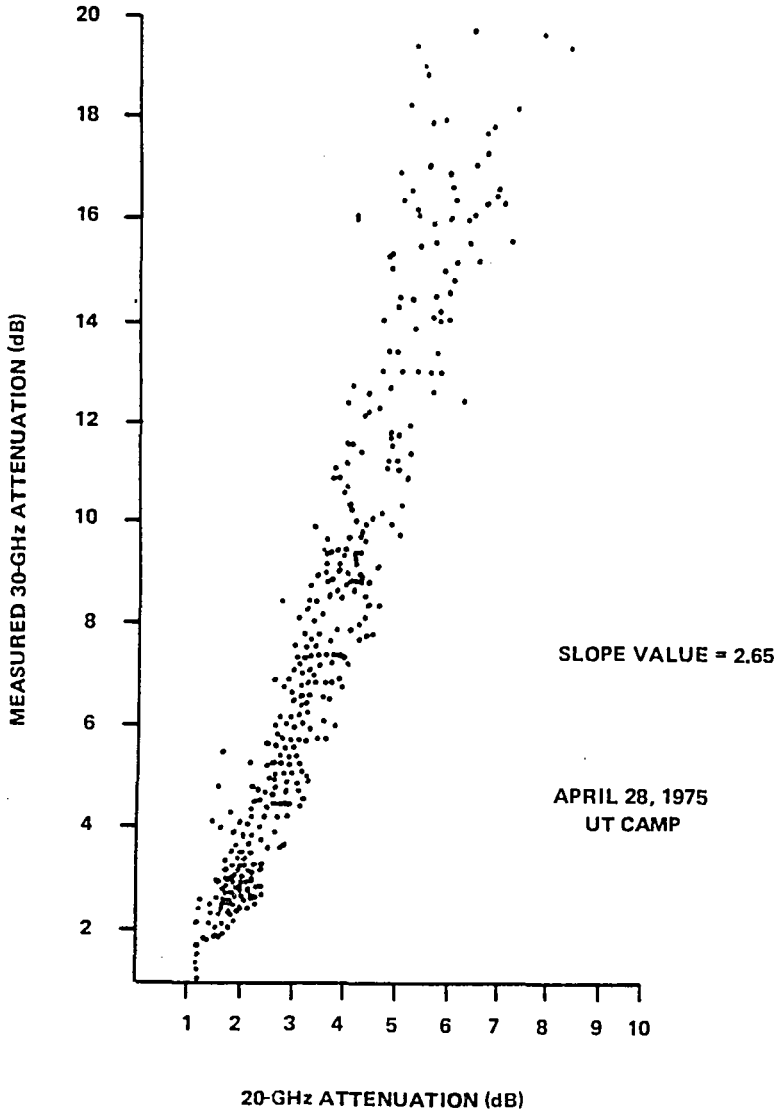

Figure 10-16. Attenuation: 20-GHz vs. 30-GHz

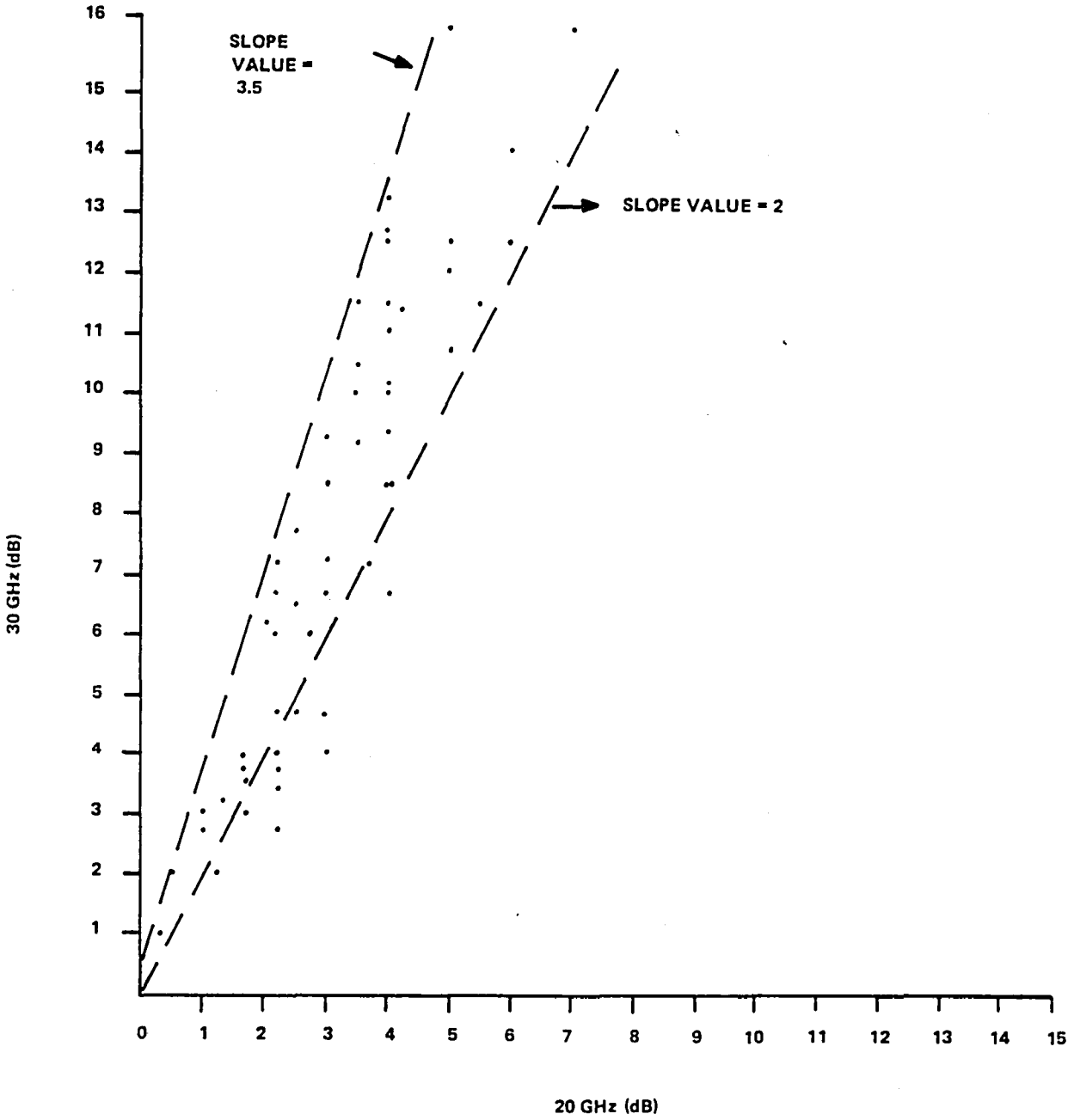

Figure 10-17. Scattergram Plot of 30-GHz Attenuation vs. 20-GHz Attenuation Measured June 6, 1975

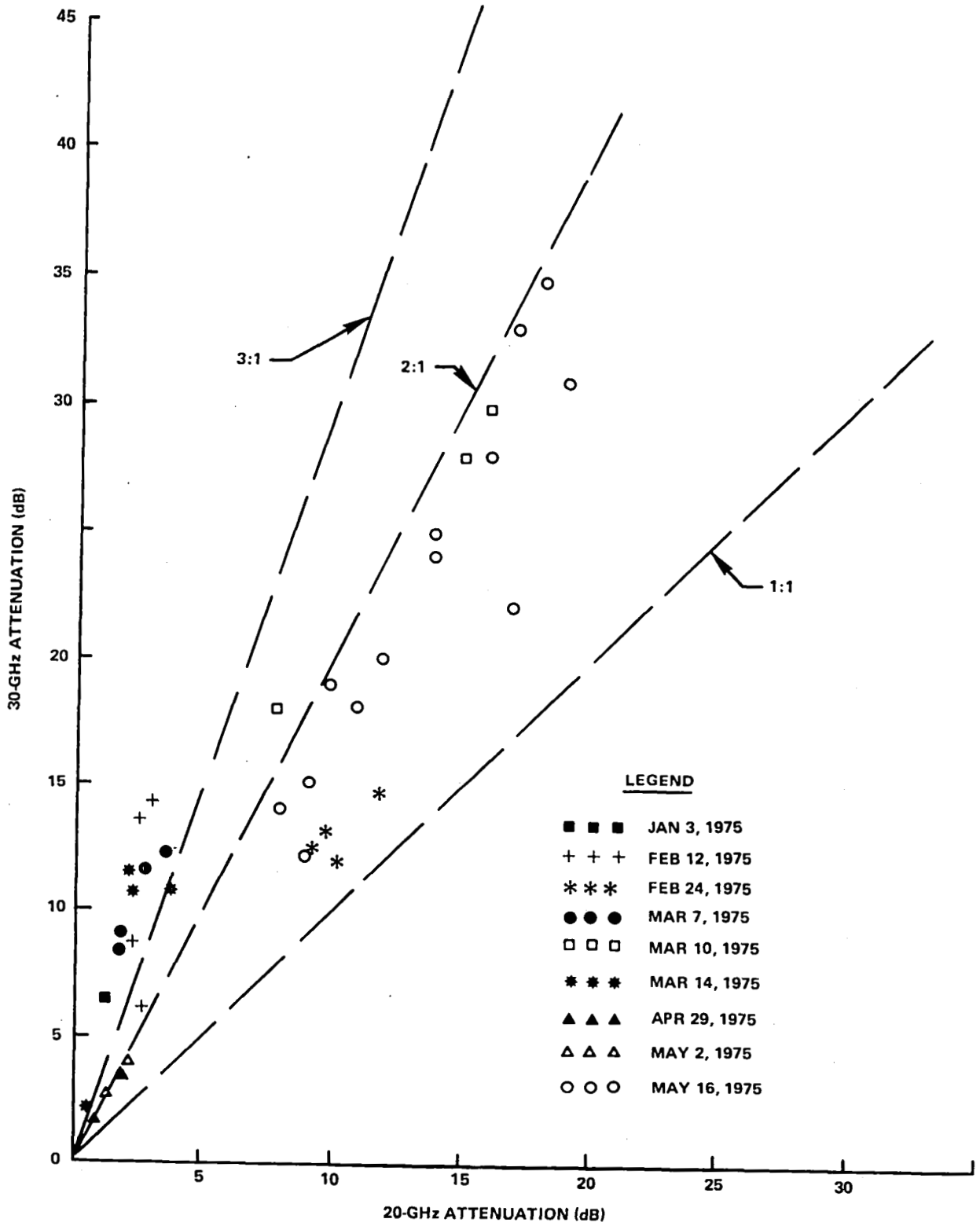

Figure 10-18. 30-GHz vs. 20-GHz Attenuation, GSFC MMW Station

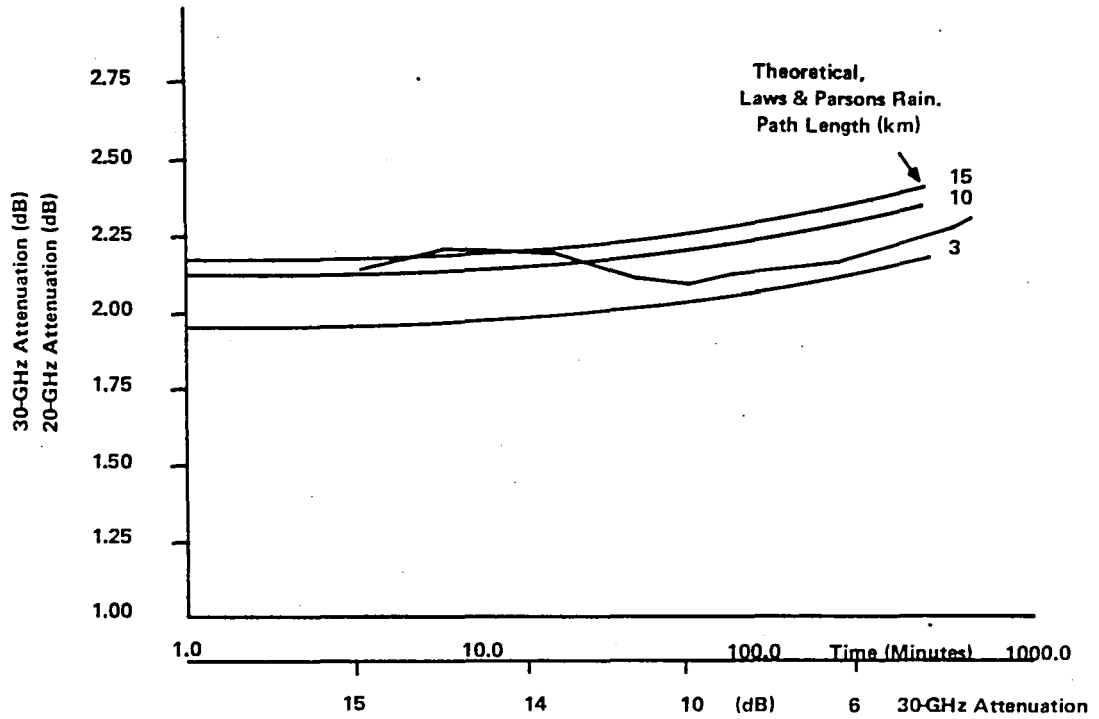

Figure 10-19. Attenuation Ratio for 30-GHz and 20-GHz Obtained from Cumulative Distributions of Attenuation for Equal-Percentage Times

The station located at Leeheim, Germany, also measured attenuation ratio values for 20-GHz and 11.4-GHz frequencies. The attenuation, A, at 11.4 GHz was obtained from sky-temperature measurements. As a result of the measurements, the following empirically derived relationship was developed.

$$\frac{A(30)}{A(11.4)} = 7.14 - 3\,(A\,(11.4))^{-1} \qquad (10\text{-}1)$$

For an attenuation at 11.4 GHz of 1 and 7 dB, the corresponding ratio values of 4.14 and 6.7 are computed from the expression. The increase in the attenuation ratio values for an increasing attenuation is opposite to the trend obtained from the concurrent 20-GHz and 30-GHz values. The divergence between expressions could result from the fact that the previous expression was derived from the attenuation values of two widely separated frequencies. Measured attenuation values (20) at attenuation at 28.56 GHz and 11.7 GHz produced a ratio value of about 4.5 for an attenuation at 11.7 GHz; A (11.7), value of about 1 dB. This corresponds to the result obtained from the German station for slightly different frequencies. Sufficient data were unavailable to note a trend in the ratio value as the A(11.7) value increased. No general conclusions regarding this divergence can be developed, because of the lack of sufficient data. However, it appears that for the A (30)/A (20) ratio values, good correspondence was obtained between the United States and European experimenters where the ratio values decrease for increasing attenuation.

In conclusion, the ratio value, quantitatively, is a complicated function of the spatial extent of the rain environment and magnitude of the respective attenuation values. However, qualitative estimates can be obtained in most cases by using simplifying assumptions of the constancy of the above parameters.

Meteorological Radar Results

The multifrequency meteorological radar operating at 3 and 8.75 GHz was located at the NASA Rosman Ground Station in North Carolina. With the use of the radar return from the 255 one hundred-meter range bins, a quantitative measurement of the rain environment was possible.

A typical computer plot of the integrated refectivity at 3 GHz versus A (20) is shown in Figure 10-20. The points represent 4-second mean values of the parameters. It is noted that the η parameter is a sensitive indicator of attenuation when A_t is less than 4 dB. Above this value, the slope tends to decrease and the scatter increases. These trends are probably a function of the threshold level set in the radar receiver. As A_t increases, more range bin returns exceed the threshold value, causing a measurable increase in the integrated η factor. As A_t continues to increase, the number of range bins exceeding the threshold value does not increase accordingly, but the signal level within the useable range bins increases, causing a smaller increase in η. Signal attenuation of the radar return from the range bin to the radar antenna is a factor in the reduced signal level. Even though the threshold of the receiver does mask the level of the radar return, a general correlation between η and A (20) does exist. From these results, it could be concluded that the accuracy of the attenuation prediction will vary inversely with attenuation.

The magnitude of the reflectivity factor, Z, that is measured, as a function of slant range, is indicative of the rain rate that exists in the elevated beam at a given time. An example of the Z-plot expressed in dB above 1 mm^6/m^3 is shown in Figure 10-21 and denoted as dB Z for the 8.75-GHz frequency. As shown, an intense rain cell is present at 1.2 km and its width is approximately 500 meters. Another wide cell of lesser intensity is shown at about 4.2 km. The dB Z response falls below the receiver threshold value at a range of 5.2 km. The response at 8.2 km is from the melting layer (zero degree isotherm). This is the transition region between rain and snow in which very large radar returns can be received.

Rain rate within a specific 100-meter range bin can be predicted from the radar return as shown in Equation 9-9, Chapter 9, this volume. An example of this prediction is shown in Figure 10-22 for range bin 1. For reference purposes, the 20-second average of rain bucket, which is directly below the range bin, is plotted. As shown, excellent correlation is obtained between the ground measured rain rate and the radar predicted rain rate mainly because of the low spatial difference between the rain bucket and the range bin. The third plot is a 20-second average of the measured wind speed within the vicinity of the rain bucket. In general, poor correlation exists between the rain-rate peaks and the wind-speed peaks. Wind speed is a measure of the turbulence that was present at the time of the measurement.

Rain-rate plots for a large spatial displacement between the rain bucket and the range bin are shown in Figure 10-23. Poor correlation exists at the low rain-rate values; however, the peak rain-rate

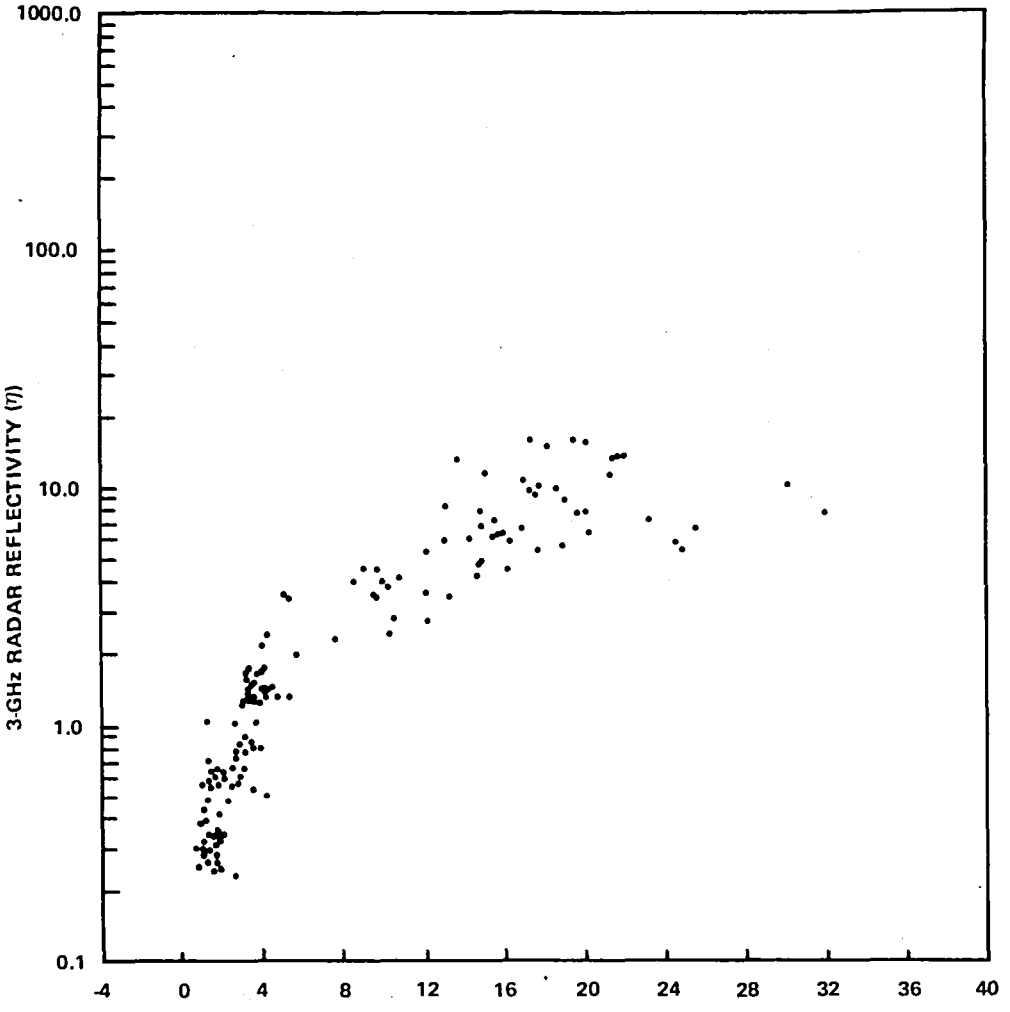

START TIME			STOP TIME				20 GHz	30 GHz
YEAR	=	1975	YEAR	=	1975	TEST MODE	CW	CW
DAY	=	89	DAY	=	89	PARAMP	OFF	OFF
GMT	=	110	GMT	=	209	S/C ANT. GAIN	HI	NA
						MULT. CHAIN	A	A

Figure 10-20. Integrated Reflectivity at 3 GHz vs. A (20)

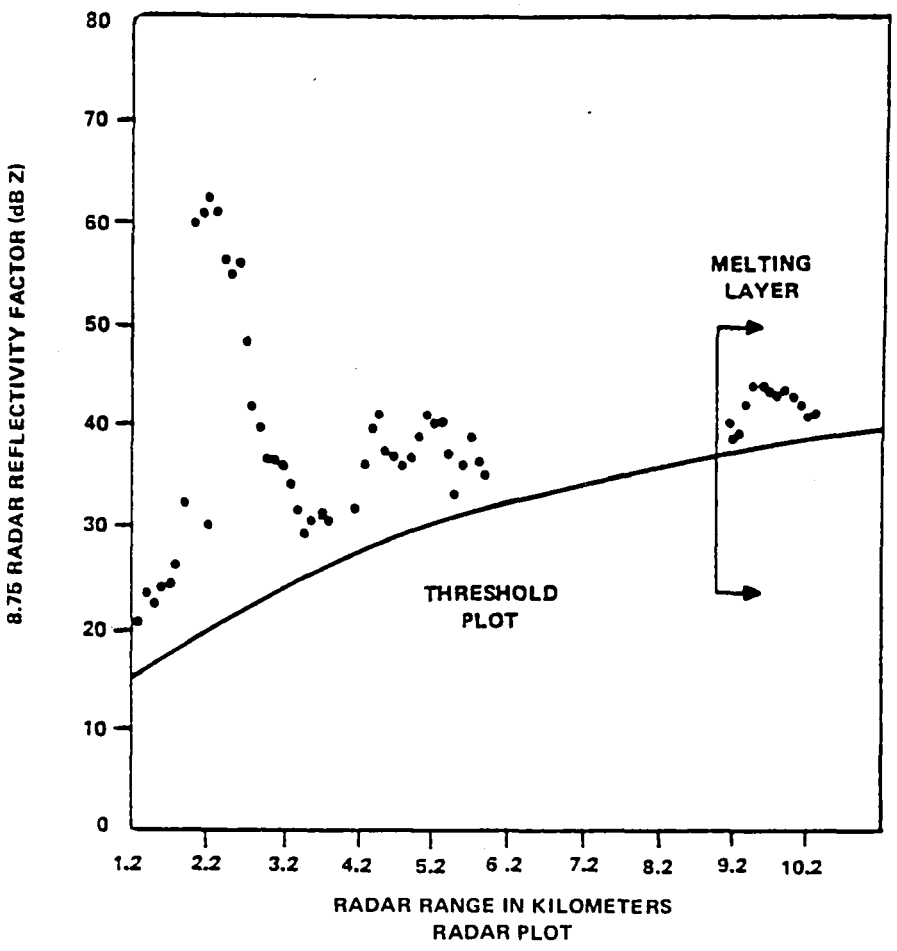

START TIME			STOP TIME		
YEAR	=	74	YEAR	=	74
DAY	=	270	DAY	=	270
GMT	=	1914	GMT	=	1935

TIME OF PLOT

GMT	=	1919
SEC	=	3

Figure 10-21. DB Z Threshold Plot (8.75 GHz)

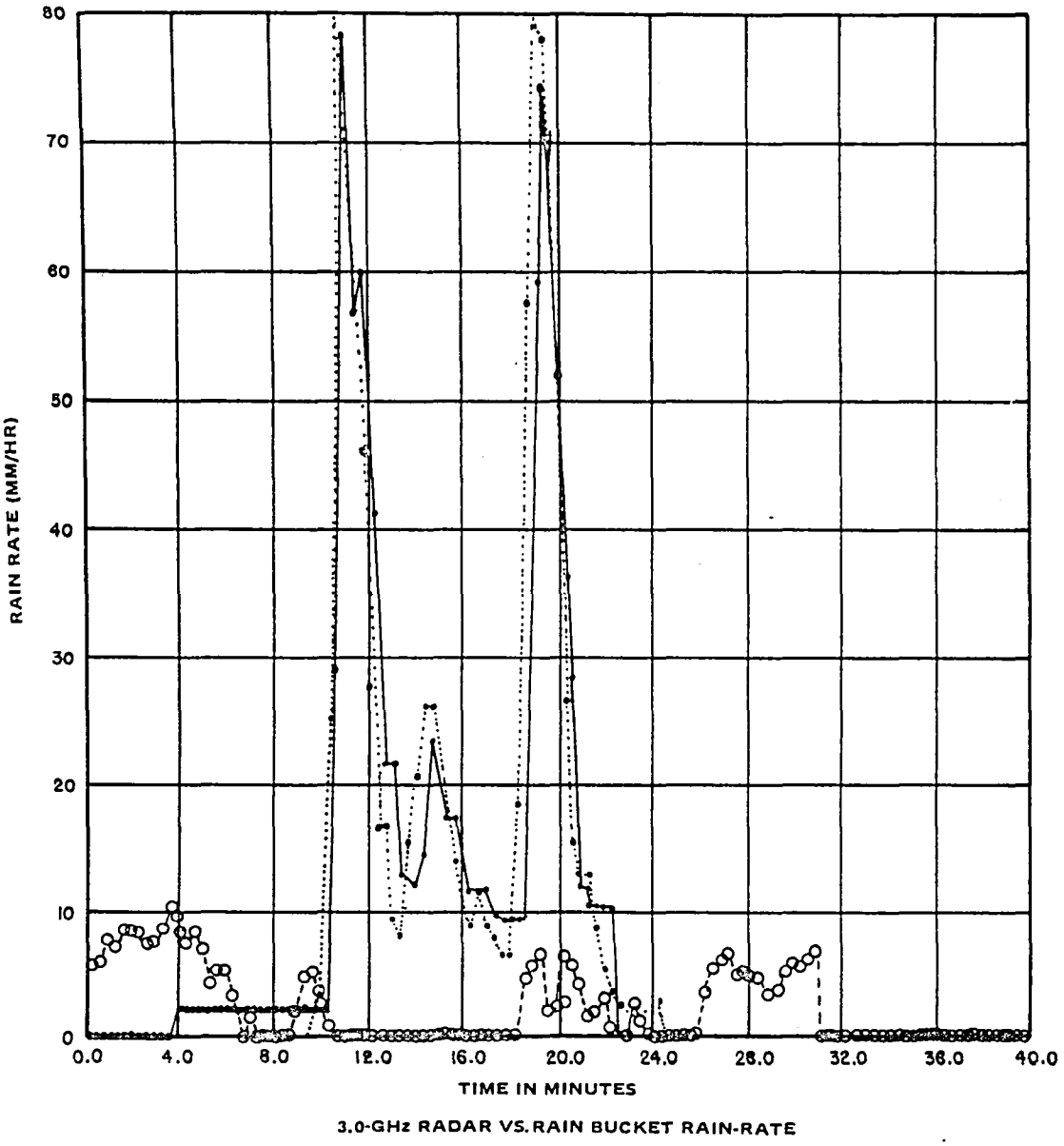

Figure 10-22. Radar Predicted and Measured Rain Rate vs. Time (Range Bin 1, Rain Bucket 2)

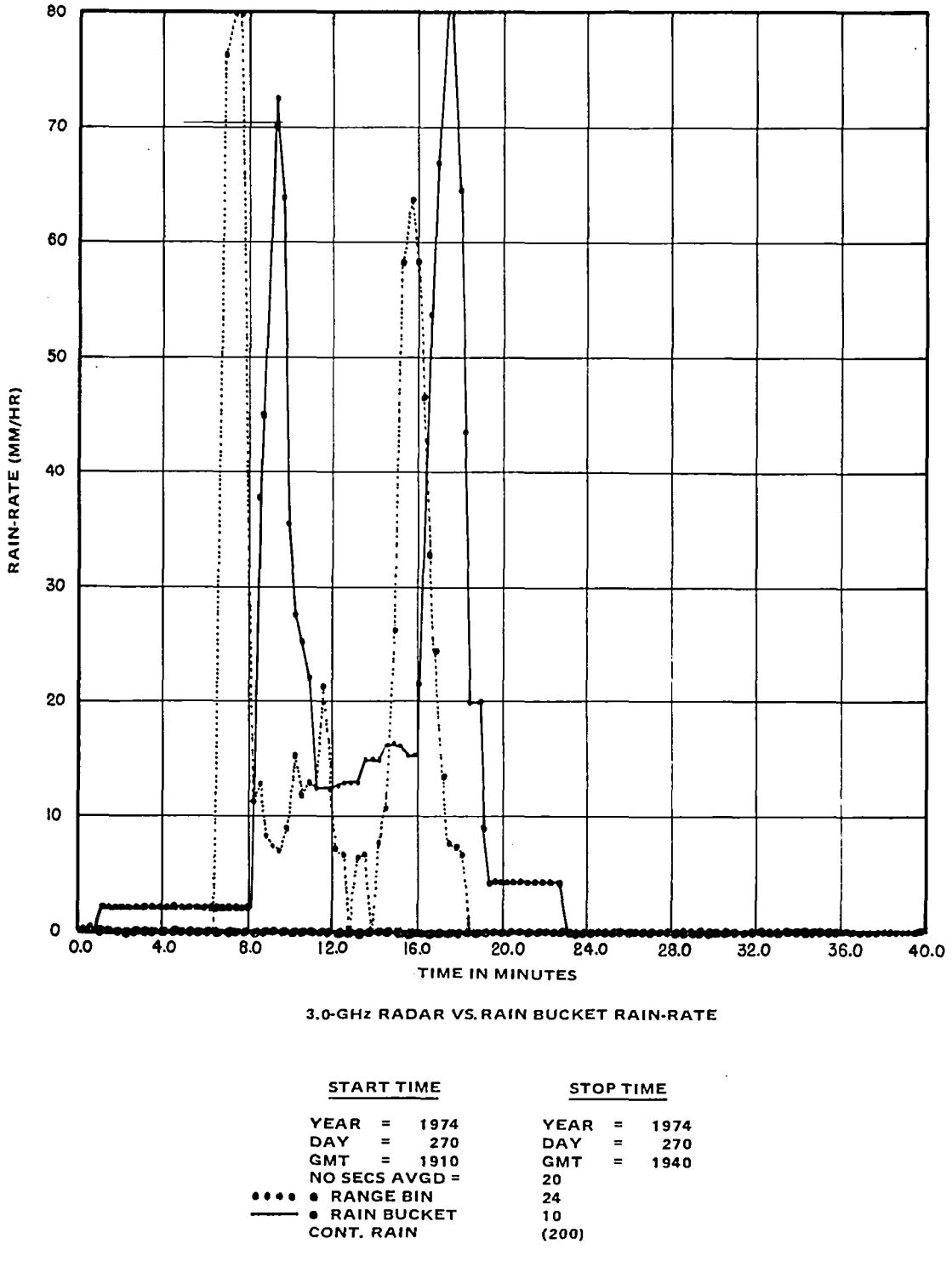

Figure 10-23. Radar Predicted and Measured Rain Rate vs. Time (Range Bin 24, Rain Bucket 10)

values still track with a time displacement of approximately 2 minutes. For this time displacement, a rain drop fall velocity of about 20 meters per second is computed. This is a very high fall velocity when compared to the usual values quoted of about 10 meters per second. At a rain rate of 80 millimeters per hour the average time between rain bucket tips is 11.43 seconds. Because of this low time interval, the 20-second average time employed in the plots can easily mask the time at which the peak rain-rate values occurred. Therefore the 2-minute time displacement should be suspect. For reasonable fall velocities of about 8 meters per second, the time displacement should have been about 5 minutes.

Rain attenuation can be predicted from the radar return equation. The radiometer is an excellent means of providing attenuation prediction for values less than approximately 10 dB. The radar technique should be investigated for attenuation prediction generally above the 10 dB value. In the high attenuation region, it is reasonable to conclude that the 3-GHz return will give a better estimate of attenuation, because of the attenuation of the 8.75-GHz return. The largest source of error for the radar prediction technique should be caused from the inaccuracies in the radar constant. Within the radar constant, the assumption that the return comes from rain only at the peak of the beam is the main reason for the error. Antenna gain should be treated as a variable, because returns will actually be received from the sidelobes and other parts of the main lobe. The simplifying assumption causes an underestimation of the actual rain intensity especially for high rain rates. In summary, the main causes of error in the radar prediction technique are the inaccuracy in the radar constant and that there is a two-way attenuation of the radar signal as it traverses the distance between range bin and the radar antenna.

Examples of the results of the radar prediction technique are shown in Figures 10-24 and 20-25. As shown in Figure 10-24, the 3-GHz frequency is the best to use because of the attenuation factor discussed previously. Figure 10-25 shows that a reasonable correlation exists between the measured and predicted values. The effect of the attenuation factor would be to underpredict the measured attenuation. The effect of the error in the radar constant could cause either an over or under prediction. At high attenuation values, an underprediction should be more prevalent. In the lower and intermediate attenuation regions, either prediction result could occur.

The Bradford ground station in England used a 9.4-GHz meteorological radar to predict attenuation. Examples of the results of the investigation are shown in Figures 10-26 and 10-27. In the former figure, a three-dimensional plot of Z (vertical axis) versus time and range is given for a thunderstorm event. The zero degree isotherm level or bright band characterized by a large Z-value but low signal attenuation is located at a slowly varying maximum range that is parallel to the time axis. The rain cells appear as a slanting ridge at intermediate range values. Intense rain cells of limited extent are clearly seen in the plot. The plot shows that intermediate and high attenuation values are caused by severe rain cells of limited extent that occur in a highly heterogeneous rain environment.

The radar predicted and measured attenuation for the storm event is shown in Figure 10-27. The general agreement for the overall time interval is good for these intermediate attenuation values. The deviations at points "a," "b," and "c" are mainly due to radar constant errors, and because no compensation was employed for the effect of the bright band on increased reflectivity.

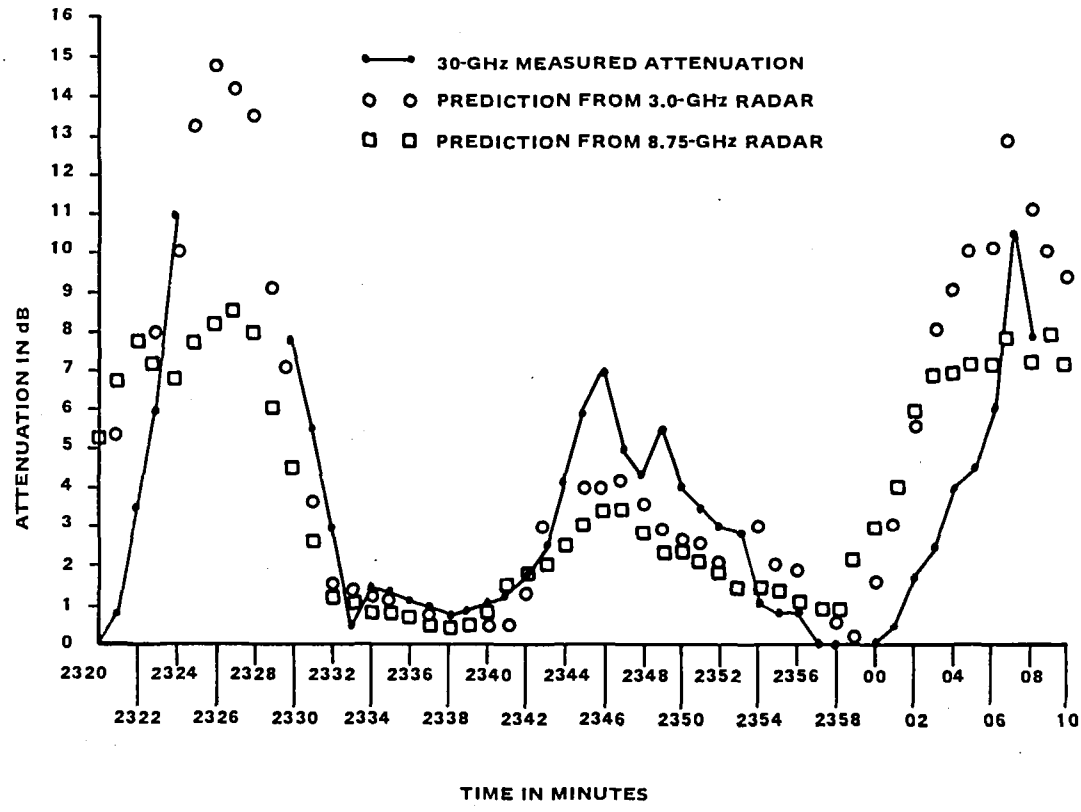

Figure 10-24. Radar Predicted and Measured Attenuation vs. Time (30-GHz Measured Attenuation)

To achieve good accuracy, it would be necessary to divide the attenuating region into three distinct zones: (1) The rain environment, (2) the zero degree isotherm region, and (3) the region beyond (Reference 2). Each region would have its own characteristic attenuation versus Z relationship. Also more accurate methods of calibrating the radar should be developed.

Path Diversity

Because large attenuation values experienced on space-Earth links are caused by intense cells for limited spatial extent, improved system service times could be attained from the concept of path diversity. Good examples of this limited spatial extent are shown in Figures 10-28 and 10-29. The data for the former figure were obtained from the fixed transportable stations located 13.2 km apart at the Ohio State University complex. The latter figure shows the respective attenuation and rain-rate time plots for the long range diversity experiment of the three stations shown in Figure 9-10, Chapter 9, this volume. In each example, peak attenuation values at the stations are not time coincident.

The defined diversity gain (E) is computed by using the joint and individual cumulative probability functions as shown in Figure 9-9, Chapter 9. An example of the distributions obtained from measured data is shown in Figure 10-30 for seven rain events recorded at Ohio State University. The E

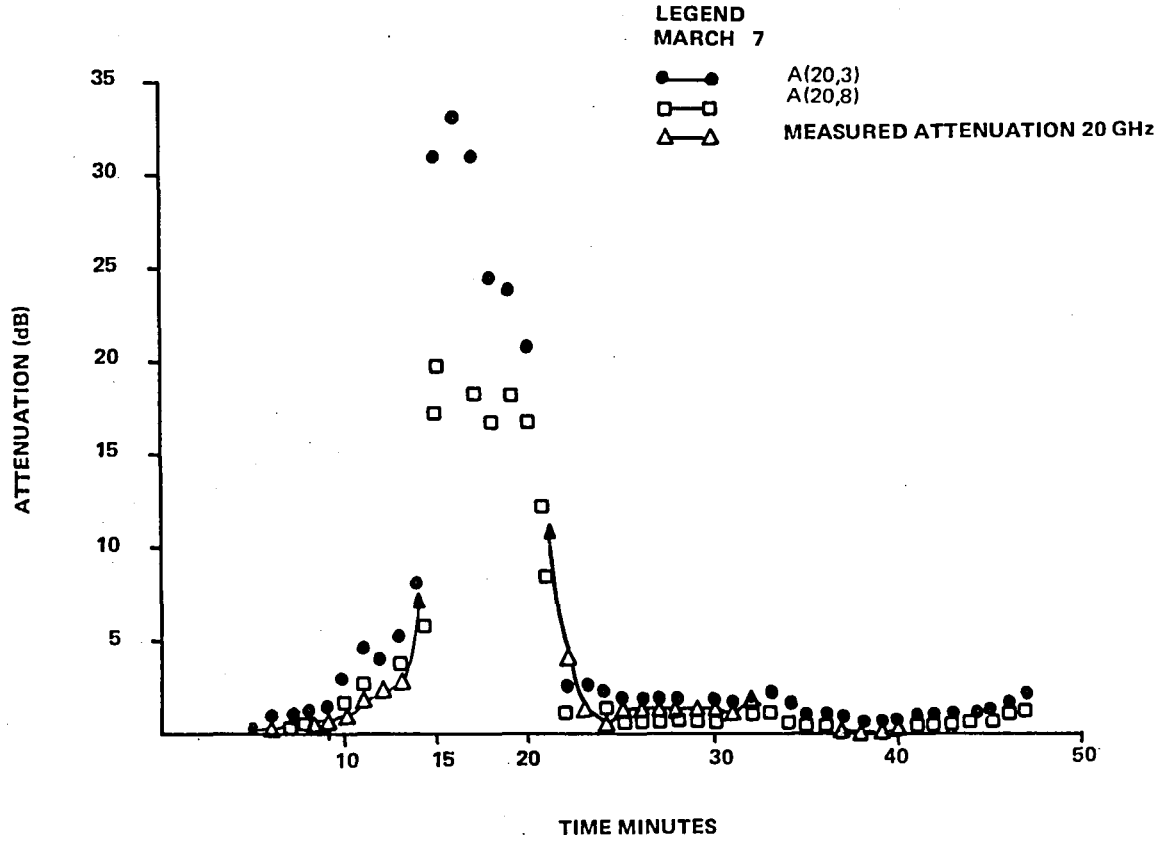

Figure 10-25. Radar Predicted and Measured Attenuation vs. Time (March 7)

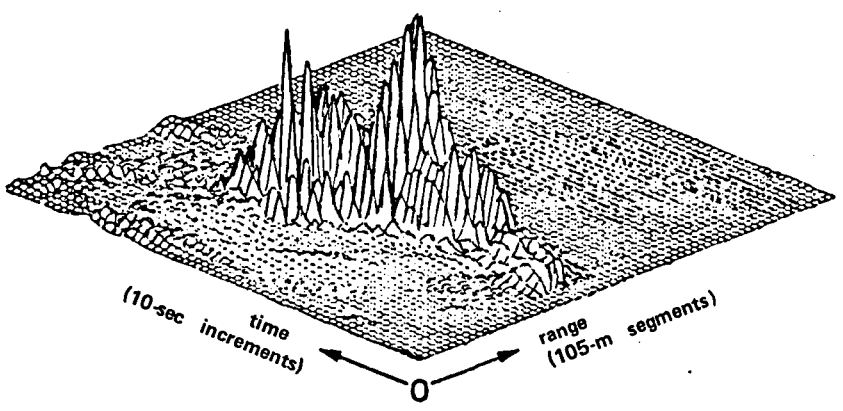

Figure 10-26. Radar Reflectivity (Vertical Axis) vs. Time on a 6.5-km Start Range

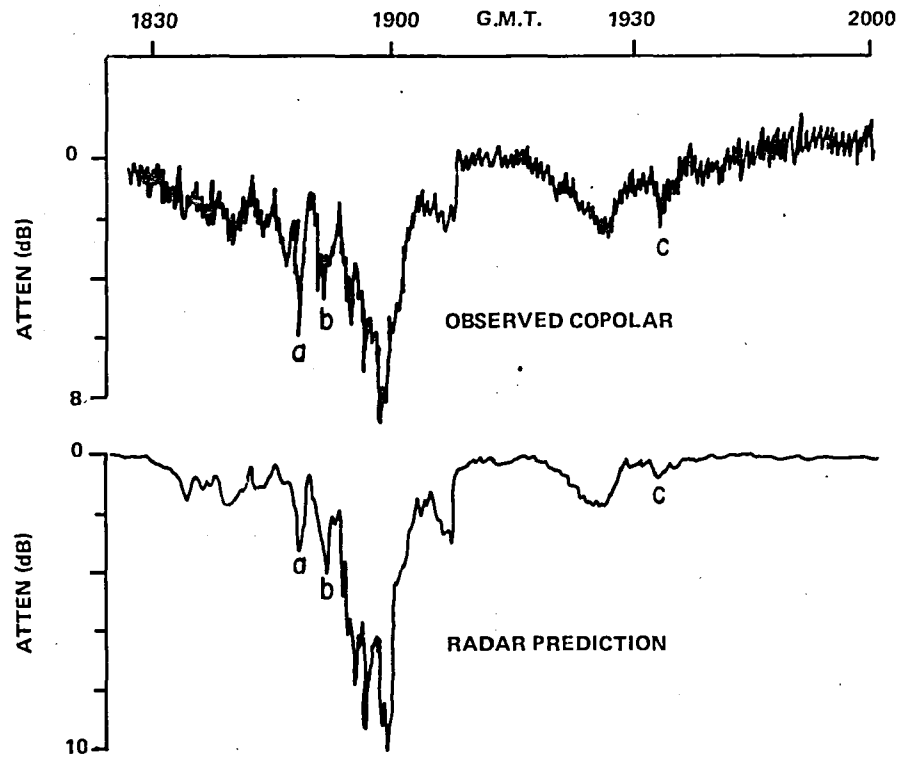

Figure 10-27. Thunderstorm Event, July 5, 1976

factor is determined from the attenuation difference for a constant percentage time between the joint and fixed cumulative distributions. Results of the computations are shown in Figure 10-31 for the above data and for data from other experimenters. As shown, the E factor reaches a limit for a site separation of about 12 km.

The diversity experiment for the University of Texas was conducted for a site separation of 11 km at a frequency of 30 GHz. Results of this experiment agree quite closely with the Ohio State results. As shown in Figure 10-31, the E factor should be about 10.5 dB for a site separation of 11 km. Results from the University of Texas show that for an A_t of 14 dB, the E factor was about 10 dB.

As the distance between sites increases past about 10 km, the E factor approaches its limiting value, which is the value of A_t obtained from the statistics for a single site. Therefore, increasing the site separation beyond 10 km should not result in a much improved E factor because of the limiting value of E.

Results of the diversity improvement for the long baseline experiment are shown in Figure 10-32. Increasing the site distance does not result in an E factor approaching its ideal value. A possible explanation of this result can be obtained from the time plots shown in Figure 10-29. Within the space of 1 hour, each of the three sites experienced brief periods of significant attenuation. Some of these periods could have been caused by a single cell intersecting two sites in turn. Others, because

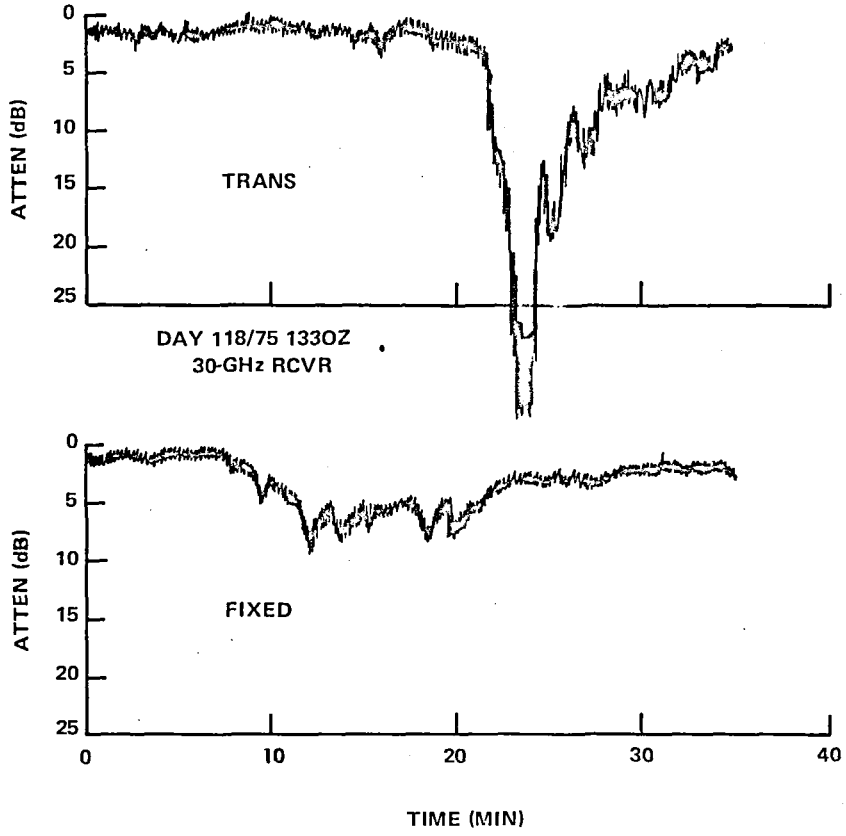

Figure 10-28. Preprocessed 30-GHz Receiver Data (April 28, 1975)

of the short length of time between fades at different sites, were caused by different cells within the general storm area. The probability of separate rain cells affecting more than one site at the same time is higher for site separations greater than 8 km.

For this reason, it may be less advantageous to have diversity sites separated by distances like 25 to 50 km, than lesser distances like 8 to 10 km. For high separation distances, site location should be chosen to minimize the probability of separate cells affecting different sites at the same time.

The ground stations located at Slough, England, also performed path diversity experiments using station spacing of 2 km (Appleton and Langley), 10.3 km (Appleton and Winkfield), and 12.3 km (Langley and Winkfield). It was found that the 2-km spacing only produced 2 dB less diversity gain than the 10.3 and 12.3 spacings. At a fade level of 12 dB, the diversity gains for the 2-km and 12.3 km spacings were 3 and 5 dB, respectively. According to Figure 10-31, the diversity gains for the above site separation should be about 6 and 8.5 dB. Approximately a 2 dB difference in gain values seems to be correct. It was concluded from the European experiment that site location is much more important than site separation. Placement of one of the sites in hilly terrain will enhance rain results at that site. Placement of one site in hilly terrain and one in flat terrain will reduce the diversity gain, because if it is raining at the flat site, it is probable that it is also raining at the hilly

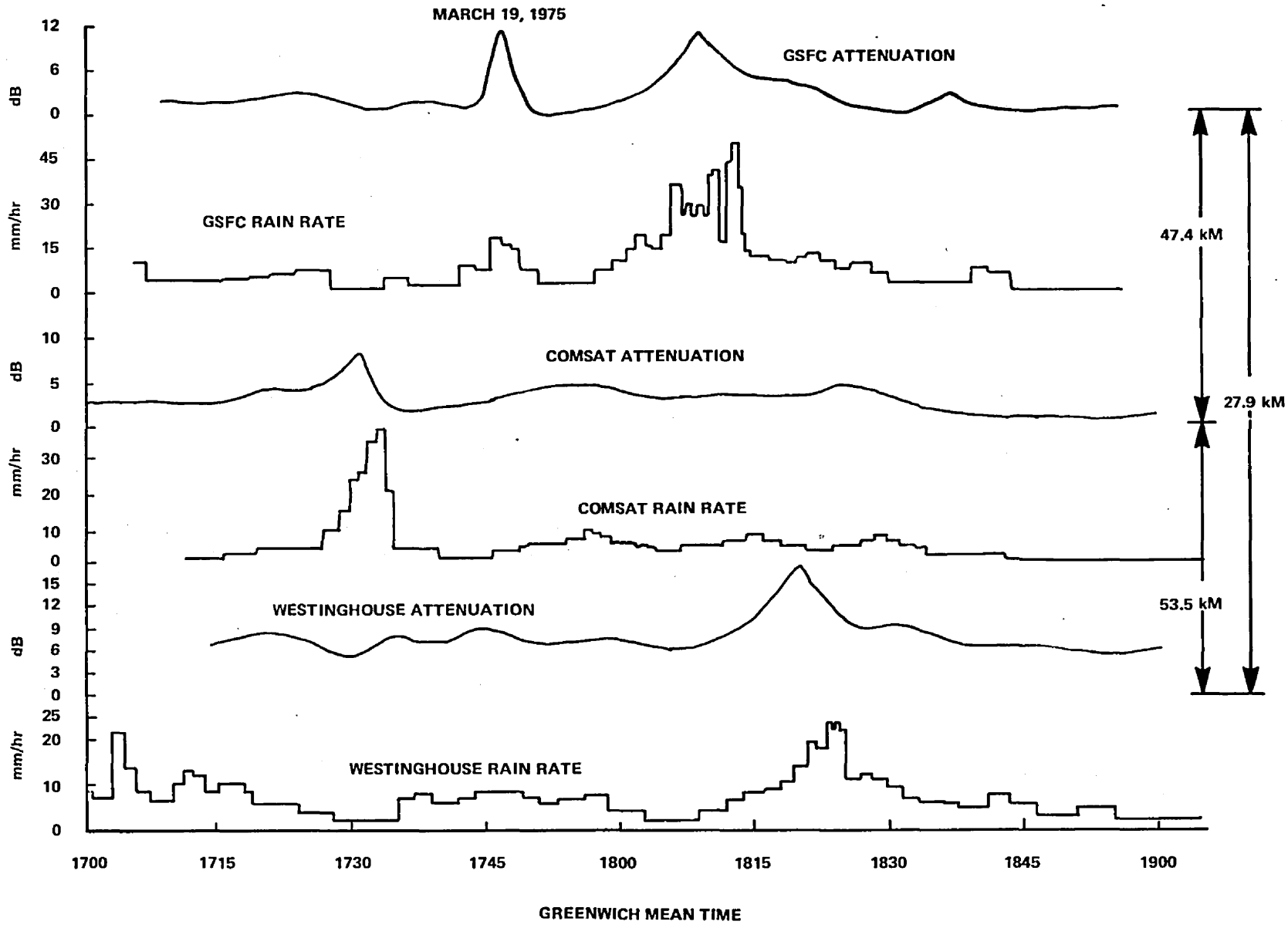

Figure 10-29. Three-Station Diversity Measurements Rain Rate and Attenuation Factors vs. Time

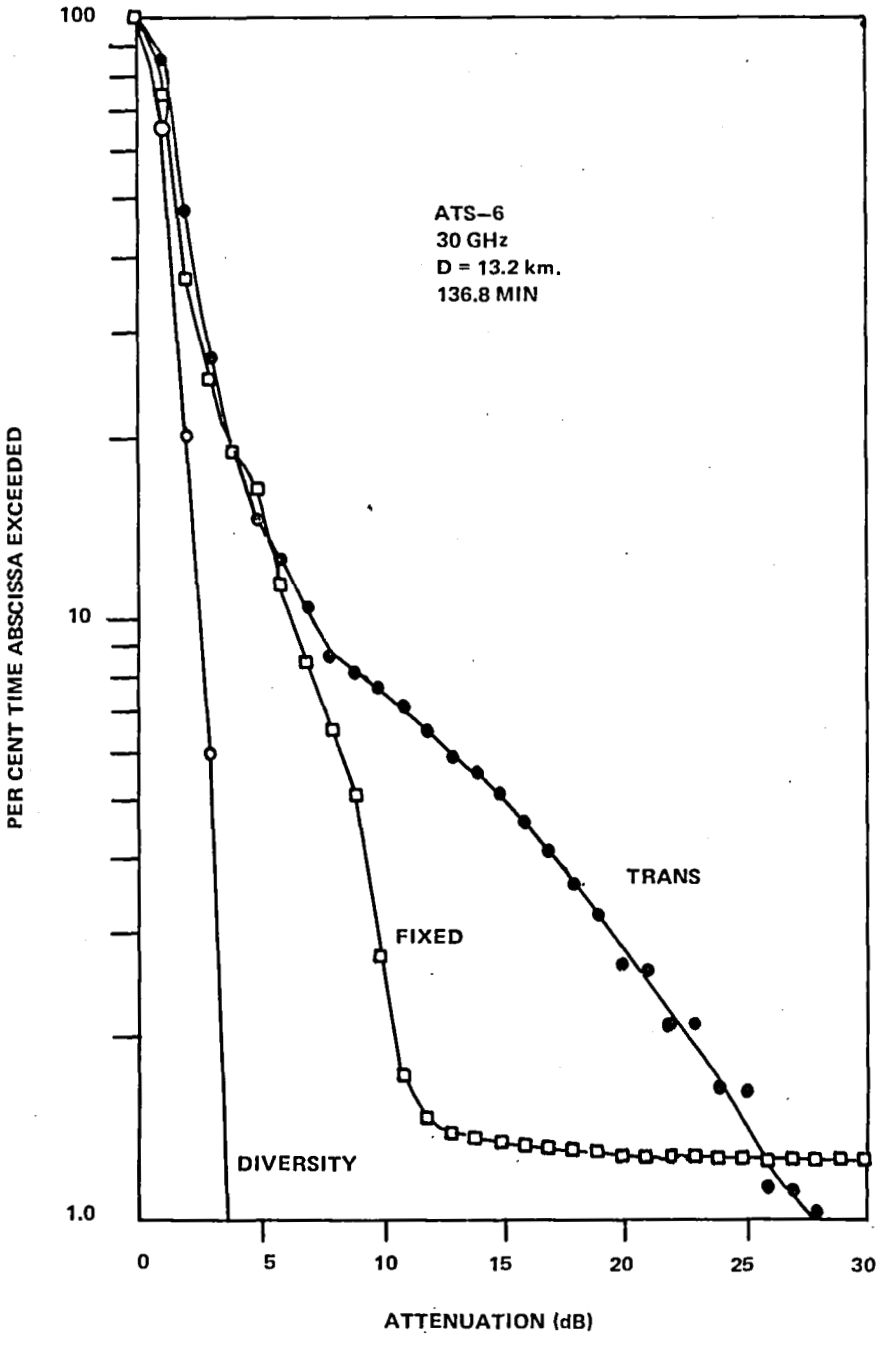

Figure 10-30. Cumulative 30-GHz Fade Distributions (Seven Events)

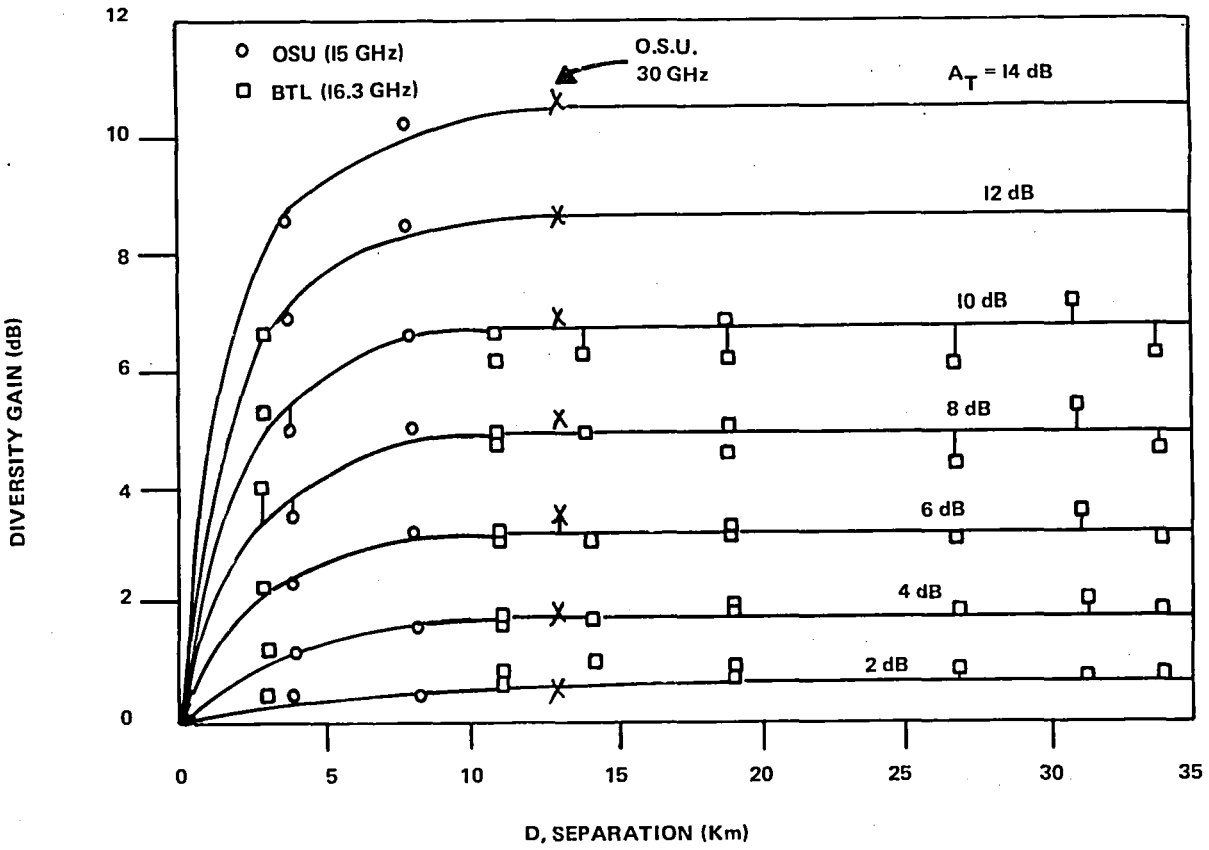

Figure 10-31. Diversity Gain vs. Terminal Separation Distance

site. Both stations should be placed in flat terrain where the probability of rain at one site will be lower if, in fact, it is raining at the other site.

Communication Parameters

Analog Signals

The first successful color video transmitted through a millimeter wave space link was demonstrated at the Rosman Ground Station in North Carolina on July 12, 1974, with signal-to-noise ratios of 31.5 dB at 20 GHz, and 36.5 dB at 30 GHz. Video quality was good and compared favorably with the 4-GHz downlink. Numerous attempts were made to observe video signal degradation during heavy rain at Rosman, but all were unsuccessful. The complexity of the uplink-downlink operations required all video tests to be prescheduled, and light rains occurred during test periods.

Digital Signals

Five different data rates and modes of operation were tested over the satellite link (Table 10-1).

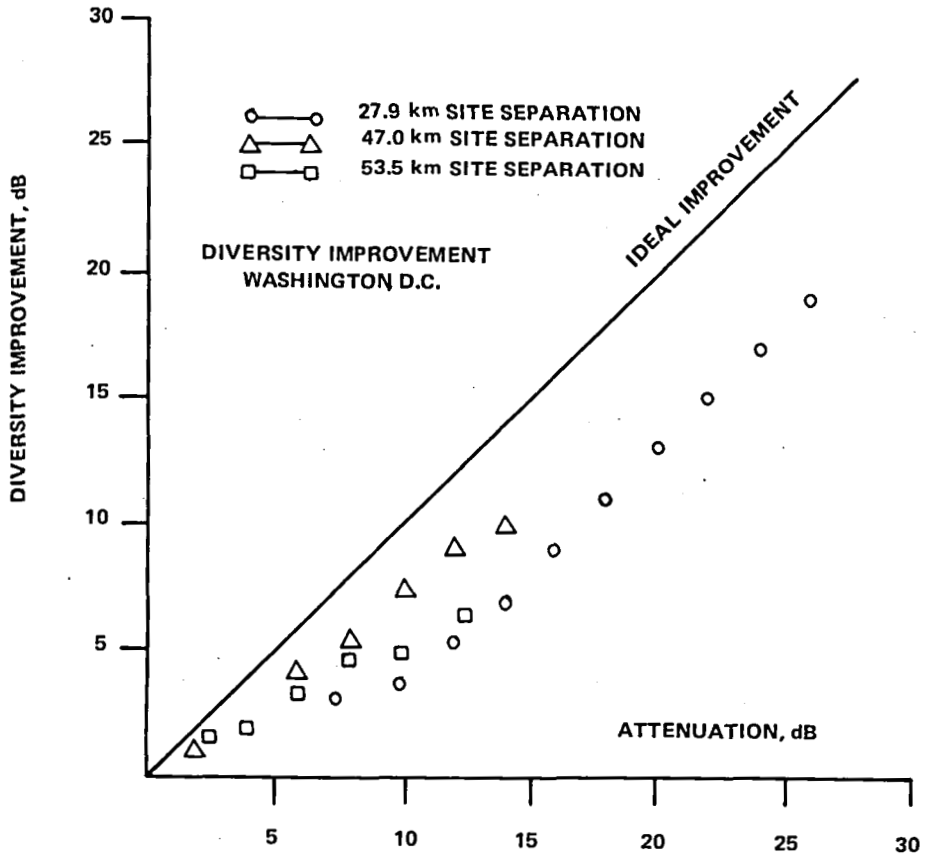

Figure 10-32. Two-Station Diversity Gain, with Respect to Higher Attenuation Sites

Table 10-1
Data Rates and Modes of Operation Tested

Test Mode	In Phase Channel Data Rate	Quadrature Channel Data Rate
1 Quadriphase	3 Mbps	100 kbps
2 Quadriphase	20 Mbps	200 kbps
3 Quadriphase	10 Mbps	10 Mbps
4 Quadriphase	10 Mbps	1 Mbps
5 Biphase	15 Mbps	–

In test 1, no measurable bit error rate (BER) was obtained, because the link parameters produced an energy per bit over spectral noise density (E_b/N_o) of 28 dB for both channels. By rotating the receive antenna polarization angle, a rain fade was simulated. This reduction in energy per bit produced bit-error-rate values greater than 10^{-6}.

In test 2, the transmit power difference in the channels was 10 dB. For the C-band downlink, the bit-error-rate for the 20-Mbps channel was 1.6×10^{-4}, which corresponds to an E_b/N_o of 12.6 dB (4.4 dB worse than the theoretical value). This degradation was due to modem deficiencies in part. No 20-GHz or 30-GHz downlink data were obtained for the test because of lock carrier problems. It was determined that there was a frequency offset problem that was eventually corrected.

No data were obtained from test 3 because no synchronization could be achieved by the carrier tracking loop even for the strong C-band link. The exact cause of this deficiency was not determined.

In test 4, a power difference between channels of 8 dB was employed. No bit-error-rate was obtained for the C-band link. Relatively high bit-error-rate values in the rates of 10^{-2} to 10^{-3} were obtained for the 20- and 30-GHz links. Performance of the 10-Mbps channel was better than the 1 Mbps-channel. This result does not follow from theory. It was concluded that a noisy environmental effect might have contributed to the poor loop test performance.

Test 5 was a differentially encoded phase-shift-keying test with the quadrature channel disabled. The data rate was 15 Mbps. The modem carrier extraction loop achieved lock for all three links. The results are shown in Figure 10-33. The performance was within 2 dB of the loop-test curve, even though the loop-test curve exhibited severe degradation. It can be concluded that the K-band links are capable of supporting 15-Mbps transmission rates, which is the most significant result for the millimeter wave experiment digital transmission.

Coherence Bandwidth

Digital and analog techniques were employed to determine the coherence bandwidth properties of a 20- and 30-GHz space-Earth link. The digital data were developed in the form of discrete 4-second mean carrier values of A (20) and A (30). These values were tabulated along with the normalized A values for each of the sidebands. The tabulated normalized values A_{ns} were computed from the following expression.

$$A_{ns}\,(\text{dB}) = A_s\,(\text{dB}) - A_c\,(\text{dB}) \qquad (10\text{-}2)$$

where A_s is the measured attenuation value of the sideband, s, and A_c is the measured attenuation of the corresponding carrier. It is estimated that the measurement error for A was approximately 1 dB. For this magnitude of error, it is apparent that no selective fading properties exist for the 4-second mean values in all instances except when A (30) is greater than 20 dB. In this case, it appears that some selective fading occurs at A_{720}. However, at these high A values, the measurement accuracy could be degraded above the 1-dB limit because of receiver noise and also because the dynamic range for the measurement of A was reduced from 5 volts to about 2.5 volts. This reduced measurement range is probably the main cause for the accuracy degradation.

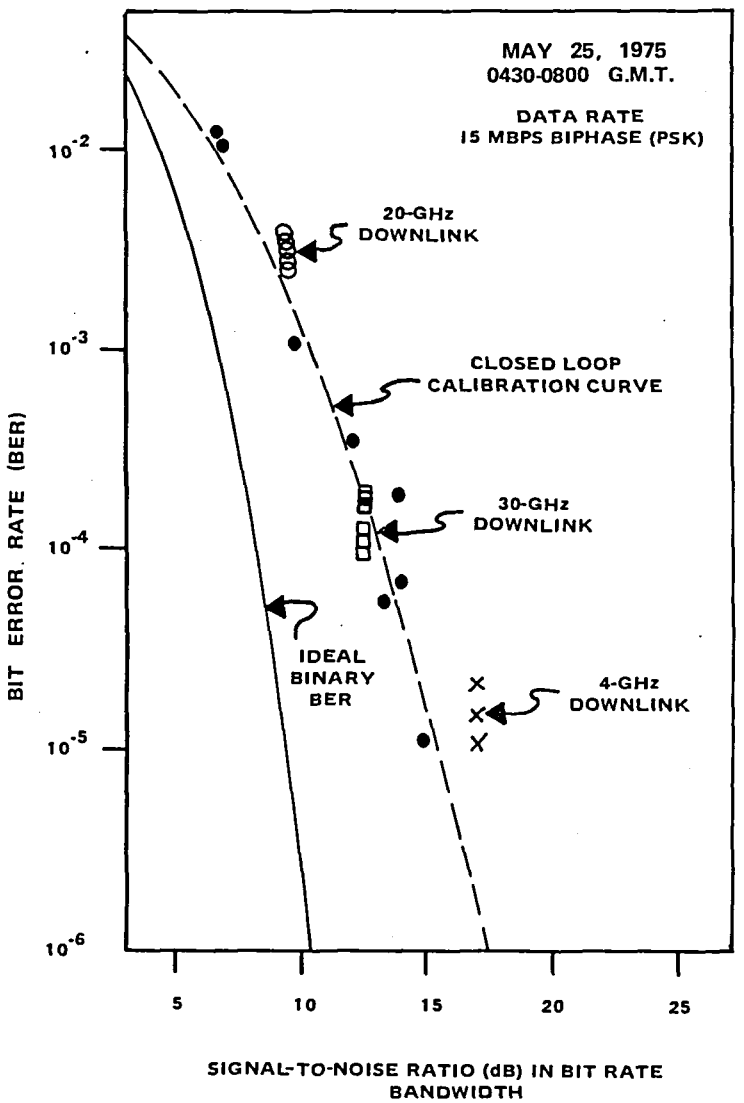

Figure 10-33. Digital Communication Link Measurements

An example of a 20-GHz differential phase measurement during a rain event is shown in Figure 10-34. Computer plots of the minutely averages of the highest sideband (±720 MHz) attenuation is also shown. The dots above the minutely averages denoted by the solid lines are the minutely standard deviation for each of the respective minutes. Almost perfect correlation exists between the attenuation plots showing that no selective fading exists for these conditions. Also the close tracking of the differential phase with the sideband attenuation shows that the phase characteristics were more a function of attenuation than the dispersive phase properties of the channel. This was probably an equipment limitation rather than a propagation phenomenon.

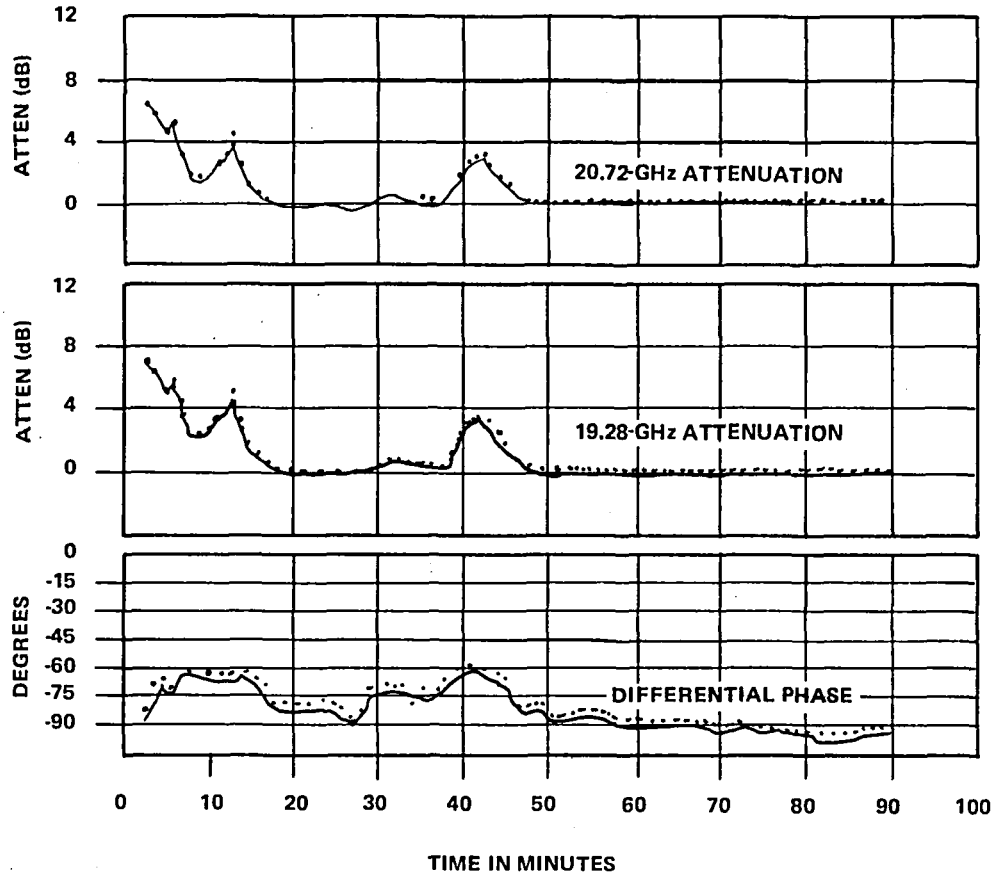

Figure 10-34. Differential Phase Measurements at 1440 MHz, Rosman Ground Station, August 9, 1974

An attempt was made to characterize the channel using a spectrum analyzer and analog tape recordings. Carrier autocorrelation functions and sideband pair crosscorrelation functions were computed from the recorded analog data. However, it was found that poor estimates of the autocorrelation function were obtained from the spectrum analyzer. This is because for all physically realizable signals, the maximum value of the function must occur at a $\tau = 0$. The correlation function is denoted by $\delta(\tau)$. The given requirement includes signals with d.c. components. Certain estimates of the autocorrelation function do not have this characteristic [i.e., $\delta(\tau)_{MAX} = \delta(0)$]. The reason for this is that very low frequency periodic components of significant amplitude were present in the signal. This has been demonstrated by power spectral plots of significant resolution to identify the very low frequency periodic components. These components are one cause of the nonstationary nature of the signal.

In dealing with sampled data systems with equally spaced sampling intervals, all frequencies down to zero are transmitted and special precautions must be taken. Serious attention must be given to the very low frequency components. It is required to distinguish between power at zero frequency and power density at zero frequency. The power spectrum of a stationary random process *with zero*

mean may have finite power density at zero frequency without having finite power there. However, finite power at zero frequency may be introduced into the data in measurements. It would be desirable to filter out the power at exactly zero frequency because of random stationary process, but this cannot be done perfectly.

In comparing the results from the spectrum analyzer and the digital program, it is important to remember that for the digital program, the overall mean for the record time length has been subtracted from each measurement before the mean lag products are calculated. In the spectrum analyzer, the mean is estimated from the previous record length and a certain percentage of the current record length rather than from the mean of the total present record. For slowly changing means, this difference in estimation can be significant. By eliminating input signals with significant low frequency periodic components, better estimates of the correlation function are possible.

The result of low frequency periodic components in the correlation functions make it extremely difficult to get a time picture of the channel behavior for the longer time records (102.4 sec). This is because of the poor estimates of the correlation function for nonwide sense stationary conditions over the long time periods.

Signal Depolarization

Virginia Polytechnic Institute (VPI) at Blacksburg, Virginia, was the main experimenter of signal depolarization for the ATS-6 Propagation Experiment. Because of various operational difficulties, a very limited amount of data was obtained and processed. The best data about the depolarization effect were obtained from a storm that occurred on March 30, 1975. The data are shown in Figure 10-35 and indicate the peak cross-polarization ratio (CPR) value was -25 dB. The striking feature of these data is the strong correlation between the rain-rate peaks and the CPR peaks. This is unlike what is usually observed on terrestrial radio systems where the attenuation and CPR are not well correlated with each other during the rain event. In another rain storm in which attenuation and rain rate values exceeded 14 dB and 80 millimeters per hour (mm/hr), no measurable CPR was detected. The only explanation offered for this effect is that the polarization angle was so close to vertical that the incident electric field was aligned with the rain drops minor axes, and so there was no depolarization.

Depolarization and signal attenuation due to snow is not generally accepted by all researchers in the field. However, researchers at VPI have concluded that these two phenomena did, in fact, occur during an intense snow storm that occurred from November 30, 1975 to December 2, 1975. Selected data from that storm are shown in Figure 10-36 for two different polarization angles. The effect of varying these angles was to change the residual CPR. At -19.5 degrees, it is no greater than -33 dB. At -16.5 degrees, it is no greater than -28 dB. The mechanism for causing the depolarization and attenuation is not presently known; however, it was concluded that the phenomenon is a function of the intensity of the snowflakes and the density of the clouds.

During the ATS-6 transition period, the depolarization effects caused by low elevation angles were measured at VPI. At an elevation angle of 5.35 degrees, it was noted that the CPR rose sharply and

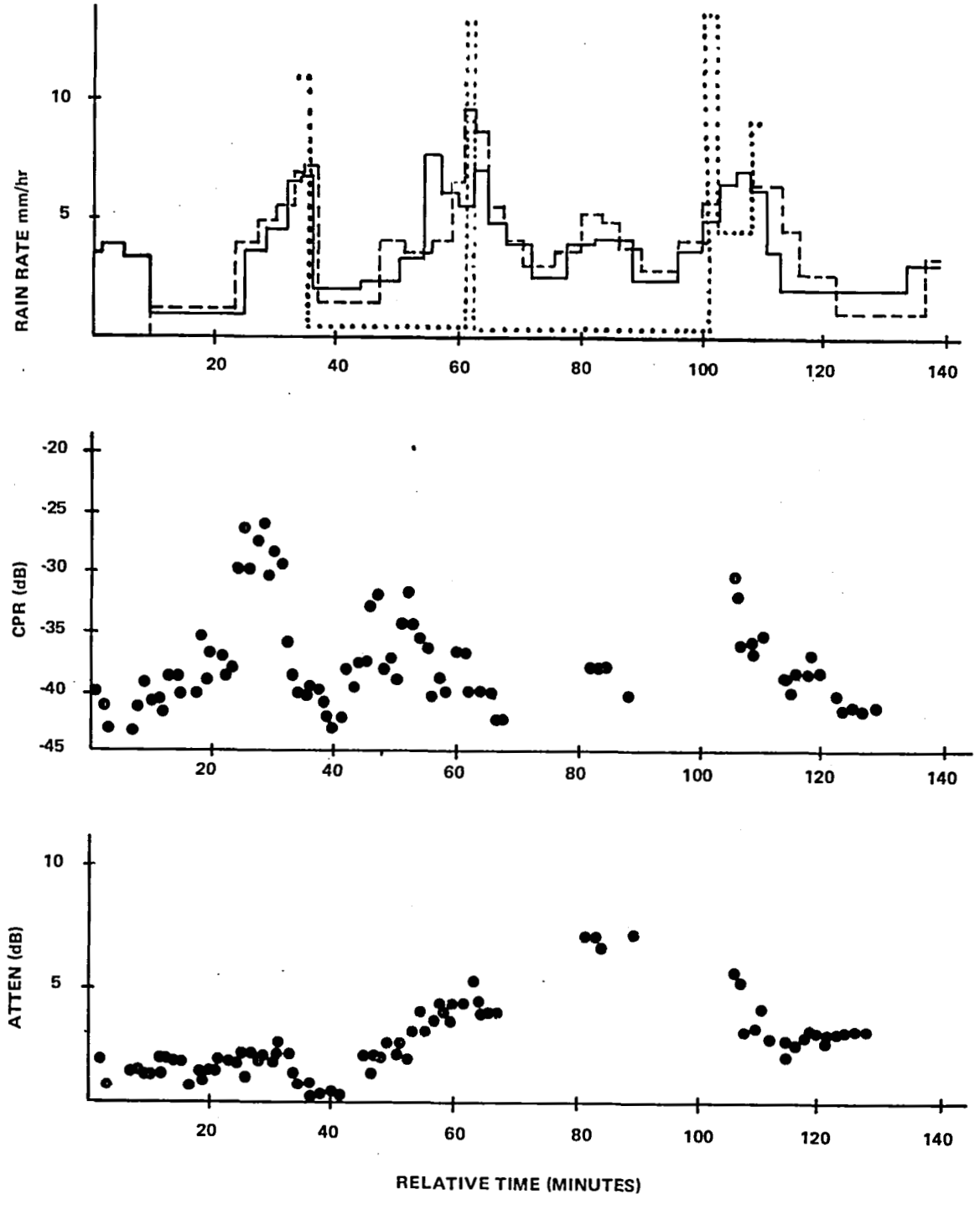

Figure 10-35. Rain Depolarization Data from the Storm of March 30, 1975

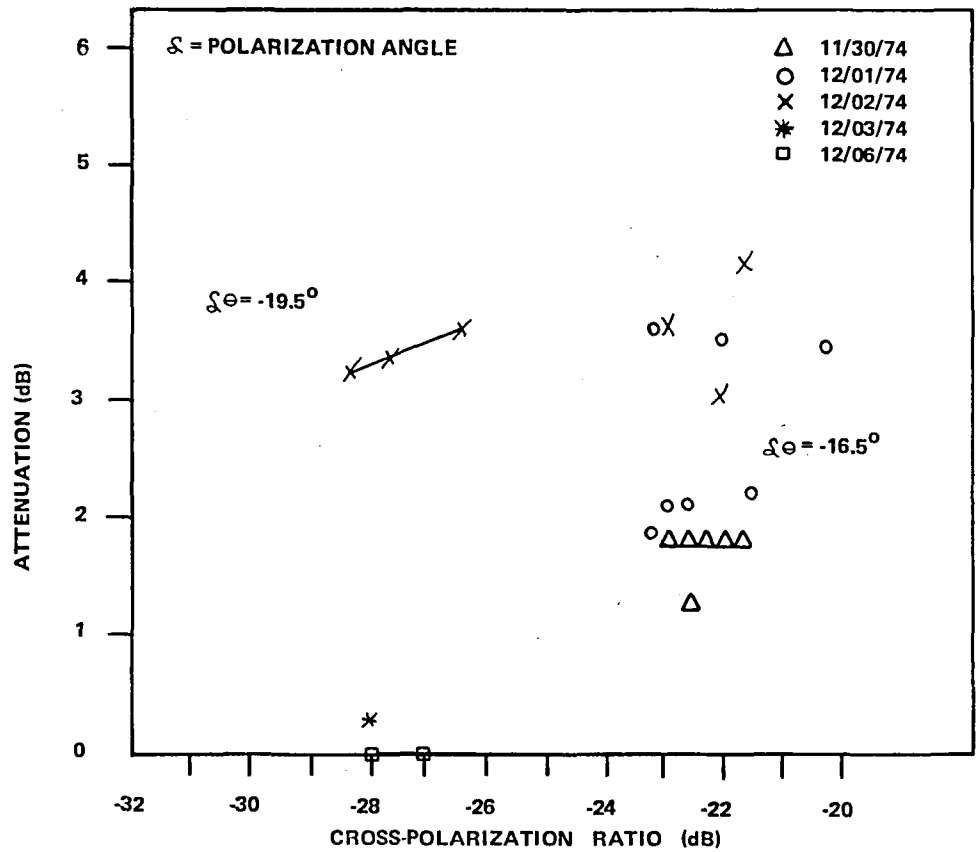

Figure 10-36. Cross-Polarization Ratio vs. Attenuation for Snow Storm of November 30 Through December 2, 1975 and the Period Following the Storm

peaked at about -12 dB. This value was measured for about 40 minutes. After an equipment check, it was determined that the high CPR value was because of severe multipath. It was concluded that the large increase in the cross-polarized signal was due to the shape of the cross-polarized pattern of the antenna that has a sharp null on axis. For the same incident polarization, a signal arriving off-axis will be out of the null and the antenna will receive a larger cross-polarized component than it would if the signal came in on-axis. Therefore, an important parameter of the depolarization process is the angle-of-arrival of the incident energy. It could be concluded that multipath depolarization is potentially a more serious problem at low elevation angles than is rain depolarization.

For relatively high elevation angles, signal depolarization is due mainly to rain and ice. The statistics of the depolarization events can be estimated by using Equation 9-10 (Chapter 9) and the measured cumulative attenuation statistics. An example of these statistics for the Rosman Ground Station while observing the 20-GHz ATS-6 beacon are shown in Figure 10-37. The ATS-6 signal was nearly vertically polarized (within 20 degrees of vertical). For these conditions the empirically determined constants were found for Equation 9-10 from which the depolarization statistics were determined as shown in Figure 10-37. For low A_t values, ice effects will start to become a factor. It was empirically

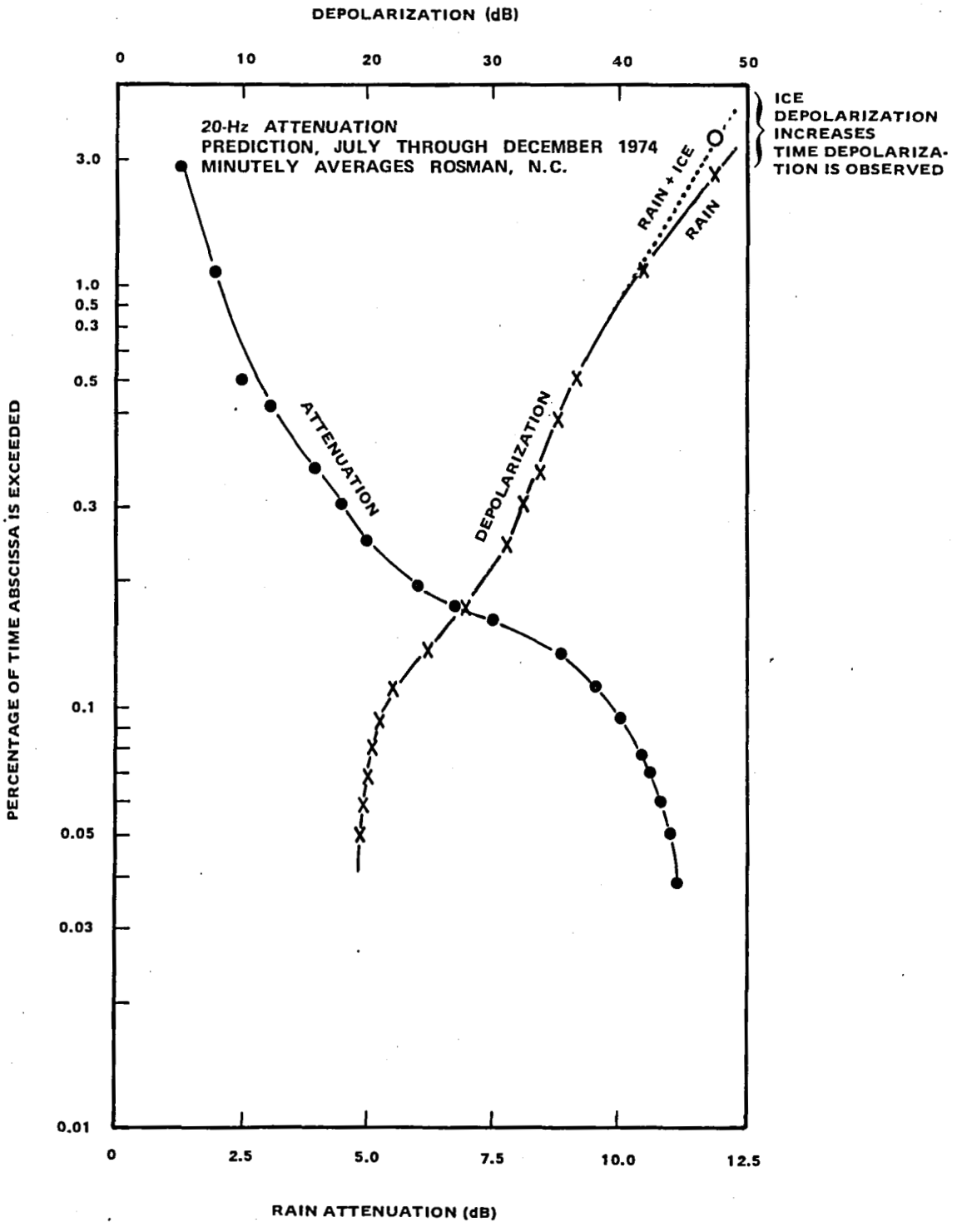

Figure 10-37. Attenuation and Depolarization Statistics for Rosman Ground Station

determined that at an A_t of 1 dB, about 30 percent more cross-polarization ratio events occur because of ice and rain, then just rain alone. This has an effect of increasing the percentage values as shown in Figure 10-37. When A_t is greater than 3 dB, only rain effects need be considered.

The European experimenters obtained a large amount of definitive information with regard to the signal depolarization process. They found correlations between the process and the amount of rain and ice in the elevated beam. Mixtures of rain and ice can also cause severe depolarization effects. It was concluded at the ground station at Ipswich, England, that ice depolarization is a more important factor than rain for a satellite-Earth link. The highest cross-polarization levels recorded due to rain were 21 dB at 20 GHz and 11 dB at 30 GHz with corresponding attenuation values of 6 dB and 16 dB. For ice depolarization, 18-dB level was measured for an attenuation of 2.1 dB at 20 GHz. At 30 GHz, the level was 14 dB with an attenuation of 1 dB. The dB level for the depolarization effect varied inversely with the intensity of the effect.

The phase difference between the copolar and cross-polar signals was measured to determine if the parameter could be used to measure the effect of the depolarization process. The station at Leeheim, Germany, did find that the phase difference was a function of the depolarization process; however, the data base was too small to obtain a meaningful relationship.

Abrupt changes in the cross-polarization effect were noted during thunderstorms at the ground stations in Bradford, England. A time plot of one of these events is shown in Figure 10-38. A meteorological radar was operating at the time and its return showed a bright band in the 9- to 10-km region with no rain at lower ranges. Hence, the cause of the depolarization must have been because of ice at ranges above 10 km. The point discharge current from a current probe showed that the peak cross-polar signal level occurred exactly at the time of a lightning stroke. Also the relative phase between the cross and copolar signals was exactly at 90 degrees. This phase corresponded to a lossless dielectric medium with differential phase shift. It was concluded that the abrupt changes in the cross-polar signal level were due to highly oriented ice particles that realigned at sudden changes of field experienced during a lightning stroke.

REFERENCES

1. Ippolito, L. J., "Effects of Precipitation on 15.3 and 31.65 GHz Earth Space, Transmissions with the ATS-5 Satellite," Proc. IEEE, Vol. 59, No. 2, February 1971, pp. 189-205.

2. Oguchi, T. and Y. Hosoya, (1974), "Scattering Properties of Oblate Raindrops and Cross Polarization of Radio Waves due to Rain (Part III) Calculations at Microwave and Millimeter Wave Regions," *Journal of the Radio Research Laboratories*, 21, No. 105, pp. 191-259.

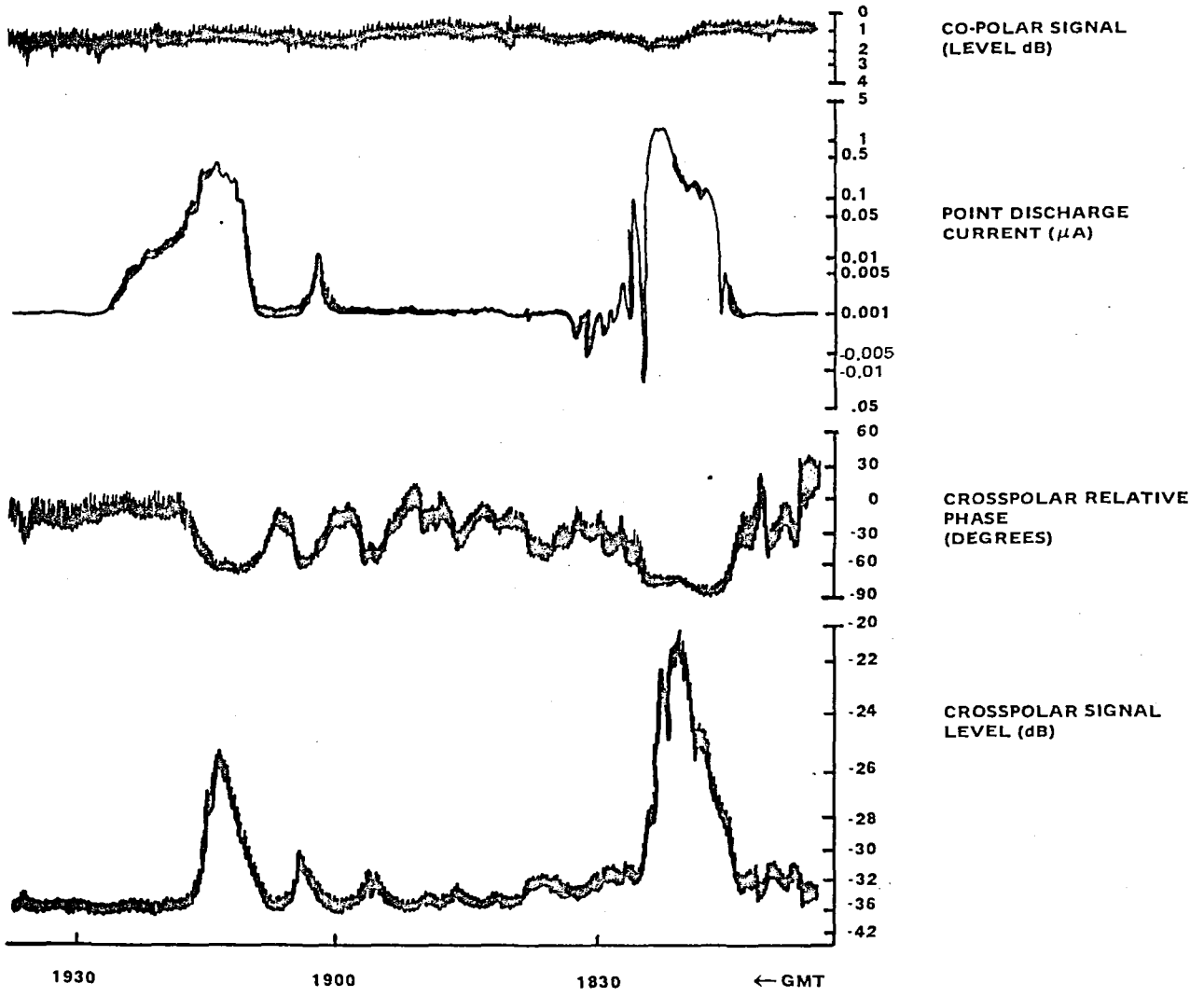

Radar was operational in a self-triggering mode, but bright band was close to edge of radar range setting (10 km). No reflections below 10 km were observed until just after this satellite session when radar triggered on heavy rain. Note near 90 degrees relative phase for ice particle cross-polarization.

Figure 10-38. Ice Particle Cross-Polarization Event Showing Correlation with Point-Discharge Current (Drawn on a True Logarithmic Scale)

CHAPTER 11

SIGNIFICANT EXPERIMENTAL RESULTS AND CONCLUSIONS– MILLIMETER WAVE PROPAGATION AT 20 AND 30 GHz

INTRODUCTION

The results of the propagation experiment have shown that a number of factors must be considered in the design of future systems that will use the 20- to 30-GHz frequency band on a space-Earth link. Because propagation parameters are an important consideration, link service time is the first factor to consider. If times of 99 percent or less are adequate, then minimal system margins due to precipitation effects need to be considered. The main propagation consideration would be from clear weather scintillation and the deleterious effects of operating at low elevation angles. If higher service times are required, then the system degradations from propagation effects in both clear sky and precipitation conditions must be considered. Hence, from a propagation standpoint, both service time and the required operating elevation angles are the primary system parameters that will determine the magnitude of the propagation effects on the system.

CLEAR WEATHER PROPAGATION EFFECTS

The propagation effects during clear weather are a critical function of elevation angle and frequency. Above 5 degrees, signal scintillation tends to be small compared to the line-of-sight signal and does not vary more than 10 dB over an elevation angle range of 5 degrees to about 45 degrees. There is a gradual decrease in scintillation activity as the elevation angle increases. In this angle range, scintillation activity increases by about 2.5 dB as the frequency increases from 20 GHz to 30 GHz.

From elevation angles lower than 5 degrees, various propagation phenomena become a factor in system performance. There was a measurable increase in scintillation activity and the frequency effects were not as pronounced. The median signal level tended to decrease in addition to the signal scintillation effects. Measured 13.2-GHz values were about 3 dB lower than the predicted clear sky signal strength. At 30 GHz, the median signal level decreased by a factor of 11 dB at an elevation angle of 2 degrees. At elevation angles below 3 degrees, the possibility of Rayleigh fading and pronounced scintillation activity can be expected.

Multipath effects due to the ground reflections or to tropospheric layer reflections add to the detrimental effects of a heterogeneous atmosphere. This additional factor tends to increase the detrimental propagation effects for low elevation angles as discussed previously. In addition, a large increase in signal depolarization is possible as a direct result of this multipath phenomenon. In fact, the multipath effect on signal depolarization was much more pronounced than the effect of rain. In summary, low elevation angle operation should be avoided to minimize the subject propagation effects during clear weather.

PROPAGATION EFFECTS DUE TO PRECIPITATION

When operating in the 20- to 30-GHz frequency band during periods of precipitation, a measurable amount of signal attenuation will be noted. The magnitude of this attenuation will be a function of elevation angle (path length through the rain environment), frequency, and the number and size of the raindrops (measure in rain rate) within the elevated beam. The attenuation in dB at 30 GHz will be about 2.5 times higher than the attenuation at 20 GHz. The magnitude of the system margin required to operate during this attenuation period will be a critical function of the required system service time, the operating frequency and the time period of the attenuation probability distribution in which the required system margin is determined.

System margin levels as a function of service times can be determined from a conditional cumulative probability distribution. These distributions are computed from the measured rain fades and from the total period of precipitation in which the fades were measured. For a given probability of occurrence, the fade level is a function of the precipitation patterns within the time period for which the distribution was computed. For a yearly period, the fade levels will be less severe than for a worst month period. Because of the limited test time available in the experiment, the distributions were only computed from the actual time period in which rain measurements were taken. Hence, the stated values will be higher than values obtained from an overall yearly period but could be lower for values obtained from a worst month period.

If it is assumed that the space-to-ground link has a system margin of 10 dB, the maximum link service time will be defined for a given period of precipitation. For cumulative probability distributions computed for the total precipitation period, the Rosman data show a service time of 95 percent for the 30-GHz frequency and 99.2 percent for the 20-GHz frequency. If path diversity is employed, where the site separation is at least 10 km, then the service times for the 30- and 20-GHz links will be increased to 99 percent and about 99.99 percent, respectively. This increase is due to a 10-dB diversity gain.

If the cumulative probability distribution is computed on the basis of the total time period in which rain attenuation measurements would have been taken, the University of Texas data show that for the 30-GHz link and a fade margin of 10 dB, the service time would be 99.83 percent. For a 10-dB diversity gain, the service time can be increased to 99.924 percent. This increase of service time of 0.094 percent can only be attained by a large increase in system complexity. For the 20-GHz link and a fade margin of 10 dB, the resulting service time would be 99.942.

The above statistics were computed from attenuation data taken at relatively high elevation angles. At the North Carolina and Texas stations, the elevation angles were 47 degrees and 54 degrees, respectively. These high angles tend to decrease the path length through the region of precipitation. For systems that operate at lower angles, the fade margins must be increased, especially at the low and intermediate values at attenuation.

If a dual channel space-to-Earth link that uses polarization discrimination is desired, then linear polarization rather than circular polarization should be employed. The degree of crosstalk between channels due to depolarization will be a function of the operational elevation angle and the intensity

of the rain and/or ice within the elevated beam. Depolarization statistics can be developed to determine the percentage of the operational time that depolarization phenomena will degrade performance.

If wide bandwidths are required for the system, values on the order of 1440 MHz can be employed without any selective frequency fading within the band. Also, no phase nonlinearity across the test band should be expected from propagation effects.

PASSIVE MEASUREMENTS OF RAIN ATTENUATION

The ATS-6 and other propagation experiments have shown that sky temperature measurements can be employed to predict rain attenuation up to levels of about 10 dB. This limit is determined by the rate that the sky temperature approaches the mean temperature of the absorbing rain medium. This rate increases as the operating frequency increases. To minimize this limit effect, it is best to obtain sky temperature measurements at lower frequencies, and then to determine the corresponding attenuation at higher frequencies by using the frequency scaling techniques. The method of obtaining attenuation statistics at a given locale is very economical when compared to direct signal measurement from a satellite.

SUMMARY OF CONCLUSIONS

Introduction

The ATS-6 Millimeter Wave Experiment (MWE) was the first experiment to obtain direct 20- and 30-GHz signal measurement on a space-Earth link. Participants in the experiment included 11 locations within the United States and 7 locations within the continent of Europe. The propagation effects that exist in a space-Earth link were determined by measuring various signal and meteorological parameters. The signal parameters that were investigated consisted of signal scintillation, rain attenuation, frequency scaling, path diversity, communications parameters, coherence bandwidth, and signal depolarization. The meteorological parameters that were measured and used to describe the actual environment consisted of sky temperature, meteorological radar returns, rain rate, and wind speed and direction.

The quantity and quality of the data were affected by various system malfunctions and operating conditions for the overall satellite system. The largest single detrimental factor that affected the experiment was the priority system that was set up to accommodate all experimenters. Because of the low priority given the ATS-6 Millimeter Wave Experiment, the satellite was not available at times when periods of precipitation occurred at the 18 locations in Europe and the United States.

The system factors that affected the results of the experiment were as follows:

1. After launch, it was determined that the 20-GHz horn traveling wave tube amplifier was inoperative; therefore, wide-angle coverage over an area similar to the United States was not available at 20 GHz.

2. The Polaris sensor on the satellite failed in September of 1975, resulting in reduced satellite stability in yaw. This affected signal depolarization measurements.

3. The 20-GHz satellite transmitter for the parabolic antenna failed in June of 1976.

Signal Scintillation

Signal scintillation was caused by the variation of the amplitude, phase and angle-of-arrival of the signal as it propagated through the troposphere. Scintillation effects were minimized during clear weather and for elevation angles greater than 10 degrees. Scintillations on the order of 2 dB peak-to-peak were measured when various types of clouds intercepted the elevated beam.

As the operational elevation angle decreased, an increase in scintillation activity was noted. Abrupt increases occurred in the region of 3 degrees. The scintillation at 30 GHz was always higher relative to the 20-GHz activity. At elevation angles above 10 degrees, it was about 4.4 dB higher. The frequency differences tended to decrease below 10 degrees. Spectral measurements of the scintillation indicated that the majority of measurements were below 2 Hz.

Below an elevation angle of 3 degrees, excess signal attenuation and scintillation activity increased relative to what was measured at 21 degrees. Also, there was evidence of Rayleigh fading in which fade levels in excess of 20 dB occurred.

Rain Effects

Rain Attenuation

Signal attenuation due to rain is mainly a function of the amount of water in the elevated beam and the distribution of its drop sizes. Since rain rate is easily measured, this parameter, along with the assumed path length through a rain environment, were used to predict the magnitude of the signal attenuation.

Measured signal attenuation A_t due to rain is usually presented in the form of time plots from individual rain events. For data accumulated over a given time period, the method of presentation is a cumulative probability distribution. Examples of the magnitudes of the measured fades and the corresponding percentages of time in which these respective fades were exceeded for the measurement period for three test stations are as follows:

Station	Measurement Time	Attenuation	Percentage
Univ. of Texas	425160 minutes (total)	25 dB (30 GHz)	0.058
NASA Greenbelt	665 minutes	14 dB (20 GHz)	0.09
GSFC	665 minutes	38 dB (30 GHz)	0.08
NASA Rosman	933 minutes	15 dB (20 GHz)	0.06
Station	1117 minutes	32 dB (30 GHz)	0.01

Rain attenuation statistics for the European experimenters showed lower attenuation values, even though the elevation angles were generally half of the operational angles employed for the U.S. stations. This implies a longer path length through the storm for the U.S. stations. The statistics for the Ipswich, England, station gave peak attenuation values of 16 dB and 7 dB for the 30- and 20-GHz frequencies, respectively. This is approximately half of what was obtained by the U.S. experimenters. Part of the problem could have been inaccessibility of the spacecraft during storm periods in Europe. Peak attenuation values of only 10 dB at 30 GHz were measured at the station in Leeheim, Germany.

On the basis of one storm event, there does not appear to be a functional relationship between point rain rate and measured attenuation. However, over a long-term basis of a number of storm events, such a relationship could exist. A relationship can be developed from concurrent long-term cumulative probability distributions of rain rate and attenuation. Rain values (rain rate and attenuation) of these parameters can be obtained for constant values of the probability of occurrence. By performing a least mean square fit of the pair values to the function $c(RR)^d$, it is possible to obtain a functional relationship between path length, L, rain rate, RR, and attenuation. From these relationships, it has been determined that L is a function of RR. For values of RR less than about 20 millimeters per hour (mm/hr), L tends to increase at a high rate as the rain rate decreases. For high values of RR (greater than 20 mm/hr), L tends to approach a constant value of about 1 kilometer (km) as the rain rate increases. This latter result stems from the fact that high rain-rate values always occur in regions of limited extent.

Because rain attenuation is due mainly to an absorption process, sky temperature measurements have a high degree of correlation with resulting signal attenuation. As a result, signal attenuation can be accurately predicted from sky temperature measurements. The maximum limit of this prediction is about 10 dB. This occurs at a point where the sky temperature is within 90 percent of the mean absorption temperature.

Frequency Scaling

Frequency scaling is the technique of predicting the attenuation at one frequency from the measured attenuation at another frequency. Three different techniques were investigated in this experiment and consisted of (1) empirical scaling, (2) specific attenuation scaling, and (3) Gaussian rain distribution scaling. The ratio of the measured data A (30)/A (20), 20-GHz attenuation A (20), and 30-GHz attenuation A (30), falls within the bounds of 2.5 to 3, whereas the specific attenuation and empirical scaling methods predict values in the 2 to 2.5 region. The Gaussian rain distribution technique predicts slope values greater than 2.5 for low values of the measured attenuation. In prediction technique (2) and (3), the ratio value gends to decrease as the attenuation values increase and tend toward a limit of 2.

Attenuation ratio values obtained at Leeheim, Germany, for A (30) and A (11.4) were 4.14 and 6.7 for A (11.4) values of 1 and 7 dB. Good correspondence was obtained from a U.S. station for the 4.14 ratio; however, there is a divergence of trends between the German and U.S. methods for varying values of the lower attenuation. The German results show an increasing ratio value as the attenuation increases and the U.S. results show the opposite trend. More data are required to resolve the problem.

Path Diversity

The concept of path diversity was developed to achieve the desired level of system reliability at a reasonable cost. The concept is based on the hypothesis that rain cells and, in particular, the intense rain cells that cause the most severe fading are limited in spatial extent. The parameters used to specify the space diversity improvement are the diversity gain, E, and the diversity improvement, I. E can be interpreted as the reduction in the required system margin at a particular percentage of time. I can be interpreted as the factor by which the fade time is reduced at a particular fade level. E and I are functions of the site separation distance, d, and the magnitude of the attenuation. E and I will increase almost linearly up to a value of d of about 10 km and asymptotically approach a limit. This limit corresponds to the distance at which uncorrelated fading at the individual Earth terminals occur.

At a site separation distance of about 13 km, E factors of 0.5 dB up to 10.5 dB were obtained for attenuation values of 2 dB and 14 dB, respectively. These results were obtained at Ohio State and Texas Universities for a 30-GHz test frequency. The ground stations located at Slough, England, also performed diversity experiments for d values of 2, 10.3, and 12.3 km. From this experiment, it was concluded that site location is much more important than site separation. Placement of a site in hilly terrain will enhance rain production. Placement of the other site in flat terrain will tend to reduce E, because if it is raining at the latter site, then it is probable that it is also raining at the hilly site. Both stations should be placed in flat terrain where the probability of rain at one site will be lower if it is raining at the other site.

Meteorological Radar Considerations

A multifrequency meteorological radar operating at frequencies of 3 GHz and 8.75 GHz, respectively, was used at NASA's Rosman Ground Station to measure meteorological conditions that existed in the elevated path at the time rain attenuation measurements were being performed. Rain rate and attenuation within 255-100 meter range intervals were measured by relating the backscatter power to the reflectivity of the rain. This reflectivity, in turn, was related to the scattering of the incident wave by the raindrops.

Rain-rate predictions within a given range bin were compared to measured rain-rate values obtained from a tipping bucket. Good correlation was obtained for low rain-rate values where the spatial difference between the bucket and the range bin was small. As the distance increased, the correlation decreased, even though the peak rain-rate values tended to track at a given time displacement.

The accuracy of using the radar for attenuation prediction was affected by the following factors: (1) errors in radar calibration, (2) high returns from the zero degree isotherm region that produced relatively low attenuation levels, and (3) two-way attenuation of the radar signal as it traversed the distance between a range bin and the radar antenna.

Attenuation prediction results have shown that the 3-GHz frequency gave the most accurate results because factor (3) was lower than in the case of the 8.75-GHz frequency. The second factor caused an over prediction and the first factor could cause either an under or over prediction of attenuation.

A 9.4-GHz radar was used at the Bradford station in England to predict attenuation. The results of the experiment show that to obtain good accuracy, the attenuating medium must be characterized by three regions: (1) rain region, (2) zero degree isotherm region, and (3) the region beyond the zero degree isotherm region. Each region would have its own characteristic attenuation versus reflectivity factor relationship.

Communication Parameters

Television and digital signals were transmitted over the space-Earth link using a 6-GHz uplink and 4-GHz, 20-GHz downlinks. Tests on the color video link showed that good quality pictures were obtained when using the 20- and 30-GHz frequencies relative to the 4-GHz downlink.

For the digital test, a two-channel (four phase) unbalanced direct mode, with one channel at a rate of 10 megabits per second (Mbps) and a second channel at a 1-Mbps rate, was tested. In addition, a 15 Mbps biphase (differentially encoded) and a 20-Mbps/20 kbps two-channel quadriphase transmission was also tested.

System problems affected the operation of the system more than the propagation effects of the downlink. Generally, the test results were within 2 dB (E_b/N_o) of the calibration curves (obtained during the field-loop tests). It should be noted, however, that the field-loop test results were worse than those obtained at Goddard Space Flight Center, which was probably caused by the noisy operational environment in the field.

The quadriphase telemetry transmission tests were the first digital transmission tests using the ATS-6 MWE links. From the results obtained, it was concluded that the K-band links can support a telemetry transmission rate in excess of 15 Mbps using biphase modulation and in excess of 30 Mbps using quadriphase modulation. In addition, C-band links provide a 20-Mbps biphase telemetry transmission capability.

Coherence Bandwidth

Tests were performed to determine if any frequency selective properties existed in amplitude and/or phase of a 1440-MHz bandwidth over 20- and 30-GHz links. Nine distinct tones at each frequency were transmitted. Digital and analog techniques were employed to measure the dispersive properties of the channel.

For the digital phase, four-second mean values of attenuation of the nine tones were employed. From the results, it was concluded that no dispersive propagation effects were present over the 1440-MHz bandwidth.

For the analog phase, a spectrum analyzer was employed to measure autocorrelation functions and cross-correlation functions using the recorded analog signals of the nine tones. These distinct functions were then used to develop an overall correlation function that was a measure of the dispersive properties of the link. Only distorted correlation functions were obtained, because the signals were nonstationary. This was caused by the presence of very low frequency components in the signal that caused the mean of the signal to vary as a function of time.

Signal Depolarization

Depolarization or changes in the polarization sense of a transmitted signal results from the nonspherical shape of raindrops, snowflakes, and ice crystals that are present in the propagation path. Also, multipaths and adverse refractive effects produce the phenomenon. It is generally agreed that circular polarization will produce the highest depolarization effect because on the average its polarization angle is oriented about 45 degrees from the major and minor axes of the oblate spheroid.

Virginia Polytechnic Institute, which was NASA's chief investigator of the depolarization process, measured cross polarization ratios (CPR) of -25 dB during a heavy rainstorm at a high elevation angle. Nominal CPR values were about -43 dB. CPR values of -28 dB were also measured during an intense snowstorm. High CPR values of -12 dB were measured at low elevation angles of about 5 degrees. It was determined that the high CPR values were mainly due to severe multipath.

The European experimenters also obtained depolarization measurements under conditions of rain, ice, and lightning discharges. The English experimenters concluded that ice depolarization is a more important factor than rain for a satellite-Earth link. The highest CPR values recorded for rain were -21 dB at 20 GHz and -11 dB at 30 GHz with corresponding attenuation values of 6 and 16 dB. For ice depolarization, CPR values of -18 dB for 20 GHz and -14 dB for 30 GHz were obtained. The corresponding attenuation values were 2.1 dB for 20 GHz and 1 dB for 30 GHz. CPR levels during a lightning discharge reached a peak of -20 dB.

APPENDIX

ACRONYMS AND ABBREVIATIONS

A

A	ampere
Å	Angstrom
ABC	analog backup controller
AC	attitude control
a.c.	alternating current
ACE	actuator control electronics
ACP	acquisition control program
acq.	acquisition
ACS	attitude control subsystem
ACSN	Appalachian Community Service Network
A/D	analog to digital
ADC	analog-to-digital converter
ADPE	automatic data processing equipment
ADS	automatic deployment sequencer
ADSS	auxiliary digital Sun sensor
ADVM	adaptive delta voice modulation
A/E	absorbtivity to emissivity
Aerosat	aeronautical satellite
AES	Ahmedabad Earth Station
AESP	Appalachian Education Satellite Project
af	audio frequency
AFC	automatic frequency control
AFTE	Advanced Thermal Control Flight Experiment
AGC	automatic gain control
AGE	aerospace ground equipment
Ah	ampere-hour
AID	Agency for International Development
AIDSAT	Agency for International Development Television Demonstration
AIR	All India Radio
ALC	automatic level control
ALED	Alaska Education Experiment
am, AM	amplitude-modulation
AMP	amplifier
AOS	acquisition of satellite
APM	antenna pattern measurement

APT	automatic picture transmission
ARC	Appalachian Regional Commission
ASC	Aerospace Corporation
ASP	automated sequential processor
ASSY	assembly
ASTP	Apollo-Soyuz Test Program
ASTP-TV	ASTP television coverage experiment
ATA	automatic threshold adjust
AT&T	American Telephone and Telegraph (Spacecraft)
ATC	air traffic control, active thermal control
ATFE	Advanced Thermal Control Flight Experiment
atm, ATMOS	atmosphere(s)
ATS	Applications Technology Satellite
ATS-6	Applications Technology Satellite-6
ATSOCC	ATS Operations Control Center
ATS-R	ATS ranging
ATSSIM	ATS simulator
Atten	attenuator (attenuation)
Aux	auxiliary

B

B&E	Broadcast and Engineering
BAM	building attenuation measurement
BB	baseband
BER	bit error rate
bps	bits per second
BRC	Balcones Research Center
BSA	bit synchronization acquisition
BTC	binary time code
BTE	bench test equipment
Btu	British thermal unit
BW	bandwidth

C

C	Celsius
Cap Com	Capsule Communicator
CCIR	International Radio Consultative Committee
CDD	command/decoder distributor
CEE	designator for "career education course for elementary-grade teachers"
CES	designator for "career education course for secondary-grade teachers"
CESP	computer executive system program
CFSS	coarse/fine Sun sensors

CIC	command interface control
CIE	cesium ion engine
C/L	capacitance-to-inductance
cm	centimeter
CM	communications module
C/M	carrier-to-multipath
CMD	command
CMOS	complimentary metal oxide semiconductor
C/N_o	carrier power to spectral noise density ratio
CNR, C/N	carrier-to-noise ratio
cntr	center
Comsat	Communications Satellite Corporation
ConUS, CONUS	Continental United States
CONV	converter
COSMOS	complimentary symmetry metal oxide semiconductor
CPI	cross polarization isolation
CPR	cross polarization ratio
CPU	central processing unit
CRT	cathode-ray tube
CSM	command-service module
CSP	command service program
CSS	coarse Sun sensor
CTNE	Companie Telephonica Nacional de Espana
CW	carrier wave, continuous wave

D

DA	design adequacy
D/A	digital to analog
DACU	data acquisition and control unit
DAF	Data Acquisition Facility
dB	decibel
dBi	decibel isotropic (gain relative to an isotropic antenna)
dB/K	decibel per degree Kelvin
dBm	decibels referred to 1 milliwatt
dBW	decibel (reference level 1 watt)
DC	downconverter
d.c.	direct current
DCP	data collection platforms
DDDF	duplex digital data formatter
DDS	digital Sun sensor
DECPSK	differentially encoded coherent phase shift key (modulated)
DEG, deg	degree

DEM	digital evaluation mode
Depl	deployment
DES	Delhi Earth Station
DESA	double electrostatic analyzer
DIB	data input buffer
div	division
DIX	data interface transmitter
DJS	Dzhusaly (designator)
DLO	dual local oscillator
DM	docking module
DOC	digital operational controller
DOD	depth-of-discharge
DOT	Department of Transportation
DOT/FAA	The Department of Transportation/Federal Aviation Administration
DOT/TSC	The Department of Transportation/Transportation Systems Center
DPRI	diagnostic and prescriptive reading instruction
DR	Copenhagen (designator)
DRR	data recorder/reproducer
DRS	direct reception system
DSS	digital Sun sensor
DSU	data switching unit
DTS	data transmission system
DUT	Denver Uplink Terminal

E

EBU	European Broadcast Union
ECH	Earth-coverage horn
ECI	Earth centered inertial
e.d.t., EDT	eastern daylight time
e.i.r.p.	effective isotropic radiated power
EME	Environmental Measurements Experiments
emi, EMI	electromagnetic interference
EML	equivalent monomolecular layer
enc	encoder
Eng.	engineering
EOL	end-of-life
EPIRB	Emergency Position Indicating Radio Beacon
EPS	electrical power subsystem
ERP	effective radiated power
ES	Earth sensor
ESA	Earth sensor assembly, European Space Agency
ESA/PSA	Earth sensor assembly/Polaris sensor assembly
e.s.t., EST	eastern standard time

ETR	Eastern Test Range
eV	electronvolt
EVM	Earth-viewing module
EVT	Eupatoria (designator)

F

f	frequency
F	Fahrenheit
FAA	Federal Aviation Administration
FCC	Federal Communications Commission
FCHP	feedback-controlled variable conductance heat pipe
FCP	flight computer program
FCT	fixed calibration terminal
f/d	ratio of focal distance to diameter
FDM	frequency diversity modulation; frequency division multiplexer
fm, FM	frequency modulated
FOV	field-of-view
FOWG	Flight Operations Working Group
Freq.	frequency
FRMS	Federation of Rocky Mountain States
fsk	frequency shift keying
FSS	fine Sun sensor
ft	foot, feet
FT	frequency translation
ft-lb	foot-pound
FTO	functional test objective
FTS	Federal Telecommunications System

G

g	grams, gravity
G	gain
GAC	ground attitude control
GEOS-3	Geodetic Earth-Orbiting Satellite-3
GFRP	graphite fiber reinforced plastic
GHz	gigahertz
gm	gram
G.m.t., GMT	Greenwich mean time
GRD	ground
GRP	group
GSFC	Goddard Space Flight Center
G/T	dB/K antenna gain over system noise temperature
GTT	ground transmit terminal
GVHRR	Geosynchronous Very High Resolution Radiometer

H

HAC	Hughes Aircraft Company
HDRSS	high data rate storage system
HET	Health, Education, Telecommunications (experiment)
HEW	Department of Health, Education, and Welfare
hf	high frequency
HGA	high gain antenna
HI	Honeywell International
HPBW	half power bandwidth
HR	hour
HSE	high-speed execute
HTR	heater; high-time resolution
Hz	hertz

I

IBM	International Business Machines
IDT	image dissector tube
IEB	interface electronics box
i.f.	intermediate frequency
IFC	in-flight calibration
IHS	Indian Health Service (Alaska)
IHSDL	interferometer high speed data link
IM	intermodulation
IMF	interplanetary magnetic field
IMP	Interplanetary Monitoring Platform
in.	inch
in.-oz	inch-ounce
Intelsat	International Telecommunications Satellite
INTF	interferometer
I/O	input/output
IPD	Information Processing Division
IR	infrared
IRAC	Interdepartment Radio Advisory Committee
ISRO	Indian Space Research Organization
IT	intensive terminal
ITS	Institute of Telecommunications Sciences
ITU	International Telecommunications Union
I-V	current voltage
IW	inertia wheel
IZMIRAN	Institute of Terrestrial Magnetism, Ionosphere and Radio Wave Propagation

J

JAM	jet-assist mode
Joburg	Johannesburg (designator)
JSC	Johnson Space Center

K

K	Kelvin
kbps	kilobits per second
keV	kiloelectronvolt
kg	kilogram
kHz	kilohertz
km	kilometer
KSC	Kennedy Space Center
kW	kilowatt

L

lb	pound
LC	inductive-capacitance
LD	linear detector
LFT	long form test
LIC	load interface circuit
LLD	lower level discriminator
LO	local oscillator
LOS	line-of-sight
LRIR	limb radiance inversion radiometer
LSB	least significant bit
LT	local time
LV	local vertical
L.V.	latch valve

M

m	meter
m^2	square meter
mA	milliamperes
Mad	Madrid
MAD-HYB	Madrid Hybrid
Mage	U.S./U.S.S.R. Magnetometer Experiment
Marad	Maritime Administration
MASEP	main sequential program
Max.	maximum

MCC-H	Mission Control Center, Houston
MCC-M	Mission Control Center, Moscow
MDAC	McDonnell-Douglas Aircraft Corporation
MDHS	meteorological data handling system
MESC	magnetoelectrostatic plasma containment
MeV	megnelectronvolts
MHz	megahertz
μf	microfarad
μm	micrometer (micron)
μs, μsec	microsecond
MILA	Merritt Island Launch Annex
min, MIN	minute
mlb	millipound
MMW	Millimeter Wave Experiment
mN	millinewton
MOCC	Multisatellite Operations Control Center
MOCR	Mission Operations Control Room
MONO	monopulse
MOR	Mission Operations Room
MOS	metal oxide semiconductor
MSB	most significant bit
ms, msec	millisecond
m/s	meters per second
MT	multitone
mV	millivolts
mW	milliwatt
MWE	Millimeter Wave Experiment
MW XMTR	microwave transmitter

N

N	Newton
NAFEC	National Aviation Facilities Experiment Center
NASA	National Aeronautics and Space Administration
Nascom	NASA Communications Network
NBFM	narrowband frequency modulation
NCC	Network Coordination Center
NCE	normal command encoder
NDR	Hamburg (designator)
nm	nanometer
NMRC	National Maritime Research Center
NOAA	National Oceanic and Atmospheric Administration
N/P	negative/positive
NRL	Naval Research Laboratories

ns	nanosecond
NTSC	National Television System Committee color (U.S.)

O

O&M	operations and maintenance
OC	orbit control
OCJ	orbit control jet
OCP	operational control program
o.d.	outside diameter
OD	Operations and Distribution (Center)
omni	omnidirectional
OSR	optical solar reflectors
OSU	Ohio State University
OYA	Helsinki (designator)

P

PA	power amplifier, preamplifier
PAL	phase alternation live color (Europe)
PAM	pulse amplitude modulated
PAO	Public Affairs Office
PARAMP	parametric amplifier
PB	phonetically balanced
PBS	Public Broadcasting Service
P_c	course phase measurement
pcm, PCM	pulse code modulation
pcm/fsk/am	pulse code modulation/frequency shift keying/amplitude modulation
PCT	portable calibration terminal
PCU	power control unit
PDM	pulse duration modulation
pf	picofarad
PFD	power flux density
PFF	prime-focus feed
PGE	PLACE ground equipment
PIC	power interface circuit
PLACE	Position Location and Aircraft Communications Experiment
PLU	Project Look-Up
PM	phase-modulated
PN	pseudo-noise
POCC	Project Operations Control Center
p-p	peak-to-peak
PPK	Petropavlovsk-Kamchatski (designator)
ppm	parts per million

P_R	reference (phase) signal
P_{rgi}	power received at ground into an isotropic antenna
P_{rsi}	power received at spacecraft into an isotropic antenna
PRU	power regulation unit
PSA	Polaris sensor assembly
P_{SE}	probability function
psia	pounds per square inch absolute
PSK	phase shift keyed
Pv	vernier phase measurement
pW	picowatt
PWR	power

Q

QCM	Quartz-crystal microbalance contamination monitor
Q-M	quadrature phase modulation

R

Radsta	U.S. Coast Guard Radio Station
R&RR	range and range rate
RBE	Radio Beacon Expriment
RCA	Radio Corporation of America
RCC	Resource Coordinating Center
RCV	receive
RDA	rotating detector assembly
REC	receive
Ref., REF	reference
Rel	release
RESA	Regional Education Service Agency
rf	radio frequency
RFC	radio-frequency compatibility
rfi	radio frequency interference
RFIME	Radio Fequency Interference Measurement Experiment
RGA	rate-gyro assembly
RME	Rocky Mountain East
RMPBN	Rocky Mountain Public Broadcast Network
rms	root mean square
RMW	Rocky Mountain West
ROT	receive-only terminal
rpm	revolutions per minute
RR	rain rate

S

S/A	solar array
SAPPSAC	Spacecraft Attitude Precision Pointing and Slewing Adaptive Control (Experiment)
SAR	search and rescue
S&R	surveillance and ranging
Satcom	Satellite Communications
SC	sudden commencement
S/C	spacecraft
SCAMA	switching, conferencing, and monitoring arrangement
SCAMP	small command antenna medium power
SE	system effectiveness
sec, s	second
SECAM	Sequential Couleurs a Memoire (III) color (U.S.S.R.)
SEL	Space Environment Laboratory
SENS	sensor
S.G.	signal generator
SITE	Satellite Instructional Television Experiment
SITEC	sudden increase in total electron content
SIU	squib interface unit
S-IVB	Saturn IB second stage
SMSD	spin motor sync detector
SNR, S/N	signal-to-noise ratio
Spec	specification
SPS	spacecraft propulsion subsystem
SPU	signal processing unit
sr	steradian
SR	Stockholm (designator)
SRT	SAPPSAC remote terminal
SSC	sudden storm commencement
SSEA	Sun sensor electronics assembly
SSR	Staff Support Room
STA	station
STADAN	Space Tracking and Data Acquisition Network
STDN	Spaceflight Tracking and Data Network
STRUCT	structural
SWBT	Southwestern Bell Telephone Company
SYN	synthesizer
SYNC	synchronous
SYSSIM	system simulator

T

TACH	tachometer
T&CS	telemetry and command subsystem
T&DRE	Tracking and Data Relay Experiment
TART	transmit and receive terminal
TASO	Television Allocation Study Organization
TBC	time base corrector
TCD	transponder command decoder
TCS	telemetry and command subsystem, thermal control subsystem
TDA	tunnel diode amplifier
TDRE	Tracking and Data Relay Experiment
TEMP	temperature
THIR	temperature-humidity infrared radiometer
TID	traveling ionospheric disturbances
TLM, TM	telemetry
TORQ	torquer
TRUST	Television Relay Using Small Terminals
TSM	thermal structural model
TSP	telemetry service program
TSU	temperature (control) and signal (conditioning) unit
TT/N	test-tone signal-to-noise ratio
TTY	teletype
TV	television
TVOC	Television Operational Control Centers
TWT	traveling wave tube
TWTA	traveling wave tube amplifier

U

UC	upconverter
UCLA	University of California at Los Angeles
UCSD	University of California at San Diego
uhf	ultrahigh frequency
UK	United Kingdom
UKTV	University of Kentucky Television
ulf	ultralow frequency
UNH	University of New Hampshire
U.S.	United States
USA	ubiquitous spectrum analyzer
USAF	United States Air Force
USCG	United States Coast Guard
USK	Ussuruisk (designator)

U.S.S.R.	Union of Soviet Socialist Republics
UT	universal time
UV	ultraviolet

V

v	velocity
V	volt
VA	Veterans Administration
VCA	voltage controlled amplifier
VCHP	passive "cold-reservoir" variable conductance heat pipe
VCXO	voltage controlled crystal oscillator
Vdc	volts direct current
V/deg	volts per degree
Vert.	vertical
vhf, VHF	very high frequency
VHRR	very high resolution radiometer
VIP	versatile information processor
VIRS	vertical interval reference signal
VITS	vertical interval test signals
VPI	Virginia Polytechnic Institute
vs.	versus
VSWR	voltage standing-wave ratio
V/T	voltage/temperature
VTR	video-tape recorder
VU MTR	VU meter

W

W	watt
WAMI	Washington, Alaska, Montana, Idaho (medical education)
WBDU	Wideband Data Unit
WBVCO	wideband voltage-controlled oscillator
WHL, WH	wheel

X

XMIT	transmit
XMTR	transmitter
XTAL	crystal
XTAL DET.	crystal detector

Y

YIRU	yaw inertial reference unit

Z

ZAZ	Z-axis azimuth
Zcoel	Z-coelevation

BIBLIOGRAPHY

1. "Air Traffic Control Experimentation and Evaluation with the NASA ATS-6 Satellite," U.S. Department of Transportation, Report No. FAA-RD-75-173.

   Volume I "Executive Summary"

   Volume II "Demonstration of Satellite-Supported Communications and Surveillance for Oceanic Air Traffic Control," April 1976

   Volume III "Summary of U.S. Aeronautical Technology Test Program," September 1976

   Volume V "Multipath Channel Characterization Test," September 1976

   Volume VI "Modem Evaluation Test," September 1976

   Volume VII "Aircraft Antenna Evaluation Test," September 1976

2. Applications Technology Satellite-6, *IEEE Transactions on Aerospace and Electronic Systems*, Volume AES-II, No. 6, November 1975.

3. "Applications Technology Satellite ATS-6 Continuing Experiment and Spacecraft Evaluation," NASA/GSFC TMX-70907, April 1975.

4. Berman, A. L., Editor, "The ATS-F COMSAT Propagation Experiment Transponder," *COMSAT Technical Review*, Vol. 3, No. 2, Fall 1973.

5. Bostian, C. W., et al., "The Influence of Polarization on Millimeter Wave Propagation through Rain," Final Report, NASA Grant NGR-47-004-091, Virginia Polytechnic Institute, Blacksburg, Virginia, January 1974. (Available from NTIS as NASA CR-143686.)

6. Bostian, C. W., et al., "Final Report for a 20 GHz Depolarization Experiment Using the ATS-6 Satellite," Contract NAS5-21984, September 10, 1975.

7. "European Communications Experiments for L-Band with ATS-6," European Space Agency, Noordwijk, The Netherlands

   Volume I "PLACE, CW and Antenna Evaluation Experiments," January 1976

   Volume II "Aeronautical Experiments (TDM)," January 1976

   Volume III "Maritime Experiments Performed by ESTEC," March 1976

   Volume IV "Maritime Experiments Performed by NTNF-CNES-CNET," December 1975

BIBLIOGRAPHY (continued)

Volume V "Maritime Voice Experiments," January 1976

Volume VI "Distress Buoy, System Design, Instrumentation and Experiment," October 1975

Volume VII "European Communication Experiments in L-Band with ATS-6 in 1975 and 1976," June 1977

8. Gibbs, Bruce, "Results of the NASA/MaRad L-Band Satellite Navigation Experiment," Supplement to IEEE EASCON-77 Proceedings.

9. Harrold, T. W., "Estimation of Rainfall using Radar–A Critical Review," Meteorological Office, Scientific Paper No. 21, London, 1965.

10. Hess, G. C., "Land Mobile Satellite Path Loss Measurements," ATS-6 Experiment Final Report, Motorola, Inc., September 6, 1978.

11. Hodge, D. B., and R. C. Taylor, "The Ohio State University Electro-Science Laboratory Radar/Radiometer Facilities for Precipitation Measurement," Report 2374-13, The Ohio State University, Department of Electrical Engineering, March 1973.

12. Hogg, D. C., "Millimeter Wave Communications through the Atmosphere," *Science*, V. 159, 1968, p. 39.

13. Ippolito, L. J., "ATS-6 Millimeter Wave Propagation and Communications Experiments at 20 and 30 GHz," *IEEE Transactions on Aerospace and Electronics Systems*, Vol. AES-11, November 1975, pp. 1067-1082.

14. Ippolito, L. J., "The ATS-F Millimeter Wave Propagation Experiment," NASA TM X-65752, Goddard Space Flight Center, October 1971.

15. Ippolito, L. J., "20 and 30 GHz Millimeter Wave Experiments with the ATS-6 Satellite," NASA TM X-70994, Goddard Space Flight Center, August 1975.

16. Jakes, Jr., W. C., Editor, *Microwave Mobile Communications*, John Wiley and Sons, New York, 1974.

17. Kaul, R., "Prediction of Attenuation on Earth-Space Paths," ORI Inc., Silver Spring, Maryland 20901, NASA GSFC Contract NAS5-23438, Mod. 68, September 1978.

18. Kaul, R., et al., "Prediction of Millimeter Wave Propagation Effects on Earth-Space Paths (10-100 GHz)," Final Report, Goddard Space Flight Center, Greenbelt, Maryland 20771, December 1978.

BIBLIOGRAPHY (continued)

19. Laws, J. O. and D. A. Parsons, "The Relation of Raindrop Size to Intensity," *Trans. AM Geophys. Union*, Vol. 24, October/November 1943, pp. 452-460.

20. Lebow, I. L., et al., "Satellite Communications to Mobile Platforms," *Proc. of the IEEE*, Vol. 59, February 1971, pp. 139-159.

21. Maruschuk, J. and D. Nace, "A Portable L-Band Voice Transceiver for Satellite Communications," NASA Technical Memorandum TM78108, Goddard Space Flight Center, Greenbelt, Maryland, March 1978.

22. McEwan, N. J., et al., "A Self Calibrating 9.4 GHz Meteorological Radar," Bradford University, Electrical Engineering Technical Report 231, Bradford, England, December 1976.

23. Nicholson, L. W., et al., "ATS-6 Spacecraft: In-Flight Antenna Pattern Measurement," NASA Technical Note TN D-8135, January 1976.

24. Oguchi, T. and Y. Hosoya, "Scattering Properties of Oblate Raindrops and Cross Polarization of Radio Waves due to Rain (Part III) Calculations at Microwave and Millimeter Wave Regions," *Journal of the Radio Research Laboratories*, 21, No. 105,1974, pp. 191-259.

25. Olsen, R. L., et al., "The aR^b Relation in the Calculation of Rain Attenuation," *IEEE Trans. Ant. and Prop.*, Vol. AP-26, March 1978, pp. 318-329.

26. Theobold, D. M., and D. B. Hodge, "Gain Degradation and Amplitude Scintillation Due to Tropospheric Turbulence," The Ohio State University Electro-Science Lab., Tech. Report 784229-6, Revision A, 1978.

27. "Transportation Systems Center/U.S. Coast Guard L-Band Maritime Satellite Test Program, Test Summary," September-November 1974, Report No. CG-D-104-75, U.S. Department of Transportation, June 1975.

28. Westerlund, L. H., et al., "The ATS-F COMSAT Millimeter Wave Propagation Experiment," *COMSAT Technical Review*, Vol. 3, No. 2, Fall 1973.

BIBLIOGRAPHIC DATA SHEET

1. Report No.	2. Government Accession No.	3. Recipient's Catalog No.
NASA RP-1080		

4. Title and Subtitle	5. Report Date
ATS-6 Final Engineering Performance Report Volume V - Propagation Experiments	November 1981
	6. Performing Organization Code 415
7. Author(s) Robert O. Wales, Editor	8. Performing Organization Report No. 81F0034
9. Performing Organization Name and Address Goddard Space Flight Center Greenbelt, Maryland 20771	10. Work Unit No.
	11. Contract or Grant No. NAS 5-25464
12. Sponsoring Agency Name and Address National Aeronautics and Space Administration Washington, D.C. 20546	13. Type of Report and Period Covered Reference Publication
	14 Sponsoring Agency Code

15. Supplementary Notes

16. Abstract

The Applications Technology Satellite 6, an experimental communications spacecraft, operated for five years in a geosynchronous orbit. The six volumes of this report provide an engineering evaluation of the design, operation, and performance of the system and subsystems of ATS-6 and the effect of their design parameters on the various scientific and technological experiments conducted.

This volume (V) describes technological experiments in the form of propagation studies from 1.5 MHz to 10 GHz.

17. Key Words (Selected by Author(s))	18. Distribution Statement
Communications Technology Satellite, Ultrahigh Frequencies, Radio Frequency Interference, Millimeter Waves, Propagation	Unclassified - Unlimited Subject Category 18

19. Security Classif. (of this report)	20. Security Classif. (of this page)	21. No. of Pages	22. Price*
Unclassified	Unclassified	302	A14

*For sale by the National Technical Information Service, Springfield, Virginia 22151.

GSFC 25-44 (10/77)

*U.S. GOVERNMENT PRINTING OFFICE: 1981 539-007/21 1-3

National Aeronautics and
Space Administration

Washington, D.C.
20546

Official Business
Penalty for Private Use, $300

SPECIAL FOURTH CLASS MAIL
BOOK

Postage and Fees Paid
National Aeronautics and
Space Administration
NASA-451

U.S.MAIL

NASA

POSTMASTER: If Undeliverable (Section 158
Postal Manual) Do Not Return